Appendix H
Deformation and Stability Analysis

December 2019

TABLE OF CONTENTS

LIST OF FIGURES

LIST OF TABLES

LIST OF ANNEXES

1 INTRODUCTION

This Appendix presents the deformation and stability analyses undertaken in connection with the failure of the Vale S.A. ("Vale") Córrego do Feijão Mine Dam I ("Dam I") in Brumadinho, Brazil. The stability and deformation analyses were completed for Dam I to assess the stability and stress state of the dam throughout its construction history and the potential triggers that caused it to fail. The analyses were completed in stages and were developed in two- and three-dimensions (2D and 3D). This Appendix describes the approach and results of the analyses. The 3D analyses are presented first because the main findings came from them. The 2D deformation analyses were supplementary and the findings from those supported the 3D analysis findings.

The deformation models were completed using the finite difference software FLAC and FLAC3D, and the limit equilibrium analyses were completed using Geostudio Slope/W.

2 OVERALL APPROACH AND SUMMARY OF FINDINGS

The approach involved three stages, as briefly described together with the key findings in the following subsections. Further details are presented later in this Appendix.

2.1 Stage 1 – Establish Pre-failure Conditions

Stage 1 of the analysis involved simulating the construction history of Dam I. The dam was constructed sequentially within the analysis in 15 stages, representing the 10 raisings of the dam construction (see Appendix A). The model geometry and layering of the tailings and containment berms in these analyses were taken from the 3D computer-aided design (CAD) model described in Appendix F.

During this stage of the analysis, the tailings were assumed to mobilize their drained strength parameters. Various model revisions were assessed. The final model revision included use of a strain-weakening constitutive model (termed "strain softening" in the FLAC software), and the 3D analysis included the assignment of stochastic distributions of state parameter to each layer of tailings within the model. These state parameter values were subsequently used to assign the strength and stiffness parameters, as well as parameters defining the post-peak strength relationship. These parameters were assigned based on laboratory testing results and state parameter values from cone penetration test (CPTu) data presented in Appendix E.

The choice to use a stochastic distribution of state parameter was made because of the wide variation of strength and stiffness observed in the laboratory testing for samples tested at different initial state parameters (ψ), as well as the wide variation of state parameter calculated from the CPTu data. This reflected the highly heterogeneous distribution of the tailings in the dam. It was considered necessary to capture this variability both within individual raisings and within the fine and coarse tailings layers. This was achieved using a local area subdivision (LAS) routine to assign a spatial variation of ψ that also honored the statistical distribution encountered in the CPTu results. This approach was demonstrated previously by Hicks and Onisiphorou (2005)[1] in their assessment of the Nerlerk Berm liquefaction failure and is discussed further in Section 3.1.5. The use of a stochastic distribution of parameters meant that it was necessary to run multiple simulations to determine a representative range of results. In this assessment 40 simulations were completed, from which four were selected as being the most representative based on the results of Stage 2 of the analysis.

The main outcome of this stage of the analysis was a series of stress distributions representing the conditions prior to failure, which could be used in the 3D analyses for testing the potential for triggers identified by the Panel to cause failure of the dam. The results of the 2D analysis were available prior to the 3D analysis results and were used to inform the selection of initial stress conditions in anisotropically consolidated triaxial laboratory strength testing.

2.2 Stage 2 – Initial Screening of Liquefaction Triggering Mechanisms

Stage 2 was completed only in the 3D analysis using the strain-weakening relationship and stochastic distribution of ψ. It continued from Stage 1 and involved assigning undrained strength and stiffness parameters to the model and then testing the effect of various potential triggering mechanisms. Consistent with the Stage 1 analyses, the undrained stiffness, as well as the peak and residual undrained strengths and the strain required to mobilize a post-peak reduction in strength were assigned using trends from laboratory testing and the stochastic distributions of ψ.

The premise for Stage 2 of the analysis was that the dam was marginally stable with the strain-weakening undrained strengths immediately prior to failure. Therefore, before testing the potential effect of identified triggers, the first step in Stage 2 was to test each of the 40 simulations discussed in Stage 1 to determine its factor of safety (FS) using the strain-weakening relationship. This stage of the assessment involved completing a strength reduction analysis, analogous to the typical shear strength reduction (SSR) FS calculations that are commonly completed in deformation analyses. In typical SSR FS calculations, the strength of all soil units is adjusted in uniform increments to identify the strengths at which the dam in the model is no longer stable; the FS is then calculated as the ratio of the applied strengths to the strengths at the point of instability in the model. In this instance, only the peak undrained strength of the saturated fine and coarse tailings was varied to reflect the uncertainty in this parameter due to variations in the distribution of tailings and their bonding throughout the dam (see Appendix E). The remaining parameters, such as the residual (or liquefied) undrained strength and the strain required to mobilize that liquefied strength were unchanged from the trends derived from laboratory testing described in Appendix E. The parameters for the berms and unsaturated tailings were not varied. It was found that once the

[1] Hicks, M.A., & Onisiphorou, C. (2005). Stochastic evaluation of static liquefaction in a predominantly dilative sand fill. *Géotechnique*, *55*, 123-133.

process of strength loss was initiated in the model, the dam would fail rapidly and the analysis could not continue.

The intent from this strength reduction analysis was to determine the FS against the onset of liquefaction in each simulation. Having determined that FS, a subset of four models was selected that had a FS against the initiation of liquefaction close to one, which were used for testing identified triggering mechanisms. These models were considered the "representative models." The FS against liquefaction triggering in these representative models ranged from 1.0 to 1.2. Where the FS was greater than 1 in these representative models, the strengths were reduced to bring the FS to 1 before testing the triggering mechanisms.

A further test was completed on these representative models prior to testing liquefaction triggering mechanisms. This test involved assessing whether the dam in this condition of FS = 1 could resist previous events that occurred at Dam I and did not cause failure of the dam. One of the events used in this test was the drilling of borehole SM-09, which was drilled in December 2018 and January 2019 on the same bench as the borehole being drilled on the day of the failure (borehole SM-13). The other event was the water pressure at the end of deep horizontal drain 15 (DHP-15) during installation, which was observed to cause disturbance of the slope during drilling but did not cause the dam to fail. Disturbance from borehole SM-09 was simulated by assuming an extreme condition in which liquefaction was assumed to occur around the depth of this borehole. This condition involved assigning a post-liquefaction strength ratio ($S_{u\text{-}liq}/p'$) of 0.01 to all zones of the model beneath the water table within a 1-meter (m) radius of the borehole. Disturbance from DHP-15 was assessed by assigning water pressures of 600 kilopascals (kPa) and 1000 kPa at the end of the DHP borehole. Despite these models having a marginal FS prior to these tests, the dam did not fail in the representative models from these events. This confirmed their suitability for use in testing the other triggering mechanisms.

The following liquefaction triggering mechanisms were assessed on these representative models:

- *Liquefaction surrounding the borehole that was being drilled on the day of the failure (SM-13).* As a simplification, this process was assessed in the same manner described earlier for SM-09, in which a $S_{u\text{-}liq}/p'$ of 0.01 was assigned to all zones in the model within a 1-m radius of the borehole. It was found that this condition did not cause significant deformations or failure of the dam in the representative models.

- *Liquefaction surrounding DHP-15*. Despite the observation that DHP-15 did not cause failure of the dam during installation in June 2018, a scenario was considered in which liquefaction occurred later around this borehole due to previous disturbance. Like the analysis of borehole SM-13, this was assessed by assigning a $S_{u\text{-}liq}/p'$ of 0.01 in a 1-m radius around the DHP. This was recognized as being an unlikely scenario because DHP-15 was completed roughly seven months prior to the failure. Nonetheless, it did not lead to failure of the dam in the representative models.

- *Loss of suction in the unsaturated zone*. This was assessed by reducing the available strength in the material above the water table by 5 kPa, 10 kPa and 15 kPa to bound the estimate of suction-related strength loss that could potentially occur due to rainfall infiltration, as determined by the seepage analysis documented in Appendix G. It was found that this reduction in strength in the unsaturated zone would not cause failure of the dam but indicated deformation of the dam slope.
- *Liquefaction around the location of springs known to exist prior to the dam construction*. A scenario was considered in which an influx of seepage water enters the dam at the location of known, pre-existing, underground springs along the northern edge of the impoundment, which in turn causes a zone of strength loss in those regions. This was treated as a localized event around the position of the springs because the piezometers did not detect a significant change in water pressure beneath the dam prior to failure. This was simulated in the representative models by assigning a $S_{u\text{-}liq}/p'$ of 0.01 to the coarse or fine tailings or slimes within a 50-m radius region around the springs. This scenario caused significant local displacements around the springs but did not result in failure of the dam. The pattern of displacements resulting from this simulation did not reflect the observations of the failure displacements from the video analysis (see Appendix D).

This stage of the analysis was based on a simplifying assumption that the undrained strengths were mobilized throughout the entire dam and that the dam was marginally stable prior to the triggering mechanism occurring. This simplification was considered appropriate because the purpose of this analysis was to test the effect of triggers on Dam I in this fragile condition. This approach was able to identify that localized events, such as drilling, would not have a significant impact on the stability of the dam and reduced the number of potential triggers to be evaluated further. Stage 3 of the assessment involved an advancement of the most influential trigger from Stage 2, which was a 15 kPa strength-loss in the unsaturated zone due to loss of suction by rainfall infiltration, by combining this with a condition of ongoing internal strain (creep) within the dam.

2.3 Stage 3 – Further Assessment of Liquefaction Triggering Mechanisms

Stage 3 continued from Stage 2 and involved assessing a condition that was observed in the laboratory triaxial testing in which loose samples will continue to accumulate strain at a constant deviator stress if the lateral stress ratio (K_0) is lower than 0.5 (i.e., higher shear stress ratio). In this context, a K_0 of 1 represents isotropic loading and a reduction in this ratio increases the shear stress. A model of this condition was first developed by calibrating the displacements of a single element analysis to the time-dependent displacements observed in triaxial test TXDW03 at various K_0 values, the results of which are presented in Appendix E. This relationship was then applied to the representative 3D models. The relationship used for this assessment was a modified version of that developed by Wedage et al. (1998).[2]

In the representative 3D models, this relationship was applied until the dam in the model displaced 1 centimeter (cm) horizontally at a set monitoring point on the face of the dam. The effect of this creep was then reviewed after this 1-cm increment by assessing if the dam remained stable or if rapid strength loss and strain accumulation would occur. If the dam did not fail after the first 1-cm increment of creep, this process was repeated in 1-cm increments until the dam failed. This method identified the amount of creep required to initiate failure in the initially marginally stable representative 3D models.

The combined effect of a loss of suction in the unsaturated zone and ongoing creep displacement was assessed by applying the strength loss due to rainfall infiltration, discussed in Stage 2, at the end of each increment of creep displacement. When compared with the earlier creep displacement results, these results showed if the dam would fail more readily with a combination of a loss of suction combined with creep than it would with creep alone.

These results show that without the addition of a 15 kPa strength reduction in the unsaturated zone, between 8 cm and 37 cm of creep displacement recorded on the face of the dam would cause failure of the dam. This reduces to 1 cm if the 15 kPa strength loss in the unsaturated zone is included in the analysis.

The total displacement measured by InSAR in the year prior to failure was 3.5 cm, suggesting that the dam could have accumulated creep in the order of 10 cm to 15 cm over the 2.5 years after tailings deposition ceased (Appendix D). However, the InSAR displacement was dominantly vertical, suggesting that total horizontal displacements in the order of only 5 cm would be a reasonable maximum estimate for the amount of creep displacement in the 2.5 year period since operations ceased. These results show that one of the four representative models would fail close to this amount of creep displacement without the inclusion of a loss of suction in the unsaturated zone and that the addition of the loss of suction causes failure to occur in all models within this range of displacements. The pattern of displacements matched the InSAR data most closely when creep was combined with a loss of suction in the unsaturated zone.

To conclude the analysis, a further step was taken to review the effect of potential disturbance associated with the borehole being drilled on the day of the failure (SM-13). This involved repeating the creep analyses without a loss of suction in the unsaturated zone and testing the effect of localized liquefaction associated with SM-13 after each increment of creep. In this analysis, liquefaction surrounding SM-13 was simulated in the same manner as described for Stage 2. This analysis showed that the inclusion of a liquefied zone around SM-13 did not lead to a significant

---

2 Wedage, A., Morgenstern, N., & Chan, D. (1998). Simulation of time-dependent movements in Syncrude tailings dyke foundation. *Canadian Geotechnical Journal*, *35*, 284-298.

difference in the amount of creep required to cause the dam to fail. This supported the conclusion from Stage 2 that drilling borehole SM-13 had no significant impact on the failure of the dam.

2.4 Supplementary Analyses

2.4.1 Factor of Safety

Limit equilibrium method (LEM) FS calculations were completed on the three analysis sections described in Appendix F.

Ahead of these analyses, the 3D models with a FS of 1 against liquefaction triggering (see discussion in Section 2.2) were used to calculate the conventional FS of Dam I using a Mohr-Coulomb constitutive model with the peak undrained strengths and no post-peak strength loss. A standard SSR approach was used for this calculation using the approach described by Dawson et al. (1999) and Griffiths and Lane (1999). This is analogous to a typical FS calculation, such as those from LEM analyses. This calculation involved three steps:

- Step 1 – Assign peak strengths as S_u/p' to each layer of coarse and fine tailings using the stochastic distribution of ψ. Calculate the conventional FS for this condition using the SSR method. This produced a FS = 1.5 based on the peak strength.

- Step 2 – Assign a single undrained strength as an S_u/p' to the coarse and fine tailings. The purpose of this step was to identify a representative value of S_u/p' for the tailings. Calculate the conventional FS for this condition. This was repeated for different S_u/p' values until the FS was equal to that from Step 1. It was found from this that an S_u/p' of 0.59, equal to the 33rd percentile of the variable strengths (i.e., 33% would have smaller values), led to a FS equal to that with the stochastic distribution of strengths.

- Step 3 – Repeat Step 2, but instead of defining the strength as S_u/p', the strength was defined as S_u/σ'_v because this is the typical way strength ratios are assigned in LEM analyses. This was also repeated until the conventional FS from this analysis was equal to that of Step 1. It was found that a S_u/σ'_v of 0.37 would lead to a FS equivalent to that of Stage 1. This can be related to S_u/p' through the following equation: $S_u/\sigma'_v = [(1+2K_0)/3] \times S_u/p'$. The difference between the Step 2 and Step 3 results implies an average K_0 of 0.45 was operative throughout the dam slope in the region of the failure.

The LEM FS calculations were made using an S_u/σ'_v of 0.37, derived from the representative 3D models. The purpose of these analyses was to assess how the stability of the dam varied throughout the history of construction and across the various cross sections. They were also intended to form a consistency check between the LEM and finite difference-based approaches. To aid this comparison, conventional SSR FS analyses were also completed in the 2D FLAC models for two of the cross-sections.

The conventional FS values for the peak strength condition from the various analyses are summarized in Table 1.

Table 1: Factor of Safety Summary for the Condition Prior to Failure based on $S_u/\sigma'_v = 0.37$

Cross-section	Limit Equilibrium[1]	2D FLAC	3D FLAC
1-1	1.5, 1.4, 1.3	1.4	1.5
2-2	1.6, 1.6, 1.2	Not calculated	
3-3	1.5, 1.7, 1.2	1.2	

Note: [1]Factors of Safety listed represent the following slip surface scenarios: Crest to Toe, Crest to Plateau, and Plateau to Toe

These results highlight the limitation of conventional FS approaches for calculating slope stability for highly brittle soils. In this case, the FS calculated by conventional methods, in which the potential for strength loss is not included, was 1.5. This means that the peak strengths of the tailings were, on average, 50% higher than the shear stresses acting on them. However, the liquefied strengths of the tailings were much lower than the shear stresses acting on the dam slope. This meant that if the more heavily stressed areas of the dam slope began to lose strength, they would cause destabilization of the entire dam due to a progressive failure mechanism. This effect was highlighted in the Stage 2 analyses, which showed that a slight reduction in shear strength would be enough to initiate this progressive failure mechanism and cause failure of the dam; therefore, although the FS using peak strengths was 1.5, the factor of safety was actually 1 because of the high brittleness and low post-liquefaction strengths.

2.4.2 Material Point Method

A final stage in the stability and deformation analyses involved using the Material Point Method (MPM) to calculate how the dam failure would develop following liquefaction triggering. This was completed because the deformation analyses described earlier could capture the stresses up to and during the initiation of failure but could not fully capture the propagation of the failure.

This analysis used a similar strain-weakening relationship as the deformation analyses and showed that once the failure was initiated it would develop into a series of retrogressive failure planes that would occur at a rate that matched the observations. This analysis provided further support for the strain-weakening relationship used in earlier analyses.

3 DETAILS OF ANALYSES

3.1 Model Development

3.1.1 Model Geometry

The 3D CAD model summarized in Appendix F was used as the basis for developing the 2D LEM and 2D and 3D FLAC models. Models were generated by incorporating containment berm geometry, tailings delineation, and staged beach surfaces developed as part of the 3D CAD model. These models are illustrated in Figure 1 through Figure 3.

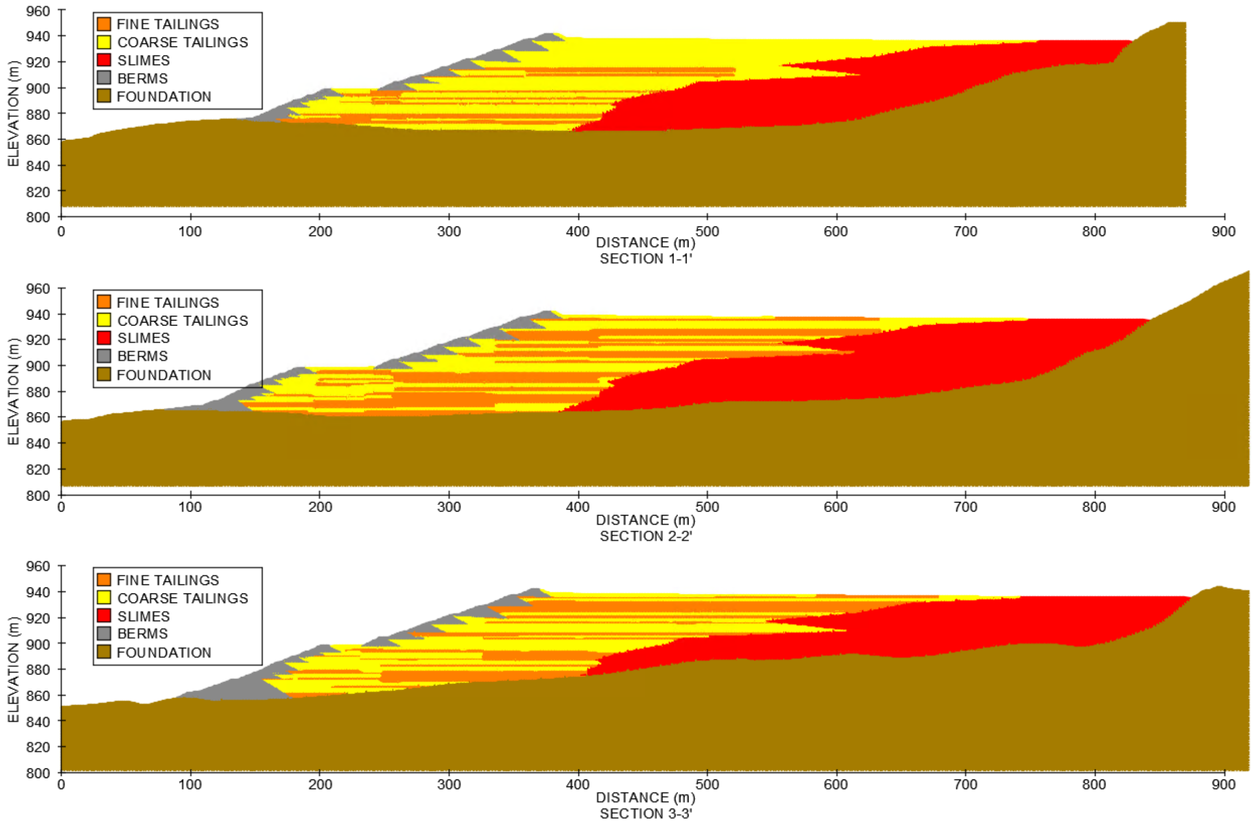

Figure 1: 2D FLAC Models – Cross-sections 1-1’, 2-2’, and 3-3’

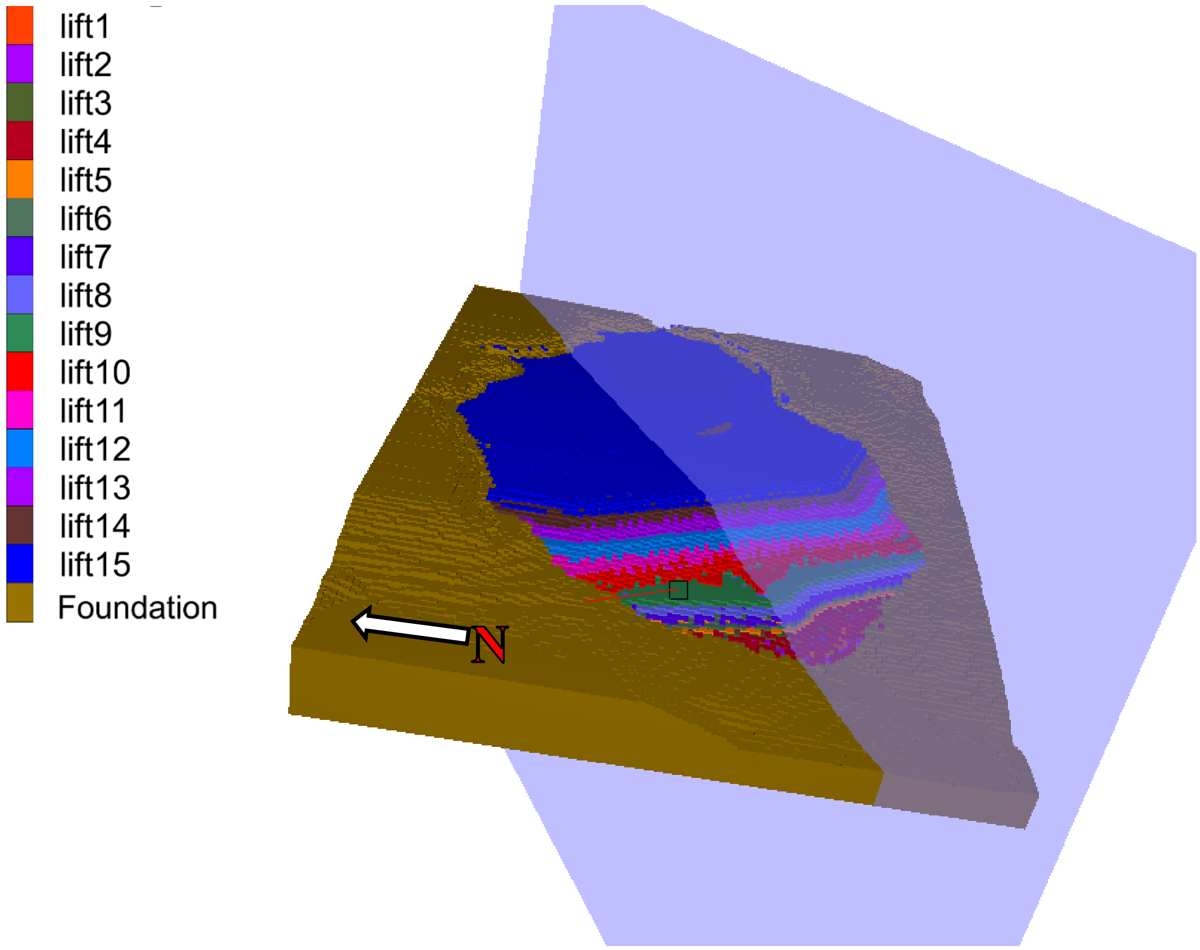

Figure 2: Oblique View of 3D FLAC Model Showing the 15 Layers in which it was Built. Section Location from Figure 3 is Shown by Vertical Plane

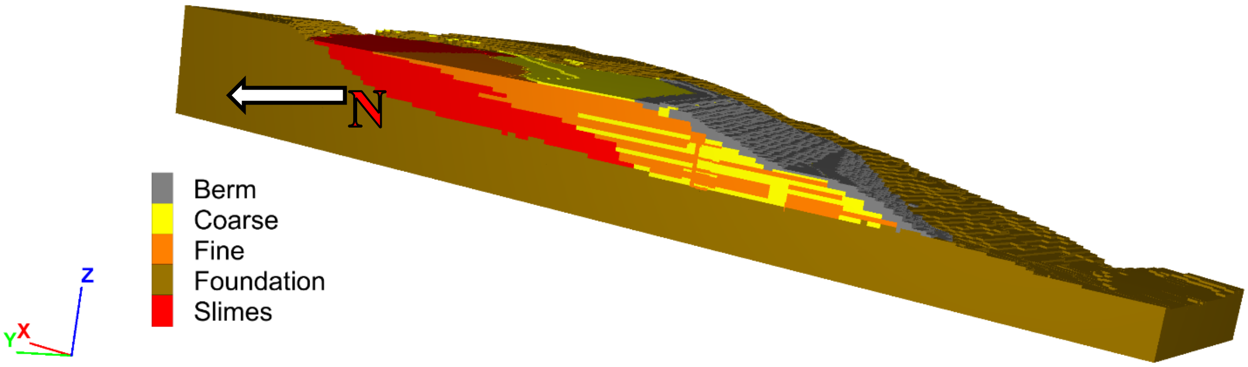

Figure 3: Oblique-Section View of 3D FLAC Model Showing Tailings Stratification

3.1.2 Model Simulation Sequence

The models were initially used to simulate the construction sequence of Dam I. This initial stage of the analysis, termed Stage 1, involved drained strength and stiffness parameters, and consisted of sequentially adding lifts of tailings in the model in a manner that reflected the stages recorded in the construction history (see Appendix A). Each lift was initially placed using elastic parameters, then the pore pressures were updated to reflect the pond and water table for that stage of construction. Then, the constitutive model for that layer was switched to the constitutive model intended for use throughout the remainder of the analysis (e.g., strain-weakening; see Section 3.1.3). This process was repeated for each of the 15 construction stages.

The subsequent stages of the analysis were described in Section 2.3 and involved testing liquefaction triggers. During these stages of the analysis, the properties assigned to the tailings were switched to the undrained strengths and stiffnesses. Where necessary, the strengths were slightly reduced to bring the model to the point of incipient failure and then the liquefaction triggers were tested on the model in this condition of marginal stability.

In summary, drained strength and stiffness parameters were used in Stage 1 and undrained parameters were used in Stages 2 and 3.

3.1.3 Constitutive Model Selection

3.1.3.1 Tailings

Throughout this investigation, analyses were completed with various constitutive models for the tailings, including:

- NorSand – only used in initial modeling of Stage 1 (drained parameters);
- Mohr-Coulomb without post-peak strength loss – only used in initial modeling of Stage 1 (drained parameters); and

- Mohr-Coulomb with post-peak strength loss (termed "strain-weakening" in this Appendix and "strain softening" in the FLAC software) – used in all three stages of the analysis (drained and undrained parameters).

The parameters for these models were presented in Appendix E together with results of element test analyses that show the way these constitutive models represent the stress-strain curves of the tailings. In summary:

- The Norsand model uses a range of parameters to define the full shape of the stress-strain curve, capturing the elastic stiffness, peak strength and post-peak strength loss. The parameters in this model automatically adjust this behavior based on the state parameter (ψ) and mean effective stress (*p'*) of the soil.

- The Mohr-Coulomb model represents the pre-failure stress-strain behavior with a linear relationship defined by two elastic constants. In this case, shear modulus (*G*) and bulk modulus (*K*) were used. This elastic relationship is used until the strength is reached. The strength was defined using a peak friction angle and no cohesion. In this model, the strength does not reduce if strain continues to accumulate beyond that associated with the peak strength.

- The strain-weakening relationship is an extension to the Mohr-Coulomb model. The same elastic relationships and strengths were used as defined for the Mohr-Coulomb analyses; however, an additional strength termed the "residual" strength was defined for this constitutive model. After the peak strength is exceeded, the strength will reduce to the residual value at a rate prescribed by setting the strain at which strength loss begins ($\varepsilon_{p\text{-}SL}$) and the strain at which the residual strength is reached. ($\varepsilon_{p\text{-}R}$).

As noted in Appendix E, the tailings in the laboratory testing were observed to develop a higher strength than typical for the ψ values tested; however, this additional component of strength was observed to be variable. This behavior was attributed to the effects of bonding between individual grains within the tailings, which was observable in the in-situ shear wave velocity data and scanning electron microscope images. This additional strength caused the soil to be stiffer and stronger than typical, but it also caused greater and more-rapid post-peak strength loss. This behavior can be captured in the NorSand model using a high value of dilatancy (χ); however, the resulting stress-strain behavior caused numerical instabilities in the full-scale models. Hence, preference was given to the strain-weakening model in the analysis because the variations in the stiffness, peak strength and post-peak stress-strain behavior could be modeled in a way that was more numerically stable than the NorSand model for these bonded tailings. The variation was captured by normalizing the assigned stiffness based on confining stress and assigning the strength and stiffness based on ψ calculated from the CPTu data (see Appendix E). The ψ was varied throughout the tailings within the final 3D simulations.

The parameters for all these constitutive models are presented in Appendix E.

3.1.3.2 Containment Berms

The containment berms on the downstream slope of the dam were modeled using a Mohr-Coulomb constitutive model with a friction angle (ϕ') of 36° and zero cohesion. These berms were modeled with a bulk and shear modulus of 28 megapascals (MPa) and 21 MPa, respectively.

3.1.3.3 Natural Soil – Foundation

The natural soil in the pre-existing valley beneath the dam was modeled using a hyperbolic-elastic constitutive model called the CHSoil model. This constitutive model represented the curved stress-strain behavior of the residual soil observed in the laboratory direct simple shear (DSS) testing completed on samples collected during the 2019 investigation (see Appendix E). It was not necessary to consider post-peak strength loss in this soil because the laboratory testing showed no significant post-peak strength loss.

The natural soil in the abutments was modeled as an elastic material with a high bulk and shear modulus of 470 MPa and 220 MPa, respectively. This was done to create a stiffness contrast with the tailings and prevent the abutments impacting the model results.

3.1.4 Input Parameters

Parameters used in the analysis were calculated from field and laboratory data, discussed in Appendix E. The Mohr-Coulomb and strain-weakening parameters are summarized below.

3.1.4.1 Mohr-Coulomb Model Inputs

Elastic moduli selected for the drained stage of Mohr-Coulomb analysis were calculated as secant moduli from drained triaxial compression test data. Relationships of shear and bulk modulus, and peak friction angle versus state parameter were developed for use in these analyses (see Appendix E for these relationships).

3.1.4.2 Strain-weakening Drained Parameters

Strain-weakening parameters for the drained stage of the analysis were developed from triaxial tests and verified with element test simulations. To model the strain-weakening response, the amount of plastic strain (i.e., strain after the peak strength has been reached) until strength loss occurs ($\varepsilon_{P\text{-}SL}$) was calculated together with the amount of strain until the residual strength is reached ($\varepsilon_{P\text{-}R}$). For input to the deformation analysis, relationships of $\varepsilon_{P\text{-}SL}$ and $\varepsilon_{P\text{-}R}$ versus state parameter were developed (see Appendix E for these relationships). Figure 4 illustrates the stress-strain relationships that result from these trends for various ψ values for an element of soil at p' = 200 kPa.

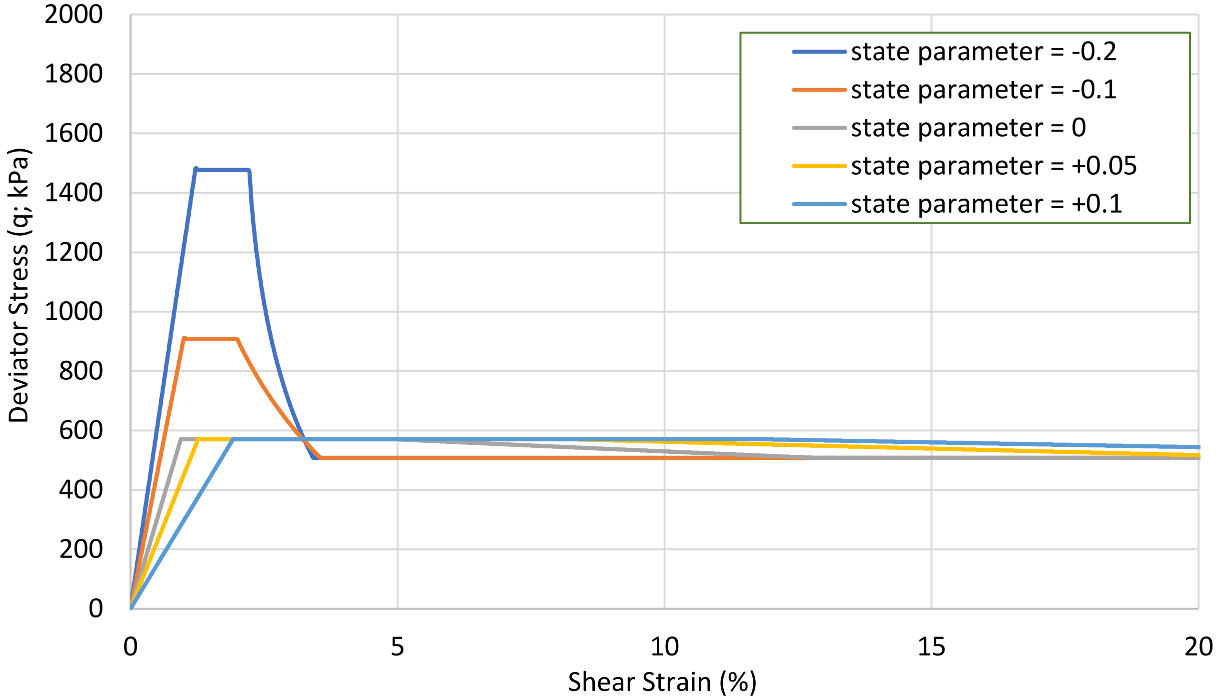

Figure 4: Example Strain-weakening Relationships at *p'* = 200 kPa – Drained Parameters

3.1.4.3 Strain-weakening Undrained Parameters

Undrained stiffness parameters for all tailings were calculated at 50% of the peak deviator stress and using a ν of 0.49.

Trends relating *G* and peak and residual undrained shear strength ratios to ψ were developed for input into the analyses. The *G* relationship was normalized by dividing by the mean effective stress. These relationships are shown in Appendix E.

K was calculated from *G* and ν using:

$$\boldsymbol{K = \frac{2G(1+v)}{3\big(1-(2v)\big)}}$$

Parameters developed to model the strain-weakening response for undrained shear were based on undrained triaxial compression tests. The $\varepsilon_{P\text{-}SL}$ and $\varepsilon_{P\text{-}R}$ versus ψ relationships for undrained shear are shown in Appendix E. Example stress-strain curves resulting from these parameters for various values of ψ at *p'* = 200 kPa are shown in Figure 5.

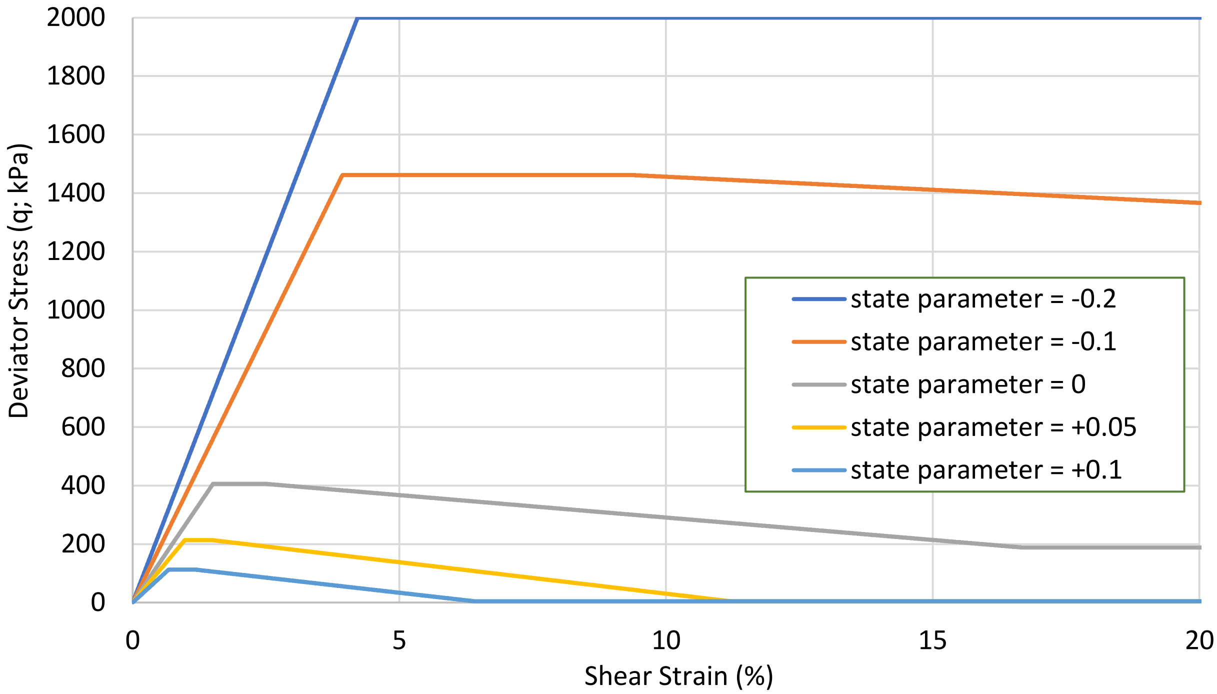

Figure 5: Example Strain-weakening Relationships at *p'* = 200 kPa – Undrained Parameters

3.1.5 Stochastic Variation of State Parameter

As mentioned in Section 3.1.4, the parameters assigned to the constitutive models were based on the ψ assigned to the fine and coarse tailings. In early model trials and in the 2D analyses, single values of ψ were assigned and sensitivity analyses were completed on this. In the final 3D analyses, a stochastic distribution of ψ was assigned to address the variability observed in the CPTu data and the impact this has on the strength and stiffness.

The method of assigning the stochastic distribution of ψ to the model was based on the autocorrelation distance and Local Area Subdivision (LAS) approach. This approach was also used in the analysis of the Nerlerk Berm liquefaction failure analysis by Hicks and Onisiphorou (2005). A description of it is in the following sections.

3.1.5.1 Autocorrelation Distance

The autocorrelation distance, δ_u, was developed by Vanmarcke (1977)[3] to characterize the local spatial variability and uncertainty of parameters within a given soil layer. The autocorrelation distance is defined as the absolute distance within which data points are expected to be correlated.

[3] Vanmarcke, E.H. (1977). Probabilistic modeling of soil profiles. *ASCE Journal of the Geotechnical Engineering Division*, *103*(GT11), 1227-1246.

Once the autocorrelation distance, δ_u, has been determined (or estimated), the variance reduction factor, $\Gamma(D_x)$, can be calculated for a region of width, D_x, using the following equation (after Vanmarcke 1977).

$$\boldsymbol{\Gamma(D_x) = \sqrt{\left(\frac{0.5\cdot\delta_u}{D_x}\right)^2\left[2\left(\frac{D_x}{0.5\cdot\delta_u} - 1 + e^{-\frac{D_x}{0.5\cdot\delta_u}}\right)\right]}}$$

Where,

D_x = Width of the region (m)

δ_u = Autocorrelation Distance (m)

$\Gamma(D_x)$ = Variance Reduction Factor

3.1.5.2 Local Area Subdivision

LAS is a stochastic modeling method developed by Fenton and Vanmarcke (1990)[4] to simulate the variation of a given material parameter based on its mean, standard deviation, and autocorrelation distance in one or more dimensions. This process is completed in stages, where Stage 0 refers to the original region of interest or soil region and, at each subsequent stage, all the previous sub-regions are divided into two equal halves. For example, Stage 1 will have two sub-regions and Stage 2 will have four sub-regions.

Once the mean, standard deviation, and autocorrelation distance have been calculated from the original data set, as discussed above, the LAS procedure can be used to assign randomized values to discrete elements within a region of interest of a model, while preserving the original mean, standard deviation, and relative spatial distribution from the original field data set.

In this method, the original mean for the data set was preserved through the process of "upwards averaging" – for each sub-region division, the mean assigned to one half was randomly generated, and the mean assigned to the second half was calculated such that averaging the two halves yielded the original mean for the entire region. The standard deviation for each stage was factored by a variance reduction factor that was calculated based on the ratio between the width of the sub-region and the autocorrelation distance. This factored standard deviation represents the expected magnitude of correlation between the data points within the sub-region, given their proximity.

The randomized values are assigned by progressively subdividing a region into halves at each stage, as per the following procedure:

---

[4] Fenton, G.A., & Vanmarcke, E. (1990). Simulation of random fields via local average subdivision. *Journal of Engineering Mechanics, 116*(8), 1733-1749.

Step 1. Assign the original mean, Z_1^0, and a standard deviation, $\sigma' \cdot \Gamma(D_x)$, to the region of interest in the model, where σ' is the standard deviation for the entire data set, and $\Gamma(D_x)$ is the variance reduction factor for a region of width D_x. This initial step is denoted Stage 0.

Step 2. In the next stage, divide each region, *j*, from the previous or "parent" stage, *i*, into two equal halves (for Stage 1, the parent stage is Stage 0, where *i* = 0 and *j* = 1). For the first sub-region, randomly generate a new mean value, Z_{2j-1}^{i+1}, in Stage *i*+1 for region 2*j*-1, based on the original or "parent" mean and standard deviation from the previous stage using the following equation:

$$\boldsymbol{Z_{2j-1}^{i+1} = X \cdot \sigma^{i} + Z_j^i}$$

Where,

i = parent stage number
j = parent region number
Z_j^i = mean from Stage *i*, Region *j*
σ^i = standard deviation for Stage *i*
X = randomly generated number from a probability distribution that matches the original data set

Then, for the second sub-region, Region 2*j*, calculate the mean value, Z_{2j}^{i+1}, using the following equation:

$$\boldsymbol{Z_{2j}^{i+1} = 2 \cdot Z_j^i - Z_{2j-1}^{i+1}}$$

The standard deviation, σ^{i+1}, for all sub-regions in Stage *i*+1 is calculated using the following equation:

$$\boldsymbol{\sigma^{i+1} = \sigma^{i} \cdot \Gamma(D_x^{i+1})}$$

Where,

σ^i = standard deviation for Stage *i*
$\Gamma\left(D_x^i\right)$ = variance reduction factor for a region of width D_x^i in Stage *i*

This process is shown in Table 2 for three adjacent sub-regions.

Table 2: Illustration of LAS Procedure

Stage	**Sub-region Mean**		
i	Z_{j-1}^i	$\boldsymbol{Z_j^i}$	Z_{j+1}^i

i+1	$Z_{2(j-1)-1}^{i+1}$	$Z_{2(j-1)}^{i+1}$	$\boldsymbol{Z_{2j-1}^{i+1}}$	$\boldsymbol{Z_{2j}^{i+1}}$	$Z_{2(j+1)-1}^{i+1}$	$Z_{2(j+1)}^{i+1}$

Step 3. Repeat Step 2, until the sub-region width, D_x, is less than the autocorrelation distance. Then randomly assign values to each element of the model based on the mean and standard deviation of the smallest LAS sub-region it is contained within using the above equations.

This approach was implemented in the FLAC3D analysis by initially subdividing the impoundment into 90-m wide regions located between the downstream toe of Dam I and the upstream edge of the impoundment, and then subdividing these regions. An autocorrelation distance of 30 m was assumed for this analysis based on typical values for natural soils, such as those summarized by El-Ramly et al. (2003),[5] and the Panel's experience with values for hydraulically discharged tailings at other mines.

3.1.5.3 State Parameter Statistics

Histograms and cumulative distribution functions of ψ for the fine and coarse tailings are plotted in Appendix E. The mean and standard deviations of these functions were used to assign state parameter values to the models. The fine tailings were assigned a mean and standard deviation of +0.16 and 0.15, respectively. The coarse tailings were assigned a mean and standard deviation of -0.02 and 0.09, respectively. Both distributions were treated as normal distributions. These distributions are illustrated in Figure 6 and Figure 7 against the distributions from the various methods of ψ calculation discussed in Appendix E.

As discussed in Appendix E, three methods were used to calculate ψ: Plewes (1992)[6]; Robertson (2009)[7]; and a CPT inversion approach after Jefferies and Been (2016).[8] Results from the three methods are shown for the coarse tailings in Figure 6. The data from Robertson (2009) is omitted from the data for the fine tailings shown in Figure 7 because the slope of the critical state line for the fine tailings is the same as the coarse tailings, which suggests the fines content correction within the Robertson (2009) method may not be appropriate for these layers. The distributions of state parameter used in the analyses was intended to capture the range of variation across the methods of ψ calculation.

---

[5] El-Ramly, H., Morgenstern, N.R., & Cruden, D.M. (2003). Probabilistic stability analysis of a tailings dyke on presheared clay-shale. *Canadian Geotechnical Journal*, *40*, 192-208.

[6] Plewes, H.D., Davies, M.P., & Jefferies, M.G. (1992). CPT based screening procedure for evaluating liquefaction susceptibility. Proceedings from *The 45th Canadian Geotechnical Conference*, 41-49. Richmond, BC: BiTech Publishers Ltd.

[7] Robertson, P.K. (2009). Interpretation of cone penetration tests – a unified approach. *Canadian Geotechnical Journal*, *46*(11), 1337-1355.

[8] Jefferies, M., & Been, K. (2016). Soil liquefaction: A critical state approach (2nd ed.). London: Taylor & Francis.

An example of the distribution of state parameter within one of the 3D models is shown in Figure 8.

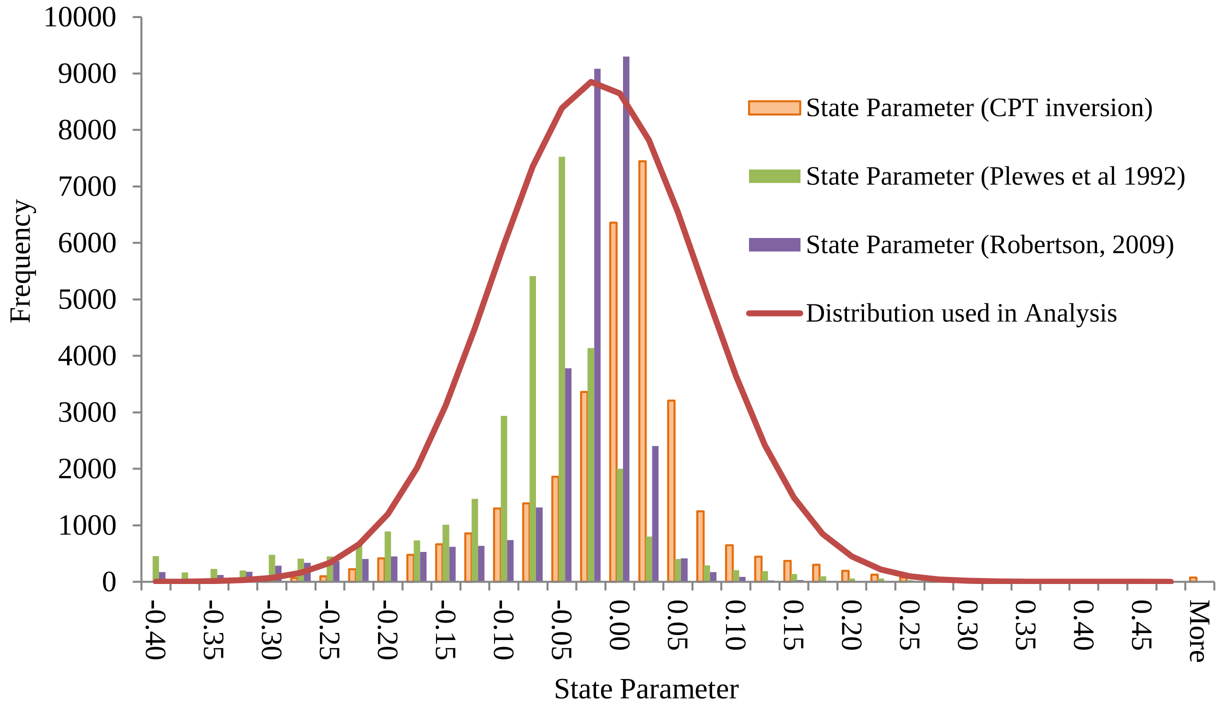

Figure 6: State Parameter (ψ) Distribution for Coarse Tailings

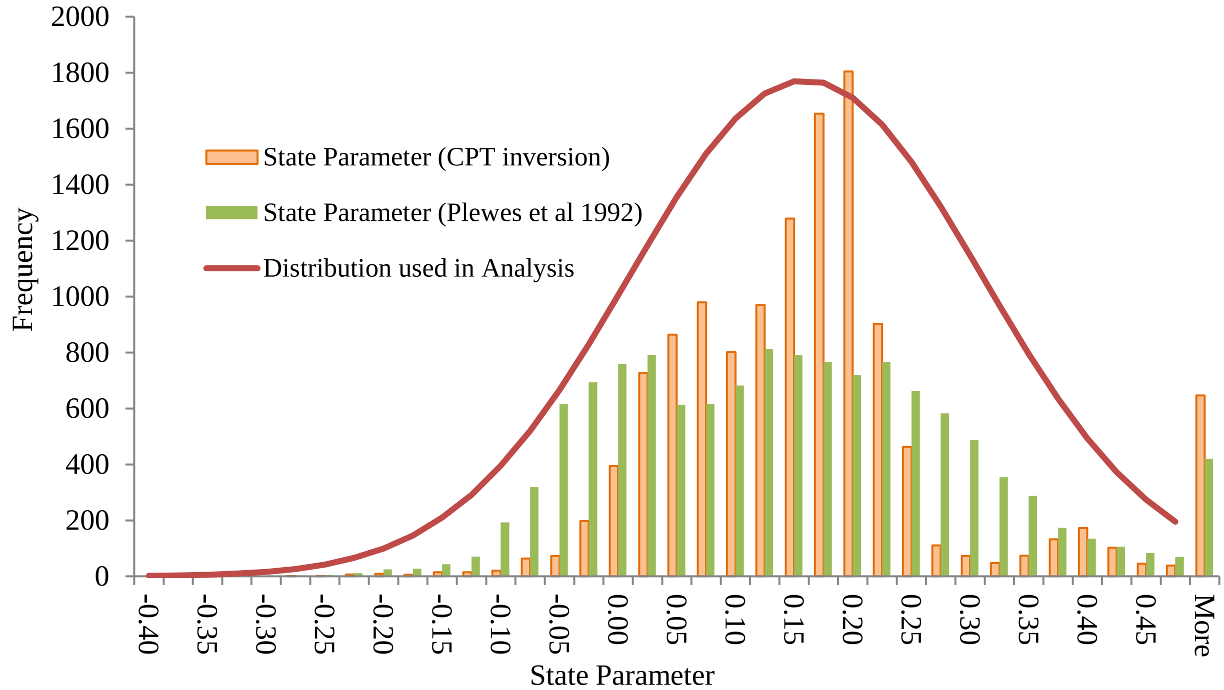

Figure 7: State Parameter (ψ) Distribution for Fine Tailings

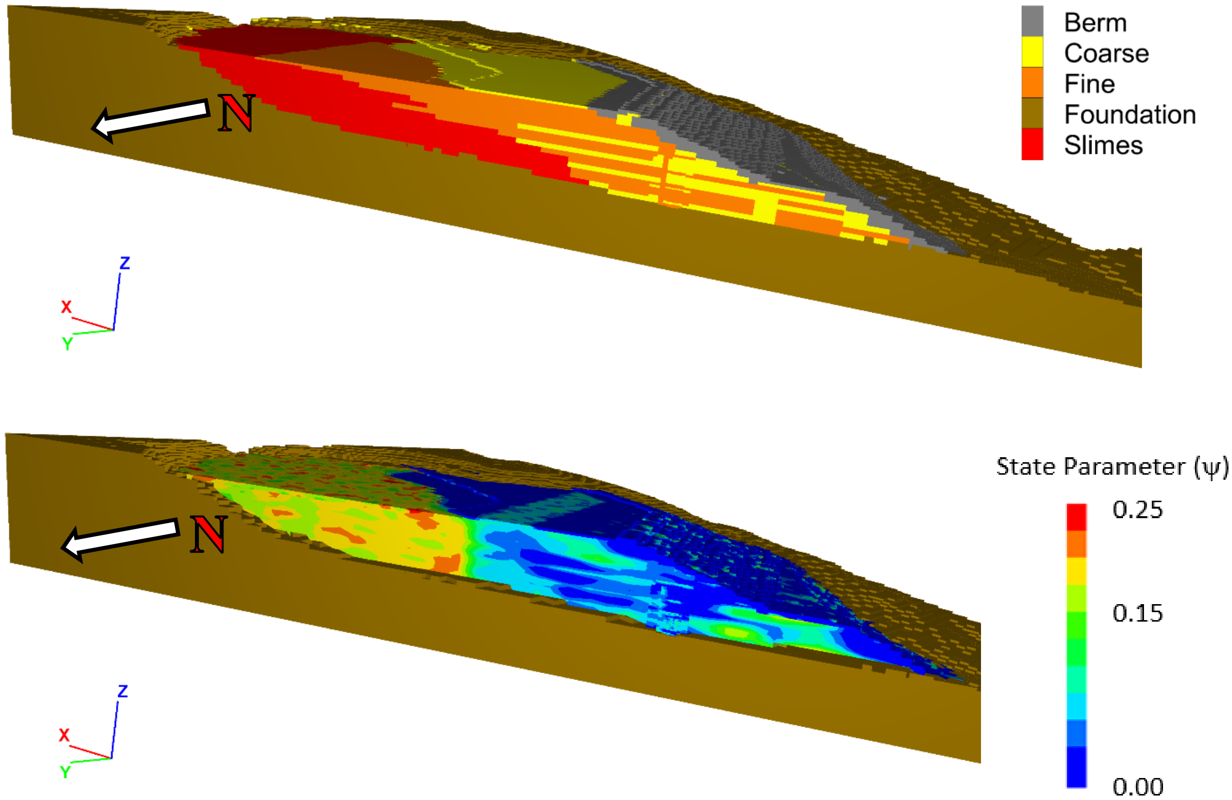

Figure 8: Example State Parameter Distribution throughout the 3D Model

3.1.6 Pore Water Pressures

Pore water pressures from the surfaces developed as part of the 3D CAD model, discussed in Appendix F, were used in these analyses in combination with a hydraulic gradient of roughly 50% of hydrostatic (based on CPTu pore pressure dissipation test data). These pore water pressures were checked and updated using the results from the seepage analysis summarized in Appendix G.

3.2 Stage 1

The main objective from Stage 1 was to assess the stress distribution in the tailings throughout construction and prior to failure. Examples of the stress distribution calculated in the 2D Mohr-Coulomb and strain-weakening analyses are shown in Figure 9 and Figure 10, respectively. The stress distributions shown on these figures are presented as η/M_{tc}, a parameter termed the mobilized instability ratio in this report. η is the ratio of the deviator stress (q) to the mean effective stress (p') and M_{tc} represents this ratio at the critical state; therefore, a higher value of η/M_{tc} indicates that the stresses are higher relative to the critical state and loose soil is potentially more vulnerable to generating a brittle undrained response if disturbed.

These 2D analyses were run with a single value of ψ of +0.06 for the fine tailings and -0.02 for the coarse tailings, with parameters assigned from these values using the relationships shown in Appendix E. These results show a higher η/M_{tc} beneath the setback at Section 3 compared with the other sections and other regions of the Section 3 dam slope. This is also the area where the first indications of the dam failure were observed in the video (see Appendix D). It was also seen that this stress concentration was higher in the strain-weakening analysis than in the Mohr-Coulomb analysis, indicating that yielding throughout the construction history of the dam would have concentrated stresses in this region.

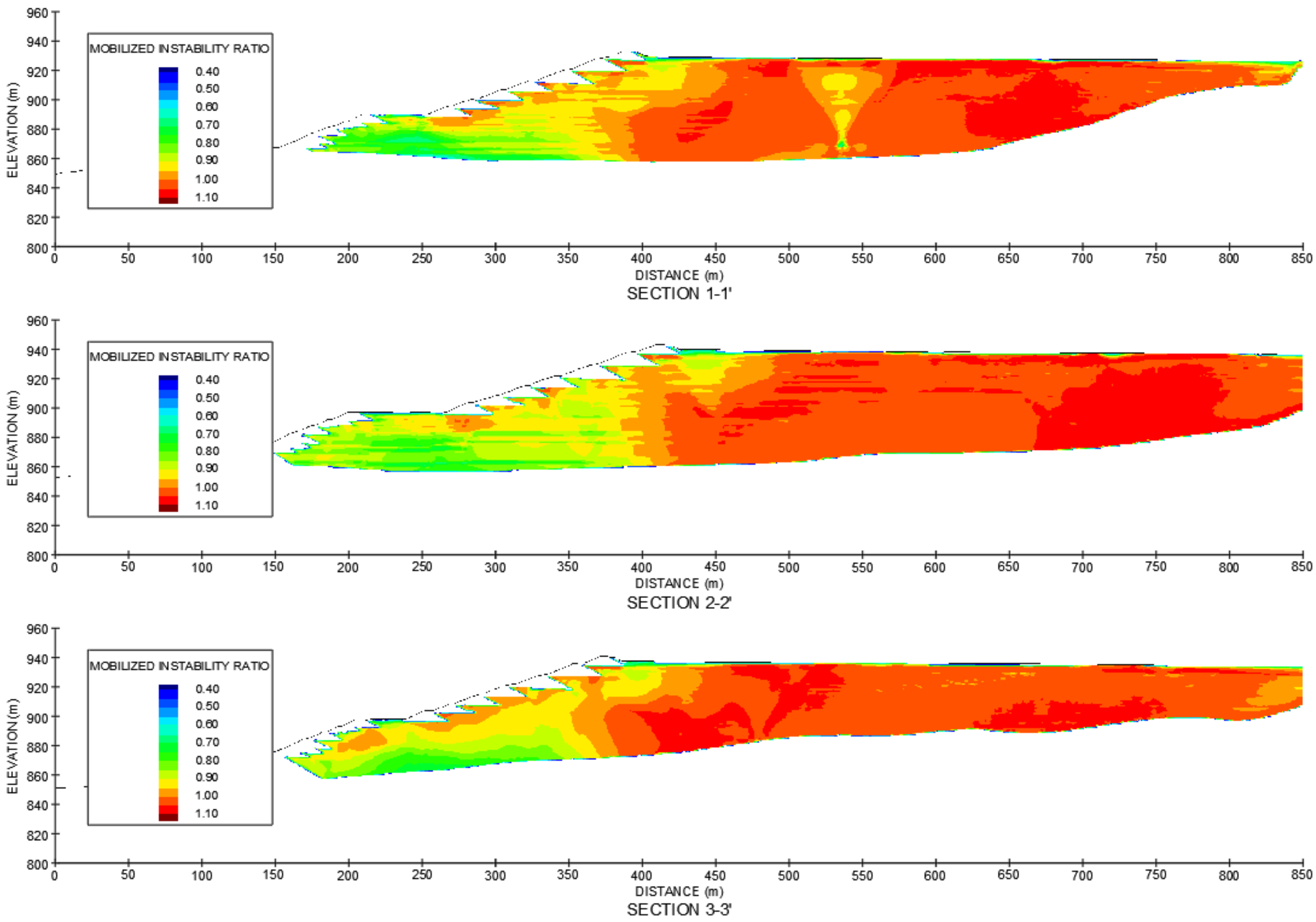

Figure 9: η/M_{tc} at Crest El. 942 m msl (Full Height) – Mohr-Coulomb Analyses

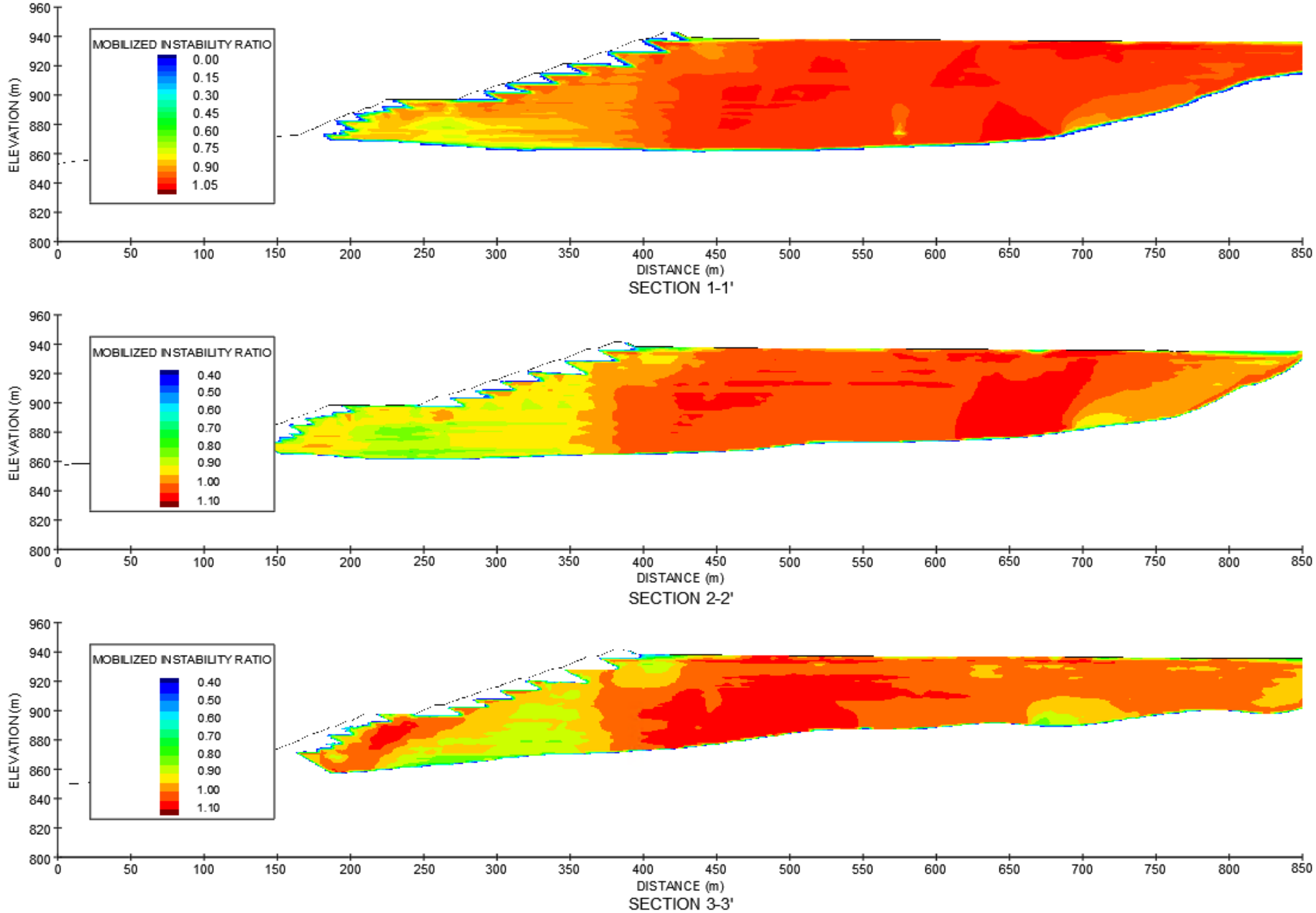

Figure 10: η/M_{tc} at Crest Elevation 942 m (Full Height) – Strain-weakening Analyses

The horizontal displacements from the 2D strain-weakening models are compared in Figure 11. These show that similar magnitudes of displacements were calculated for the three cross-sections; however, the displacements in Section 3 were concentrated closer to the dam face than the other sections. It is these displacements resulting from the steeper slope that created the higher stress ratios in this region.

The simulated displacements in Figure 11 represent the displacements at the end of construction. There are no displacement records from most of the construction history against which to compare these; however, it is known that no localized or widespread instability was recorded during the construction period of the dam, suggesting that any displacements would have been modest. These results show a maximum horizontal displacement in the order of roughly 0.5 m towards the toe of the dam and very little in the upper slope which is consistent with the inferred observation that displacements were generally minor. The InSAR analyses (Appendix D) indicated horizontal displacements in the toe region of around 10mm/year with some areas higher for the 1-year period prior to failure.

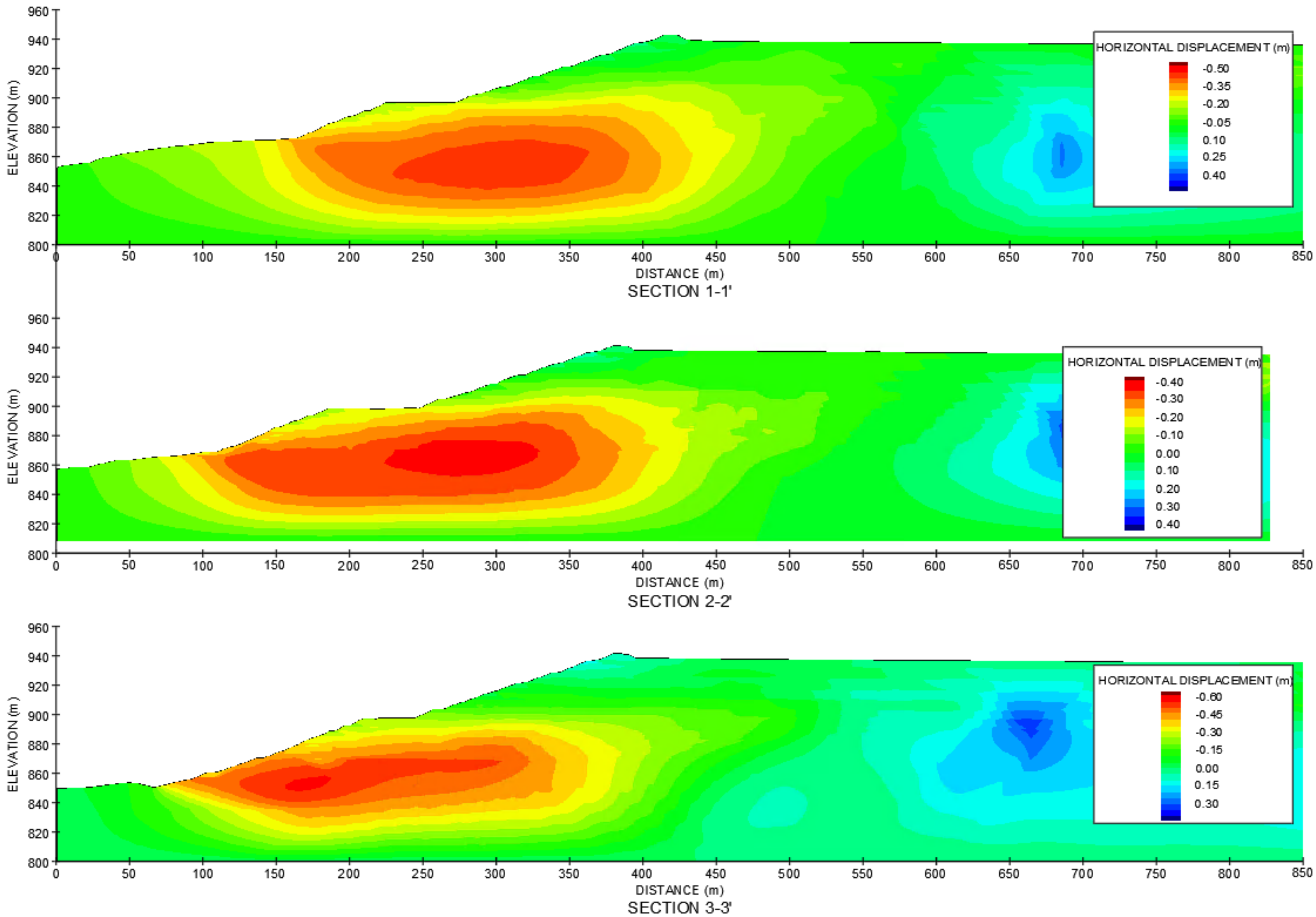

Figure 11: Horizontal Displacements (in Cross-sections 1-1, 2-2 and 3-3) at the End of Construction – 2D Strain-weakening Models

The results of the 3D analysis were consistent with these 2D results and showed an accumulation of shear stress and displacement in the region of Section 3 (see Figure 12).

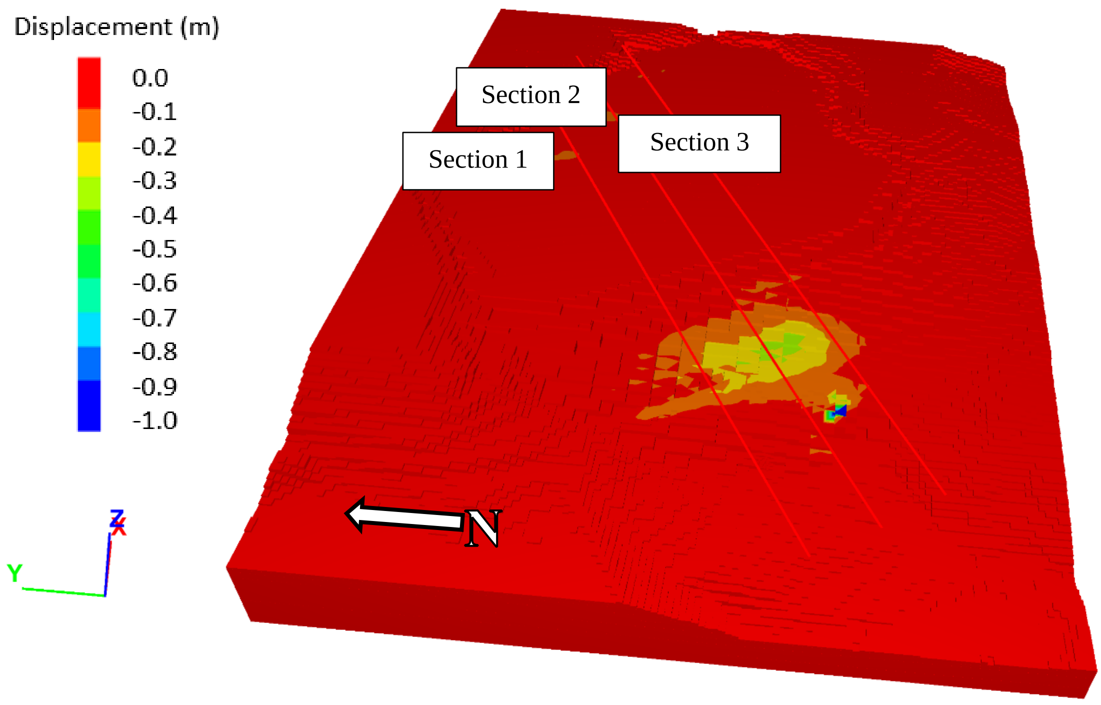

Figure 12: Oblique View of 3D Model at End of Construction Showing Horizontal Displacements Concentrating in Region of Section 3

3.3 Stage 2

3.3.1 Approach used to Test Liquefaction Triggers

As discussed in Section 2.2, the purpose of these Stage 2 analyses was to test the effect of various liquefaction triggers on the models that had a marginal factor of safety against liquefaction triggering. The triggers assessed were:

- Liquefaction in the region surrounding the borehole being drilled on the day of the failure (SM-13);
- Liquefaction in the region surrounding a DHP that was drilled in 2018 (DHP-15). This was considered an unlikely trigger because DHP-15 was completed roughly seven months before the failure but was included to capture the possible effects of any potential weakening mechanisms that may have developed during or following installation;
- Liquefaction in the regions surrounding springs that existed on the right abutment prior to the dam construction, potentially resulting from an influx of water from the surrounding

terrain. This was treated as a localized event in the analysis because the piezometers in the dam did not identify a trend of increasing pore pressure before the failure; and

- Strength loss associated with a loss of suction in the unsaturated zone (tailings and containment berms above the water table) of the dam resulting from rainfall infiltration.

The methodology for this stage was outlined in Section 2.2 and initially involved establishing the FS against liquefaction triggering by completing SSR calculations in which the peak strength of the saturated coarse and fine tailings was progressively reduced until widespread strength loss and displacements occurred in the model. The ratio of the strength assigned to the tailings versus the strength at which instability occurred is the FS.

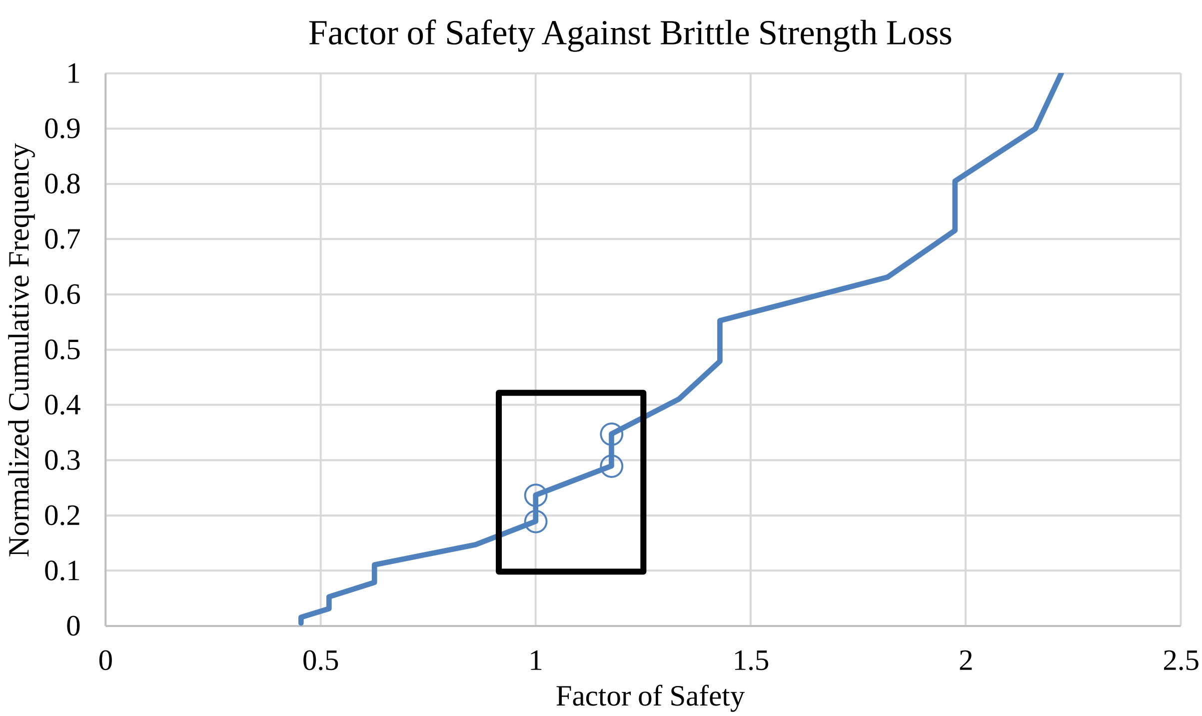

Figure 13: FS Against Liquefaction Triggering (i.e., Brittle Strength Loss) and Selection of Representative Models

This stage of the analysis showed that the FS against liquefaction triggering could range between 0.5 and 2.2, depending on the spatial distribution of ψ. Since the intent of this analysis was to assess the effect of liquefaction triggers on models of the dam with a marginal stability, a subset of four of these models was selected for further assessment. These models were referred to as the representative models and are identified with a black outline in Figure 13. The representative models had FS values between 1 and 1.16. The peak undrained strength in the models with a FS > 1 were reduced to achieve a FS of 1 before testing liquefaction triggers.

The pattern of displacements at failure in these analyses was consistent with the observations of the failure from the video (see Appendix D) and with those of subsequent conventional FS calculations (see Section 3.5.2). An example of the displacements during failure from one of the analyses is shown in Figure 14.

These displacements were used to confirm that the resulting failure would occur in the correct location and to identify a suitable monitoring location for assessing the displacements resulting from the liquefaction triggering analyses. After reviewing this pattern of displacements, a point on the dam slope was selected to be monitored throughout the triggering analyses. It was important to monitor displacements in this region specifically because the intent of this analysis was not only to determine if the triggers would cause failure of the dam, but that they would cause failure in the location in which it was observed to occur.

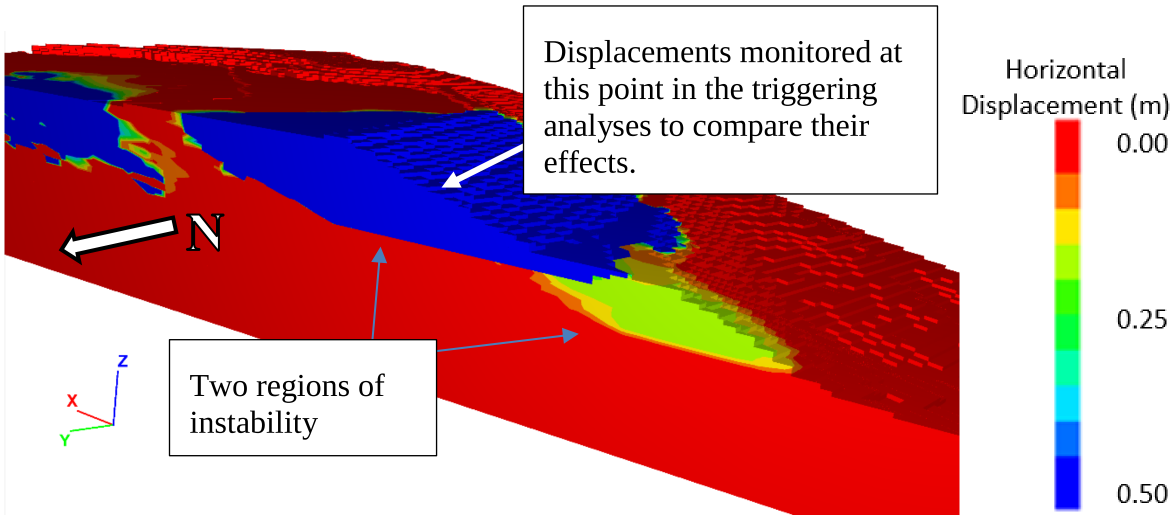

Figure 14: Patterns of Displacement Developed as Instability Occurred in Strength Reduction Analyses on Peak Strength of Saturated Tailings

As described in Section 2.2, a further test was completed on these representative models prior to testing liquefaction triggering mechanisms. This test involved assessing whether the dam in this condition of FS = 1 could resist previous events that occurred at Dam I and did not cause failure of the dam. One of the events used in this test was the drilling of borehole SM-09, which was drilled in December 2018 to January 2019 on the same bench as borehole SM-13. The other event was the water pressure at the end of DHP-15 during installation, which was observed to cause disturbance of the slope during drilling but did not cause the dam to fail. Disturbance from borehole SM-09 was simulated by assuming an extreme condition in which liquefaction was assumed to occur around the depth of this borehole. This condition involved assigning a post-liquefaction strength ratio ($S_{u\text{-liq}}/p'$) of 0.01 to all zones of the model beneath the water table within a 1-m radius of the borehole. Disturbance from DHP-15 was assessed by assigning water pressures of 600 kPa and 1000 kPa at the end of the DHP location. Despite these models having a marginal FS prior to these tests, the dam did not fail in the representative models from these events. This confirmed their suitability for use in testing the other triggering mechanisms. Results from the analysis of SM-09 were similar to those of the later assessment of SM-13 (see Figure 19).

Having identified the models to use in testing the effect of potential liquefaction triggers and the point on the dam slope to monitor their effects, the triggers discussed above were assessed as follows:

- The borehole (SM-13) and deep horizontal drain (DHP-15) were both assessed by setting all zones within a 1-m radius of the borehole or DHP to a liquefied strength. A strength ratio ($S_{u\text{-liq}}/p'$) of 0.01 was used in this analysis.
    - The location of SM-13 is shown in Figure 15. It was necessary to reduce the size of the analysis mesh around this location and to gradually increase it away from the borehole) to capture this local event. This reduced mesh size is shown in Figure 16.
    - The location of DHP-15 is shown in Figure 17. The mesh size was also reduced around this location.
- The assessment of liquefaction associated with an influx of water from the springs was modeled in the same way as the effect of the borehole and DHP, but in this case the zone of liquefaction was assumed to extend to the coarse and fine tailings within a 50-m radius of the spring locations. These 50-m radius regions are shown in Figure 18.
- The assessment of a loss of suction in the unsaturated zone was simulated by calculating the mobilized strength of the zones above the water table from the friction angle and effective confining stress, reducing it by an amount equal to the loss of suction and then reassigning this reduced strength to the zones. Three model revisions were completed with strength losses of 5 kPa, 10 kPa and 15 kPa to bound the range identified in the seepage analyses (see Appendix G).

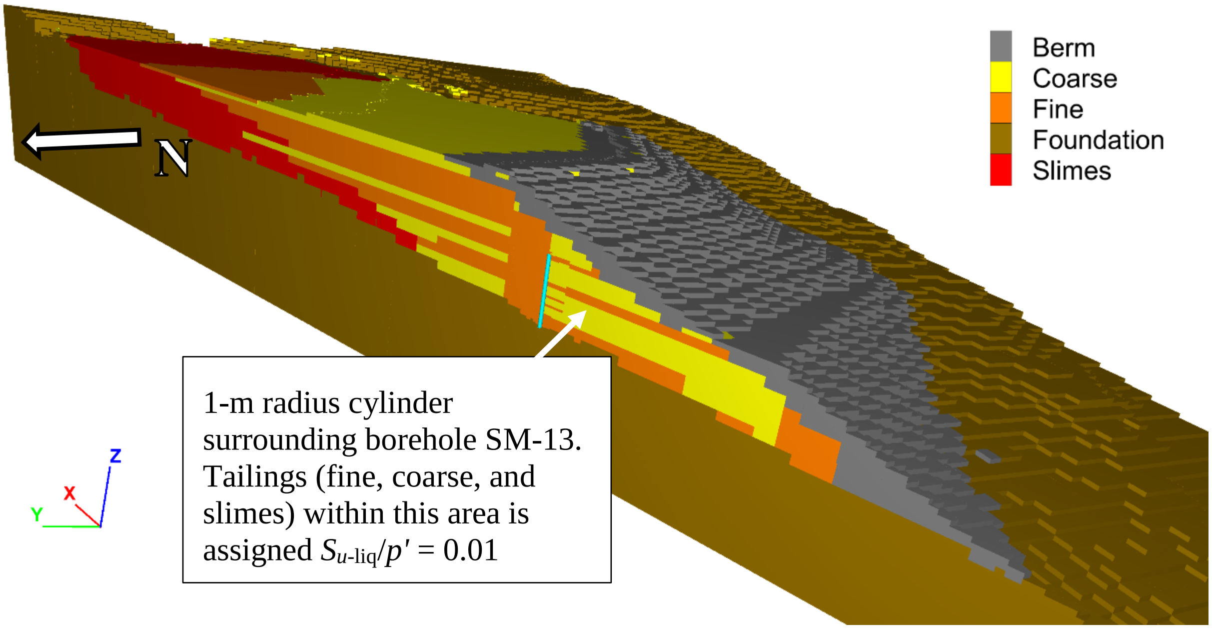

Figure 15: Liquefaction Triggering Mechanism – Borehole SM-13

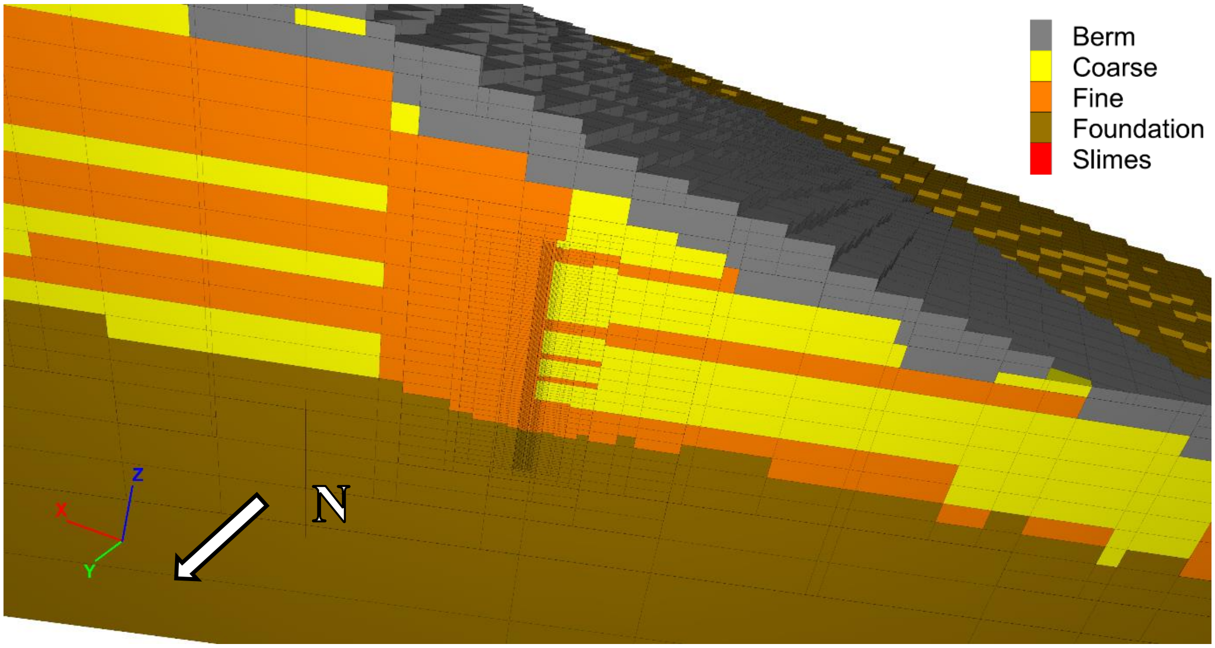

Figure 16: Reduced Mesh Size Around Borehole SM-13

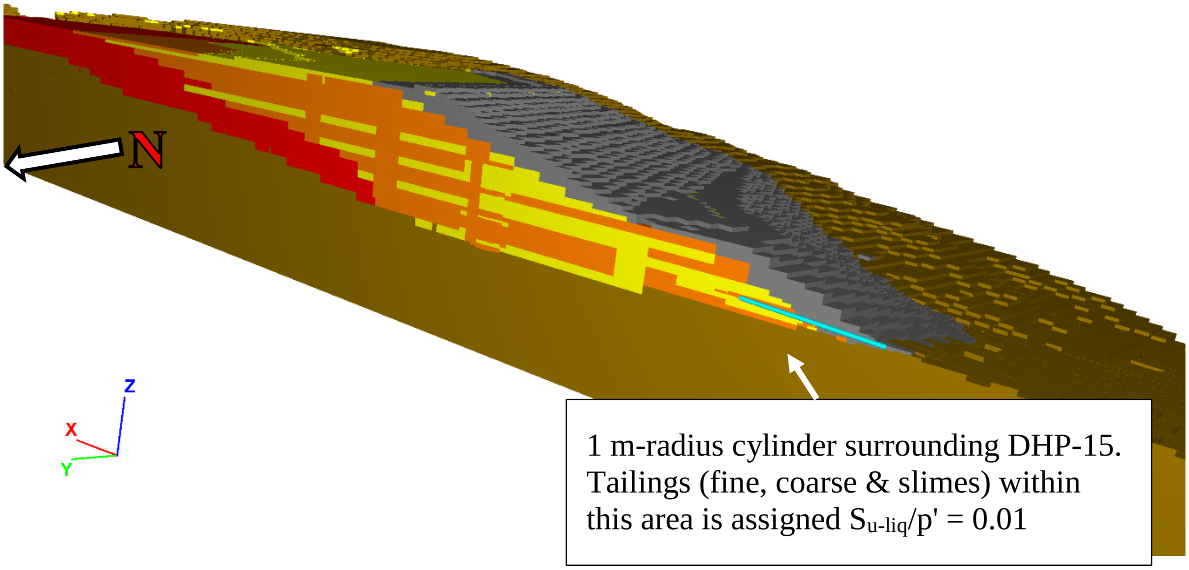

Figure 17: Liquefaction Triggering Mechanism – Deep Horizontal Drain

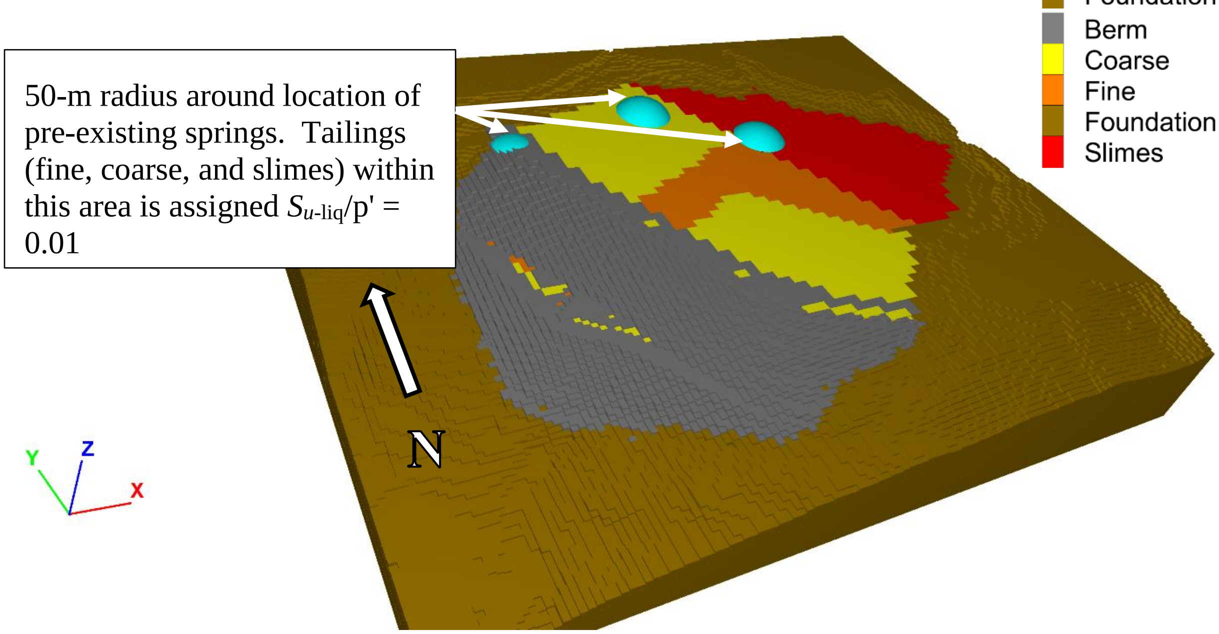

Figure 18: Liquefaction Triggering Mechanism – Springs

3.3.2 Results

The results of the Stage 2 analyses are:

- Liquefaction surrounding borehole SM-13 had very little effect on the dam. Displacements on the dam slope were typically < 1 cm. An example of the displacement patterns resulting from this trigger is shown in Figure 19.

- Liquefaction surrounding DHP-15 had a more significant effect than borehole SM-13 and caused displacements up to around 1 cm at the toe of the dam; however, the displacements associated with liquefaction around DHP-15 were localized to the region of the dam close to the DHP, and it had very little effect on the dam in the region where failure actually occurred. An example of the displacement patterns resulting from this trigger is shown in Figure 20. The calculated displacements are very similar to those detected by the ground-based radar at the time of DHP 15.

- Liquefaction around the pre-existing springs caused extensive displacements near the spring locations but did not have a significant effect in the region where the dam failure occurred. An example of the displacement patterns resulting from this trigger is shown in Figure 21.

- It was found that a strength reduction due to a loss of suction in the unsaturated zone would cause displacements in the region where the dam failure occurred. These displacements increased proportionally with increasing strength reductions. The displacement values ranged from a minimum of 4 cm to a maximum of 22 cm when 5 kPa to 15 kPa of strength reduction was applied. Example displacement patterns resulting from this trigger are shown in Figure 22 through Figure 24.

The results from all the representative models are summarized in Figure 25.

Whilst none of the triggers assessed in these Stage 2 analyses were found to cause failure of the dam, a 15 kPa strength reduction due to loss of suction in the unsaturated zone from rainfall infiltration was found to have the greatest impact in the region where the failure occurred. As a result, this loss of suction was considered to have potentially contributed to the failure. This led to this mechanism being selected for further evaluation in the Stage 3 analyses.

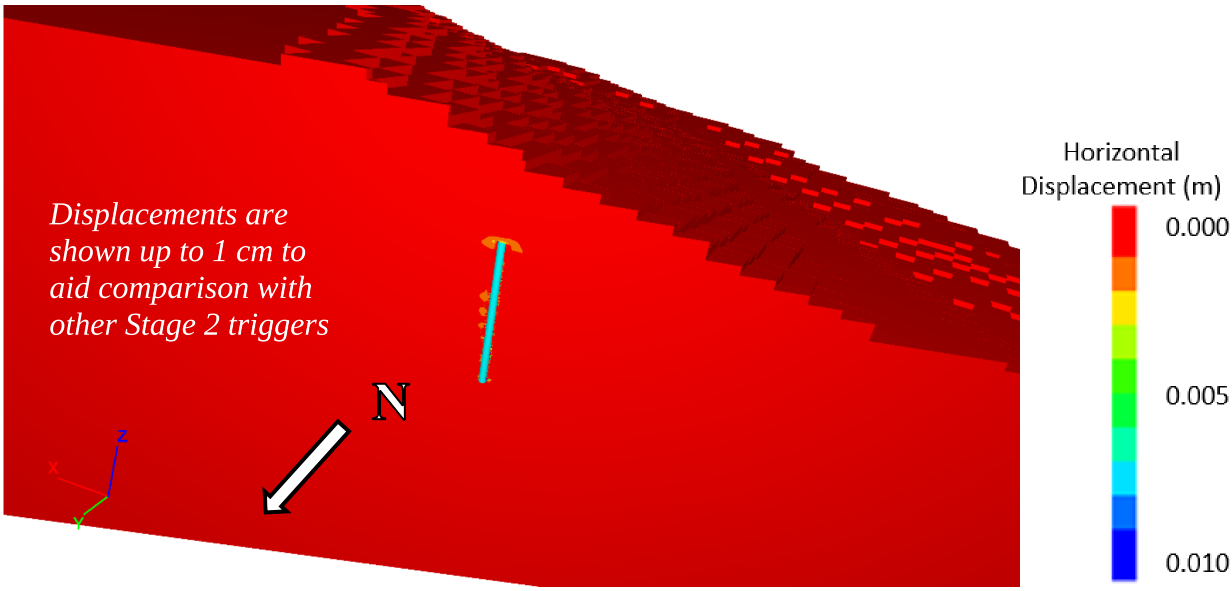

Figure 19: Horizontal Displacements Associated with Liquefaction in a 1-m Radius Surrounding Borehole SM-13

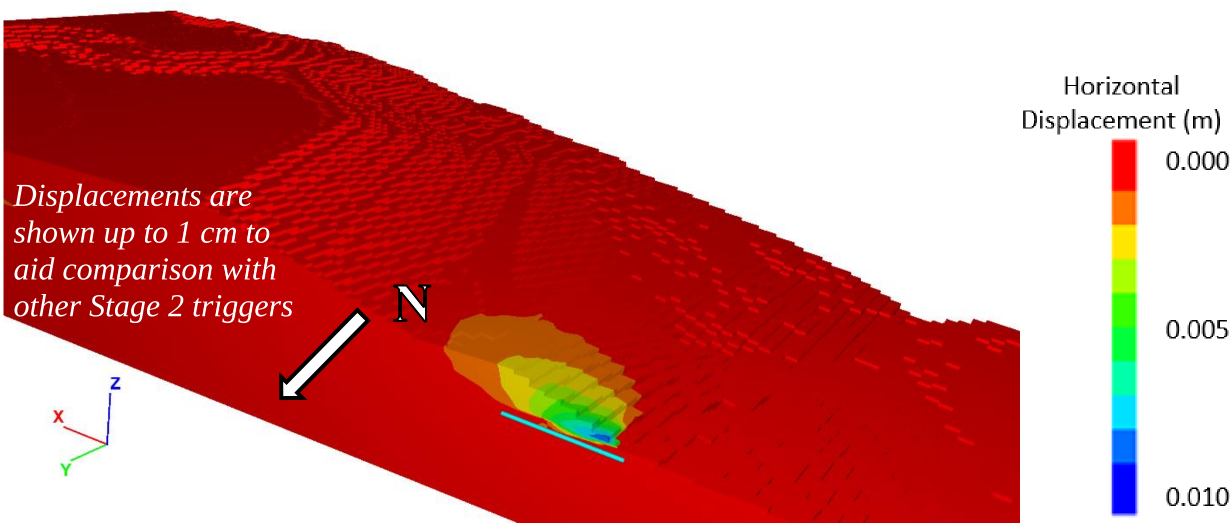

Figure 20: Horizontal Displacements Associated with Liquefaction in a 1-m Radius Surrounding DHP-15

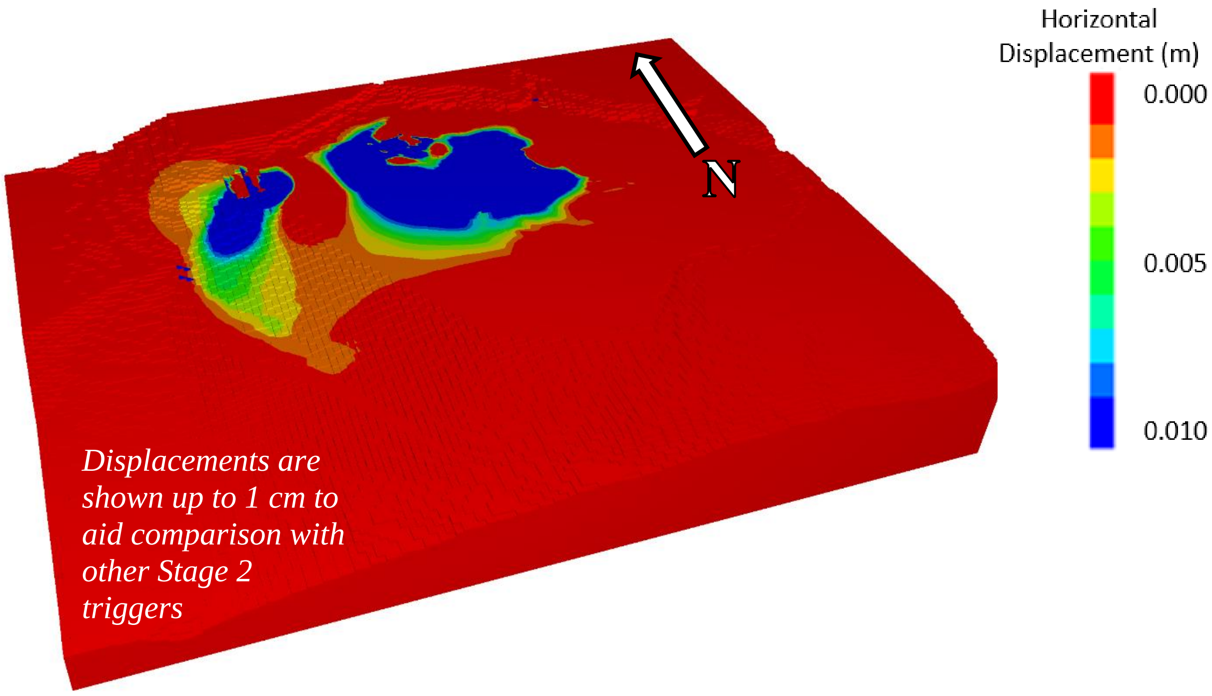

Figure 21: Oblique View of Horizontal Displacements Associated with Liquefaction in a 50-m Radius Surrounding the Locations of Pre-Existing Springs

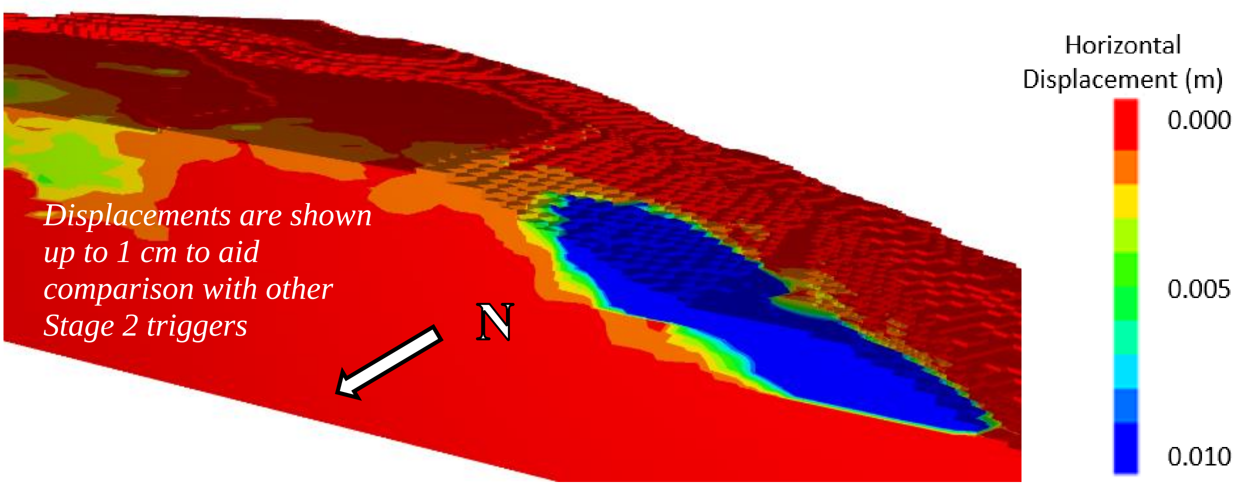

Figure 22: Section View of Horizontal Displacements Associated with a Strength Reduction of 5 kPa in the Unsaturated Zone

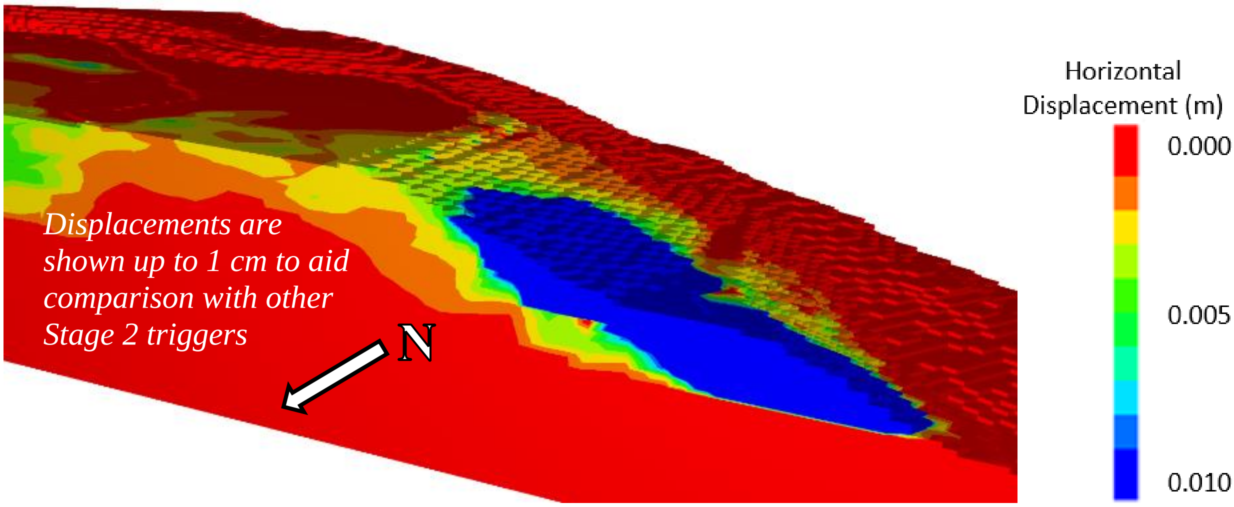

Figure 23: Section View of Horizontal Displacements Associated with a Strength Reduction of 10 kPa in the Unsaturated Zone

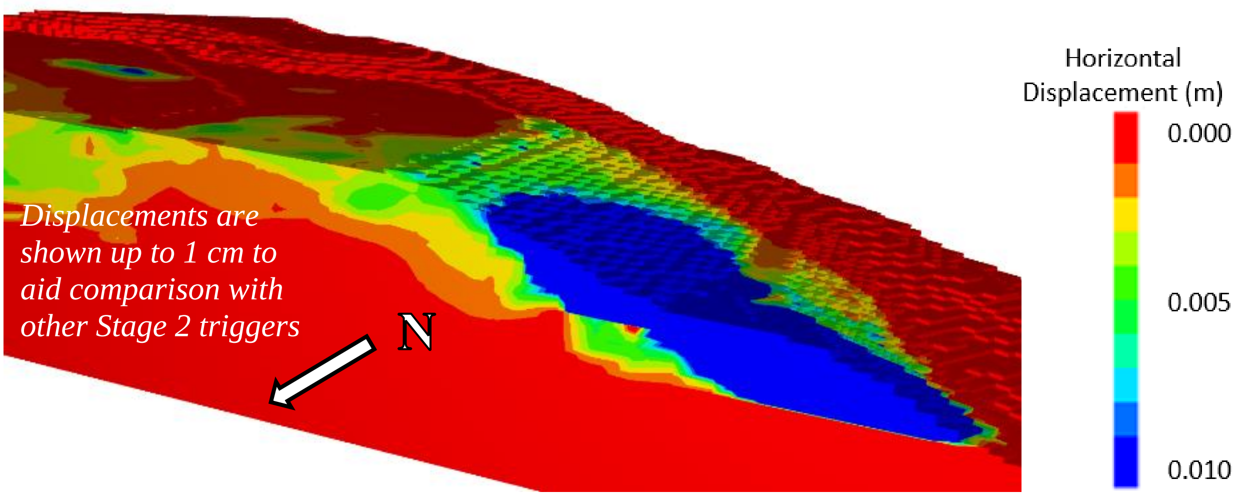

Figure 24: Section View of Horizontal Displacements Associated with a Strength Reduction of 15 kPa in the Unsaturated Zone

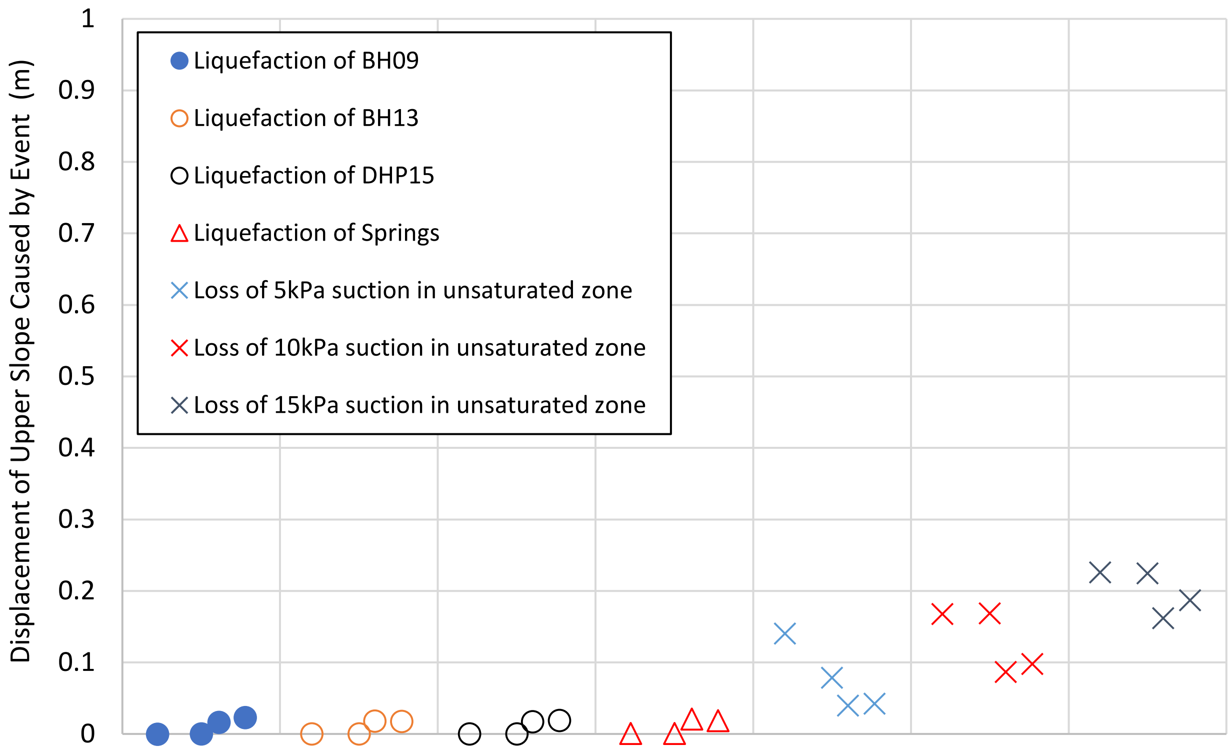

Figure 25: Displacements Caused by the Stage 2 Triggers on Representative Models

3.4 Stage 3

3.4.1 Methodology – Wedage et al. (1998)

As described in Section 2.3, the final stage in this assessment involved assessing the potential impact of ongoing strains within the dam. The reasons for considering this mechanism were:

- Small (up to 35 mm) displacements were identified in the InSAR data for the year prior to failure;
- The laboratory testing had shown that bonding in the tailings led to a higher strength than typical but also caused the samples to lose strength at low strains; and
- Laboratory testing found that strains in samples of loose tailings continued to accumulate at a constant deviator stress within the range of stress ratios identified in the Stage 1 modeling.

A method for simulating time-dependant displacements was developed by Wedage et. al. (1998). This method involves adjusting the shear strength of a material based on the shear strain rate and it has been applied previously to ongoing displacements in the foundation soil beneath tailings dams. The parameters for this method were modified for application to the Dam I tailings, and it was implemented using a subroutine in FLAC3D. The parameters for this method were determined by calibration to the strain accumulated under constant shear stress in triaxial test TXDW03, and the results of this calibration are shown in Figure 26. This calibration focused on the results at K_0 = 0.4 because the deformation analyses, including the later slope stability calculations (see Section 3.5.2) suggested the stresses in the dam slope were typically in this range. The results matched well to the displacements observed at K_0 = 0.4 and matched the observation that the sample failed between K_0 = 0.4 and K_0 = 0.3. The results slightly overpredicted the displacements at K_0 = 0.5 but matched the overall trend of reducing strain accumulation with increasing K_0.

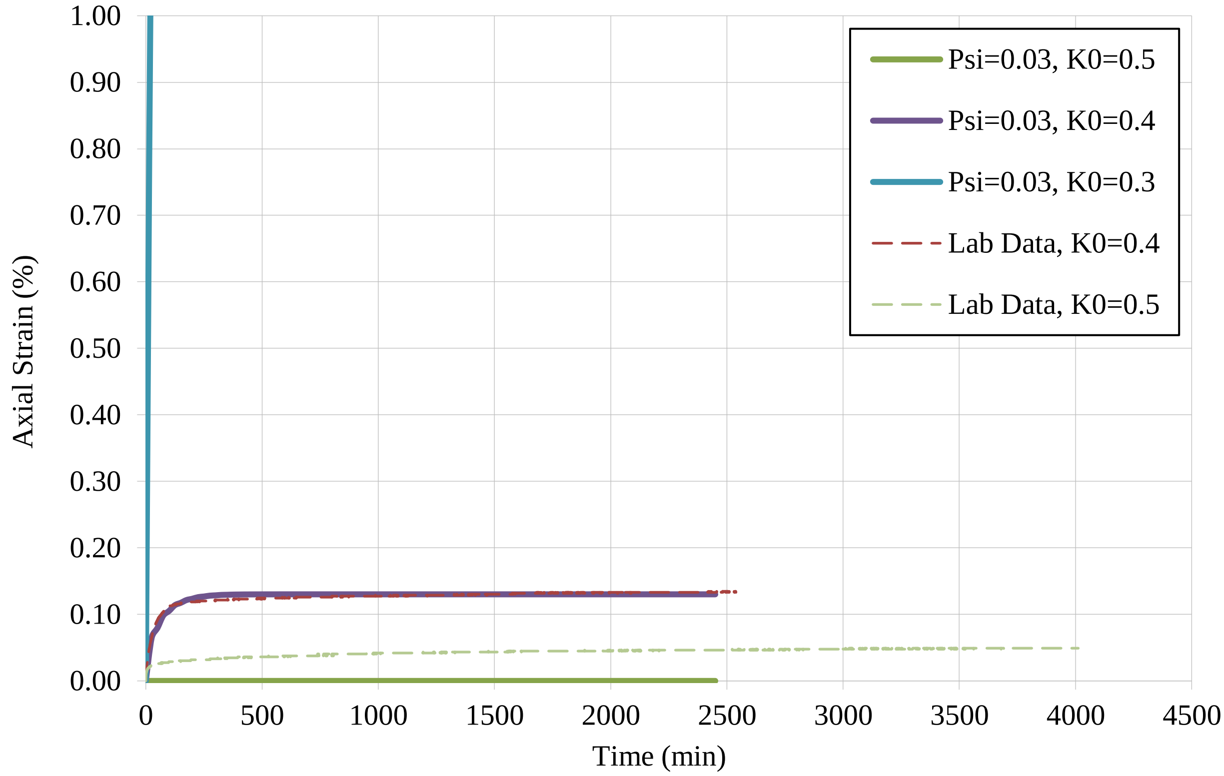

Figure 26: Calibration of the Wedage (1998) Model Parameters to Creep Test TXDW03. ψ of this test was +0.03

After calibration, this creep mechanism was applied in the representative 3D models to all coarse and fine tailings with a ψ > 0. This creep mechanism was applied sequentially, and the stability of the dam was tested after each increment of creep. The method used for this involved enabling the creep mechanism until 1 cm of displacement had developed at the monitoring location used in the Stage 2 analyses (see Figure 14); the creep mechanism was then disabled and the model analysis was solved to see if the dam was stable; if the dam was still stable, the analysis was repeated with 2 cm of creep. This process was continued until the amount of creep required to cause dam instability was determined. It should be noted, that the 1 cm increments of creep were monitored at a specific location on the face of the dam; therefore, whilst 1 cm of creep was measured at this location, greater displacements occurred in other areas of the dam. This is illustrated later.

Three variants of this process were completed:

- Variant 1: Creep only. This is the process described above.
- Variant 2: Creep combined with a loss of suction in the unsaturated zone. In this case, a 15 kPa strength loss was applied to the unsaturated zone at the end of the increment of creep.
- Variant 3: Creep combined with liquefaction of borehole SM-13. In this case, liquefaction surrounding SM-13 was applied in the manner described in Section 3.3.1 at the end of the increment of creep.

3.4.2 Results

The results are summarized in Figure 27. These results show that without the addition of a 15 kPa strength reduction in the unsaturated zone, between 8 cm and 37 cm of creep displacement recorded on the face of the dam would cause failure of the dam. This reduces to 1 cm if the 15 kPa strength loss in the unsaturated zone is included in the analysis. When the effect of borehole SM-13 is included in the analysis, the creep displacements required to cause failure of the dam are unchanged from those without the borehole, further supporting the Stage 2 observation that any localized liquefaction around the borehole would not have a significant impact on the stability of the dam.

As discussed in Section 2.3, the total displacement measured by InSAR in the year prior to failure was 3.5 cm, suggesting that the dam could have accumulated creep in the order of 10 cm to 15 cm over the 2.5 years since tailings deposition ceased; however, the InSAR displacement was dominantly vertical, suggesting that horizontal displacements in the order of 5 cm would be a reasonable maximum estimate for the amount of creep displacement in the 2.5 years after operations ceased. These results show that one of the four representative models would fail close to this amount of creep displacement without the inclusion of a loss of suction in the unsaturated zone and that the addition of the loss of suction causes failure to occur in all models within this range of displacements.

The pattern of displacements that developed from the creep mechanism are shown in Figure 28 through 31. This shows that the creep mechanism developed displacements that were dominantly vertical/roughly parallel with the face of the dam throughout most of the slope and shifting to more horizontal towards the base. This reflects the pattern suggested by the InSAR data; however, the displacement magnitudes when creep is combined with a loss of suction (Figure 29) align more closely with those of the InSAR data. Overall, it was found that displacements significantly greater than those of the InSAR data would be required for creep to cause dam failure on its own, but that this would reduce to very little displacement, consistent with the InSAR data, when creep was combined with loss of strength in the unsaturated zone. The models with creep combined with a 15 kPa loss of suction in the unsaturated zone were, therefore, considered the most representative of the failure. "Failure" in the models was defined as large displacements (>1 m) in the region where the failure actually occurred, and an inability of the model to reach an equilibrium state.

The strain prior to the onset of failure for the creep model with a 15 kPa strength reduction in the unsaturated zone due to suction was around 0.5%. This is consistent with the laboratory test results (see Appendix E) that showed that failure could initiate at shear strains of < 1% and the field observations in which significant displacements were not observed prior to failure.

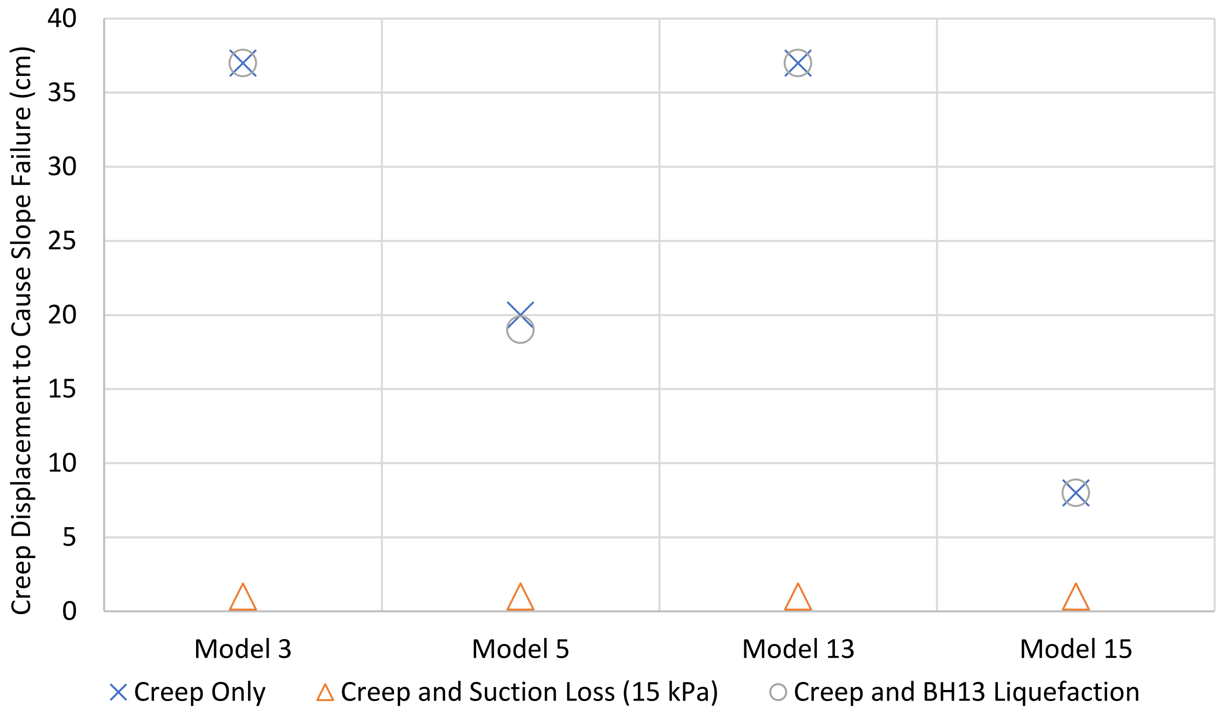

Figure 27: Creep Displacement Required to Cause Dam Failure in the Representative 3D Models

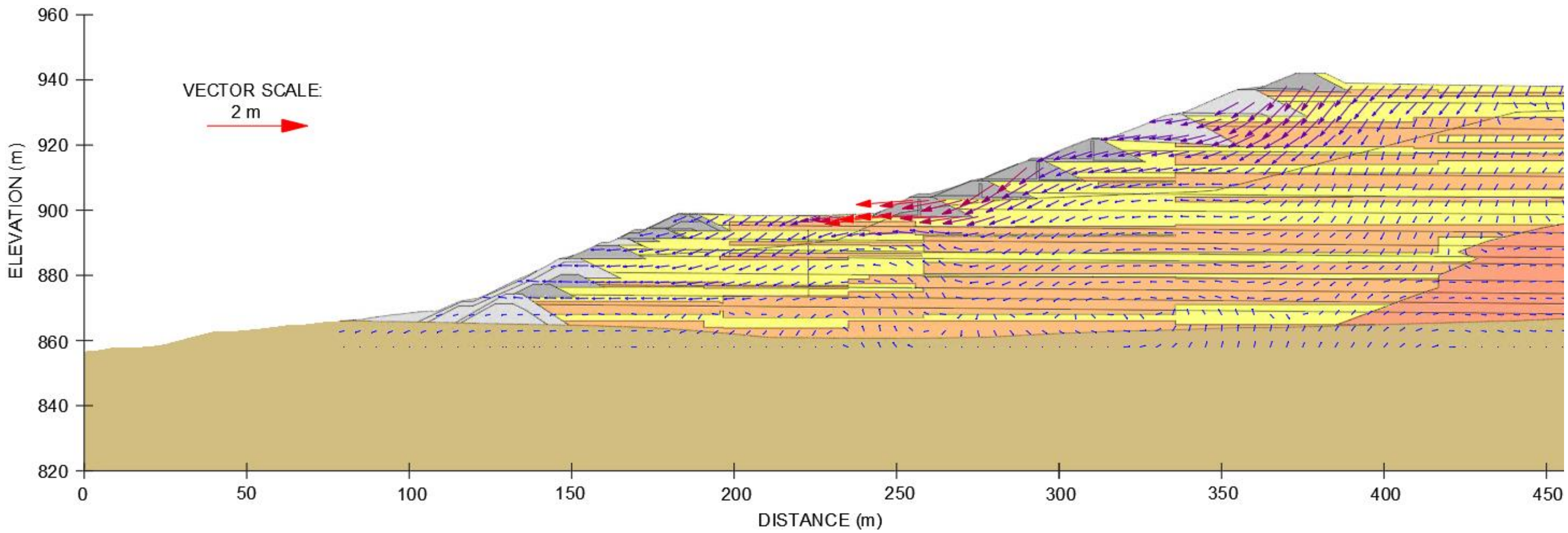

Figure 28: Example Illustration of Displacement Vectors at the End of Creep Displacement – Variant 1: Creep Only

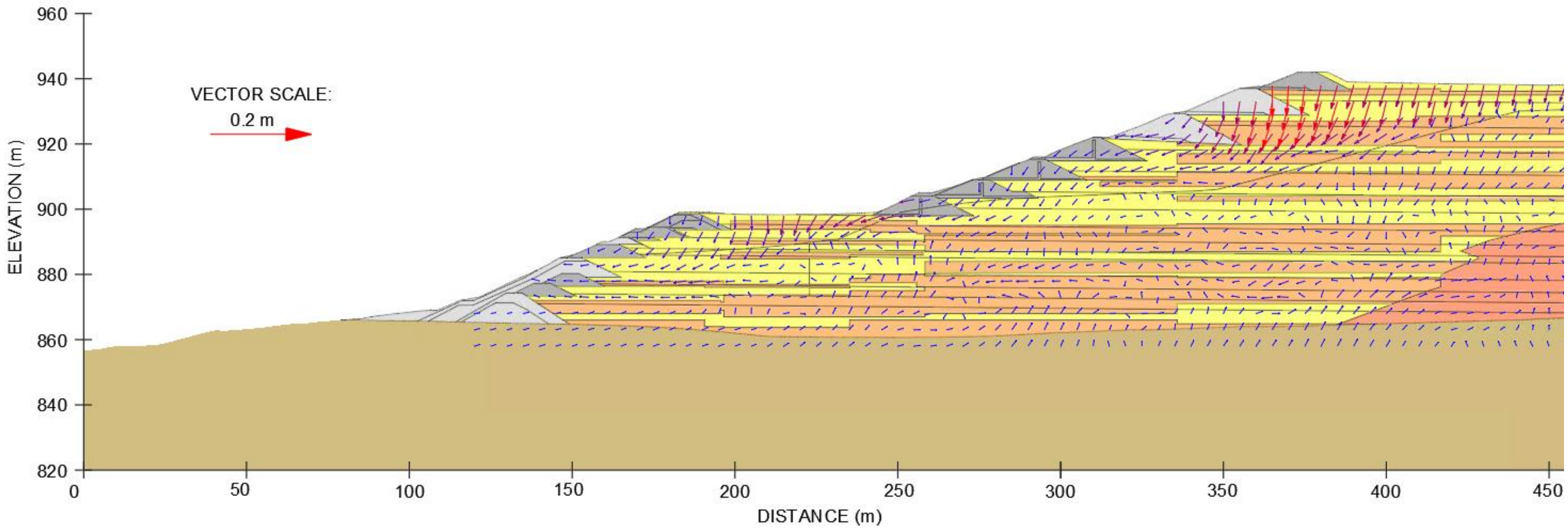

Figure 29: Example Illustration of Displacement Vectors at the End of Creep Displacement – Variant 2: Creep and Loss of Suction

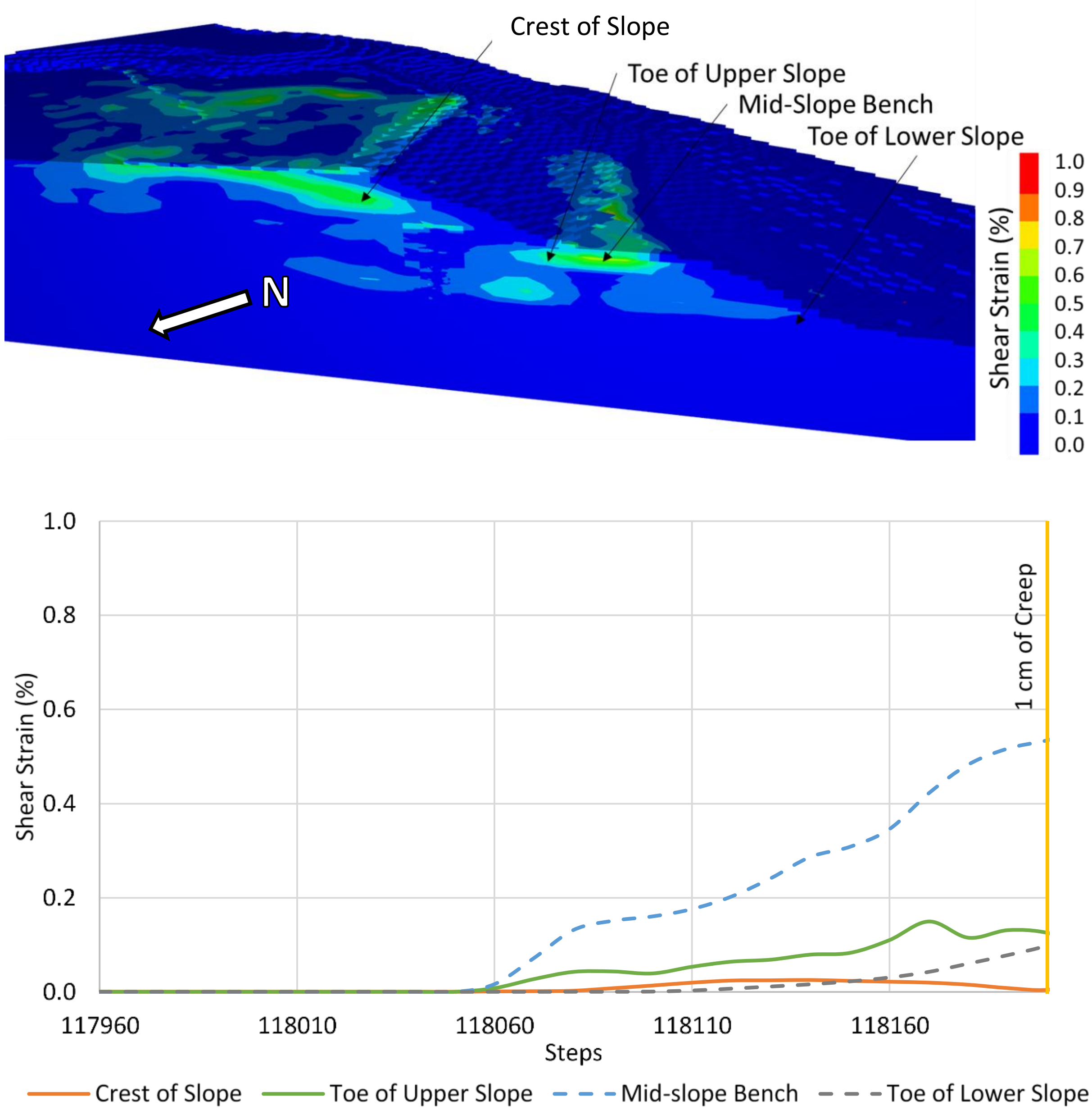

Figure 30: Development of Creep Strain within the Dam – Variant 2: Creep and Loss of Suction

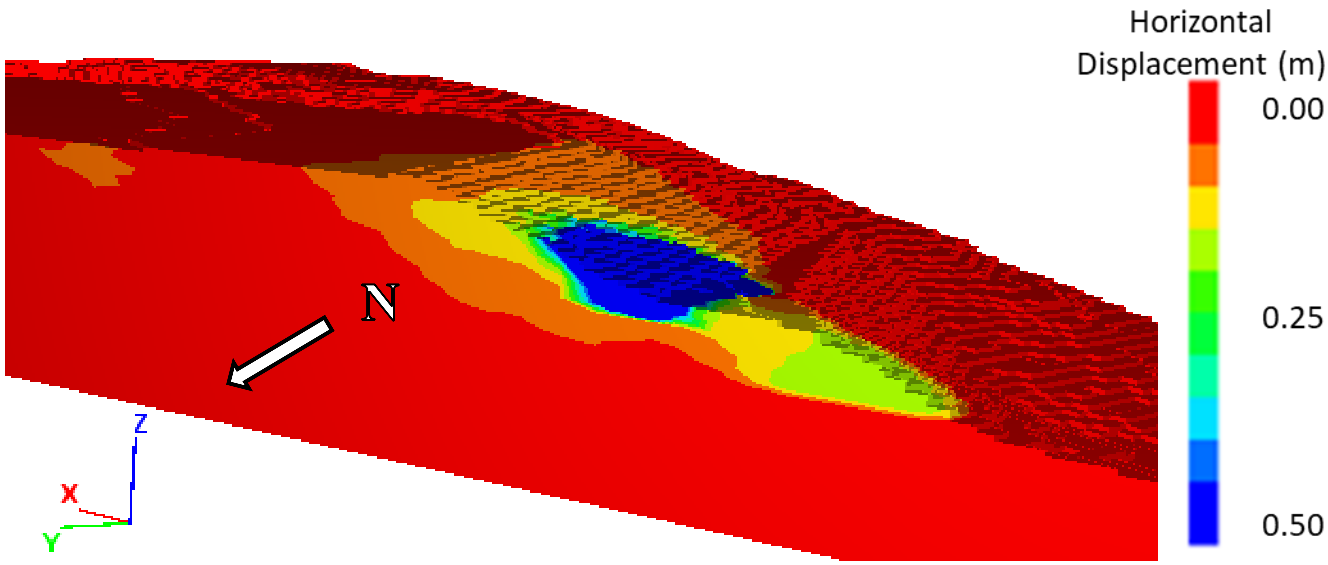

Figure 31: Dam Failure Developing from Creep Displacements - Variant 2: Creep and Loss of Suction

3.5 Supplementary Analyses

3.5.1 Factor of Safety – FLAC3D – Peak Strengths

Conventional FS calculations were completed on the 3D model using a standard SSR analysis. The purpose of this was to calculate the conventional FS of the dam using the peak undrained shear strength and standard methods of analysis for comparison with the low FS against liquefaction calculated earlier (see Section 3.3). This analysis was completed on the representative models that had a FS against liquefaction triggering of 1.

This analysis involved changing the constitutive model of the tailings from strain-weakening to Mohr-Coulomb and then assigning the peak undrained shear strengths based on the ψ, as described previously. The conventional FS from this analysis was 1.5. The displacement patterns associated with this FS are shown in Figure 32, which illustrate the development of two “slip surfaces”: one through the upper slope and one through the slope below the plateau. This reflects the observations from the video analysis that showed failure occurring in both of these regions.

After completing this FS calculation using the stochastic distribution of undrained strength, a second series of analyses was completed in which a single undrained strength ratio (S_u/p') was assigned to the coarse and fine tailings. The purpose of this step was to identify a representative value of S_u/p' for the tailings. This was repeated for different S_u/p' values until the FS from Step 1 was determined. It was found from this that an S_u/p' of 0.59, equal to the 33rd percentile of the variable strengths, led to a FS equal to that with the stochastic distribution of strengths. These results are shown in Figure 33.

Having identified the equivalent strength ratio in terms of S_u/p', the analysis was repeated using a strength ratio defined by S_u/σ'_v. The purpose of this was to determine a representative strength that could be used in LEM calculations, and the strengths in those analyses are commonly defined using S_u/σ'_v. It was found that a S_u/σ'_v of 0.37 would lead to a FS equivalent to that of the variable undrained strength (see Figure 33). This can be related to S_u/p' through the following equation: $S_u/\sigma'_v = [(1+2K_0)/3] \times S_u/p'$. The difference between the S_u/p' and S_u/σ'_v calculations implies an average K_0 of 0.45 was operative throughout the dam slope in the region of the failure.

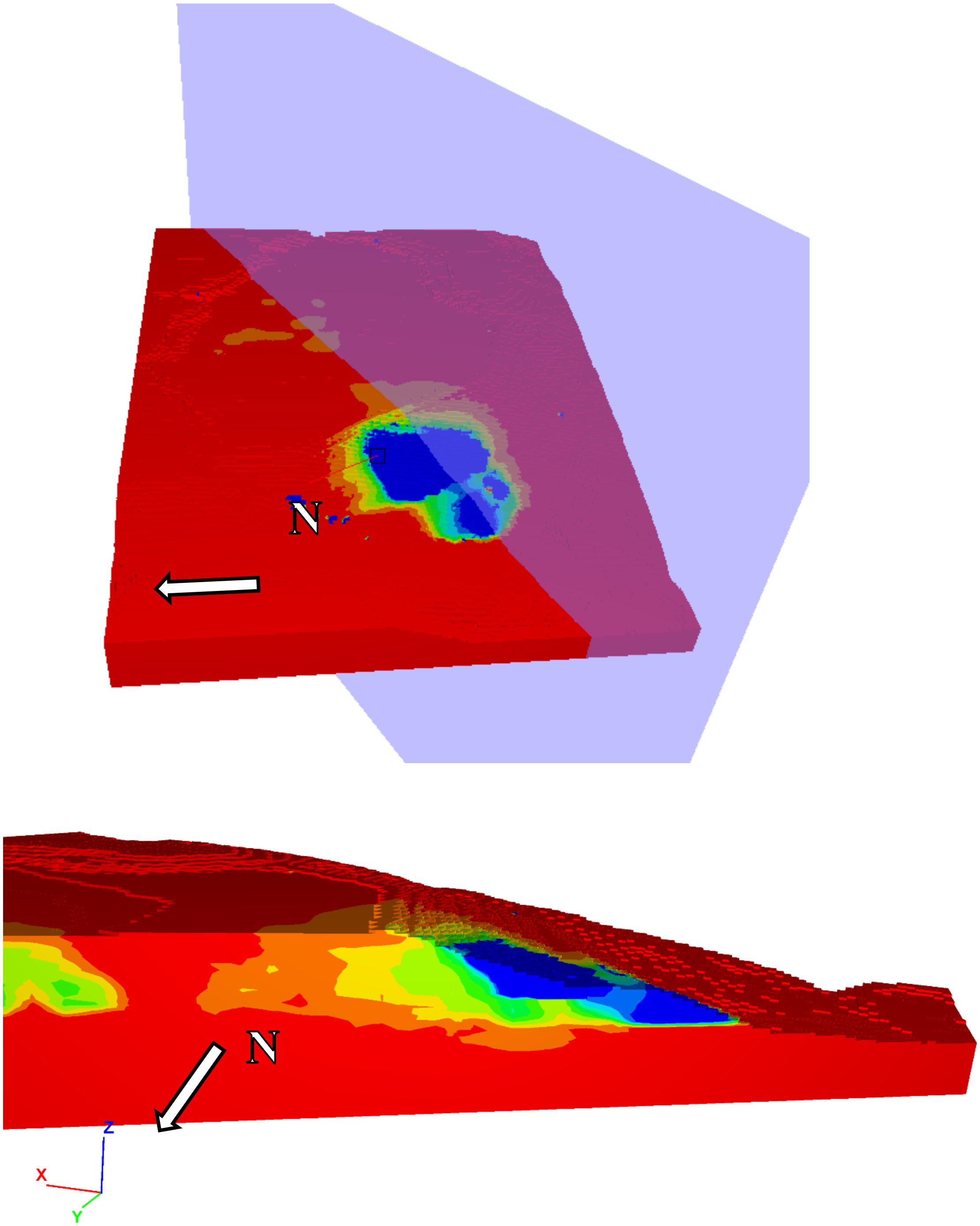

*Factor of Safety = **1.5** – Peak Undrained Strengths, Variable State Parameter*

Figure 32: Displacement Pattern Illustrating the "Slip Surface" Calculated in the Strength Reduction Stability Analysis

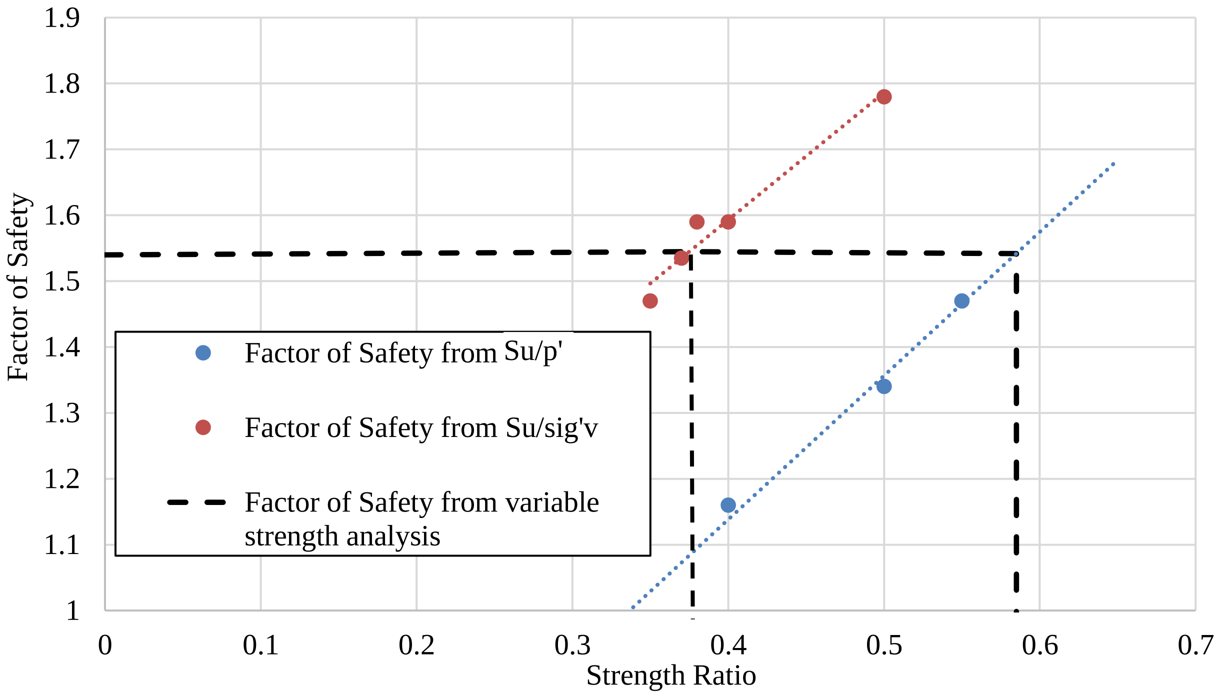

Figure 33: Determination of Equivalent Uniform Strength to the Variable Undrained Strength Analysis

3.5.2 Factor of Safety – Limit Equilibrium – Peak Undrained Strength

The undrained strength ratio of $S_u/\sigma'_v = 0.37$ was used in 2D LEM analyses to calculate: (i) how the LEM FS would have varied throughout the history of Dam I; (ii) how it varied across the analysis sections; and (iii) how it varied at different locations on each cross section. Calculations were made for each construction stage on Sections 1, 2, and 3. The LEM FS was calculated for a slip surface going: (i) from the dam crest to the dam toe; (ii) from the crest to the plateau; and (iii) from the plateau to the dam toe.

The results from the dam crest to the dam toe at the full dam height are shown in Figure 34 through Figure 36. These results showed the LEM FS for this slip surface ranged between 1.5 and 1.6 for the conditions prior to failure. Results for an intermediate dam construction stage when the Dam I crest elevation was 916.5 m msl are shown in Figure 37 through Figure 39. The trend of LEM FS for this slip surface versus dam crest elevation is shown in Figure 40, which shows a similar value throughout the history of construction once the dam crest elevation was above 905 m. This corresponds to the elevation when the crest was raised above the setback.

Figures showing all LEM FS results are shown in Annex 2.

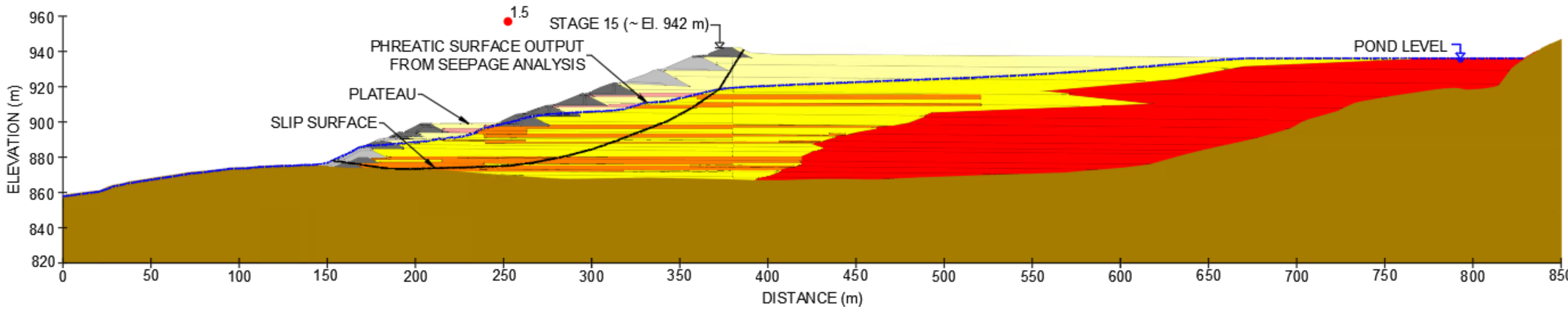

Figure 34: 2D Limit Equilibrium Analysis Result – Cross-section 1-1', El. 942 m msl (Crest to Toe Failure) $\mathbf{S_u/\sigma'_v}$ = 0.37

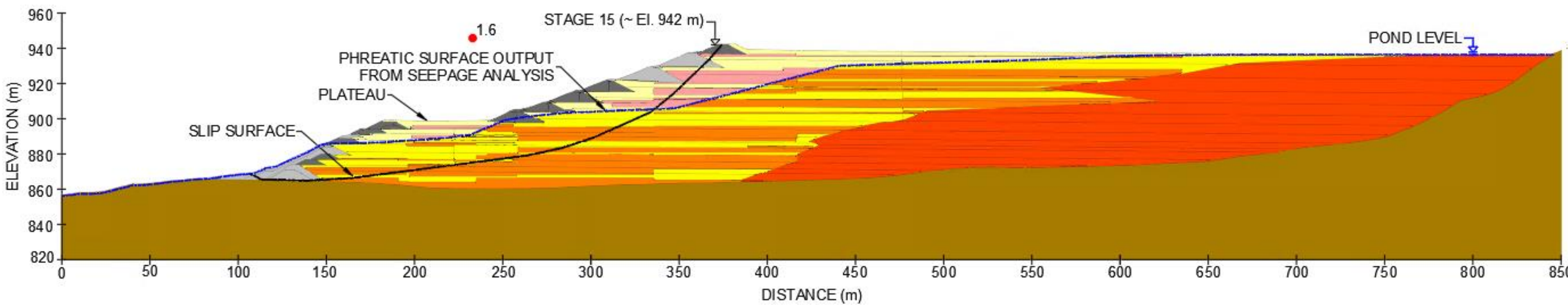

Figure 35: 2D Limit Equilibrium Analysis Result – Cross-section 2-2', El. 942 m msl (Crest to Toe Failure) $\mathbf{S_u/\sigma'_v}$ = 0.37

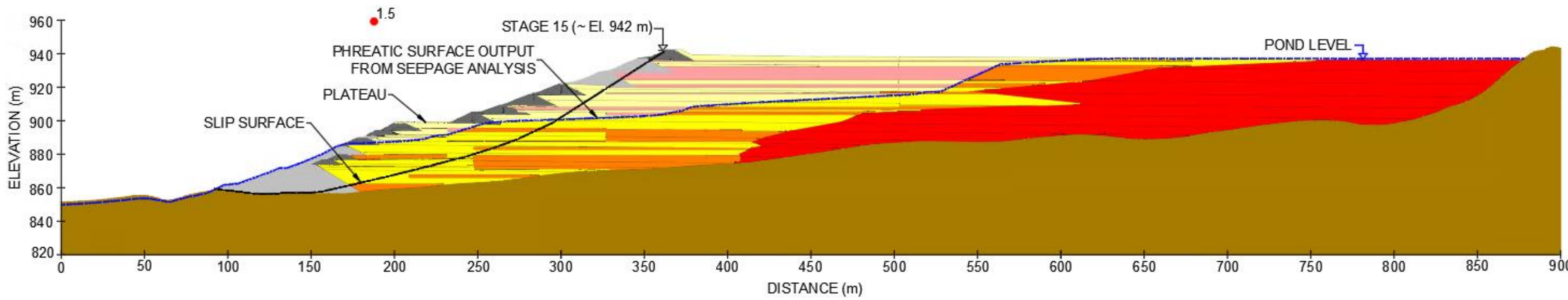

Figure 36: 2D Limit Equilibrium Analysis Result – Cross-section 3-3', El. 942 m msl (Crest to Toe Failure) $\mathbf{S_u/\sigma'_v}$ = 0.37

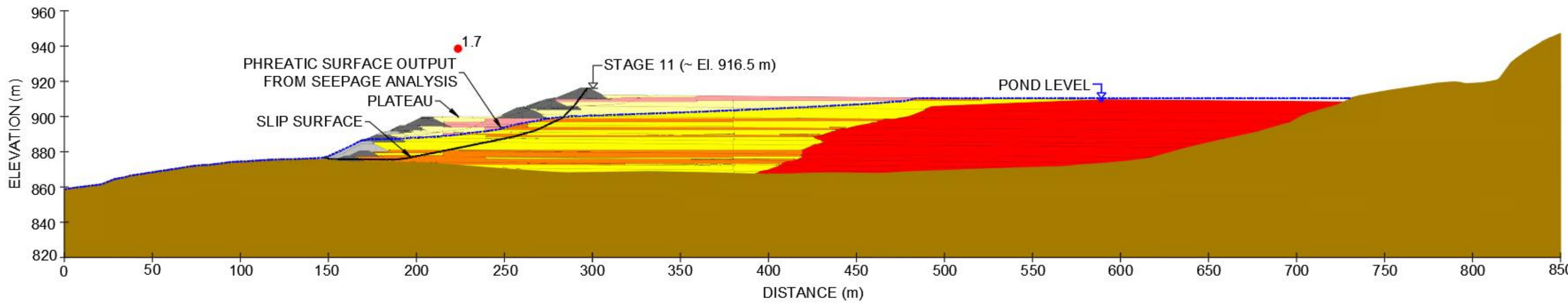

Figure 37: 2D Limit Equilibrium Analysis Result – Cross-section 1-1', El. 916.5 m msl (Crest to Toe Failure) $\mathbf{S_u/\sigma'_v}$ = 0.37

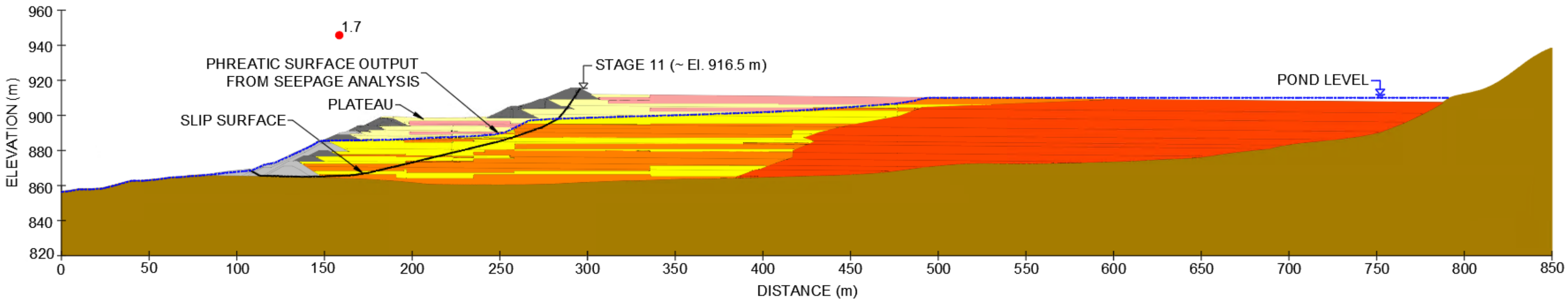

Figure 38: 2D Limit Equilibrium Analysis Result – Cross-section 2-2', El. 916.5 m msl (Crest to Toe Failure) $\mathbf{S_u/\sigma'_v}$ = 0.37

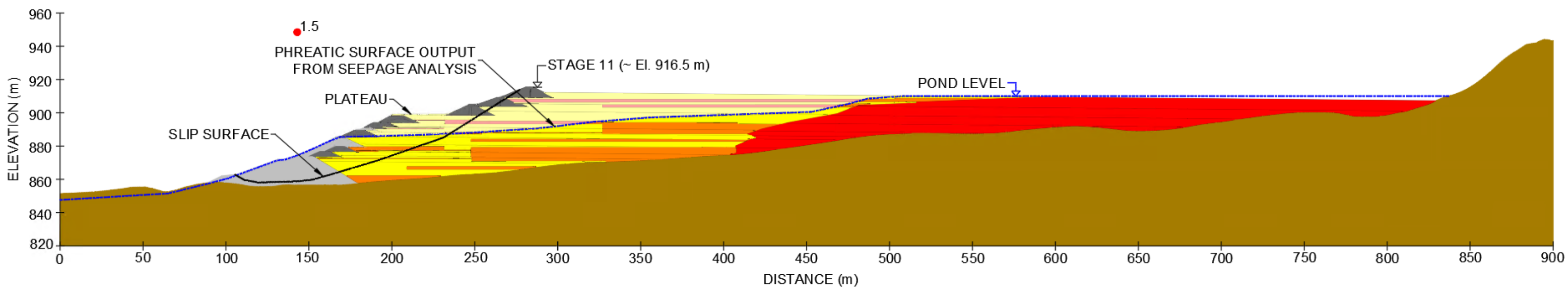

Figure 39: 2D Limit Equilibrium Analysis Result – Cross-section 3-3', El. 916.5 m msl (Crest to Toe Failure) $\mathbf{S_u/\sigma'_v}$ = 0.37

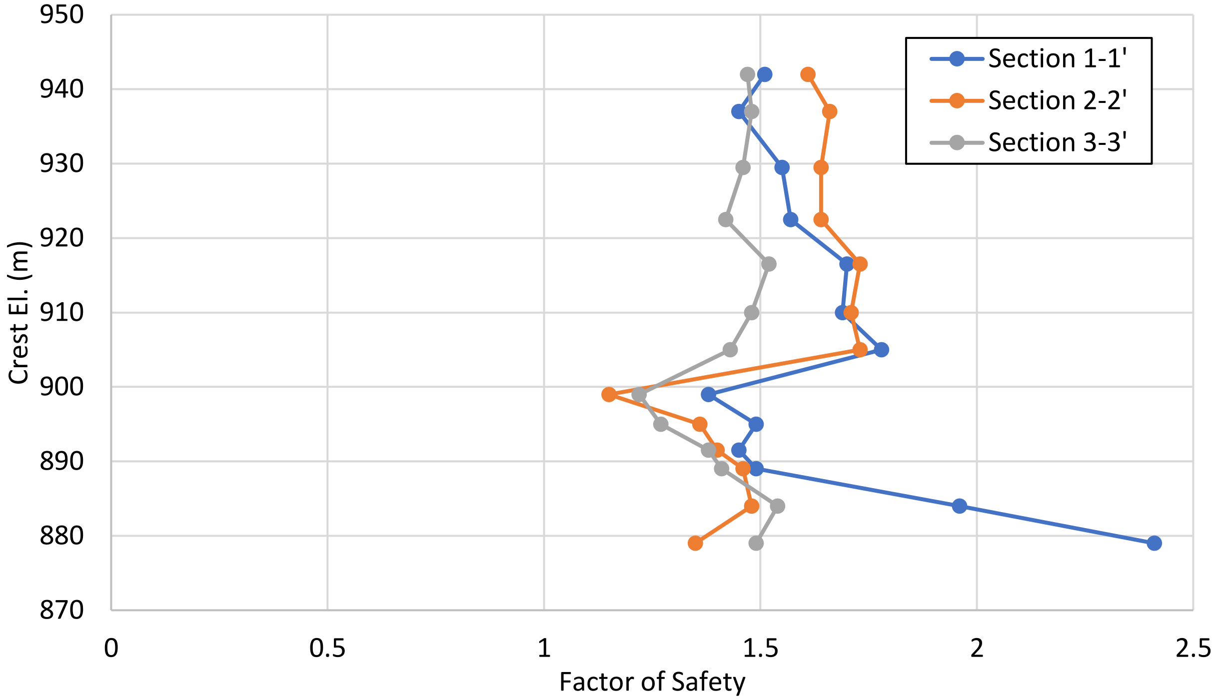

Figure 40: 2D Limit Equilibrium Stability Analysis Results (Peak Strengths) – Crest to Toe Failures

The results for a slip surface from the dam crest to the plateau are shown in Figure 41 through Figure 43. These results showed the LEM FS for this slip surface ranged between 1.4 and 1.7 for the conditions prior to failure. Results for an intermediate dam construction stage when the Dam I crest elevation was 916.5 m msl are shown in Figure 44 through Figure 46. The trend of LEM FS for this slip surface versus dam crest elevation is shown in Figure 47, which depicted a reducing trend with dam crest elevation until crest El. 916.5 m msl after which it remained consistently at the values mentioned above.

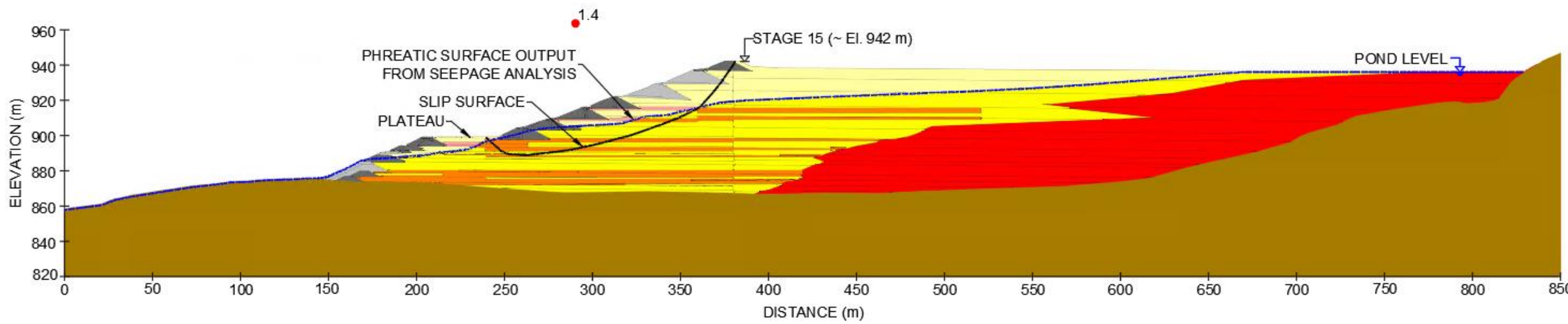

Figure 41: 2D Limit Equilibrium Analysis Result – Cross-section 1-1', El. 942 m msl (Crest to Plateau Failure) $\mathbf{S_u}/\sigma'_v = 0.37$

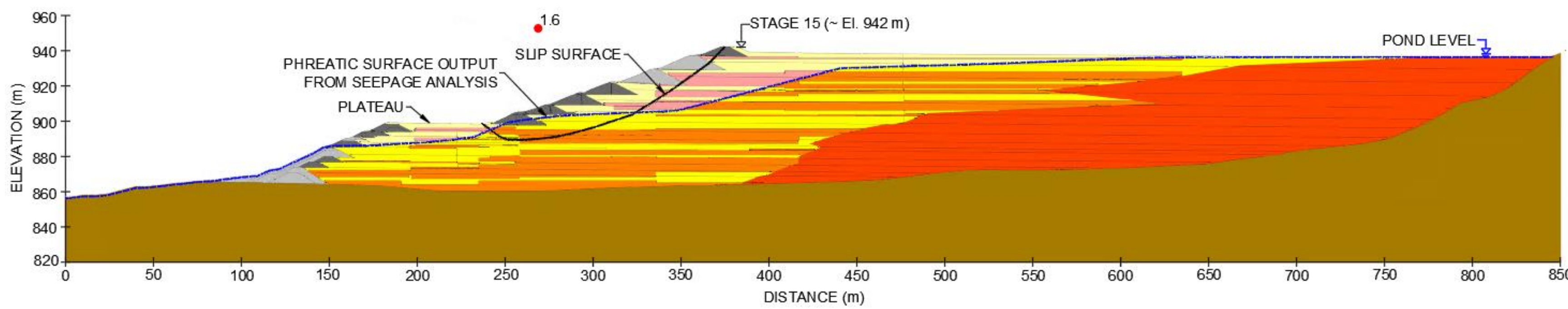

Figure 42: 2D Limit Equilibrium Analysis Result – Cross-section 2-2', El. 942 m msl (Crest to Plateau Failure) $\mathbf{S_u}/\sigma'_v = 0.37$

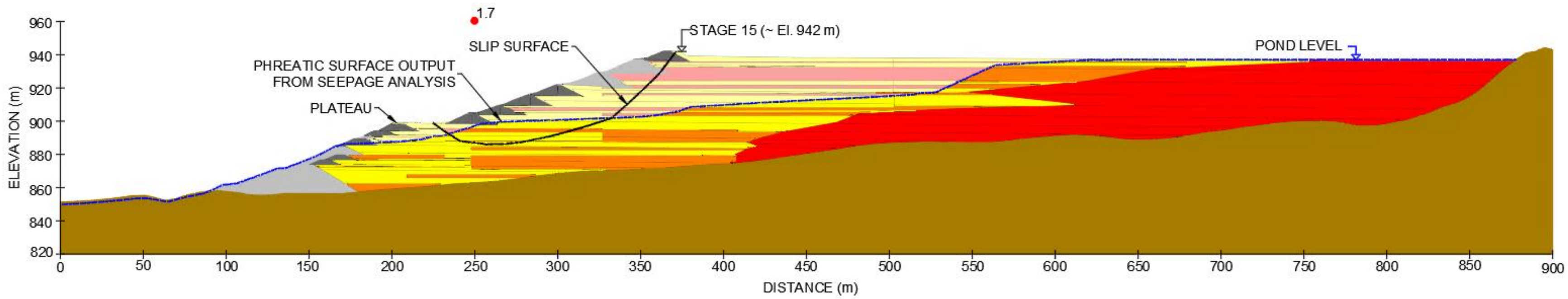

Figure 43: 2D Limit Equilibrium Analysis Result – Cross-section 3-3’, El. 942 m msl (Crest to Plateau Failure) $\mathbf{S_u}/\sigma'_v = 0.37$

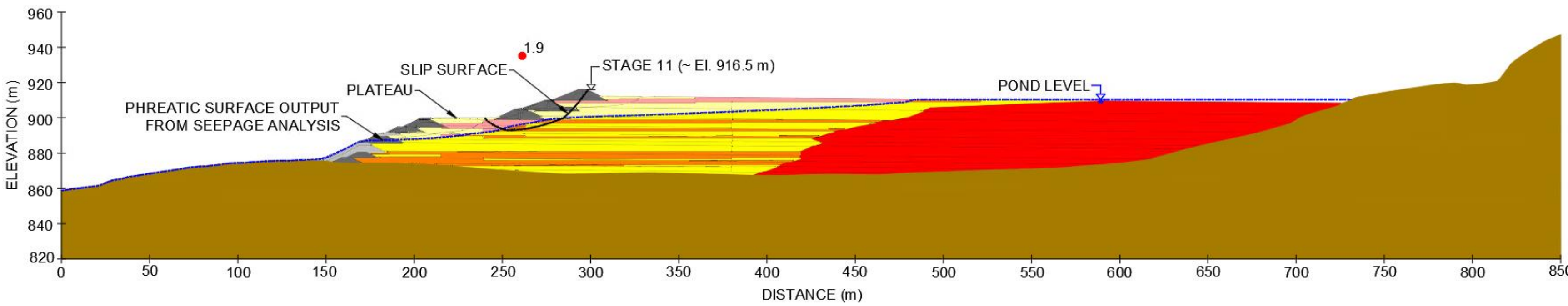

Figure 44: 2D Limit Equilibrium Analysis Result – Cross-section 1-1’, El. 916.5 m msl (Crest to Plateau Failure) $\mathbf{S_u}/\sigma'_v = 0.37$

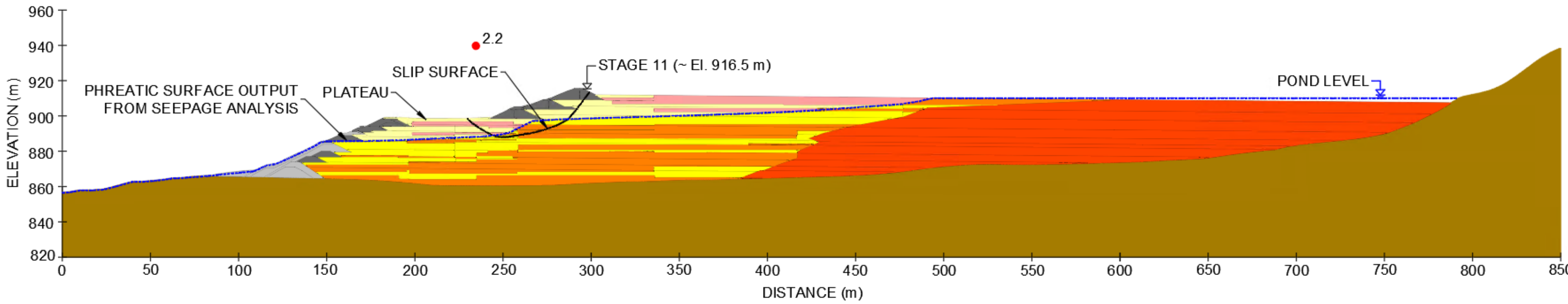

Figure 45: 2D Limit Equilibrium Analysis Result – Cross-section 2-2', El. 916.5 m msl (Crest to Plateau Failure) $\mathbf{S_u}/\sigma'_v = 0.37$

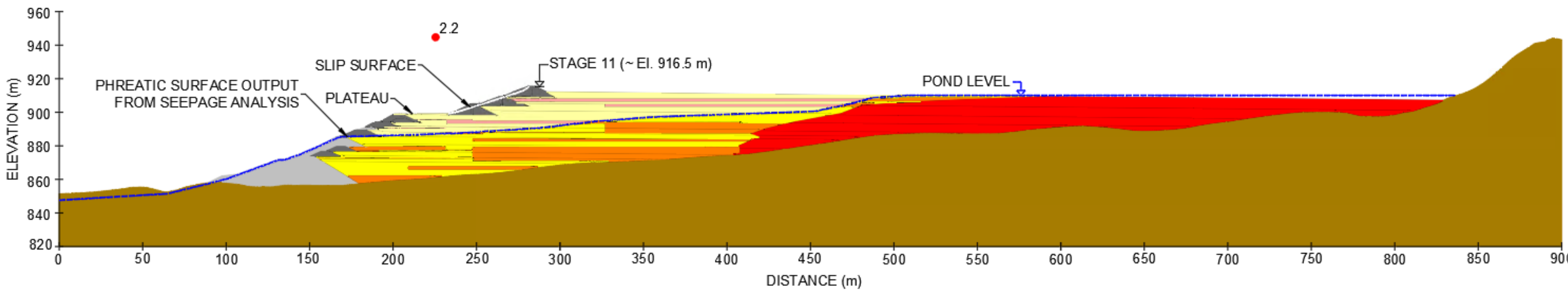

Figure 46: 2D Limit Equilibrium Analysis Result – Cross-section 3-3', El. 916.5 m msl (Crest to Plateau Failure) $\mathbf{S_u}/\sigma'_v = 0.37$

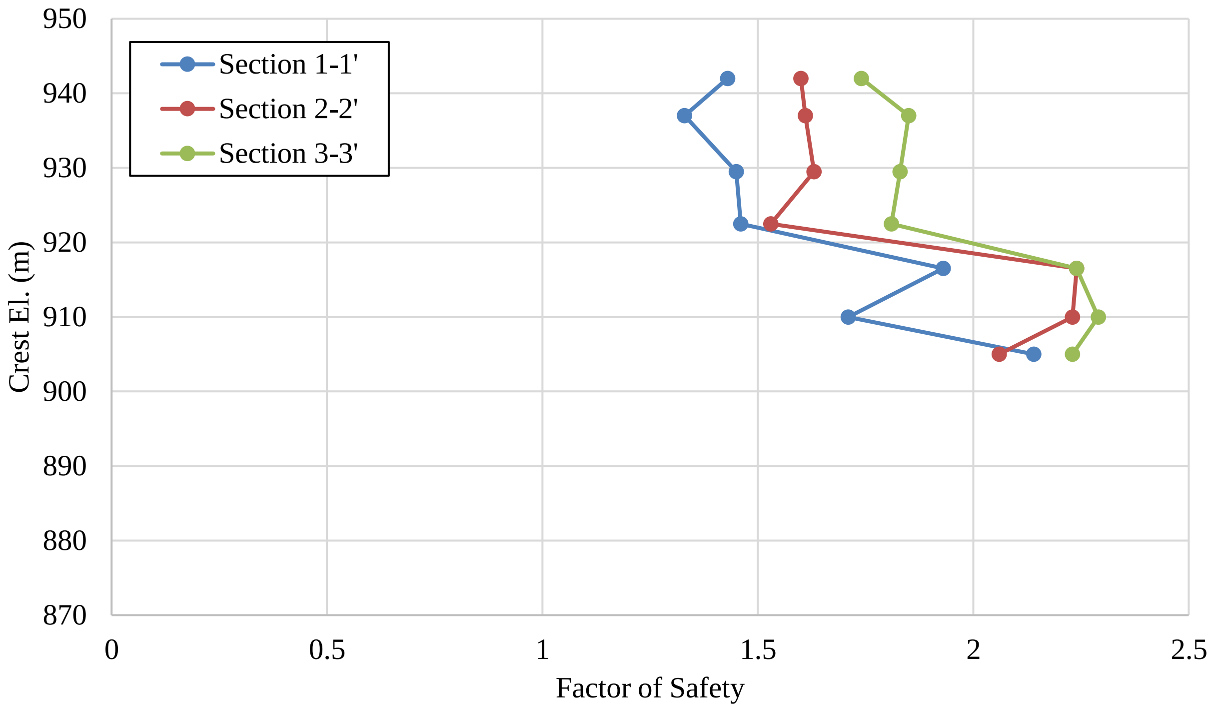

Figure 47: 2D Limit Equilibrium Stability Analysis Results (Peak Strengths) – Crest to Plateau Failures

The results for a slip surface from the plateau to the toe are shown in Figure 48 through Figure 50. These results showed the LEM FS for this slip surface ranged between 1.2 and 1.3 for the conditions prior to failure. Results for an intermediate dam construction stage when the Dam I crest elevation was 916.5 m msl are shown in Figure 51 through Figure 53. The trend of LEM FS for this slip surface versus dam crest elevation is shown in Figure 54, which remained relatively unchanged throughout the construction history.

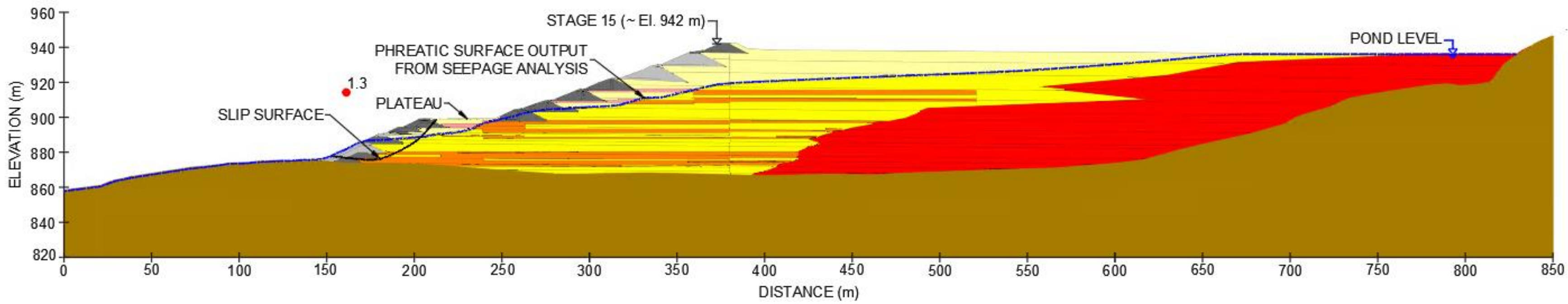

Figure 48: 2D Limit Equilibrium Analysis Result – Cross-section 1-1', El. 942 m msl (Plateau to Toe Failure) $\mathbf{S_u/\sigma'_v}$ = 0.37

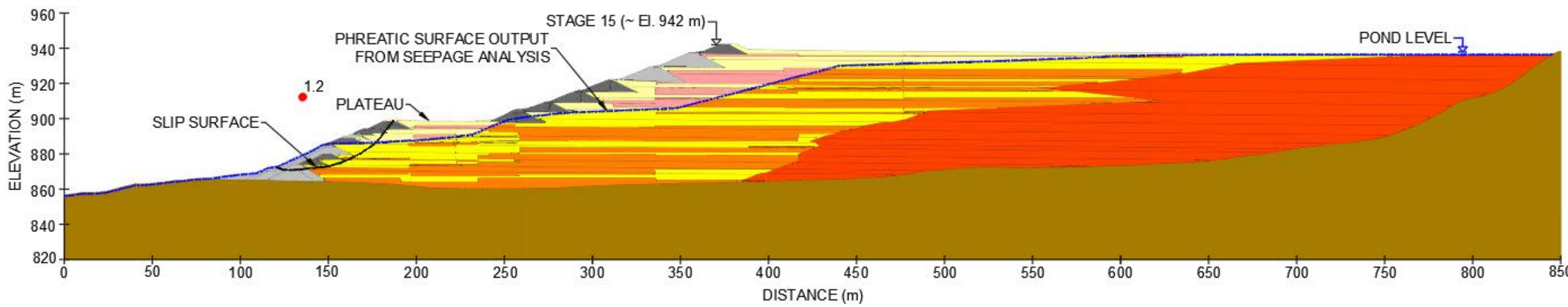

Figure 49: 2D Limit Equilibrium Analysis Result – Cross-section 2-2', El. 942 m msl (Plateau to Toe Failure) $\mathbf{S_u/\sigma'_v}$ = 0.37

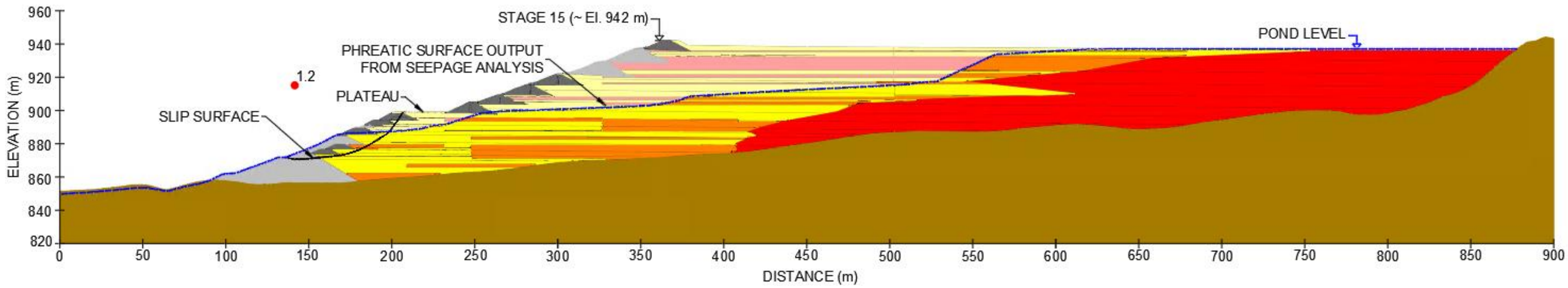

Figure 50: 2D Limit Equilibrium Analysis Result – Cross-section 3-3’, El. 942 m msl (Plateau to Toe Failure) $\mathbf{S_u/\sigma'_v}$ = 0.37

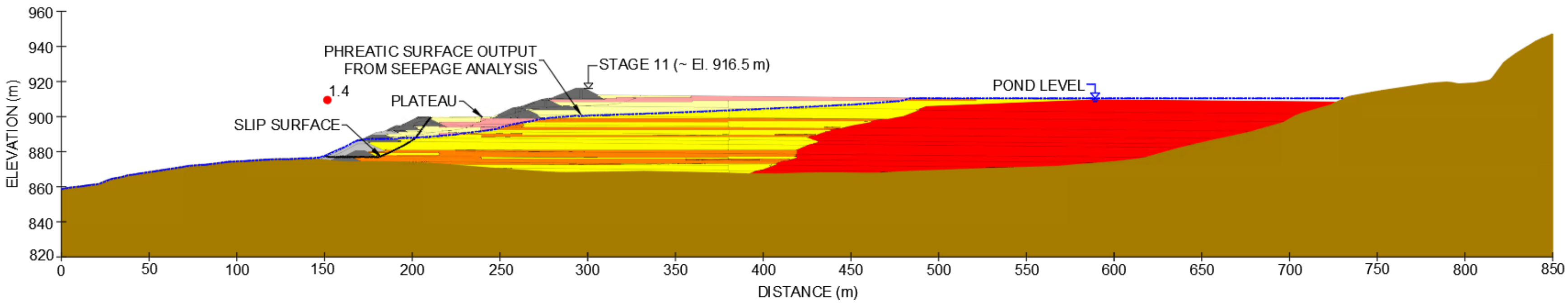

Figure 51: 2D Limit Equilibrium Analysis Result – Cross-section 1-1’, El. 916.5 m msl (Plateau to Toe Failure) $\mathbf{S_u/\sigma'_v}$ = 0.37

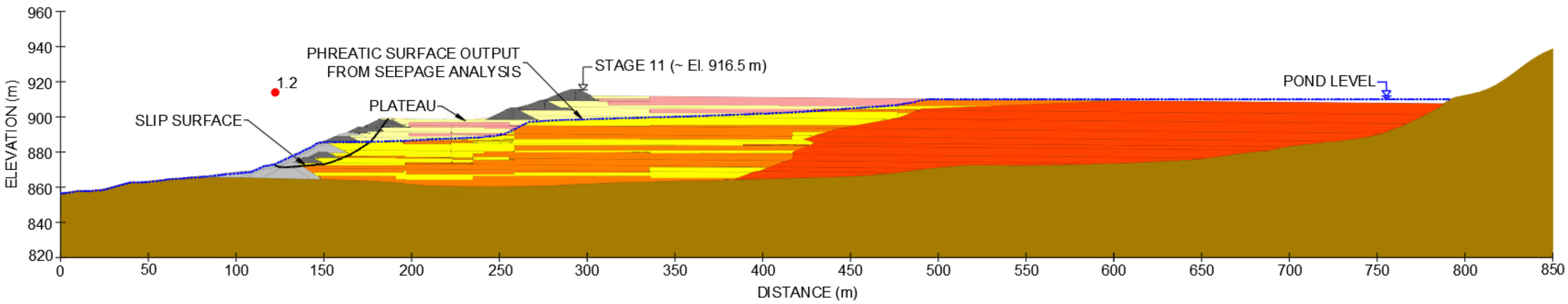

Figure 52: 2D Limit Equilibrium Analysis Result – Cross-section 2-2', El. 916.5 m msl (Plateau to Toe Failure) $\mathbf{S_u/\sigma'_v}$ = 0.37

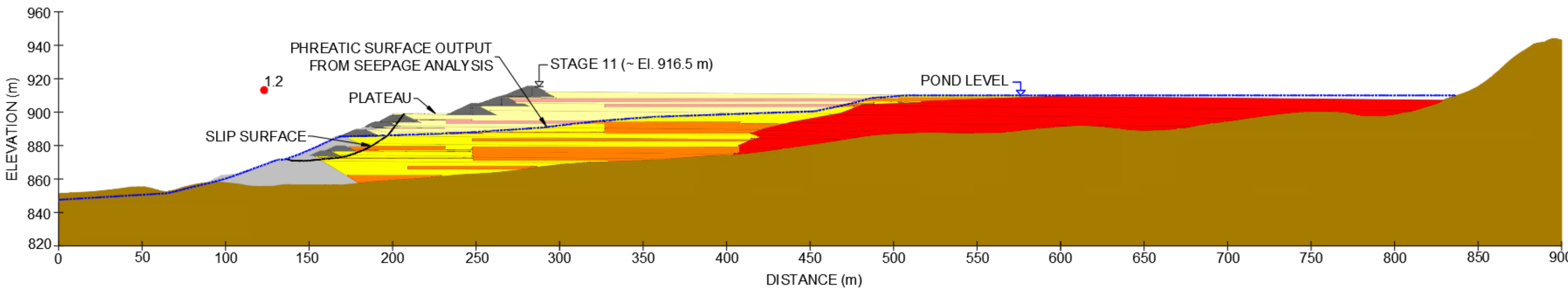

Figure 53: 2D Limit Equilibrium Analysis Result – Cross-section 3-3', El. 916.5 m msl (Plateau to Toe Failure) $\mathbf{S_u/\sigma'_v}$ = 0.37

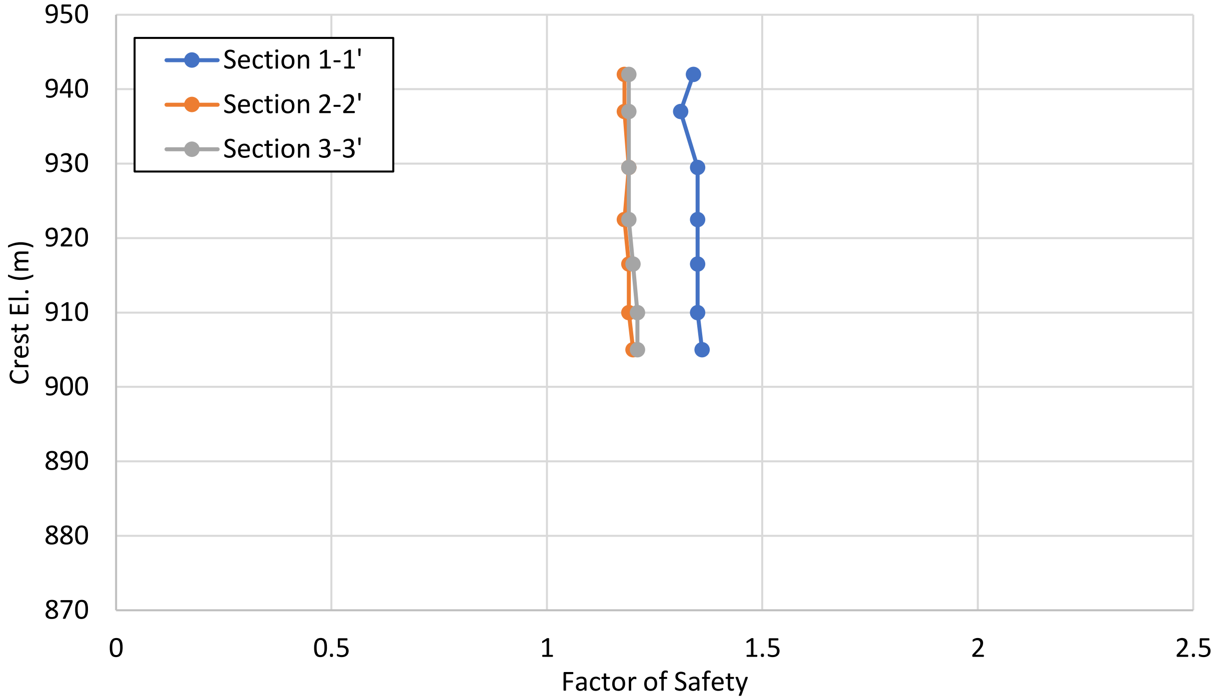

Figure 54: 2D Limit Equilibrium Stability Analysis Results (Peak Strengths) – Plateau to Toe Failures

3.5.3 Factor of Safety – FLAC2D – Peak Strengths

Conventional SSR FS calculations were completed for the conditions prior to failure in FLAC2D for comparison with the LEM results as a check on the equivalency between these methods and to aid comparison of the conventional FLAC3D FS and LEM FS results. This analysis was completed on Sections 1 and 3 to bracket the LEM results.

The results for Section 1 are shown in Figure 55. The conventional FS in this analysis was 1.4, compared with 1.3 from the LEM analysis.

The results for Section 3 are shown in Figure 56. The conventional FS in this analysis was 1.2, compared with 1.2 from the LEM analysis.

Overall, these results showed general consistency between the conventional SSR FS and LEM FS calculation methods, with both methods identifying the lowest FS to be from the plateau to the dam toe and to produce similar FS values.

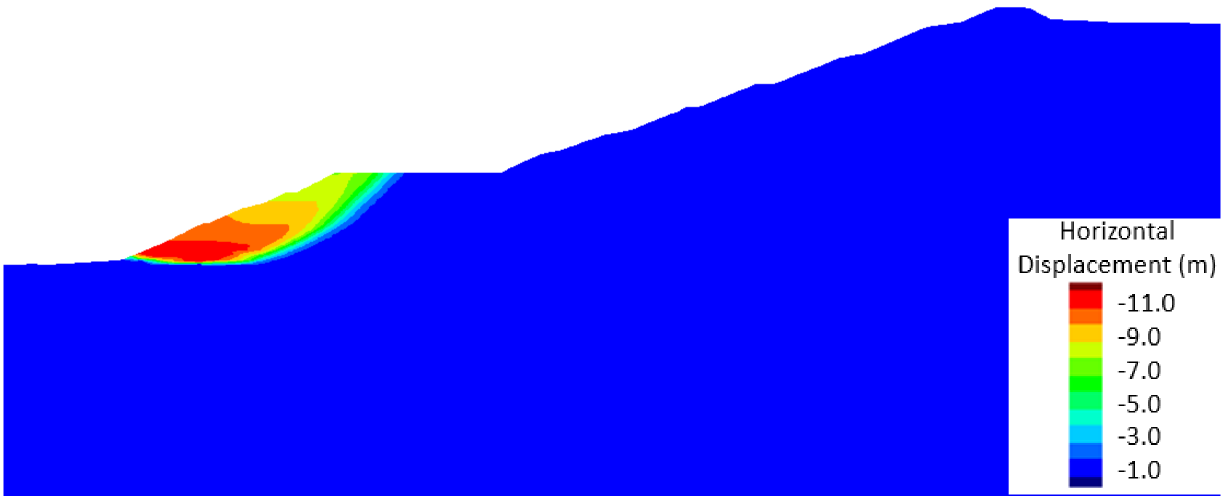

*Factor of Safety = **1.4** – Peak Undrained Strengths, S_u/σ'_v of 0.37*

Figure 55: 2D FLAC Analysis – Factor of Safety Result (Cross-section 1-1')

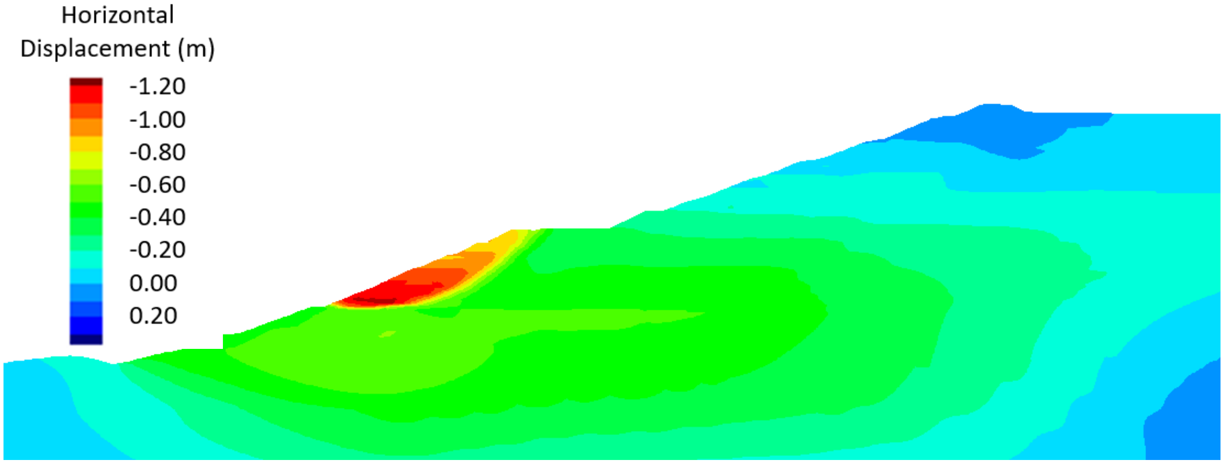

*Factor of Safety = **1.2** – Peak Undrained Strengths, S_u/σ'_v of 0.37*

Figure 56: 2D FLAC Analysis – Factor of Safety Result (Cross-section 3-3')

3.5.4 Factor of Safety – LEM – Liquefied Strengths

FS values were also calculated in the LEM analyses for each section using a post-liquefaction shear strength ratio of $S_{u\text{-liq}}/\sigma'_v = 0.01$. This method resulted in FS values ranging between 0.1 and 0.3 among the various sections and slip surfaces discussed in Section 3.5.2. This strength is a lower-bound from the laboratory testing, recognizing the visibly low shear resistance observable in the video.

3.5.5 Factor of Safety - Summary

The conventional FS values calculated for the various methods are summarized in Table 3.

Table 3: Conventional Factor of Safety Summary for the Condition Prior to Failure

Cross-section	Limit Equilibrium[1]	Conventional SSR 2D FLAC	Conventional SSR 3D FLAC
1-1	1.5, 1.4, 1.3	1.4	1.5
2-2	1.6, 1.6, 1.2	Not calculated	
3-3	1.5, 1.7, 1.2	1.2	

Note: [1]Factors of Safety listed represent the following slip surface scenarios: Crest to Toe, Crest to Plateau, and Plateau to Toe

This analysis showed that the conventional FS using peak strengths prior to failure was 1.5. Lower values, in the range of 1.2, were calculated for the toe of the dam using 2D analyses; however, the curvature of this area led to an increased FS of 1.5 in 3D analyses. These conventional FS results were based on an elastic-perfectly plastic stress-strain relationship and were calculated using the typical strength reduction approach described by Dawson et al. (1999) and Griffiths and Lane (1999). This method is built into the FLAC software. This method is different from the FS against liquefaction triggering discussed in Section 3.3.1 because it does not capture the effect of progressive failure in which a sequence of instability can develop as a result of over-stressing any area of the dam slope. Therefore, although the overall conventional FS was relatively high, local areas were stressed close to failure and would cause failure of the dam once strength loss in these areas was triggered.

This effect is highlighted by the conventional FS analyses with post-liquefaction strengths, which developed FS values significantly < 1.

3.5.6 Material Point Method

The final analysis in this assessment involved using the MPM to calculate how the dam failure would develop following liquefaction triggering. This was completed because the deformation analyses described earlier could capture the stresses and displacements up to and during the initiation of failure but could not fully capture the propagation of the failure. The methodology to develop the MPM model followed the approach developed by Llano-Serna et al. (2016).[9]

The analysis was completed in 2D on Section 2 and used a simplified version of the tailings delineation used for the FLAC analyses. The analysis involved assigning a stress distribution

[9] Llano-Serna, M.A., Farias, M.M., & Pedroso, D.M. (2015). An assessment of the material point method for modelling large scale run-out processes in landslides. *Landslides*, *5*(13), 1057-1066.

using a gradual switching-on-gravity approach. A strain-weakening constitutive model was used that was similar to the constitutive model used in the FLAC analyses.

The initial strength ratio in this analysis was $S_{u\text{-}liq}/\sigma'_v = 0.24$, which was sufficiently low to initiate the failure mechanism in the model and observe the progression of failure.

Table 4 summarises the MPM model results. The MPM model results were compared with the available video footage to assess the evolution of dam failure. At t = 2 seconds (s), a velocity of around 5 meters per second (m/s) was estimated within the body of the tailings behind the face. At t = 5s, transverse cracks were observed on the video footage. The numerical model shows a concentration of deviatoric strain reaching unity at the toe of the dam that propagates upwards behind the berms at this stage. At t = 7s, bulging of the face is evident from both the video recording and the model. Continued crest settlement and retrogression of multiple slip surfaces occurred in the model in a manner representative of the video footage. The kinematic plot in Figure 61. shows an approximate total acceleration of 3 m/s^2 from t = 0s to t = 10s when the failed mass reaches a maximum velocity of around 30 m/s (i.e., 100 km/hr). At t = 15s the failure is well developed over the entire height of the dam; the run-out velocity shown in Figure 61 indicates values ranging between 25 m/s and 30 m/s.

In summary, this analysis showed that once the failure was initiated, it would develop into a series of retrogressive failure planes that would occur at a rate that matched the observations. This analysis provided further support for the strain-weakening relationship used in earlier analyses.

Table 4: Illustration of the Main Results from the MPM Analysis Showing Progression of Failure

<table>
<tr><td>0 (Initial stress)</td><td>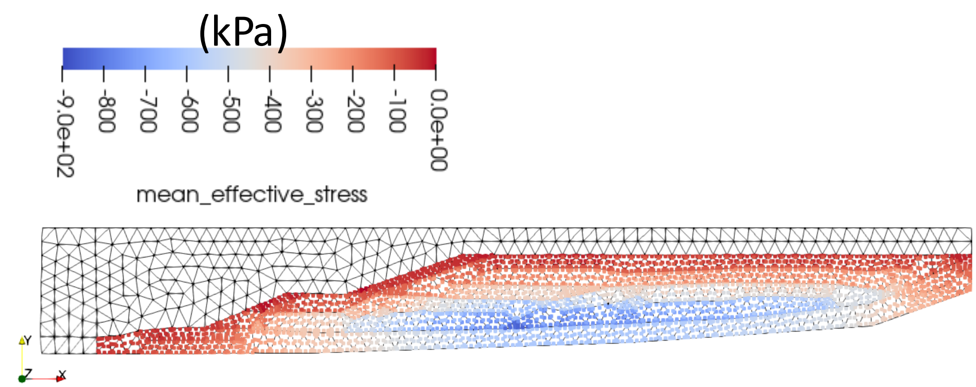
</td></tr>
<tr><td>1 second</td><td>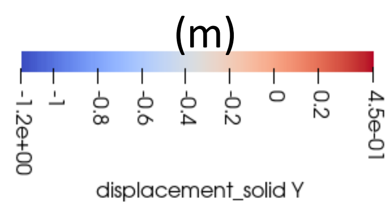

Maximum vertical displacement of 1.2 m at crest
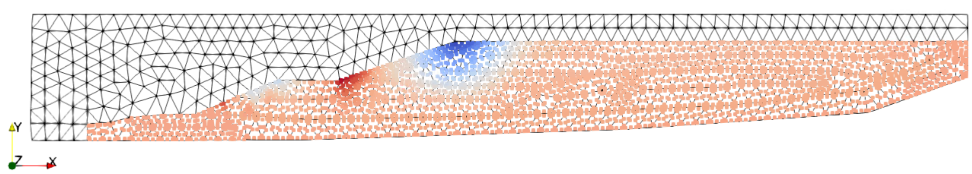</td></tr>
<tr><td>2 seconds</td><td>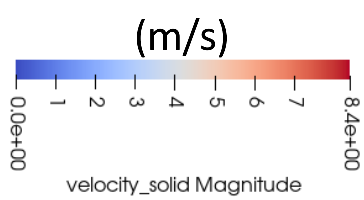

Total velocity indicates that initial signs of failure were observable in the upper section of the dam.
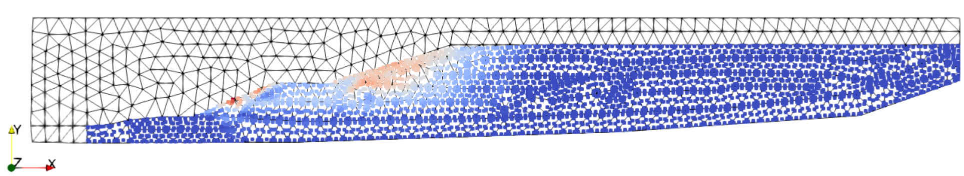</td></tr>
</table>

3 seconds	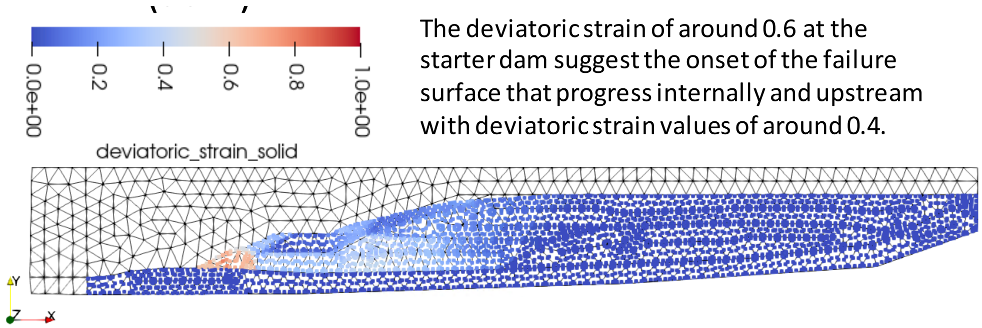 The deviatoric strain of around 0.6 at the starter dam suggest the onset of the failure surface that progress internally and upstream with deviatoric strain values of around 0.4.
4 seconds	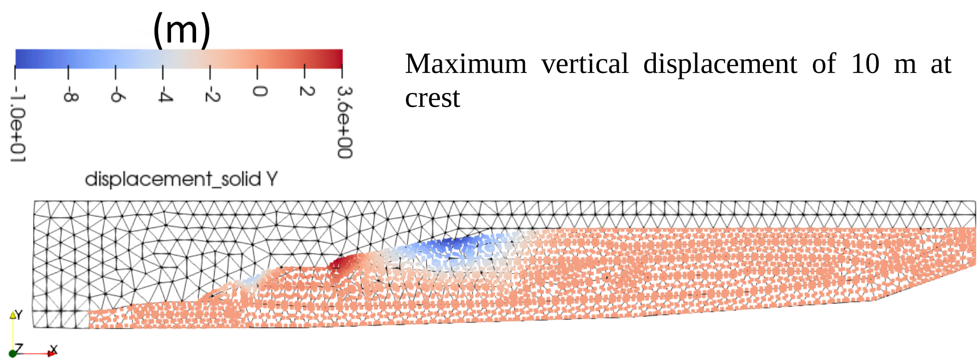 Maximum vertical displacement of 10 m at crest
5 seconds	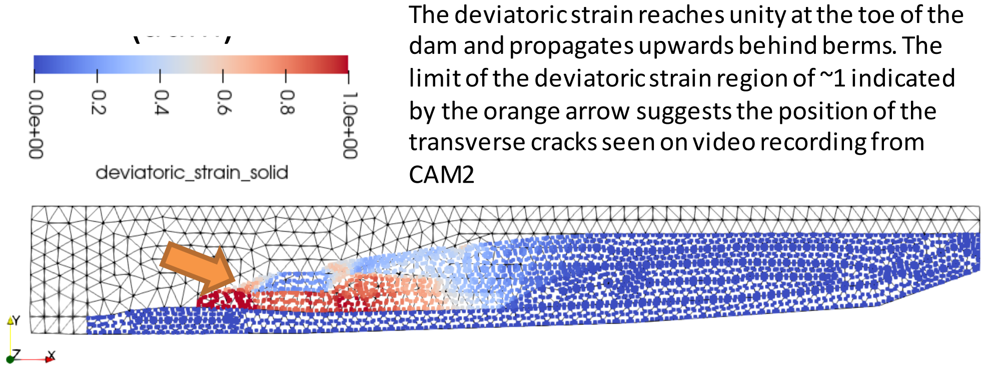 The deviatoric strain reaches unity at the toe of the dam and propagates upwards behind berms. The limit of the deviatoric strain region of ~1 indicated by the orange arrow suggests the position of the transverse cracks seen on video recording from CAM2
6 seconds	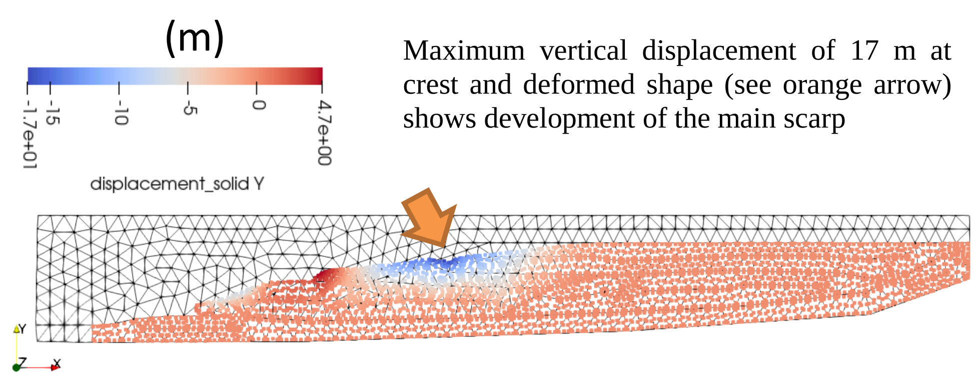 Maximum vertical displacement of 17 m at crest and deformed shape (see orange arrow) shows development of the main scarp

7 seconds	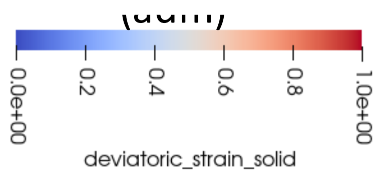 Concentration of deviatoric strain equal to unity at toe. Purple arrow shows bulging. Green arrow shows concentration of deviatoric strain equal to one in the location of the backscarp from video analysis 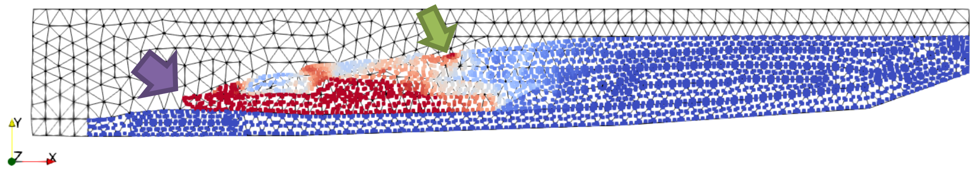
8 seconds	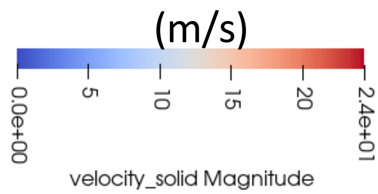 Advancing toe progresses at a speed between 20.0 and 24.0 m/s. Cone of depletion (orange broken line) extents towards rear of the facility 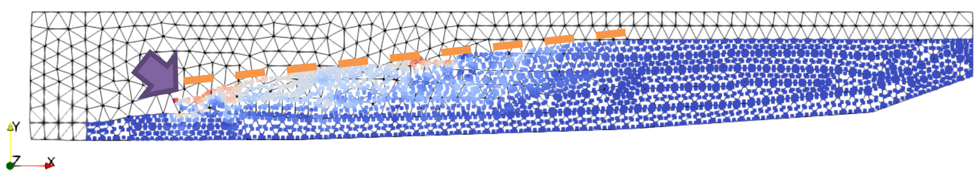
9 seconds	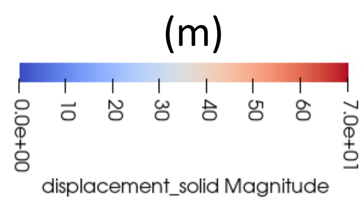 Maximum displacement of the failed mass reaches 70.0 m. Model is capable to reproduce the bulging seen on the video recording from CAM1 (see purple arrow). The sub transverse fissures seen on the video recording are localised in the region of maximum displacement described by the model (see broken red line contour). 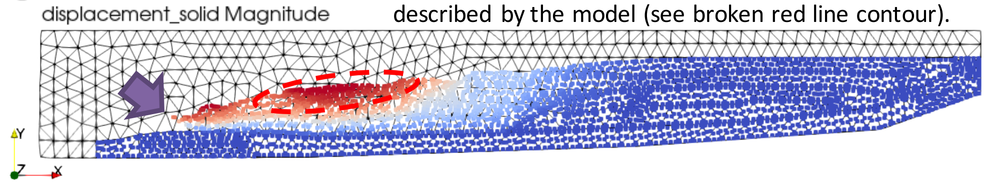
10 seconds	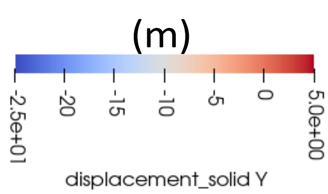 Video recording from CAM1 shows a well developed scarp that progress towards the rear of the facility. The numerical model shows the scarp regressing progressively. The computed scarp height ranges between 15.0m to 25.0 m. CAM1 shows water spouting coming from the advancing toe. 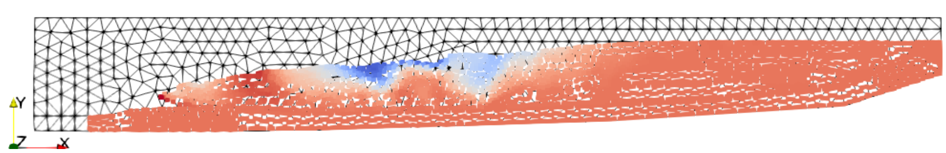

15 seconds	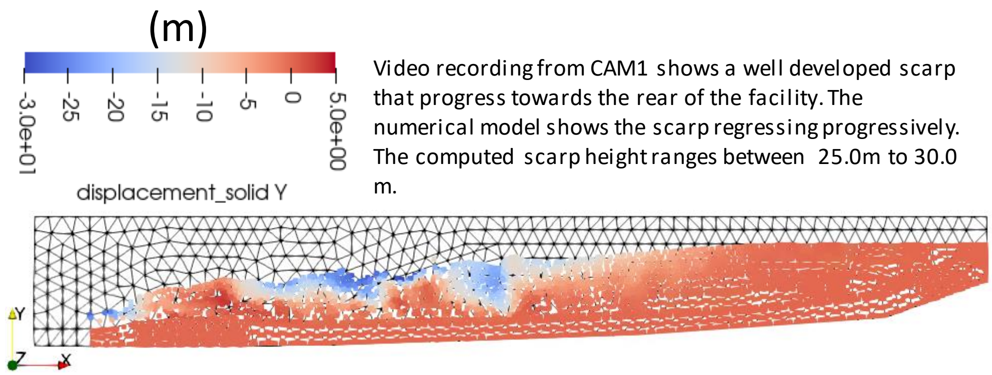 Video recording from CAM1 shows a well developed scarp that progress towards the rear of the facility. The numerical model shows the scarp regressing progressively. The computed scarp height ranges between 25.0m to 30.0 m.

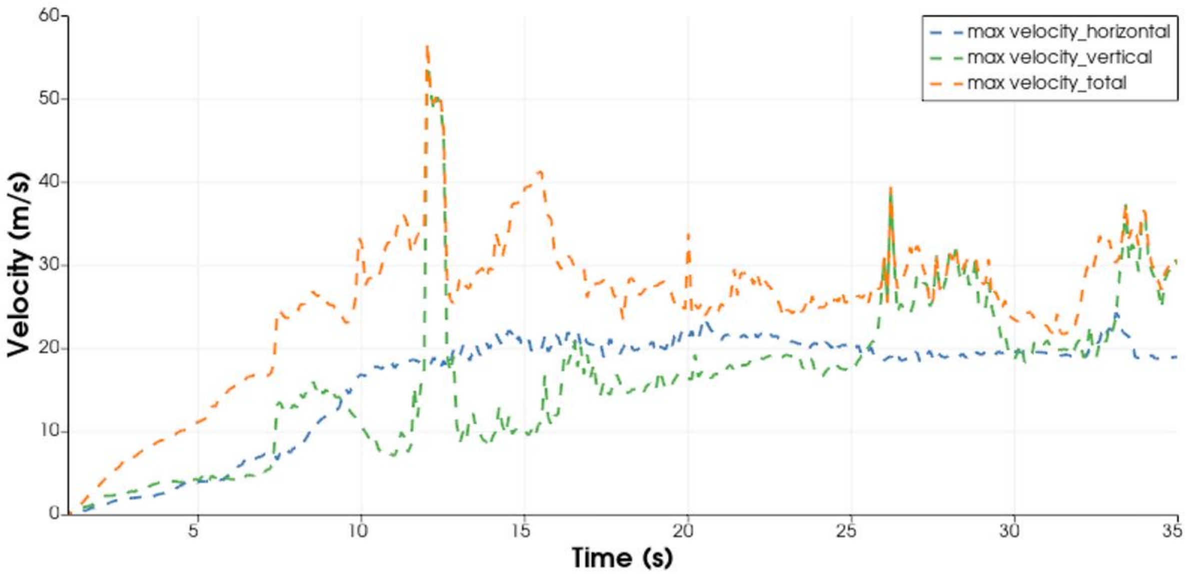

Figure 57: Change of Maximum Velocity during Failure as a Function of Time

Appendix H

Annex 1 – 2D FLAC Deformation Results

December 2019

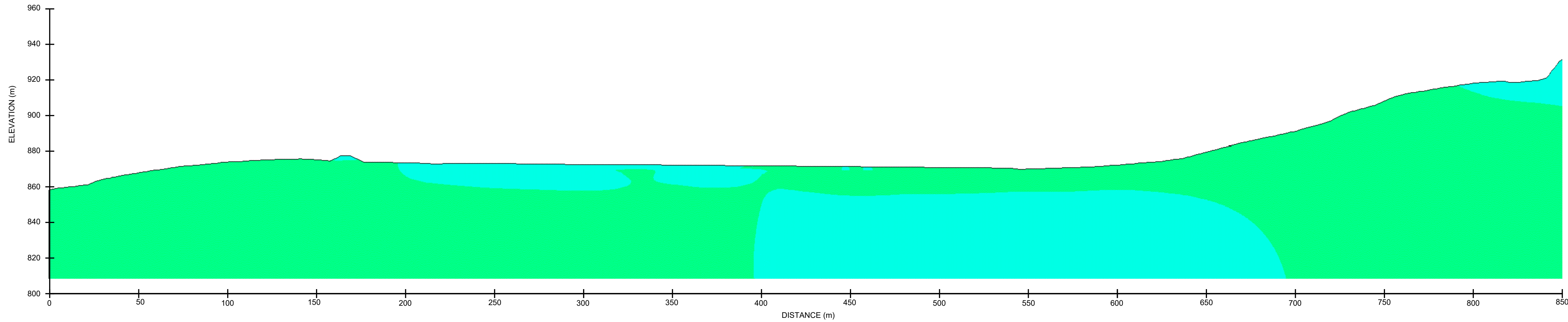

HORIZONTAL DISPLACEMENTS

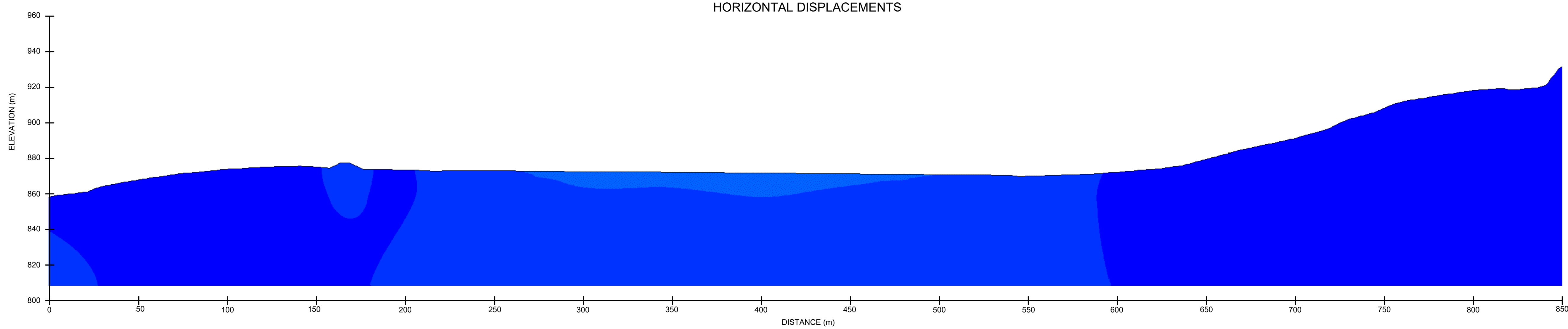

VERTICAL DISPLACEMENTS

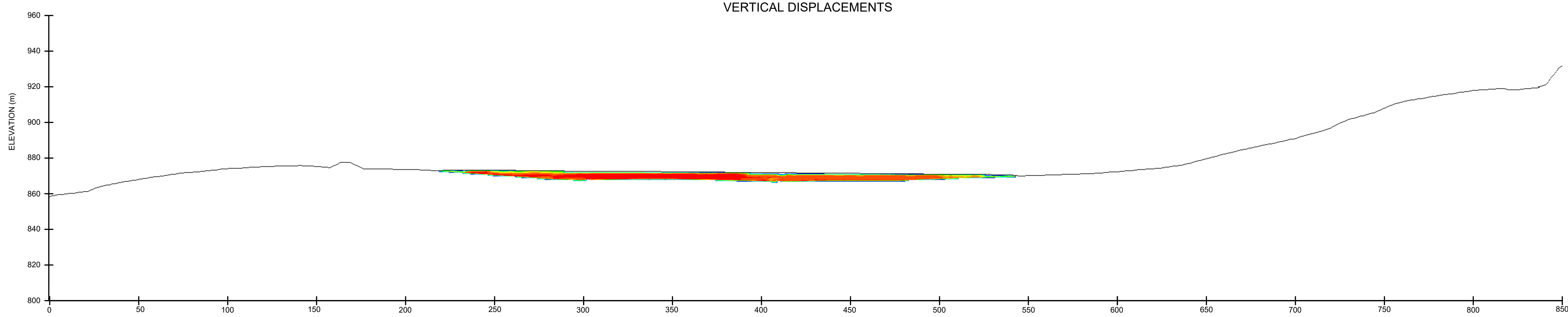

MOBILIZED STABILITY RATIO

1:2,500 0 25 50 m BASED ON A 11"X 17" DRAWING SIZE

NOTES:

1. ALL DIMENSIONS AND ELEVATIONS ARE IN METERS UNLESS STATED OTHERWISE.
2. MATERIAL PARAMETERS ARE OUTLINED IN APPENDIX E.

LEGEND:

HORIZONTAL DISPLACEMENTS (m)	VERTICAL DISPLACEMENTS	MOBILIZED INSTABILITY RATIO
-0.40	-2.10	0.40
-0.30	-1.80	0.50
-0.20	-1.50	0.60
-0.10	-1.20	0.70
0.0	-0.90	0.80
0.10	-0.60	0.90
0.20	-0.30	1.00
	0.00	1.10

CLIENT

PROJECT
REPORT OF THE EXPERT PANEL ON THE TECHNICAL CAUSES OF THE FAILURE OF FEIJÃO DAM 1

TITLE
APPENDIX H
2D DEFORMATION ANALYSIS RESULTS
MOHR COULOMB MODEL
SECTION 1-1' - EL. 877 m

SCALE	PROJECT No.	FIG. No.
1:2,500		1

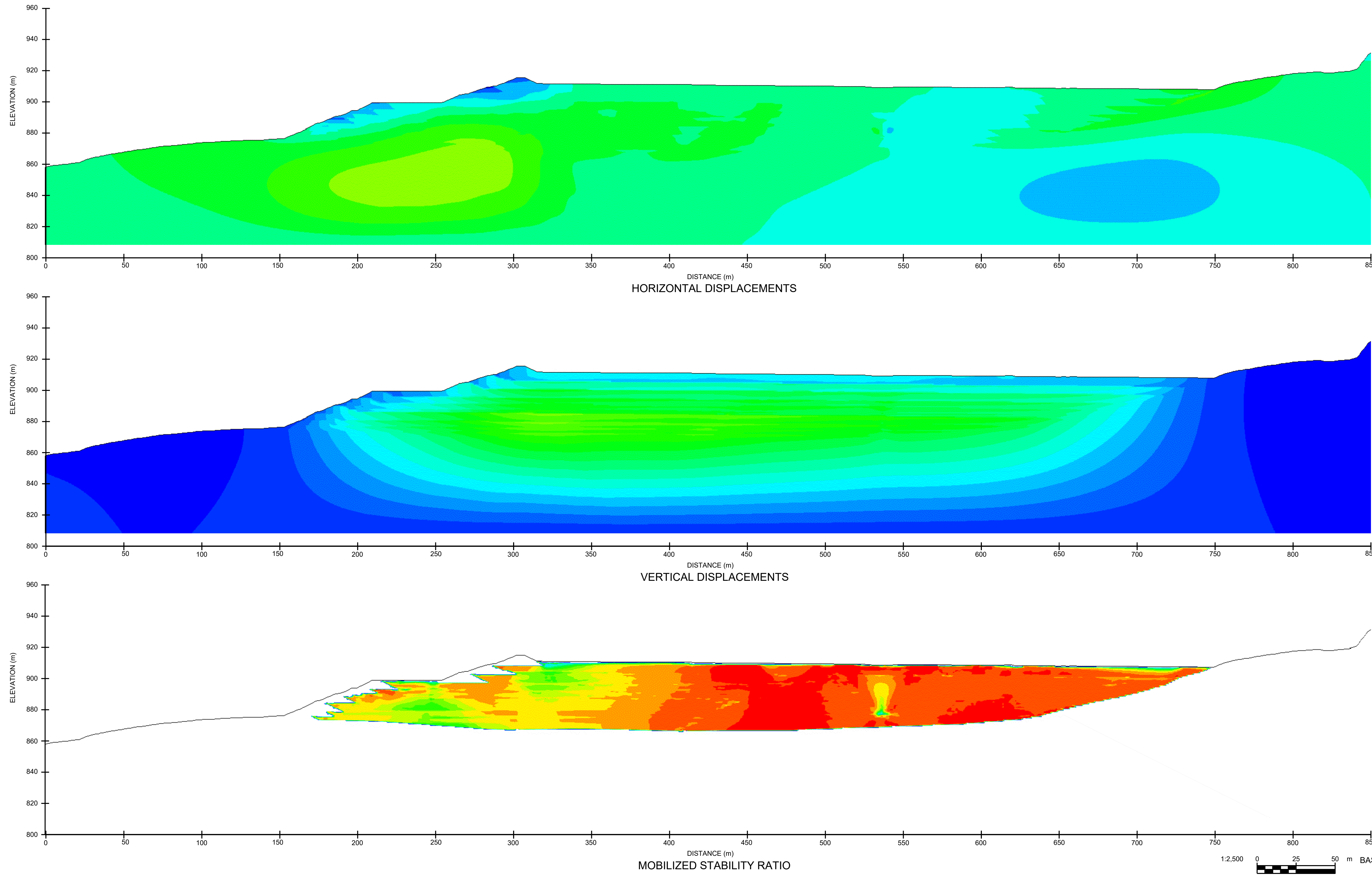

1:2,500 0 25 50 m BASED ON A 11"X 17" DRAWING SIZE

NOTES:

1. ALL DIMENSIONS AND ELEVATIONS ARE IN METERS UNLESS STATED OTHERWISE.
2. MATERIAL PARAMETERS ARE OUTLINED IN APPENDIX E.

LEGEND:

HORIZONTAL DISPLACEMENTS (m)	VERTICAL DISPLACEMENTS	MOBILIZED INSTABILITY RATIO
-0.40	-2.10	0.40
-0.30	-1.80	0.50
-0.20	-1.50	0.60
-0.10	-1.20	0.70
0.0	-0.90	0.80
0.10	-0.60	0.90
0.20	-0.30	1.00
	0.00	1.10

CLIENT

PROJECT
REPORT OF THE EXPERT PANEL ON THE TECHNICAL CAUSES OF THE FAILURE OF FEIJÃO DAM 1

TITLE
APPENDIX H
2D DEFORMATION ANALYSIS RESULTS
MOHR COULOMB MODEL
SECTION 1-1' - EL. 916.5 m

SCALE	PROJECT No.	FIG. No.
1:2,500		2

KCB-FIG-B-L

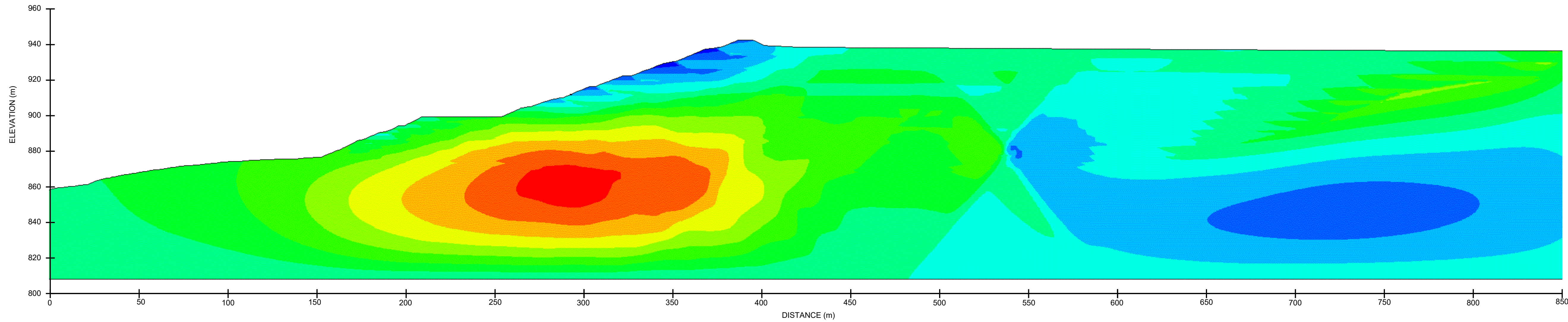

HORIZONTAL DISPLACEMENTS

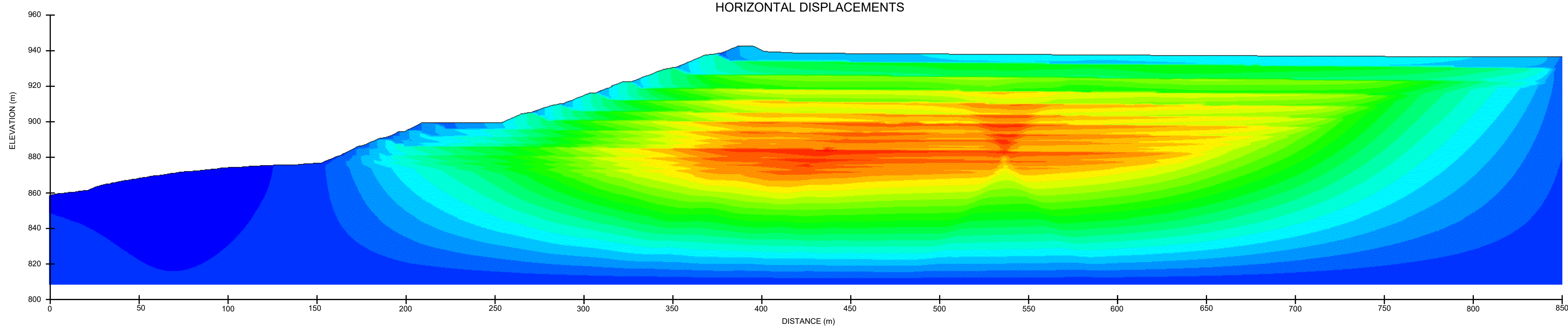

VERTICAL DISPLACEMENTS

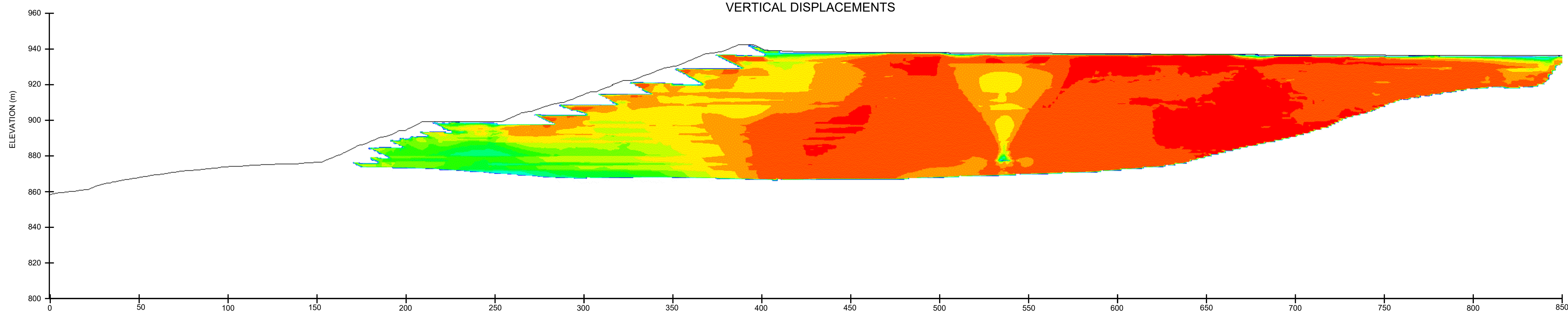

MOBILIZED STABILITY RATIO

1:2,500 0 25 50 m BASED ON A 11"X 17" DRAWING SIZE

NOTES:

1. ALL DIMENSIONS AND ELEVATIONS ARE IN METERS UNLESS STATED OTHERWISE.
2. MATERIAL PARAMETERS ARE OUTLINED IN APPENDIX E.

LEGEND:

HORIZONTAL DISPLACEMENTS (m)	VERTICAL DISPLACEMENTS	MOBILIZED INSTABILITY RATIO
-0.40	-2.10	0.40
-0.30	-1.80	0.50
-0.20	-1.50	0.60
-0.10	-1.20	0.70
0.0	-0.90	0.80
0.10	-0.60	0.90
0.20	-0.30	1.00
	0.00	1.10

CLIENT

PROJECT
REPORT OF THE EXPERT PANEL ON THE TECHNICAL CAUSES OF THE FAILURE OF FEIJÃO DAM 1

TITLE
APPENDIX H
2D DEFORMATION ANALYSIS RESULTS
MOHR COULOMB MODEL
SECTION 1-1' - EL. 942 m

SCALE	PROJECT No.	FIG. No.
1:2,500		3

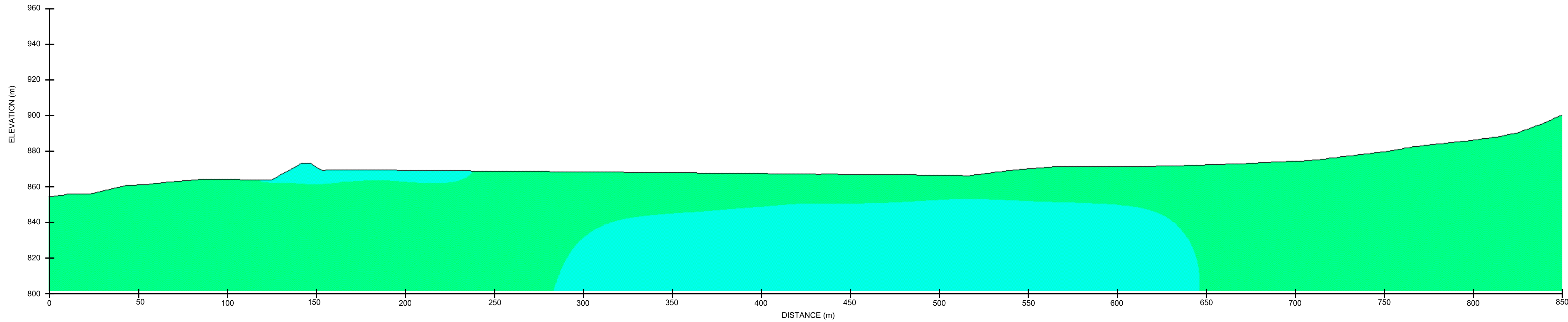

HORIZONTAL DISPLACEMENTS

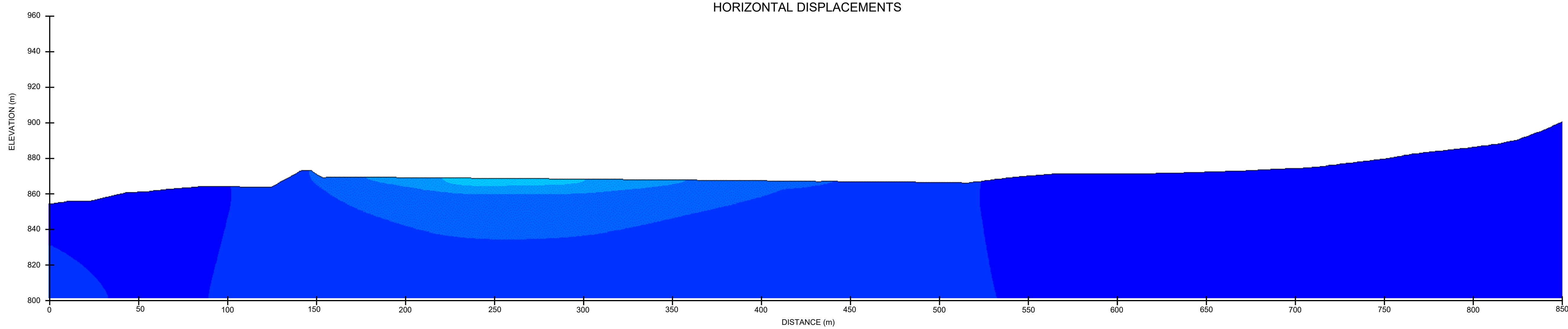

VERTICAL DISPLACEMENTS

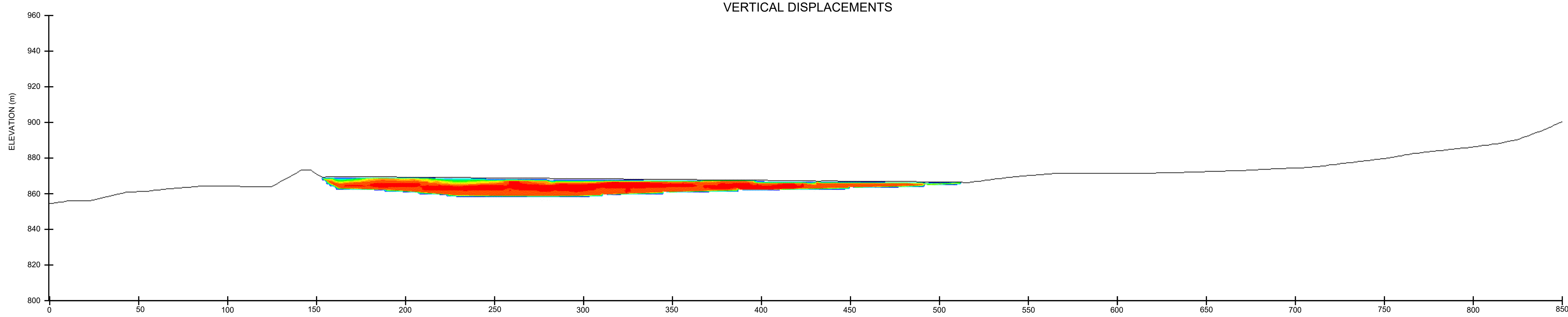

MOBILIZED STABILITY RATIO

1:2,500 0 25 50 m BASED ON A 11"X 17" DRAWING SIZE

NOTES:

1. ALL DIMENSIONS AND ELEVATIONS ARE IN METERS UNLESS STATED OTHERWISE.
2. MATERIAL PARAMETERS ARE OUTLINED IN APPENDIX E.

LEGEND:

HORIZONTAL DISPLACEMENTS (m)	VERTICAL DISPLACEMENTS	MOBILIZED INSTABILITY RATIO
-0.40	-2.10	0.40
-0.30	-1.80	0.50
-0.20	-1.50	0.60
-0.10	-1.20	0.70
0.0	-0.90	0.80
0.10	-0.60	0.90
0.20	-0.30	1.00
	0.00	1.10

CLIENT

PROJECT
REPORT OF THE EXPERT PANEL ON THE TECHNICAL CAUSES OF THE FAILURE OF FEIJÃO DAM 1

TITLE
APPENDIX H
2D DEFORMATION ANALYSIS RESULTS
MOHR COULOMB MODEL
SECTION 2-2' - EL. 874 m

SCALE	PROJECT No.	FIG. No.
1:2,500		4

KCB-FIG-B-L

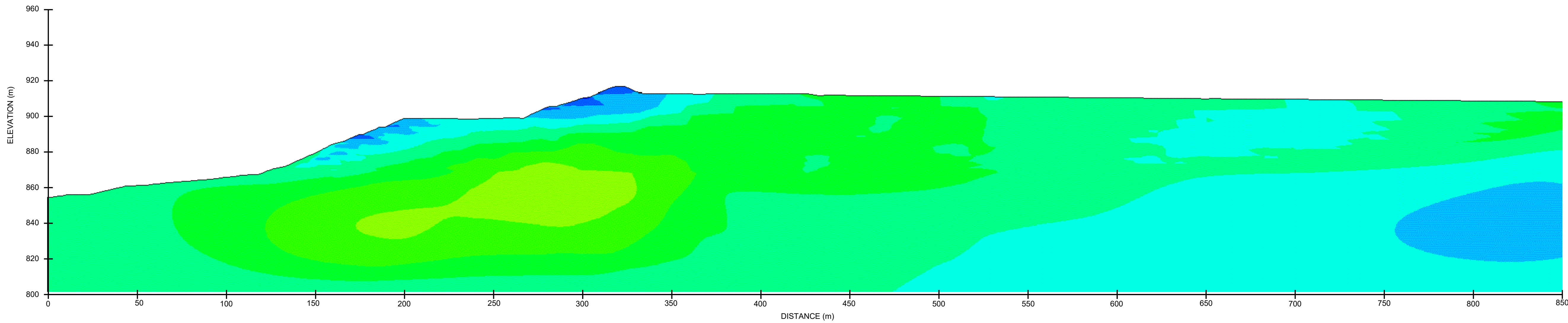

HORIZONTAL DISPLACEMENTS

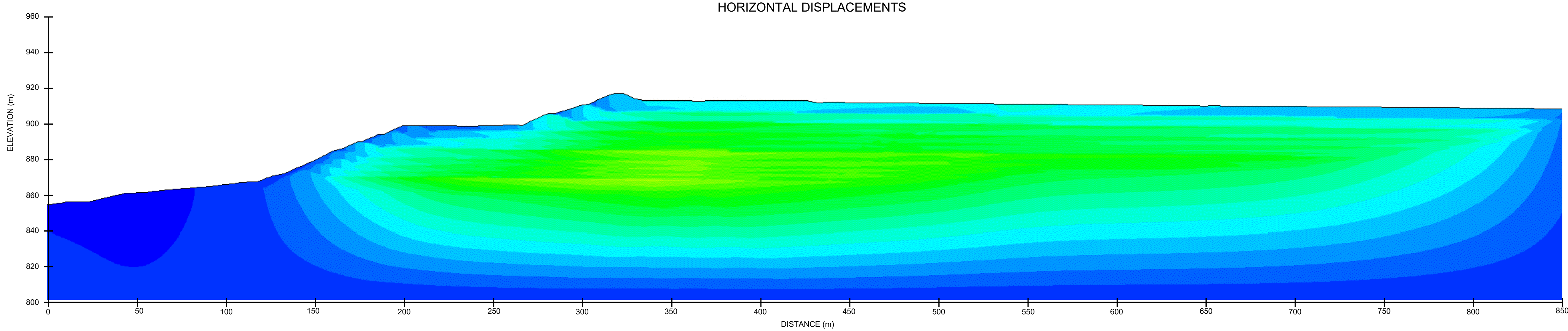

VERTICAL DISPLACEMENTS

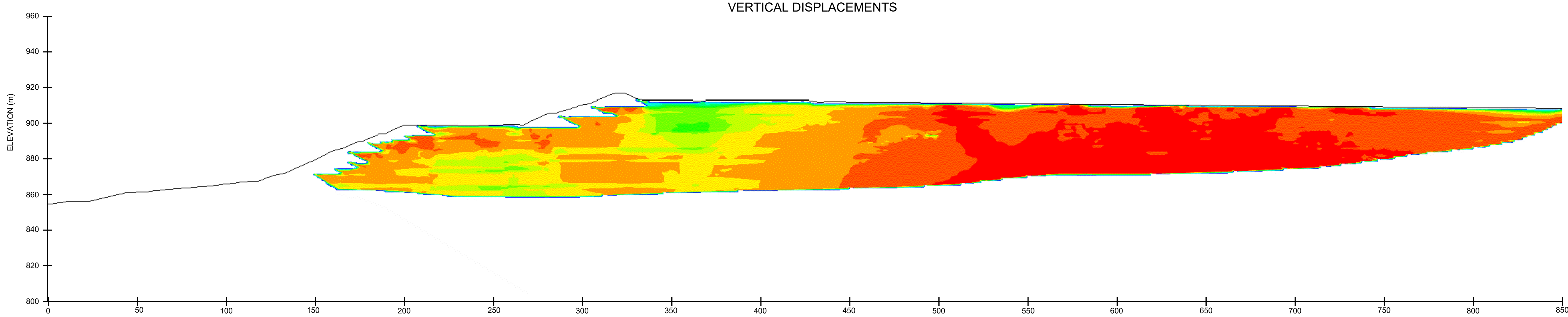

MOBILIZED STABILITY RATIO

1:2,500 0 25 50 m BASED ON A 11"X 17" DRAWING SIZE

NOTES:

1. ALL DIMENSIONS AND ELEVATIONS ARE IN METERS UNLESS STATED OTHERWISE.
2. MATERIAL PARAMETERS ARE OUTLINED IN APPENDIX E.

LEGEND:

HORIZONTAL DISPLACEMENTS (m)	VERTICAL DISPLACEMENTS	MOBILIZED INSTABILITY RATIO
-0.40	-2.10	0.40
-0.30	-1.80	0.50
-0.20	-1.50	0.60
-0.10	-1.20	0.70
0.0	-0.90	0.80
0.10	-0.60	0.90
0.20	-0.30	1.00
	0.00	1.10

CLIENT

PROJECT
REPORT OF THE EXPERT PANEL ON THE TECHNICAL CAUSES OF THE FAILURE OF FEIJÃO DAM 1

TITLE
APPENDIX H
2D DEFORMATION ANALYSIS RESULTS
MOHR COULOMB MODEL
SECTION 2-2' - EL. 916.5 m

SCALE	PROJECT No.	FIG. No.
1:2,500		5

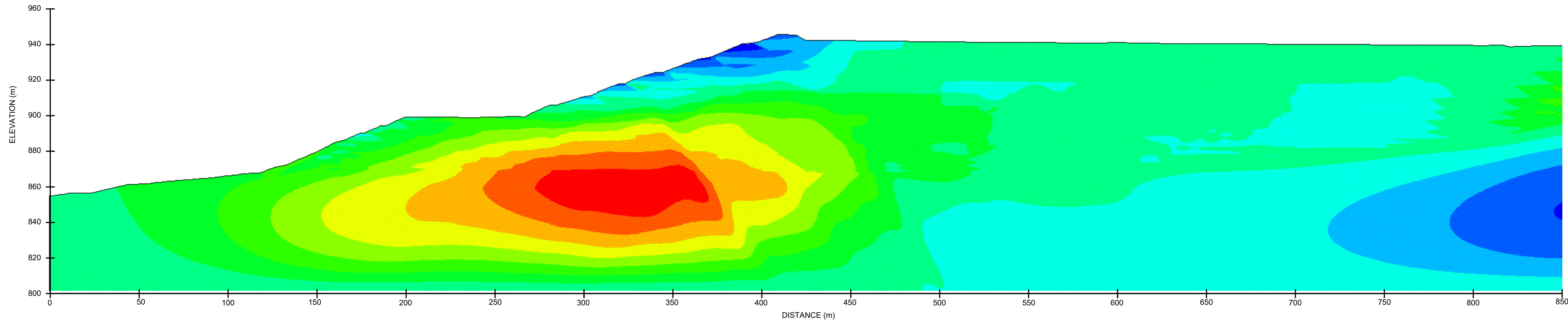

HORIZONTAL DISPLACEMENTS

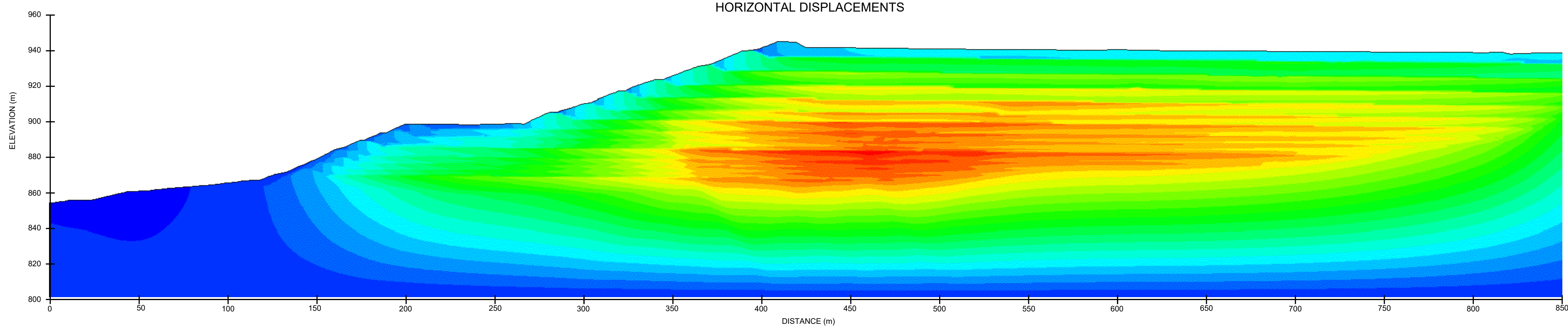

VERTICAL DISPLACEMENTS

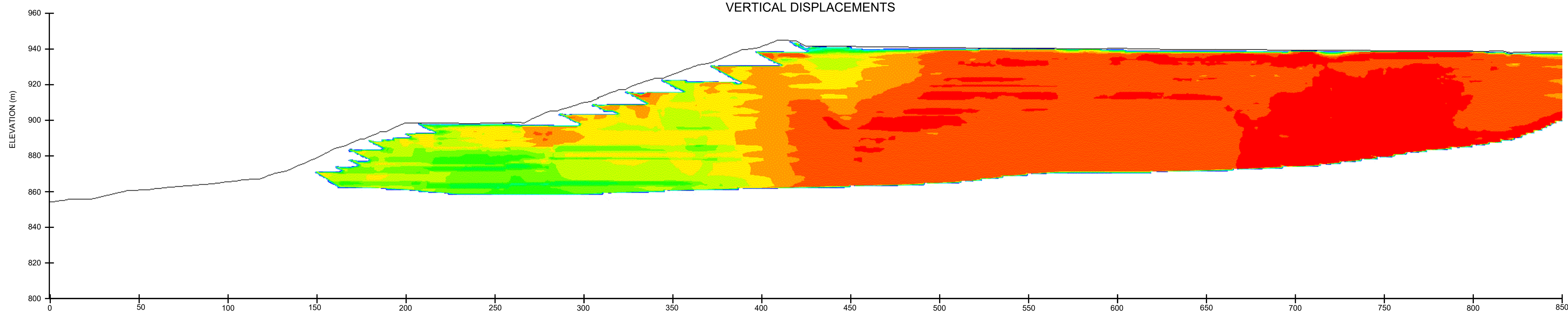

MOBILIZED STABILITY RATIO

1:2,500 0 25 50 m BASED ON A 11"X 17" DRAWING SIZE

NOTES:

1. ALL DIMENSIONS AND ELEVATIONS ARE IN METERS UNLESS STATED OTHERWISE.
2. MATERIAL PARAMETERS ARE OUTLINED IN APPENDIX E.

LEGEND:

HORIZONTAL DISPLACEMENTS (m)	VERTICAL DISPLACEMENTS	MOBILIZED INSTABILITY RATIO
-0.40	-2.10	0.40
-0.30	-1.80	0.50
-0.20	-1.50	0.60
-0.10	-1.20	0.70
0.0	-0.90	0.80
0.10	-0.60	0.90
0.20	-0.30	1.00
	0.00	1.10

CLIENT

PROJECT
REPORT OF THE EXPERT PANEL ON THE TECHNICAL CAUSES OF THE FAILURE OF FEIJÃO DAM 1

TITLE
APPENDIX H
2D DEFORMATION ANALYSIS RESULTS
MOHR COULOMB MODEL
SECTION 2-2' - EL. 942 m

SCALE	PROJECT No.	FIG. No.
1:2,500		6

KCB-FIG-B-L

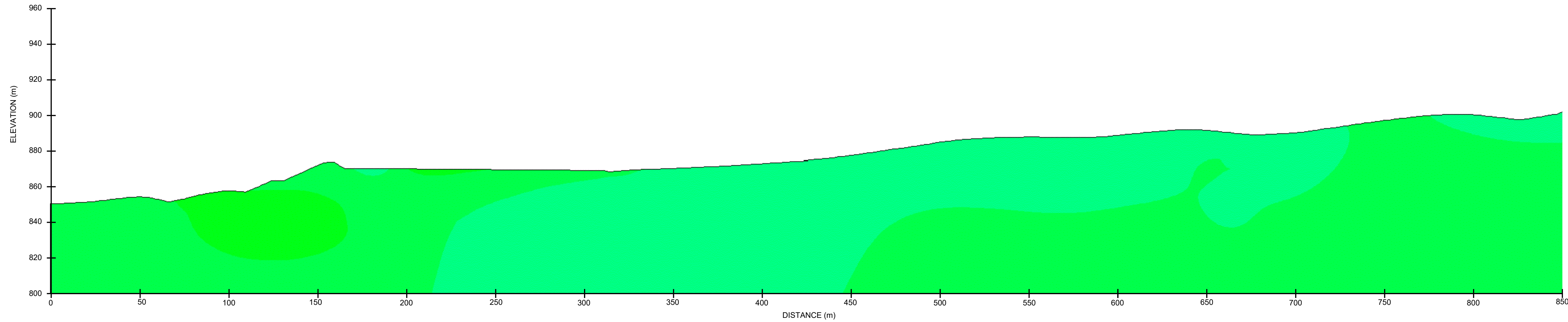

HORIZONTAL DISPLACEMENTS

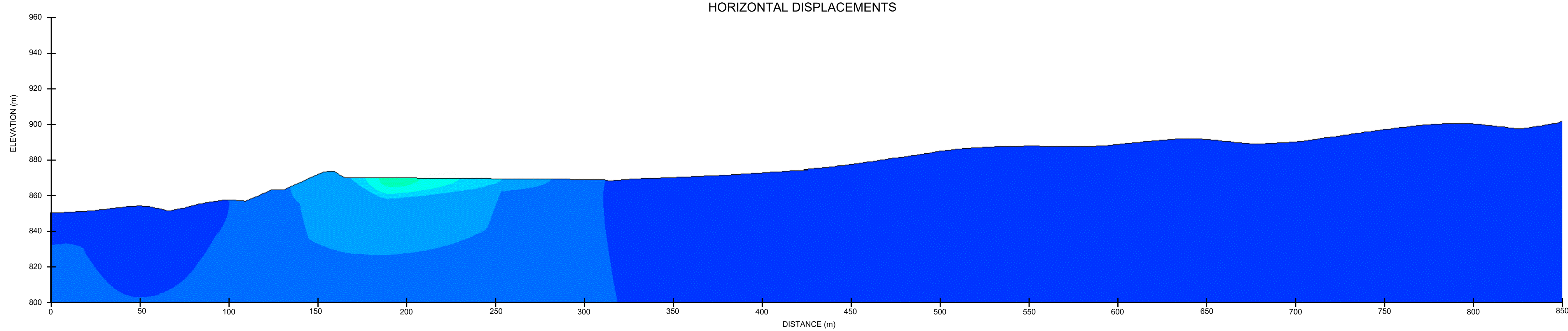

VERTICAL DISPLACEMENTS

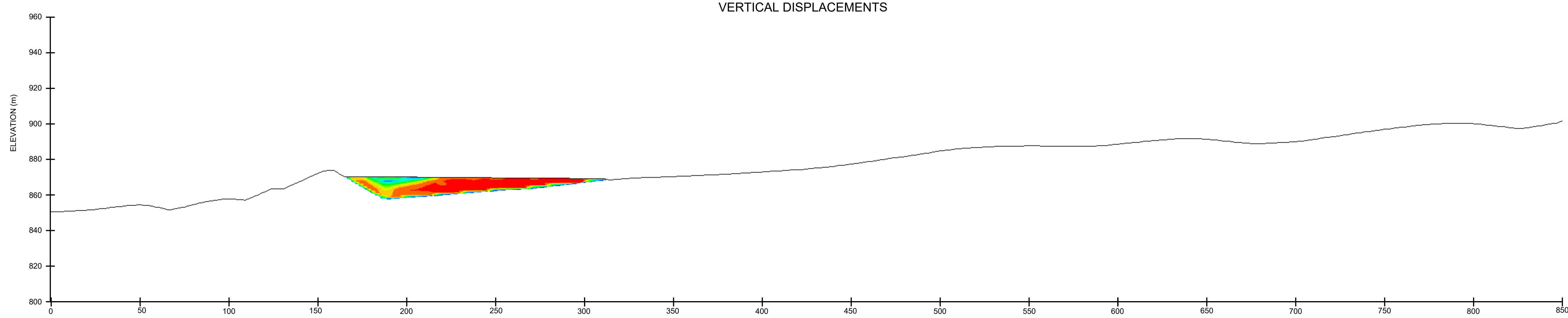

MOBILIZED STABILITY RATIO

1:2,500 0 25 50 m BASED ON A 11"X 17" DRAWING SIZE

NOTES:

1. ALL DIMENSIONS AND ELEVATIONS ARE IN METERS UNLESS STATED OTHERWISE.
2. MATERIAL PARAMETERS ARE OUTLINED IN APPENDIX E.

LEGEND:

HORIZONTAL DISPLACEMENTS (m)	VERTICAL DISPLACEMENTS	MOBILIZED INSTABILITY RATIO
-0.40	-2.10	0.40
-0.30	-1.80	0.50
-0.20	-1.50	0.60
-0.10	-1.20	0.70
0.00	-0.90	0.80
0.10	-0.60	0.90
0.20	-0.30	1.00
	-0.00	1.10

CLIENT

PROJECT
REPORT OF THE EXPERT PANEL ON THE TECHNICAL CAUSES OF THE FAILURE OF FEIJÃO DAM 1

TITLE
APPENDIX H
2D DEFORMATION ANALYSIS RESULTS
MOHR COULOMB MODEL
SECTION 3-3' - EL. 874 m

SCALE	PROJECT No.	FIG. No.
1:2,500		7

KCB-FIG-B-L

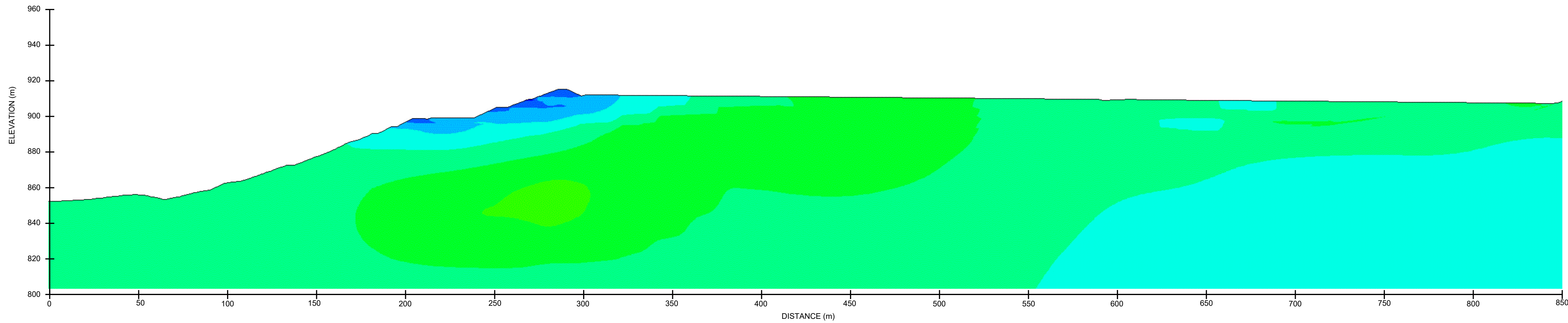

HORIZONTAL DISPLACEMENTS

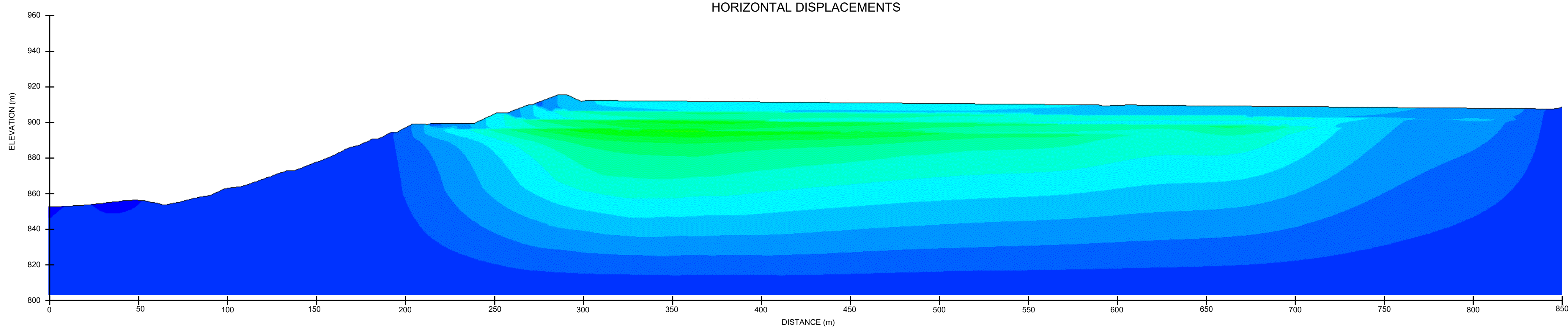

VERTICAL DISPLACEMENTS

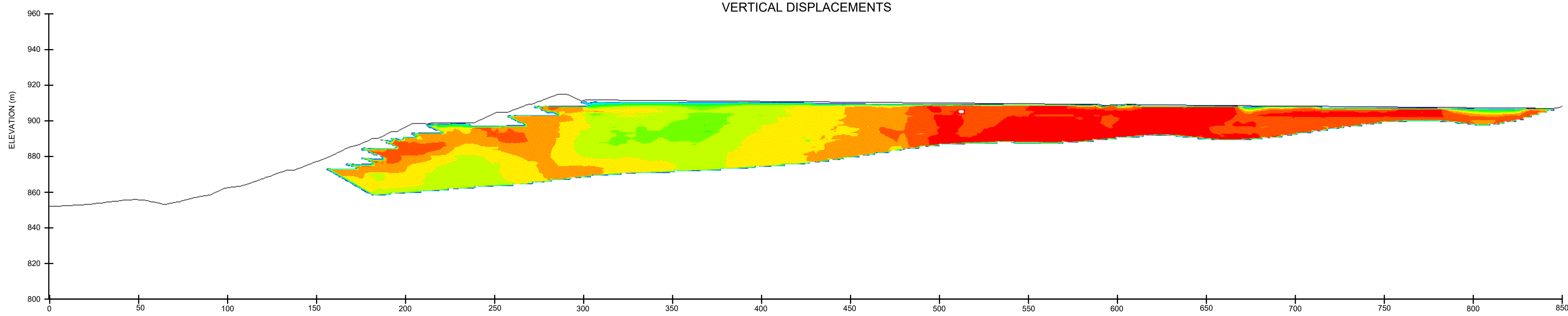

MOBILIZED STABILITY RATIO

1:2,500 0 25 50 m BASED ON A 11"X 17" DRAWING SIZE

NOTES:

1. ALL DIMENSIONS AND ELEVATIONS ARE IN METERS UNLESS STATED OTHERWISE.
2. MATERIAL PARAMETERS ARE OUTLINED IN APPENDIX E.

LEGEND:

HORIZONTAL DISPLACEMENTS (m)	VERTICAL DISPLACEMENTS	MOBILIZED INSTABILITY RATIO
-0.40	-2.10	0.40
-0.30	-1.80	0.50
-0.20	-1.50	0.60
-0.10	-1.20	0.70
0.00	-0.90	0.80
0.10	-0.60	0.90
0.20	-0.30	1.00
	-0.00	1.10

CLIENT

PROJECT
REPORT OF THE EXPERT PANEL ON THE TECHNICAL CAUSES OF THE FAILURE OF FEIJÃO DAM 1

TITLE
APPENDIX H
2D DEFORMATION ANALYSIS RESULTS
MOHR COULOMB MODEL
SECTION 3-3' - EL. 916.5 m

SCALE	PROJECT No.	FIG. No.
1:2,500		8

KCB-FIG-B-L

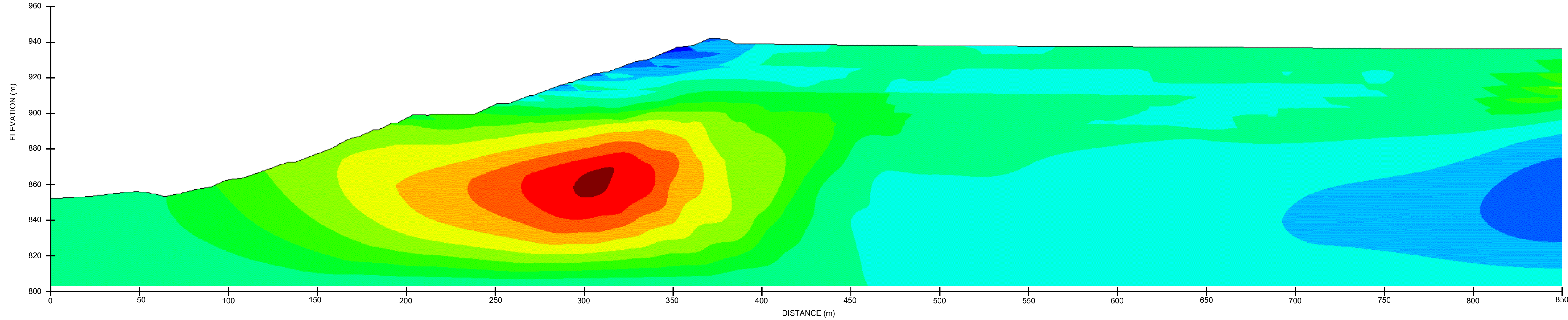

HORIZONTAL DISPLACEMENTS

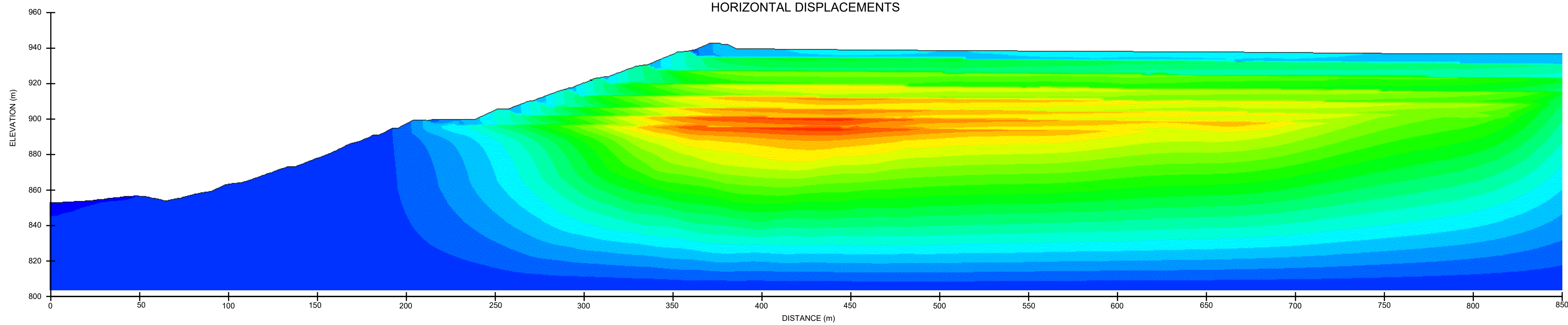

VERTICAL DISPLACEMENTS

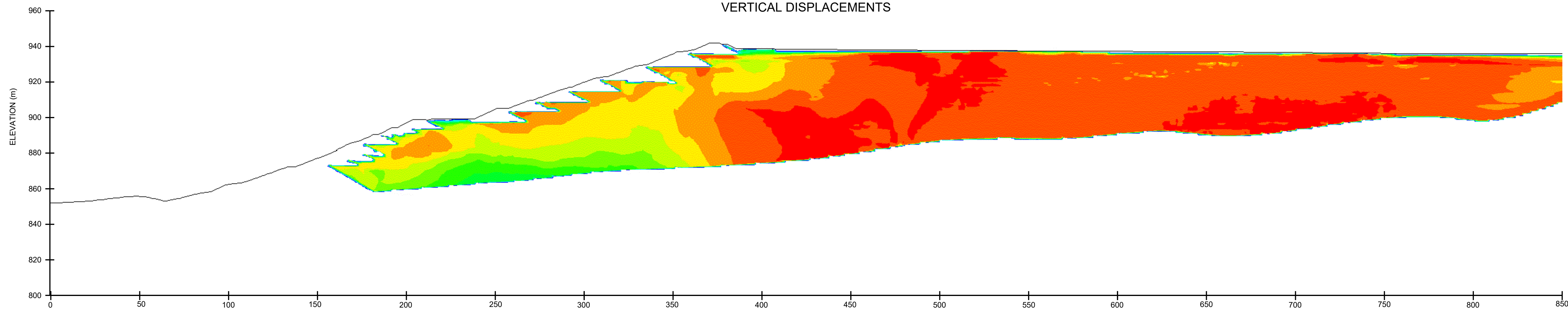

MOBILIZED STABILITY RATIO

1:2,500 0 25 50 m BASED ON A 11"X 17" DRAWING SIZE

NOTES:

1. ALL DIMENSIONS AND ELEVATIONS ARE IN METERS UNLESS STATED OTHERWISE.
2. MATERIAL PARAMETERS ARE OUTLINED IN APPENDIX E.

LEGEND:

HORIZONTAL DISPLACEMENTS (m)	VERTICAL DISPLACEMENTS	MOBILIZED INSTABILITY RATIO
-0.40	-2.10	0.40
-0.30	-1.80	0.50
-0.20	-1.50	0.60
-0.10	-1.20	0.70
0.00	-0.90	0.80
0.10	-0.60	0.90
0.20	-0.30	1.00
	-0.00	1.10

CLIENT

PROJECT
REPORT OF THE EXPERT PANEL ON THE TECHNICAL CAUSES OF THE FAILURE OF FEIJÃO DAM 1

TITLE
APPENDIX H
2D DEFORMATION ANALYSIS RESULTS
MOHR COULOMB MODEL
SECTION 3-3' - EL. 942 m

SCALE	PROJECT No.	FIG. No.
1:2,500		9

KCB-FIG-B-L

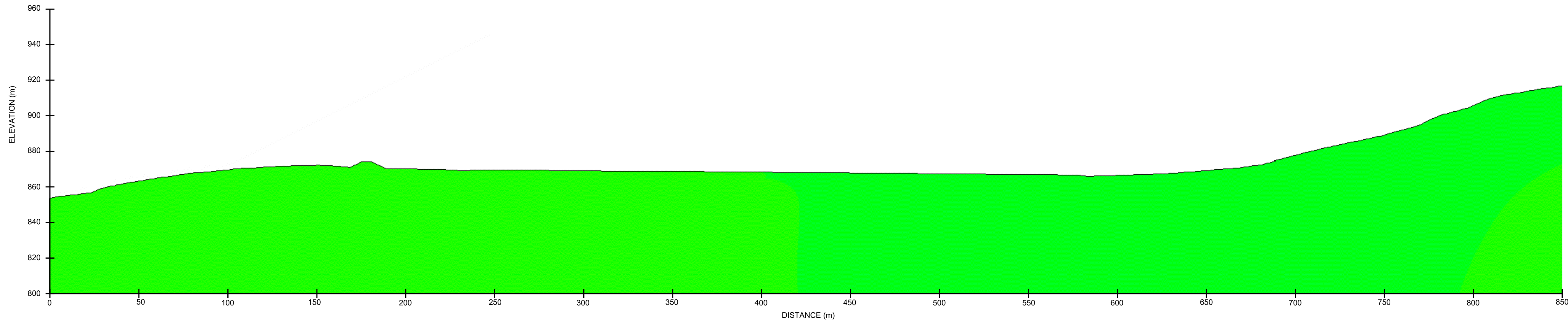

HORIZONTAL DISPLACEMENTS

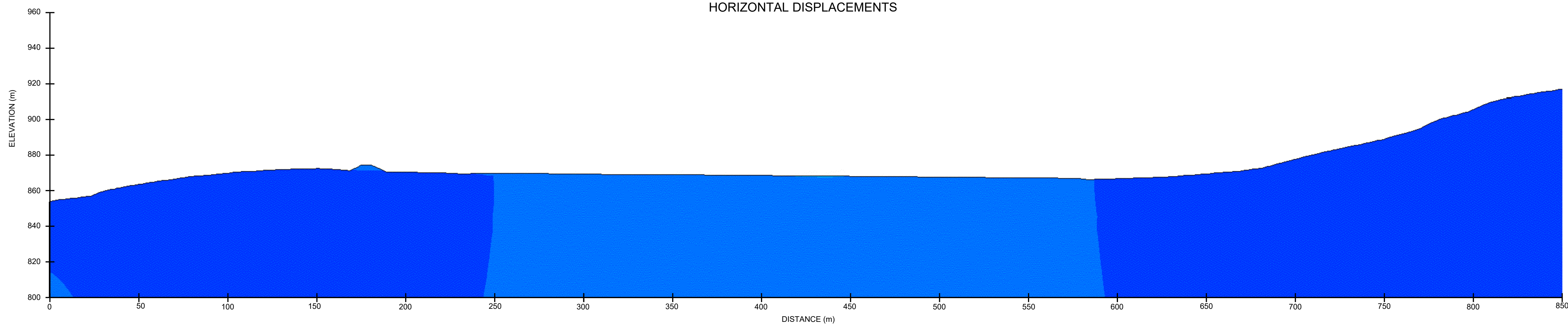

VERTICAL DISPLACEMENTS

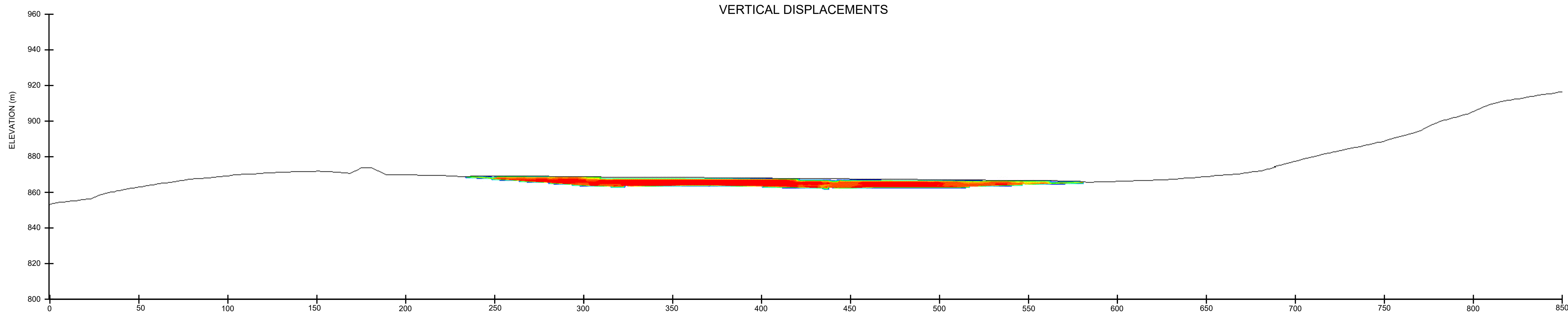

MOBILIZED STABILITY RATIO

1:2,500 0 25 50 m BASED ON A 11"X 17" DRAWING SIZE

NOTES:

1. ALL DIMENSIONS AND ELEVATIONS ARE IN METERS UNLESS STATED OTHERWISE.
2. MATERIAL PARAMETERS ARE OUTLINED IN APPENDIX E.

LEGEND:

HORIZONTAL DISPLACEMENTS (m)	VERTICAL DISPLACEMENTS	MOBILIZED INSTABILITY RATIO
-0.50	-1.70	0.40
-0.35	-1.40	0.50
-0.20	-1.10	0.60
-0.05	-0.80	0.70
0.10	-0.50	0.80
0.25	-0.20	0.90
0.40	-0.10	1.00
		1.10

CLIENT

PROJECT
REPORT OF THE EXPERT PANEL ON THE TECHNICAL CAUSES OF THE FAILURE OF FEIJÃO DAM 1

TITLE
APPENDIX H
2D DEFORMATION ANALYSIS RESULTS
STRAIN WEAKENING MODEL
SECTION 1-1' - EL. 877 m

SCALE 1:2,500 | PROJECT No. | FIG. No. 10

KCB-FIG-B-L

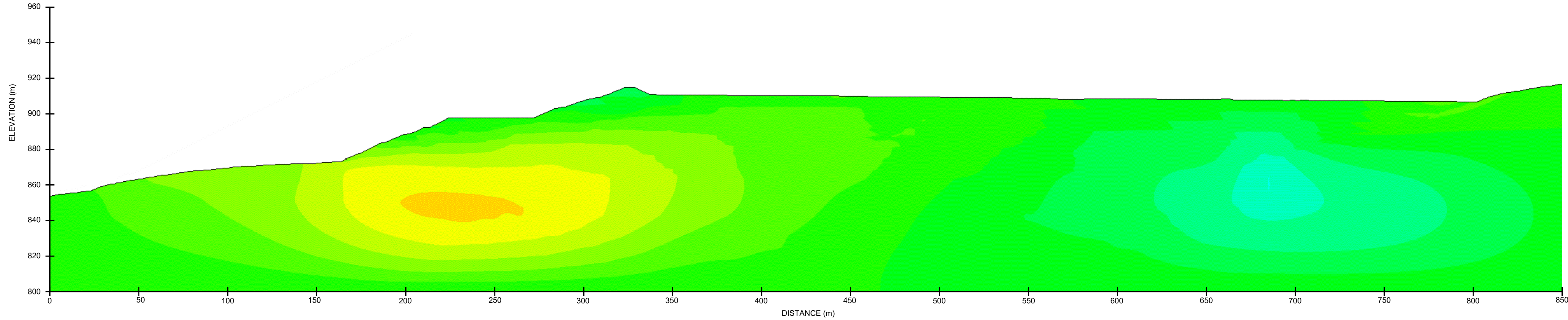

HORIZONTAL DISPLACEMENTS

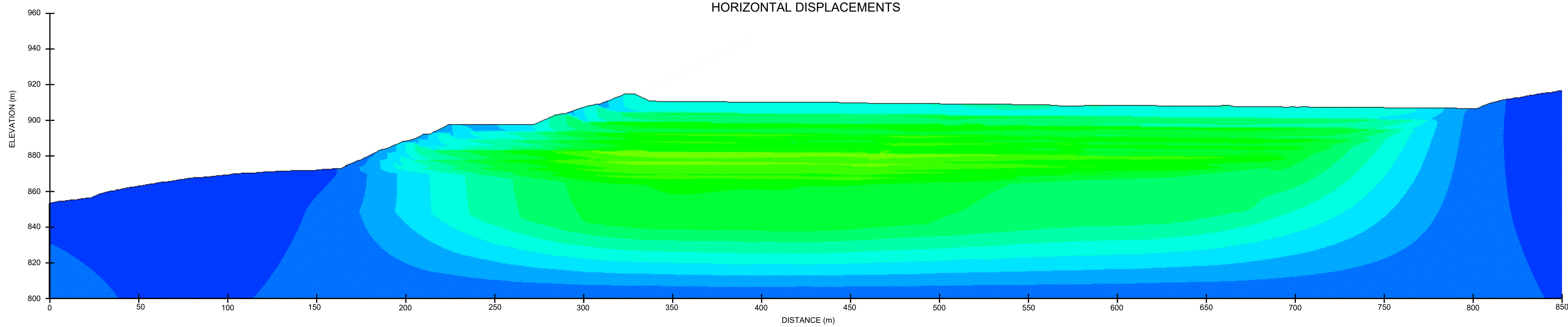

VERTICAL DISPLACEMENTS

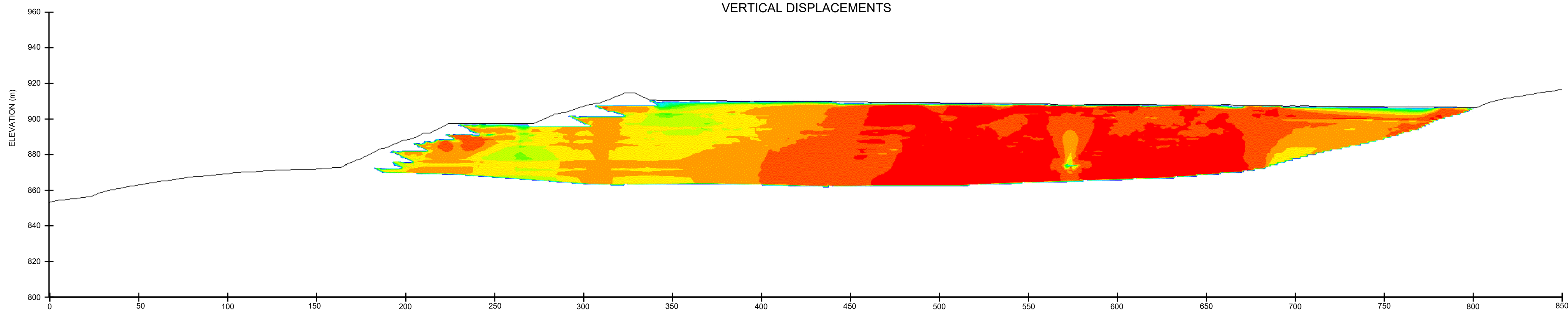

MOBILIZED STABILITY RATIO

1:2,500 0 25 50 m BASED ON A 11"X 17" DRAWING SIZE

NOTES:

1. ALL DIMENSIONS AND ELEVATIONS ARE IN METERS UNLESS STATED OTHERWISE.
2. MATERIAL PARAMETERS ARE OUTLINED IN APPENDIX E.

LEGEND:

HORIZONTAL DISPLACEMENTS (m)	VERTICAL DISPLACEMENTS	MOBILIZED INSTABILITY RATIO
-0.50	-1.70	0.40
-0.35	-1.40	0.50
-0.20	-1.10	0.60
-0.05	-0.80	0.70
0.10	-0.50	0.80
0.25	-0.20	0.90
0.40	-0.10	1.00
		1.10

CLIENT

PROJECT
REPORT OF THE EXPERT PANEL ON THE TECHNICAL CAUSES OF THE FAILURE OF FEIJÃO DAM 1

TITLE
APPENDIX H
2D DEFORMATION ANALYSIS RESULTS
STRAIN WEAKENING MODEL
SECTION 1-1' - EL. 916.5 m

SCALE	PROJECT No.	FIG. No.
1:2,500		11

KCB-FIG-B-L

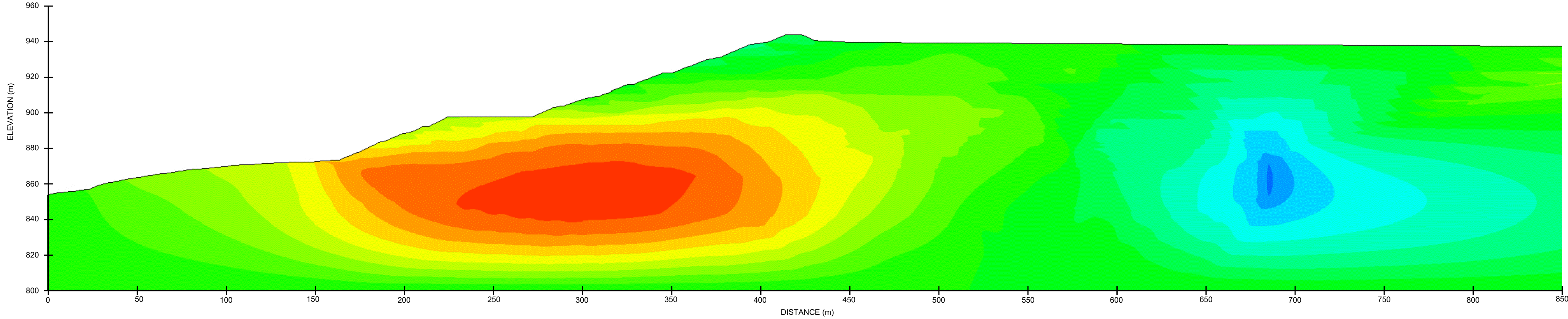

HORIZONTAL DISPLACEMENTS

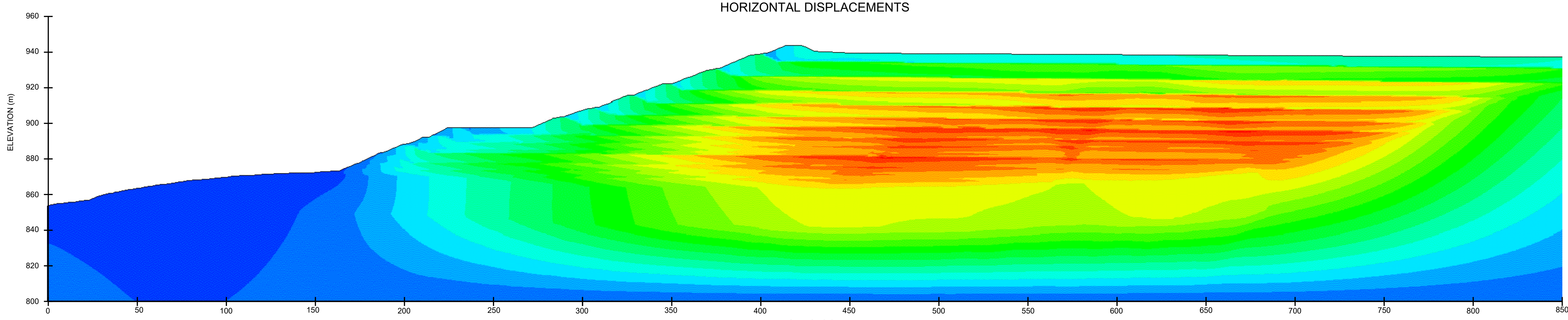

VERTICAL DISPLACEMENTS

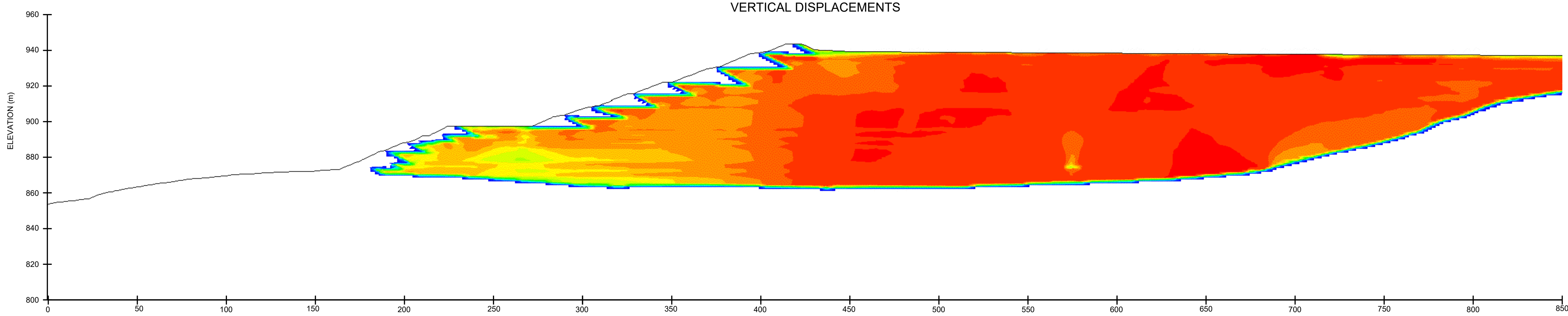

MOBILIZED STABILITY RATIO

1:2,500 0 25 50 m BASED ON A 11"X 17" DRAWING SIZE

NOTES:

1. ALL DIMENSIONS AND ELEVATIONS ARE IN METERS UNLESS STATED OTHERWISE.
2. MATERIAL PARAMETERS ARE OUTLINED IN APPENDIX E.

LEGEND:

HORIZONTAL DISPLACEMENTS (m)	VERTICAL DISPLACEMENTS	MOBILIZED INSTABILITY RATIO
-0.50	-1.70	0.00
-0.35	-1.40	0.15
-0.20	-1.10	0.30
-0.05	-0.80	0.45
0.10	-0.50	0.60
0.25	-0.20	0.75
0.40	-0.10	0.90
		1.05

CLIENT

PROJECT
REPORT OF THE EXPERT PANEL ON THE TECHNICAL CAUSES OF THE FAILURE OF FEIJÃO DAM 1

TITLE
APPENDIX H
2D DEFORMATION ANALYSIS RESULTS
STRAIN WEAKENING MODEL
SECTION 1-1' - EL. 942 m

SCALE 1:2,500 | PROJECT No. | FIG. No. 12

KCB-FIG-B-L

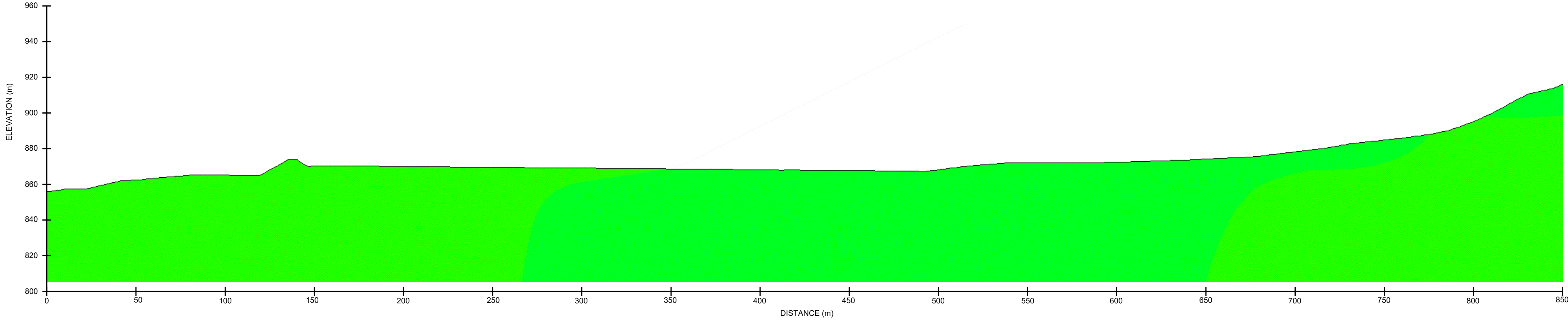

HORIZONTAL DISPLACEMENTS

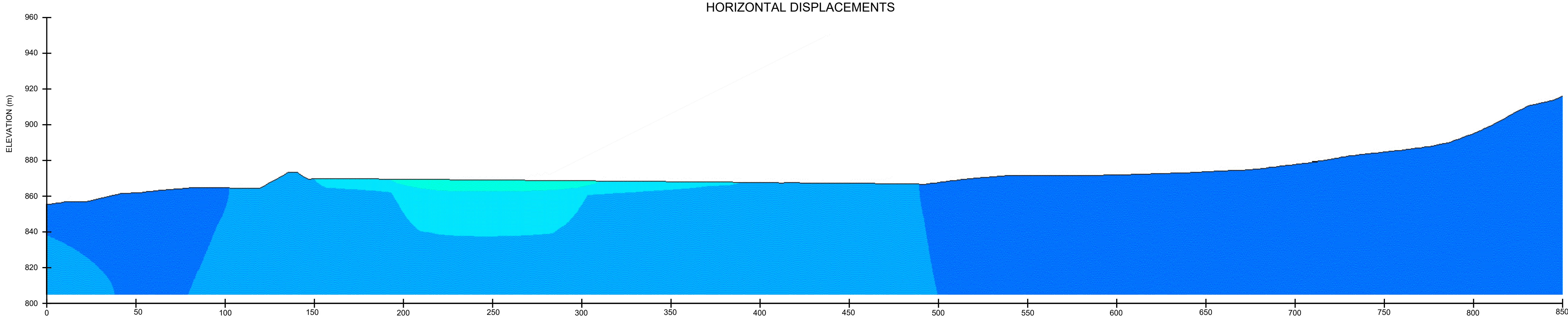

VERTICAL DISPLACEMENTS

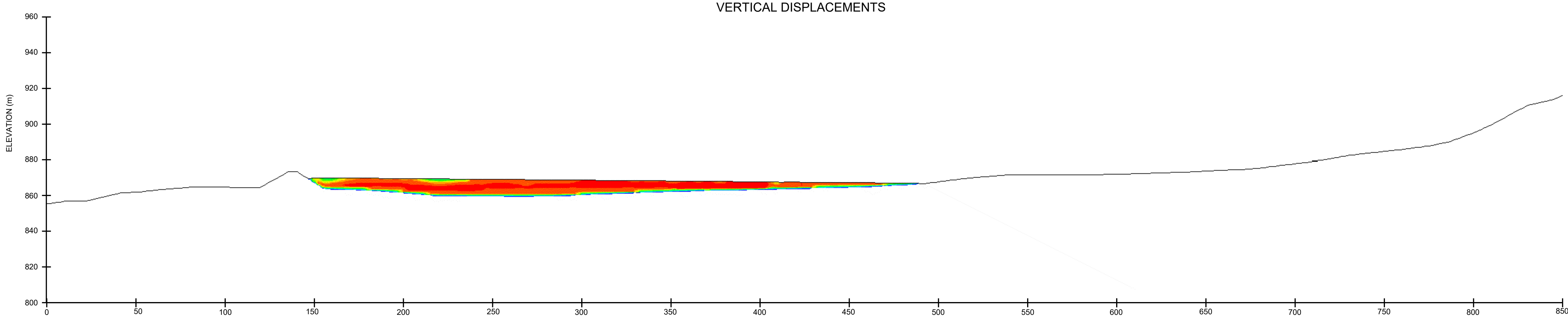

MOBILIZED STABILITY RATIO

1:2,500 0 25 50 m BASED ON A 11"X 17" DRAWING SIZE

NOTES:

1. ALL DIMENSIONS AND ELEVATIONS ARE IN METERS UNLESS STATED OTHERWISE.
2. MATERIAL PARAMETERS ARE OUTLINED IN APPENDIX E.

LEGEND:

HORIZONTAL DISPLACEMENTS (m)	VERTICAL DISPLACEMENTS	MOBILIZED INSTABILITY RATIO
-0.40	-1.70	0.40
-0.30	-1.40	0.50
-0.20	-1.10	0.60
-0.05	-0.80	0.70
0.00	-0.50	0.80
0.10	-0.20	0.90
0.20	-0.10	1.00
0.30		1.10
0.40		

CLIENT

PROJECT
REPORT OF THE EXPERT PANEL ON THE TECHNICAL CAUSES OF THE FAILURE OF FEIJÃO DAM 1

TITLE
APPENDIX H
2D DEFORMATION ANALYSIS RESULTS
STRAIN WEAKENING MODEL
SECTION 2-2' - EL. 874 m

SCALE	PROJECT No.	FIG. No.
1:2,500		13

KCB-FIG-B-L

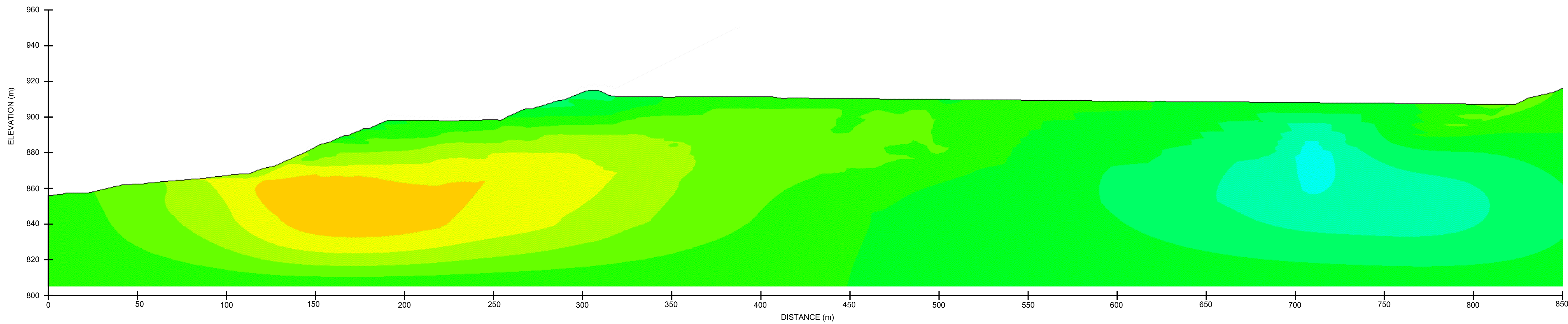

HORIZONTAL DISPLACEMENTS

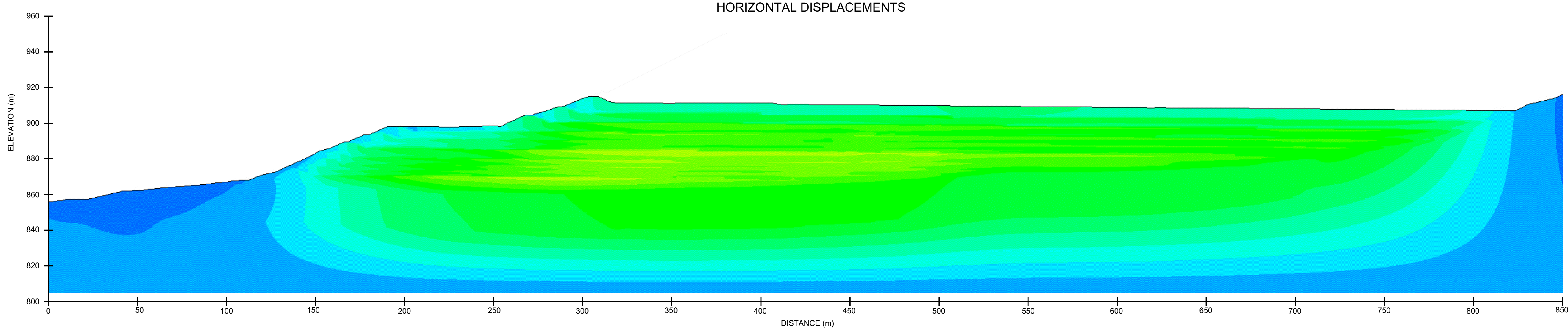

VERTICAL DISPLACEMENTS

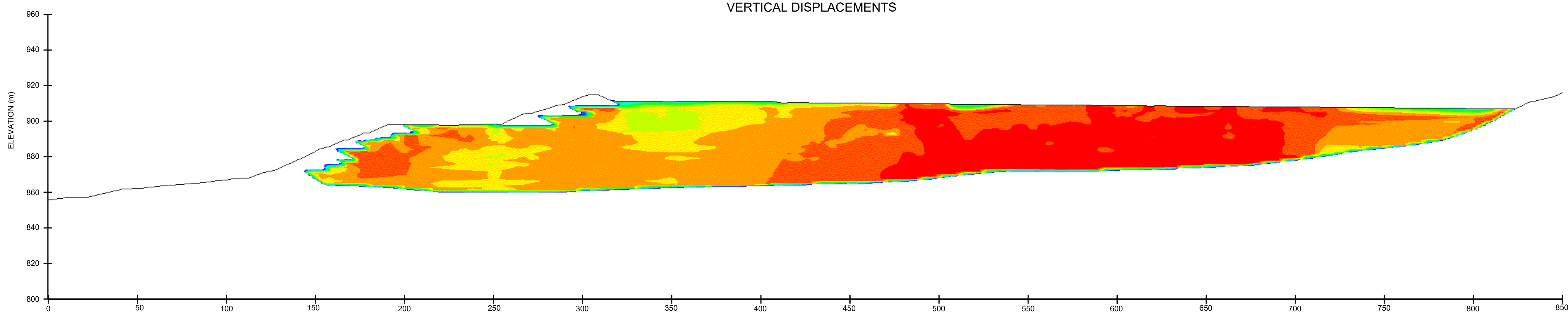

MOBILIZED STABILITY RATIO

1:2,500 0 25 50 m BASED ON A 11"X 17" DRAWING SIZE

NOTES:

1. ALL DIMENSIONS AND ELEVATIONS ARE IN METERS UNLESS STATED OTHERWISE.
2. MATERIAL PARAMETERS ARE OUTLINED IN APPENDIX E.

LEGEND:

HORIZONTAL DISPLACEMENTS (m)	VERTICAL DISPLACEMENTS	MOBILIZED INSTABILITY RATIO
-0.40	-1.70	0.40
-0.30	-1.40	0.50
-0.20	-1.10	0.60
-0.05	-0.80	0.70
0.00	-0.50	0.80
0.10	-0.20	0.90
0.20	-0.10	1.00
0.30		1.10

CLIENT

PROJECT
REPORT OF THE EXPERT PANEL ON THE TECHNICAL CAUSES OF THE FAILURE OF FEIJÃO DAM 1

TITLE
APPENDIX H
2D DEFORMATION ANALYSIS RESULTS
STRAIN WEAKENING MODEL
SECTION 2-2' - EL. 916.5 m

SCALE	PROJECT No.	FIG. No.
1:2,500		14

KCB-FIG-B-L

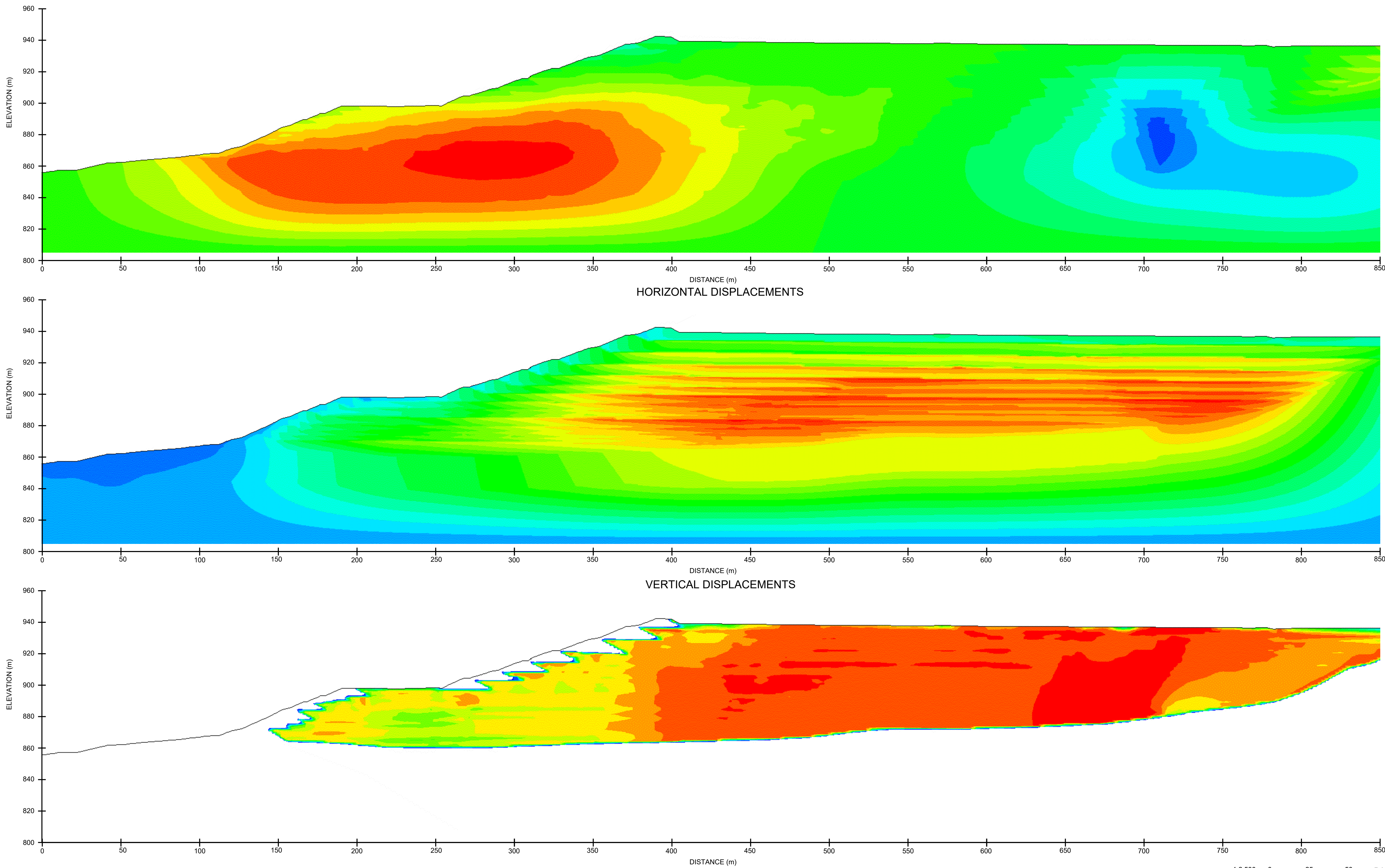

1:2,500 0 25 50 m BASED ON A 11"X 17" DRAWING SIZE

NOTES:

1. ALL DIMENSIONS AND ELEVATIONS ARE IN METERS UNLESS STATED OTHERWISE.
2. MATERIAL PARAMETERS ARE OUTLINED IN APPENDIX E.

LEGEND:

HORIZONTAL DISPLACEMENTS (m): -0.40, -0.30, -0.20, -0.05, 0.00, 0.10, 0.20, 0.30

VERTICAL DISPLACEMENTS: -1.70, -1.40, -1.10, -0.80, -0.50, -0.20, -0.10

MOBILIZED INSTABILITY RATIO: 0.40, 0.50, 0.60, 0.70, 0.80, 0.90, 1.00, 1.10

CLIENT	PROJECT
	REPORT OF THE EXPERT PANEL ON THE TECHNICAL CAUSES OF THE FAILURE OF FEIJÃO DAM 1
	TITLE: APPENDIX H 2D DEFORMATION ANALYSIS RESULTS STRAIN WEAKENING MODEL SECTION 2-2' - EL. 942 m

SCALE	PROJECT No.	FIG. No.
1:2,500		15

KCB-FIG-B-L

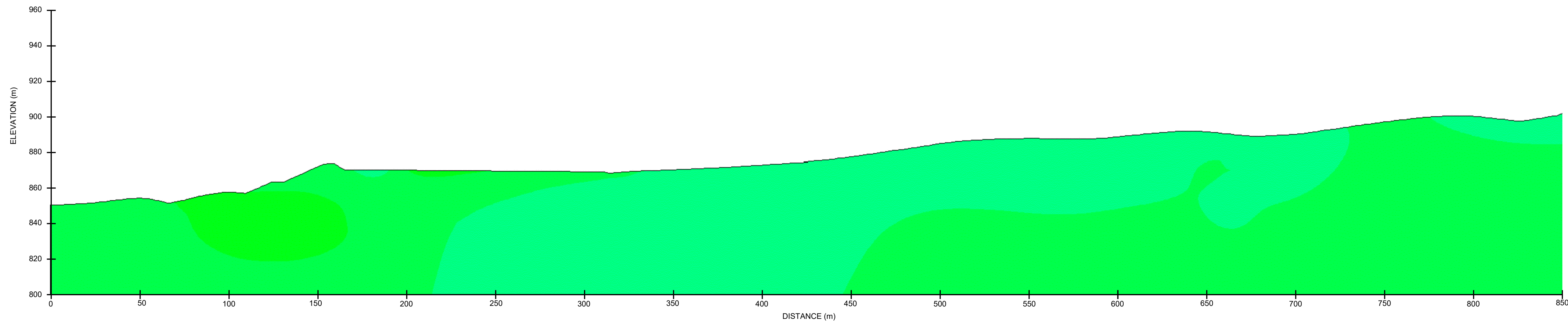

HORIZONTAL DISPLACEMENTS

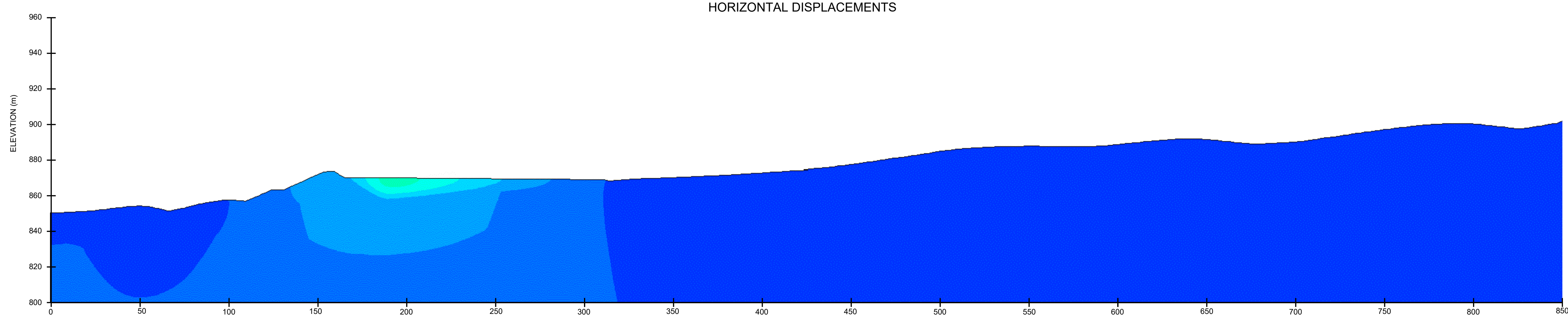

VERTICAL DISPLACEMENTS

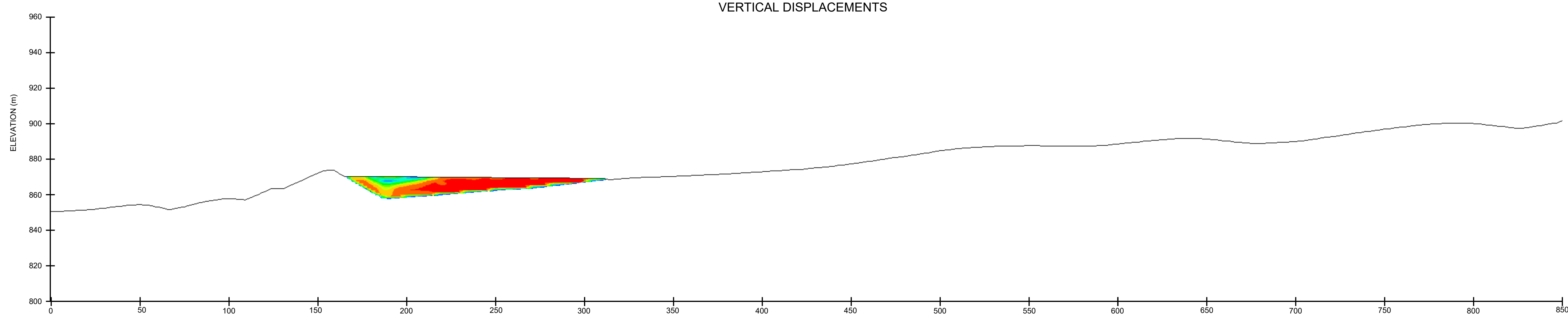

MOBILIZED STABILITY RATIO

1:2,500 0 25 50 m BASED ON A 11"X 17" DRAWING SIZE

NOTES:

1. ALL DIMENSIONS AND ELEVATIONS ARE IN METERS UNLESS STATED OTHERWISE.
2. MATERIAL PARAMETERS ARE OUTLINED IN APPENDIX E.

LEGEND:

HORIZONTAL DISPLACEMENTS (m)	VERTICAL DISPLACEMENTS	MOBILIZED INSTABILITY RATIO
-0.60	-1.80	0.55
-0.45	-1.50	0.65
-0.30	-1.20	0.75
-0.15	-0.90	0.85
0.00	-0.60	0.95
0.15	-0.30	1.05
0.30	-0.00	

CLIENT

PROJECT
REPORT OF THE EXPERT PANEL ON THE TECHNICAL CAUSES OF THE FAILURE OF FEIJÃO DAM 1

TITLE
APPENDIX H
2D DEFORMATION ANALYSIS RESULTS
STRAIN WEAKENING MODEL
SECTION 3-3' - EL. 874 m

SCALE	PROJECT No.	FIG. No.
1:2,500		16

KCB-FIG-B-L

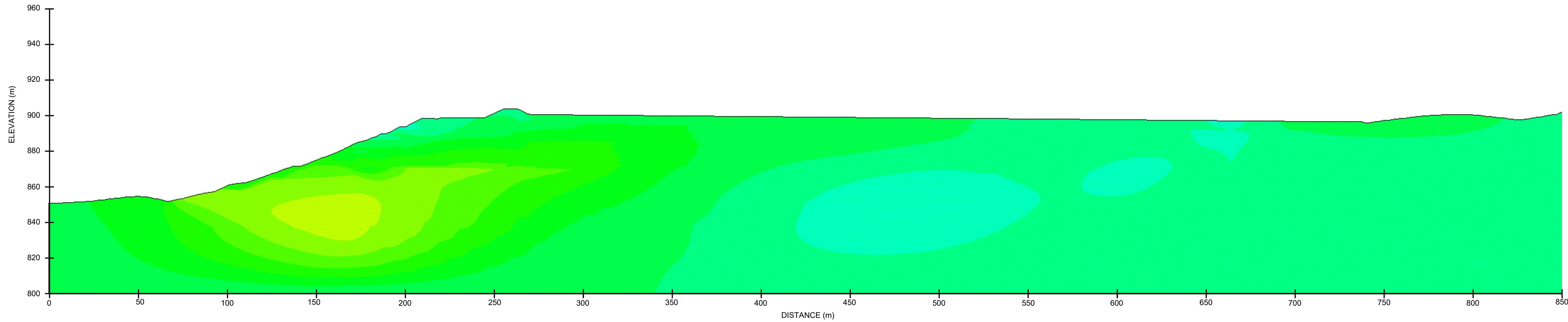

HORIZONTAL DISPLACEMENTS

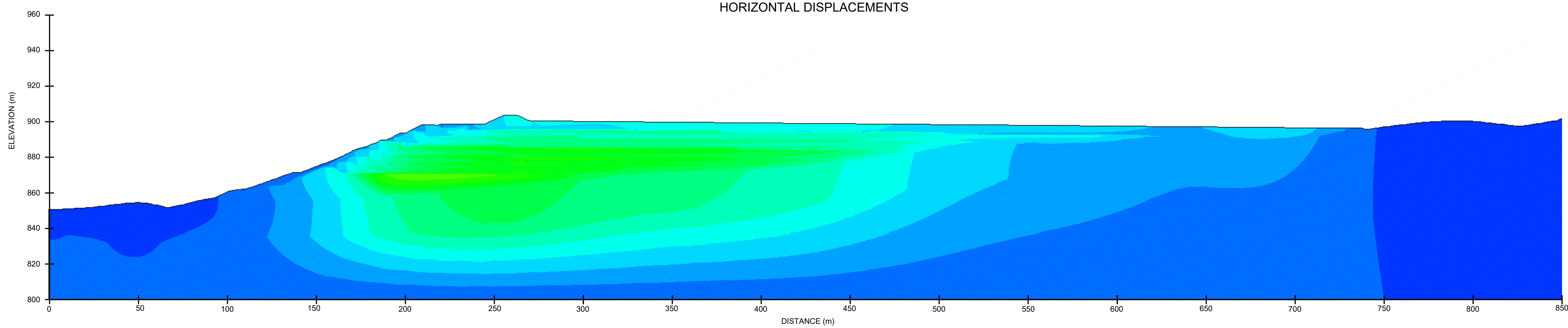

VERTICAL DISPLACEMENTS

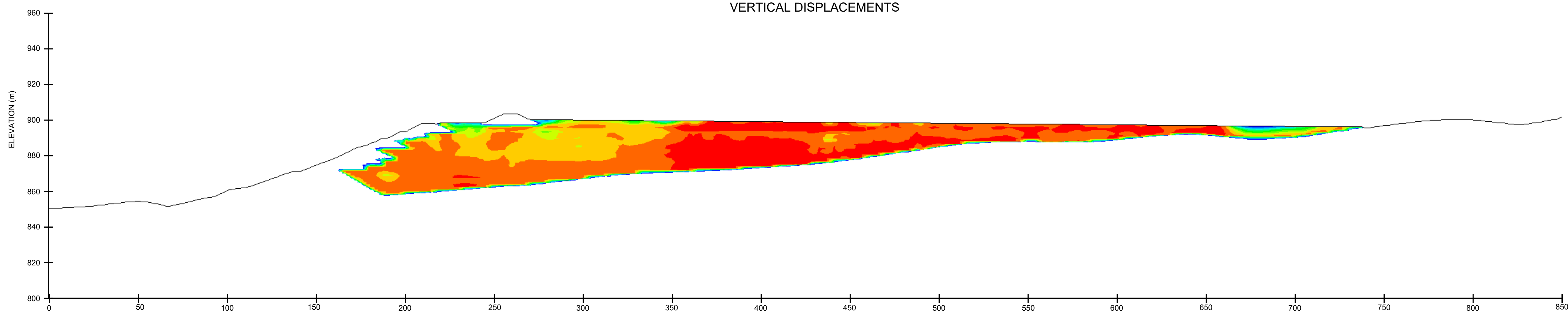

MOBILIZED STABILITY RATIO

1:2,500 0 25 50 m BASED ON A 11"X 17" DRAWING SIZE

NOTES:

1. ALL DIMENSIONS AND ELEVATIONS ARE IN METERS UNLESS STATED OTHERWISE.
2. MATERIAL PARAMETERS ARE OUTLINED IN APPENDIX E.

LEGEND:

HORIZONTAL DISPLACEMENTS (m)	VERTICAL DISPLACEMENTS	MOBILIZED INSTABILITY RATIO
-0.60	-1.80	0.55
-0.45	-1.50	0.65
-0.30	-1.20	0.75
-0.15	-0.90	0.85
0.00	-0.60	0.95
0.15	-0.30	1.05
0.30	-0.00	

CLIENT

PROJECT
REPORT OF THE EXPERT PANEL ON THE TECHNICAL CAUSES OF THE FAILURE OF FEIJÃO DAM 1

TITLE
APPENDIX H
2D DEFORMATION ANALYSIS RESULTS
STRAIN WEAKENING MODEL
SECTION 3-3' - EL. 916.5 m

SCALE	PROJECT No.	FIG. No.
1:2,500		17

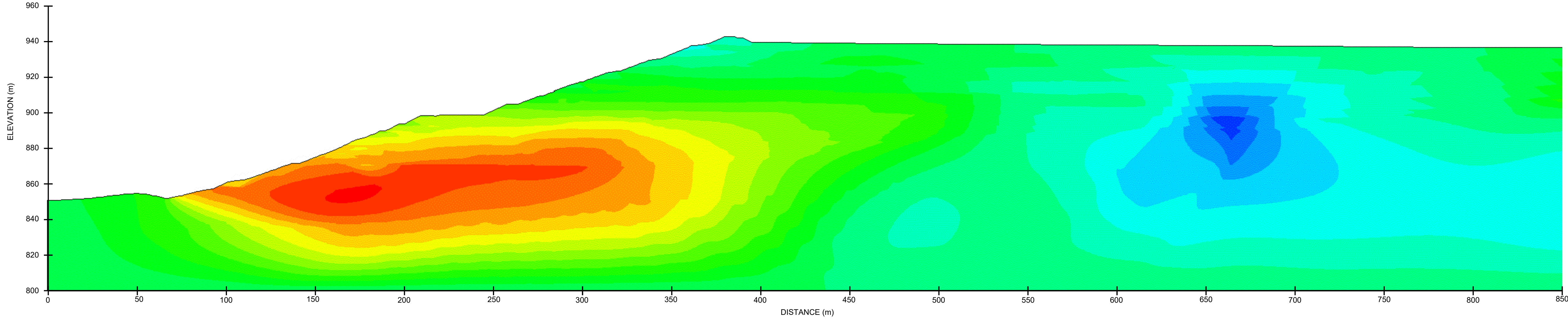

HORIZONTAL DISPLACEMENTS

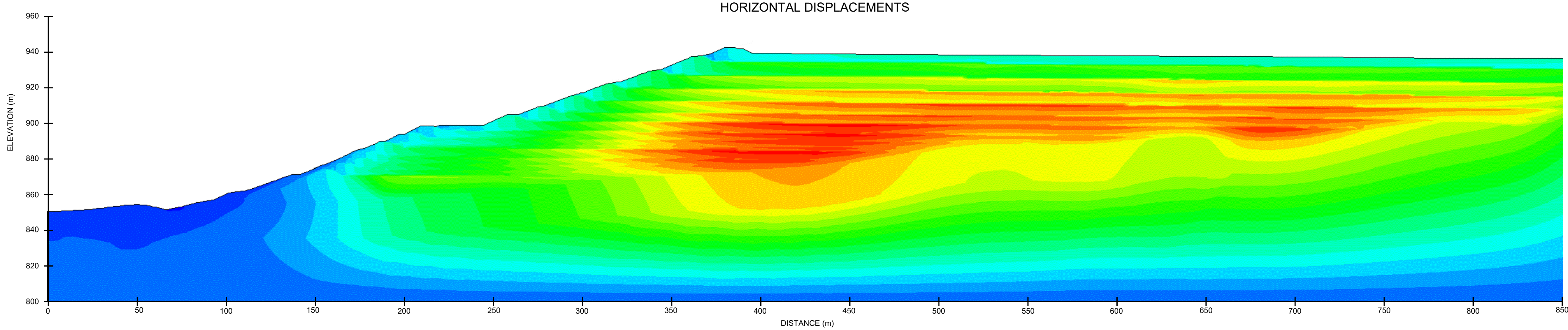

VERTICAL DISPLACEMENTS

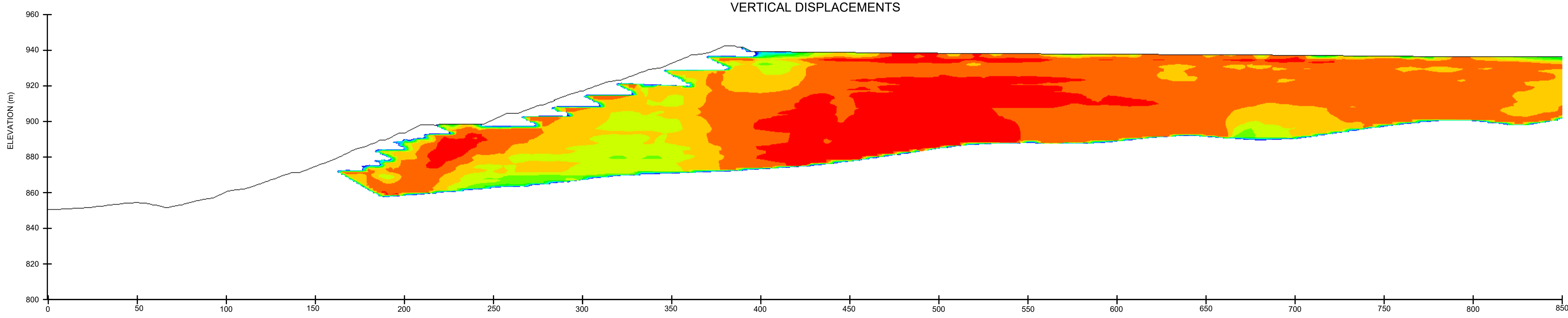

MOBILIZED STABILITY RATIO

1:2,500 0 25 50 m BASED ON A 11"X 17" DRAWING SIZE

NOTES:

1. ALL DIMENSIONS AND ELEVATIONS ARE IN METERS UNLESS STATED OTHERWISE.
2. MATERIAL PARAMETERS ARE OUTLINED IN APPENDIX E.

LEGEND:

HORIZONTAL DISPLACEMENTS (m)	VERTICAL DISPLACEMENTS	MOBILIZED INSTABILITY RATIO
-0.60	-1.80	0.55
-0.45	-1.50	0.65
-0.30	-1.20	0.75
-0.15	-0.90	0.85
0.00	-0.60	0.95
0.15	-0.30	1.05
0.30	-0.00	

CLIENT

PROJECT
REPORT OF THE EXPERT PANEL ON THE TECHNICAL CAUSES OF THE FAILURE OF FEIJÃO DAM 1

TITLE
APPENDIX H
2D DEFORMATION ANALYSIS RESULTS
STRAIN WEAKENING MODEL
SECTION 3-3' - EL. 942 m

SCALE	PROJECT No.	FIG. No.
1:2,500		18

Appendix H

Annex 2 – 2D Equilibrium Stability Results

December 2019

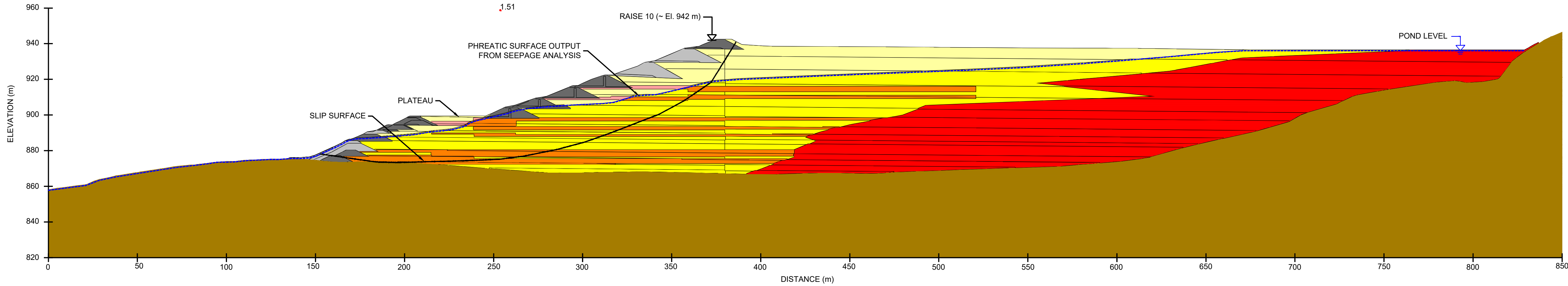

CASE 1-01A - CREST TO TOE

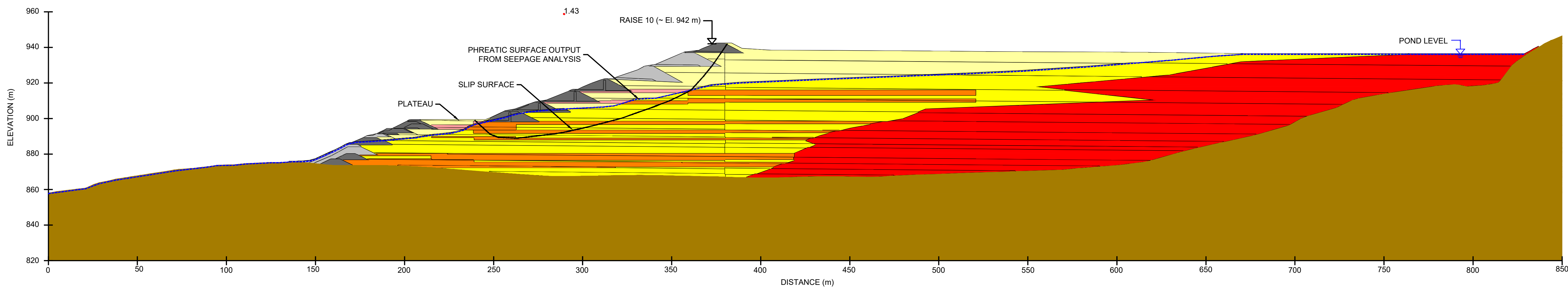

CASE 1-01B - CREST TO PLATEAU

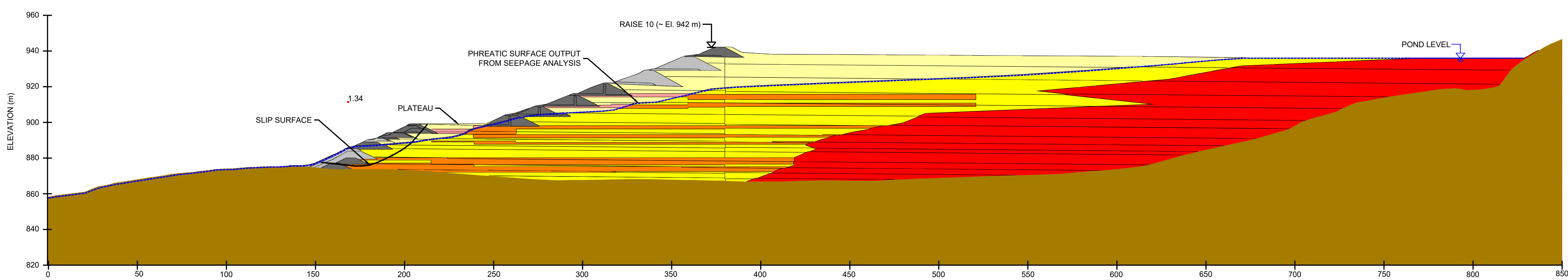

CASE 1-01C - PLATEAU TO TOE

1:2,500 0 25 50 m BASED ON A 11"X 17" DRAWING SIZE

NOTES:

1. ALL DIMENSIONS AND ELEVATIONS ARE IN METERS UNLESS STATED OTHERWISE.
2. MATERIAL PARAMETERS ARE OUTLINED IN APPENDIX E.
3. ONLY SLIP SURFACES CONSIDERED MOST CRITICAL ARE PRESENTED.

LEGEND:

- COARSE TAILINGS
- FINE TAILINGS
- COMPACTED BERM FILL (TAILINGS)
- COMPACTED BERM FILL (RESIDUAL SOIL)
- FOUNDATION SOIL
- SLIMES
- COARSE TAILINGS (DRAINED)
- FINE TAILINGS (DRAINED)
- PHREATIC SURFACE
- POND LEVEL

CLIENT

PROJECT
REPORT OF THE EXPERT PANEL ON THE TECHNICAL CAUSES OF THE FAILURE OF FEIJÃO DAM 1

TITLE
STABILITY ANALYSIS RESULTS
SECTION 1-1' - EL. 942 m
PEAK STRENGTH

SCALE	PROJECT No.	FIG. No.
1:2,500	A03355A01	1

KCB-FIG-B-L

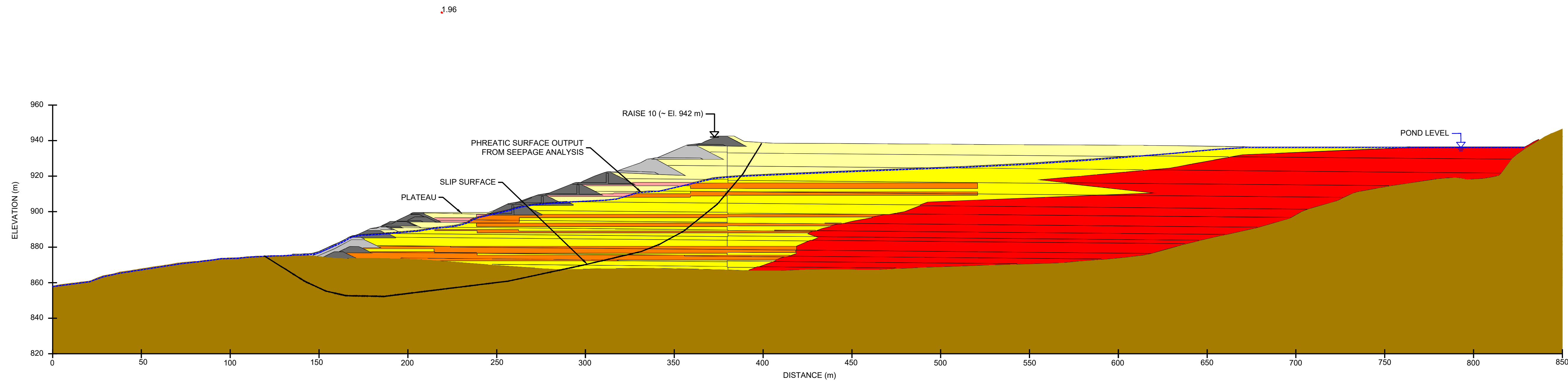

CASE 1-01D - CREST TO TOE

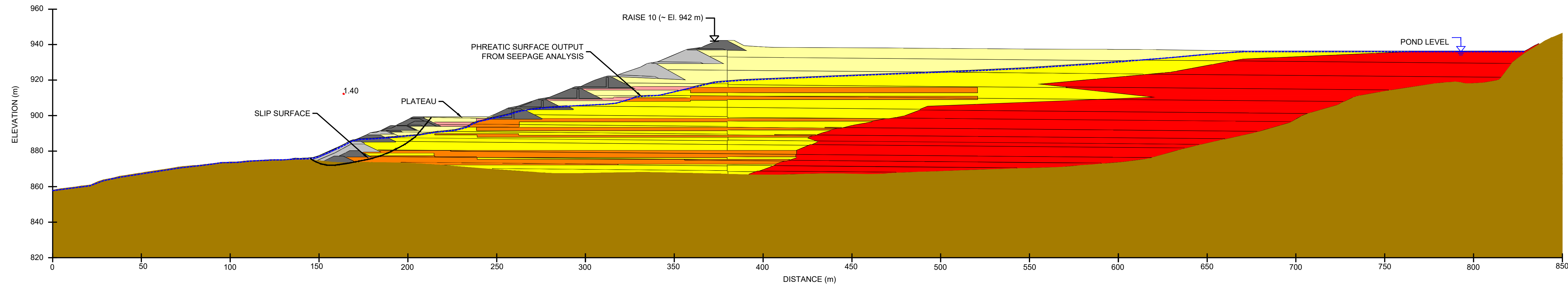

CASE 1-01E - PLATEAU TO TOE

1:2,500 0 25 50 m BASED ON A 11"X 17" DRAWING SIZE

NOTES:

1. ALL DIMENSIONS AND ELEVATIONS ARE IN METERS UNLESS STATED OTHERWISE.
2. MATERIAL PARAMETERS ARE OUTLINED IN APPENDIX E.
3. ONLY SLIP SURFACES CONSIDERED MOST CRITICAL ARE PRESENTED.

LEGEND:

- COARSE TAILINGS
- FINE TAILINGS
- COMPACTED BERM FILL (TAILINGS)
- COMPACTED BERM FILL (RESIDUAL SOIL)
- FOUNDATION SOIL
- SLIMES
- COARSE TAILINGS (DRAINED)
- FINE TAILINGS (DRAINED)
- PHREATIC SURFACE
- POND LEVEL

CLIENT	PROJECT
	REPORT OF THE EXPERT PANEL ON THE TECHNICAL CAUSES OF THE FAILURE OF FEIJÃO DAM 1
	TITLE: STABILITY ANALYSIS RESULTS SECTION 1-1' - EL. 942 m PEAK STRENGTH

SCALE	PROJECT No.	FIG. No.
1:2,500	A03355A01	2

KCB-FIG-B-L

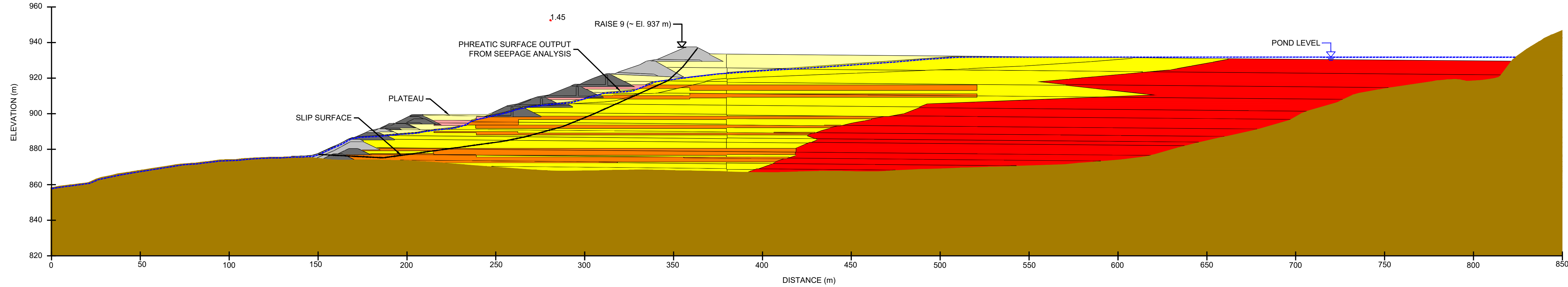

CASE 1-02A - CREST TO TOE

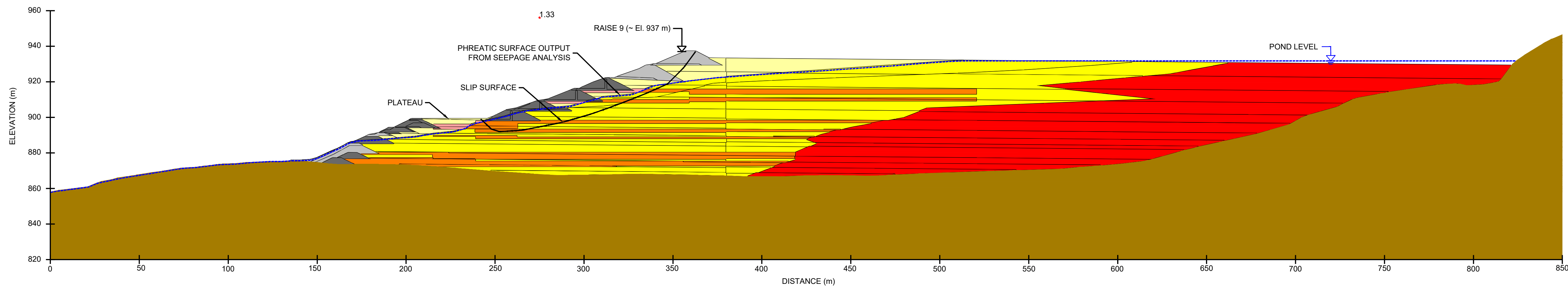

CASE 1-02B - CREST TO PLATEAU

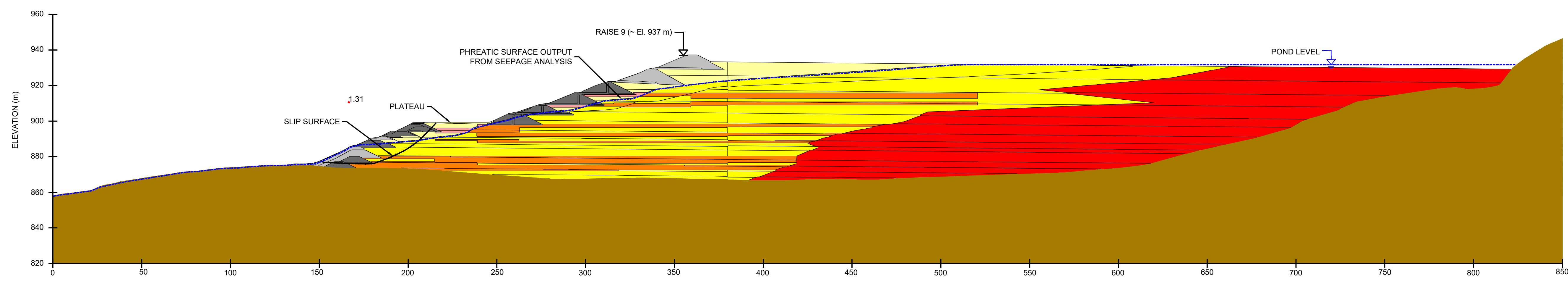

CASE 1-02C - PLATEAU TO TOE

1:2,500 0 25 50 m BASED ON A 11"X 17" DRAWING SIZE

NOTES:

1. ALL DIMENSIONS AND ELEVATIONS ARE IN METERS UNLESS STATED OTHERWISE.
2. MATERIAL PARAMETERS ARE OUTLINED IN APPENDIX E.
3. ONLY SLIP SURFACES CONSIDERED MOST CRITICAL ARE PRESENTED.

LEGEND:

- COARSE TAILINGS
- FINE TAILINGS
- COMPACTED BERM FILL (TAILINGS)
- COMPACTED BERM FILL (RESIDUAL SOIL)
- FOUNDATION SOIL
- SLIMES
- COARSE TAILINGS (DRAINED)
- FINE TAILINGS (DRAINED)
- PHREATIC SURFACE
- POND LEVEL

CLIENT	PROJECT REPORT OF THE EXPERT PANEL ON THE TECHNICAL CAUSES OF THE FAILURE OF FEIJÃO DAM 1
	TITLE STABILITY ANALYSIS RESULTS SECTION 1-1' - EL. 937 m PEAK STRENGTH
	SCALE 1:2,500 / PROJECT No. A03355A01 / FIG. No. 3

KCB-FIG-B-L

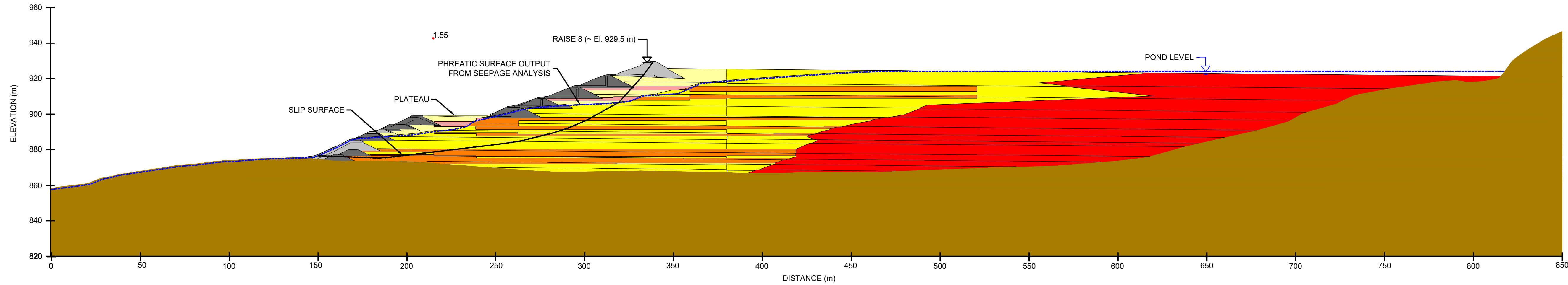

CASE 1-03A - CREST TO TOE

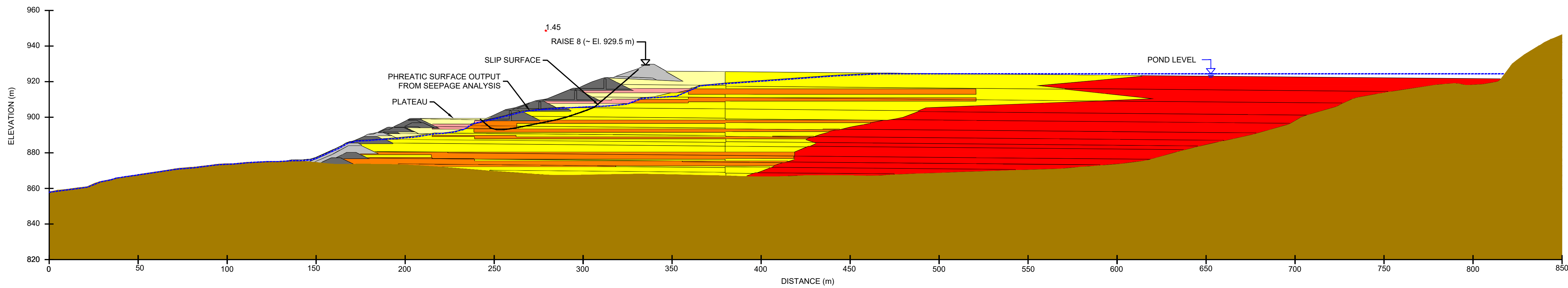

CASE 1-03B - CREST TO PLATEAU

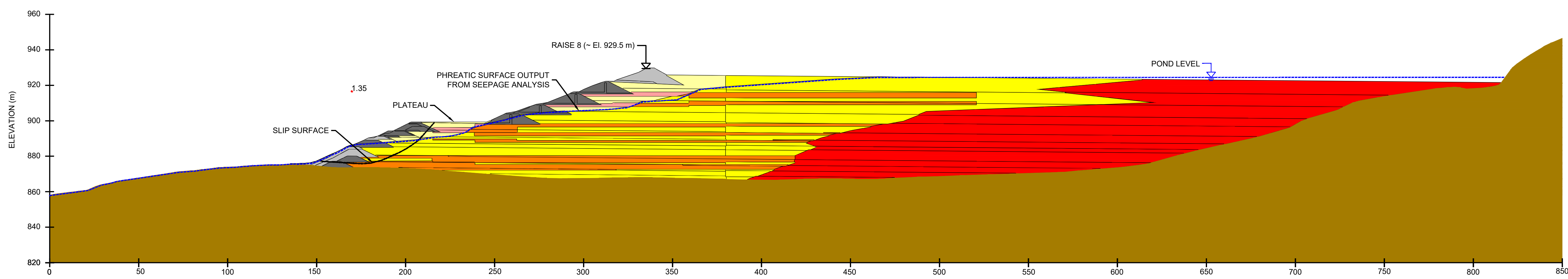

CASE 1-03C - PLATEAU TO TOE

1:2,500 0 25 50 m BASED ON A 11"X 17" DRAWING SIZE

NOTES:

1. ALL DIMENSIONS AND ELEVATIONS ARE IN METERS UNLESS STATED OTHERWISE.
2. MATERIAL PARAMETERS ARE OUTLINED IN APPENDIX E.
3. ONLY SLIP SURFACES CONSIDERED MOST CRITICAL ARE PRESENTED.

LEGEND:

- COARSE TAILINGS
- FINE TAILINGS
- COMPACTED BERM FILL (TAILINGS)
- COMPACTED BERM FILL (RESIDUAL SOIL)
- FOUNDATION SOIL
- SLIMES
- COARSE TAILINGS (DRAINED)
- FINE TAILINGS (DRAINED)
- PHREATIC SURFACE
- POND LEVEL

CLIENT

PROJECT
REPORT OF THE EXPERT PANEL ON THE TECHNICAL CAUSES OF THE FAILURE OF FEIJÃO DAM 1

TITLE
STABILITY ANALYSIS RESULTS
SECTION 1-1' - EL. 929.5 m
PEAK STRENGTH

SCALE	PROJECT No.	FIG. No.
1:2,500	A03355A01	4

KCB-FIG-B-L

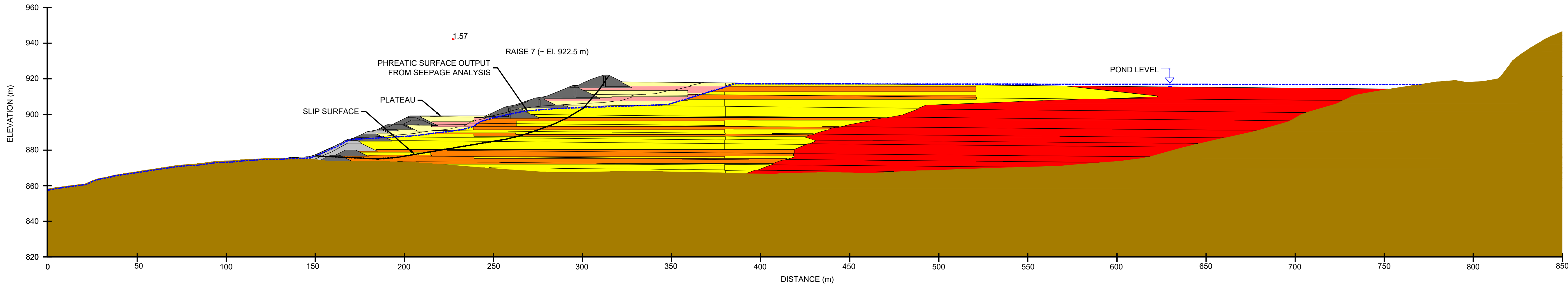

CASE 1-04A- CREST TO TOE

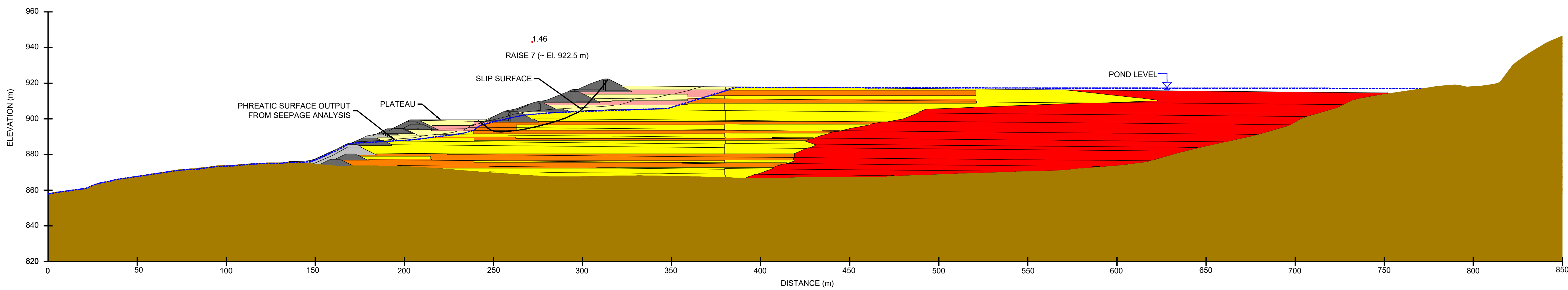

CASE 1-04B - CREST TO PLATEAU

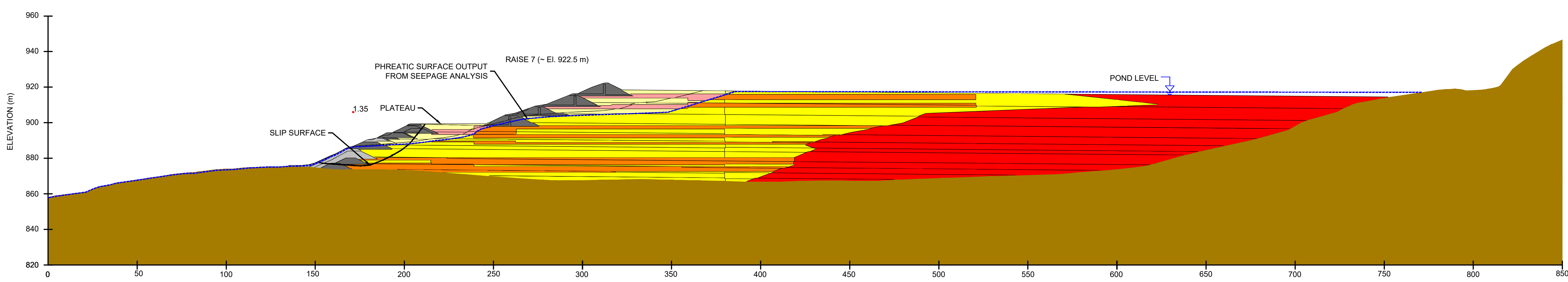

CASE 1-04C - PLATEAU TO TOE

1:2,500 0 25 50 m BASED ON A 11"X 17" DRAWING SIZE

NOTES:

1. ALL DIMENSIONS AND ELEVATIONS ARE IN METERS UNLESS STATED OTHERWISE.
2. MATERIAL PARAMETERS ARE OUTLINED IN APPENDIX E.
3. ONLY SLIP SURFACES CONSIDERED MOST CRITICAL ARE PRESENTED.

LEGEND:

- COARSE TAILINGS
- FINE TAILINGS
- COMPACTED BERM FILL (TAILINGS)
- COMPACTED BERM FILL (RESIDUAL SOIL)
- FOUNDATION SOIL
- SLIMES
- COARSE TAILINGS (DRAINED)
- FINE TAILINGS (DRAINED)
- PHREATIC SURFACE
- POND LEVEL

CLIENT

PROJECT
REPORT OF THE EXPERT PANEL ON THE TECHNICAL CAUSES OF THE FAILURE OF FEIJÃO DAM 1

TITLE
STABILITY ANALYSIS RESULTS
SECTION 1-1' - EL. 922.5 m
PEAK STRENGTH

SCALE	PROJECT No.	FIG. No.
1:2,500	A03355A01	5

KCB-FIG-B-L

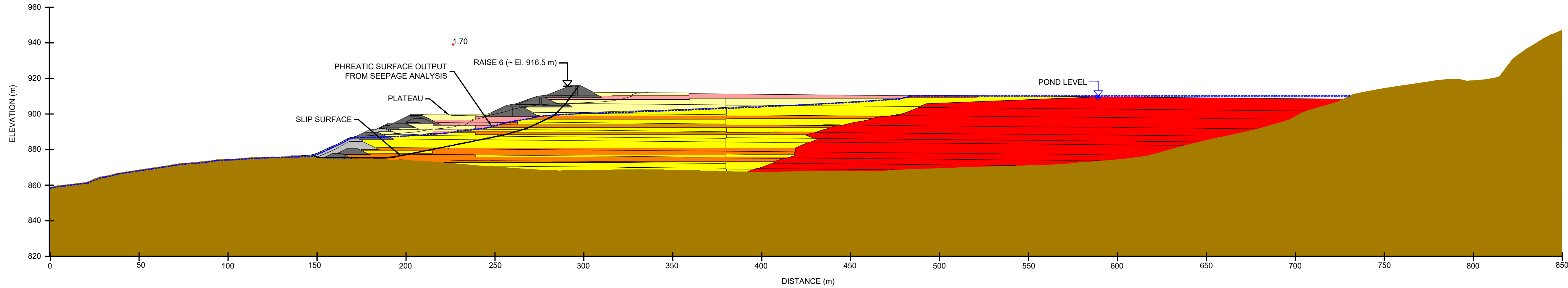

CASE 1-05A - CREST TO TOE

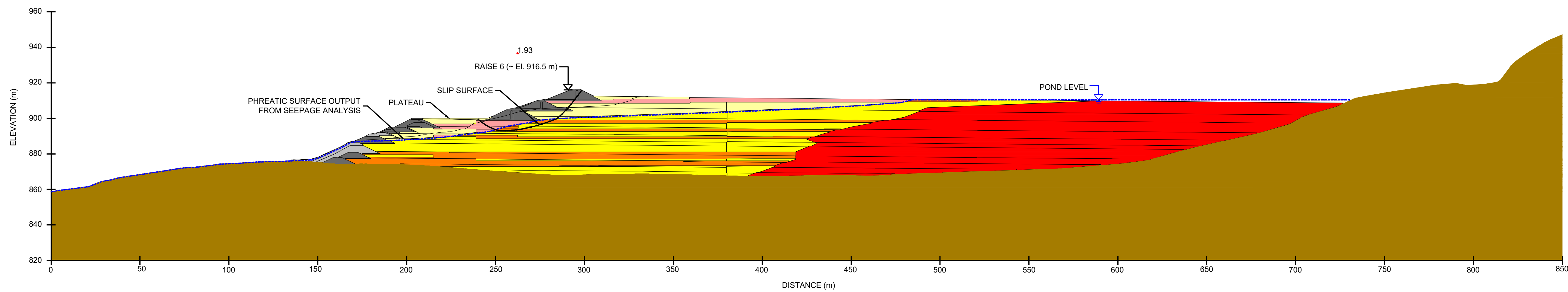

CASE 1-05B - CREST TO PLATEAU

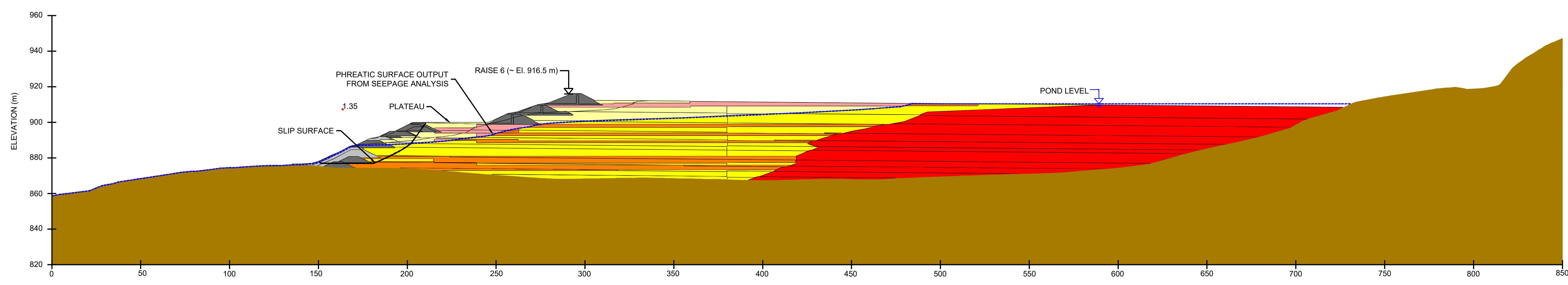

CASE 1-05C - PLATEAU TO TOE

1:2,500 0 25 50 m BASED ON A 11"X 17" DRAWING SIZE

NOTES:

1. ALL DIMENSIONS AND ELEVATIONS ARE IN METERS UNLESS STATED OTHERWISE.
2. MATERIAL PARAMETERS ARE OUTLINED IN APPENDIX E.
3. ONLY SLIP SURFACES CONSIDERED MOST CRITICAL ARE PRESENTED.

LEGEND:

- COARSE TAILINGS
- FINE TAILINGS
- COMPACTED BERM FILL (TAILINGS)
- COMPACTED BERM FILL (RESIDUAL SOIL)
- FOUNDATION SOIL
- SLIMES
- COARSE TAILINGS (DRAINED)
- FINE TAILINGS (DRAINED)
- PHREATIC SURFACE
- POND LEVEL

CLIENT

PROJECT
REPORT OF THE EXPERT PANEL ON THE TECHNICAL CAUSES OF THE FAILURE OF FEIJÃO DAM 1

TITLE
STABILITY ANALYSIS RESULTS
SECTION 1-1' - EL. 916.5 m
PEAK STRENGTH

SCALE	PROJECT No.	FIG. No.
1:2,500	A03355A01	6

KCB-FIG-B-L

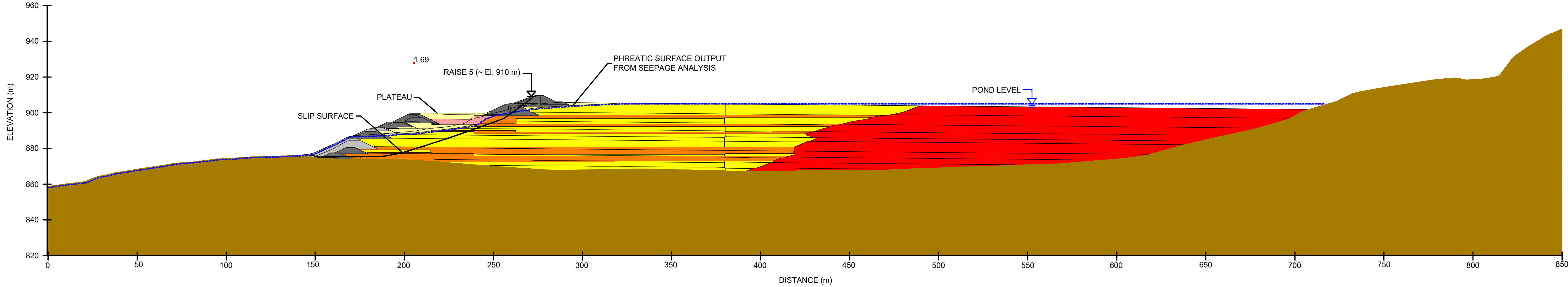

CASE 1-06A - CREST TO TOE

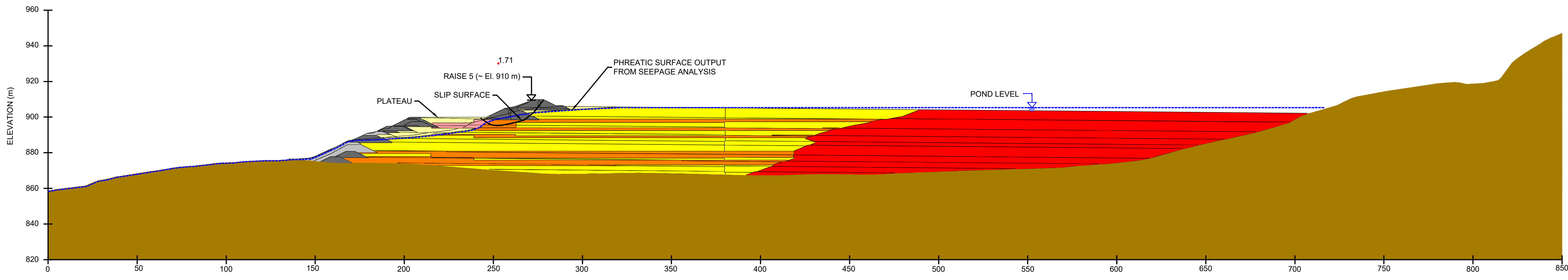

CASE 1-06B - CREST TO PLATEAU

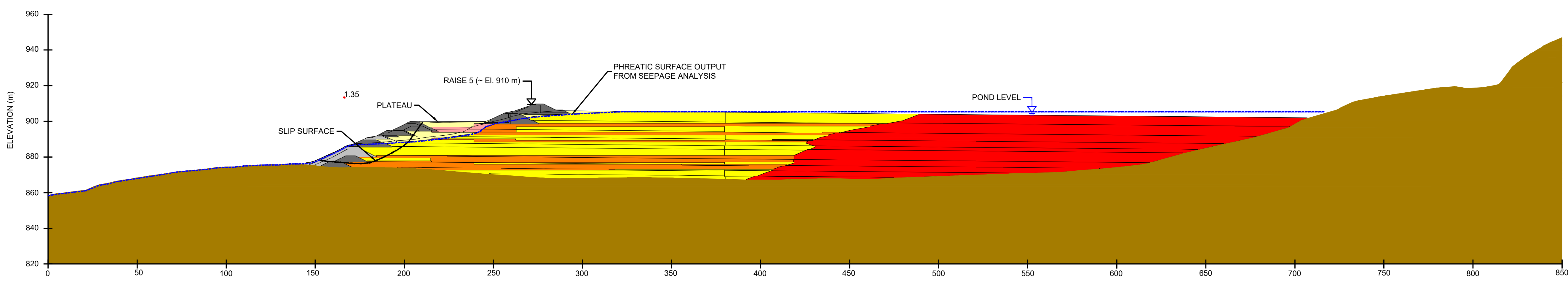

CASE 1-06C - PLATEAU TO TOE

1:2,500 0 25 50 m BASED ON A 11"X 17" DRAWING SIZE

NOTES:

1. ALL DIMENSIONS AND ELEVATIONS ARE IN METERS UNLESS STATED OTHERWISE.
2. MATERIAL PARAMETERS ARE OUTLINED IN APPENDIX E.
3. ONLY SLIP SURFACES CONSIDERED MOST CRITICAL ARE PRESENTED.

LEGEND:

- COARSE TAILINGS
- FINE TAILINGS
- COMPACTED BERM FILL (TAILINGS)
- COMPACTED BERM FILL (RESIDUAL SOIL)
- FOUNDATION SOIL
- SLIMES
- COARSE TAILINGS (DRAINED)
- FINE TAILINGS (DRAINED)
- PHREATIC SURFACE
- POND LEVEL

CLIENT

PROJECT
REPORT OF THE EXPERT PANEL ON THE TECHNICAL CAUSES OF THE FAILURE OF FEIJÃO DAM 1

TITLE
STABILITY ANALYSIS RESULTS
SECTION 1-1' - EL. 910 m
PEAK STRENGTH

SCALE	PROJECT No.	FIG. No.
1:2,500	A03355A01	7

KCB-FIG-B-L

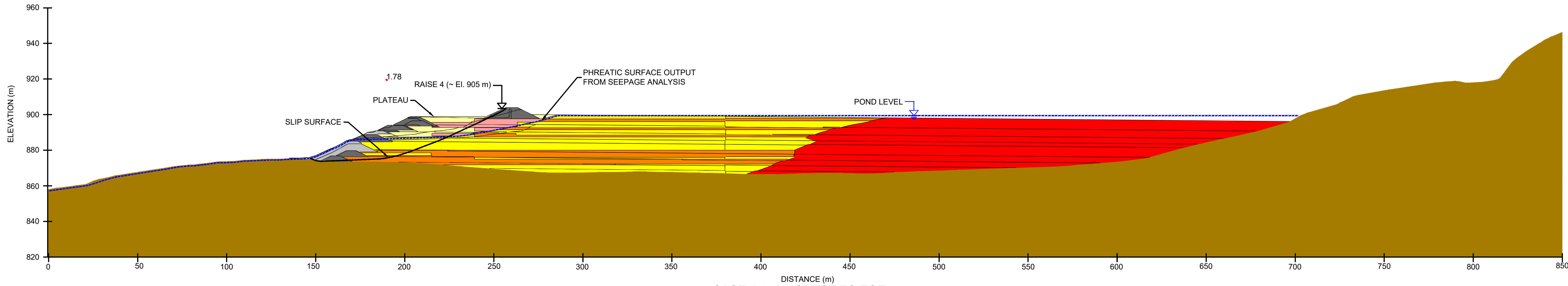

CASE 1-07A - CREST TO TOE

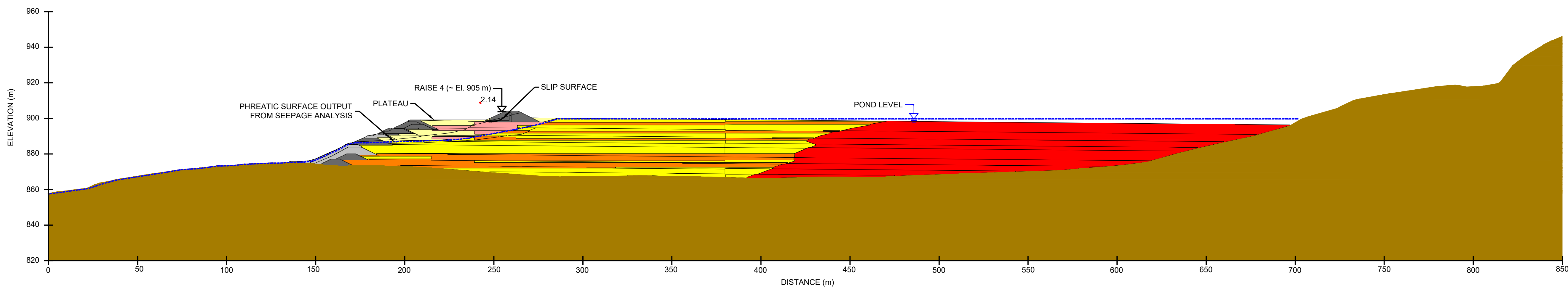

CASE 1-07B - CREST TO PLATEAU

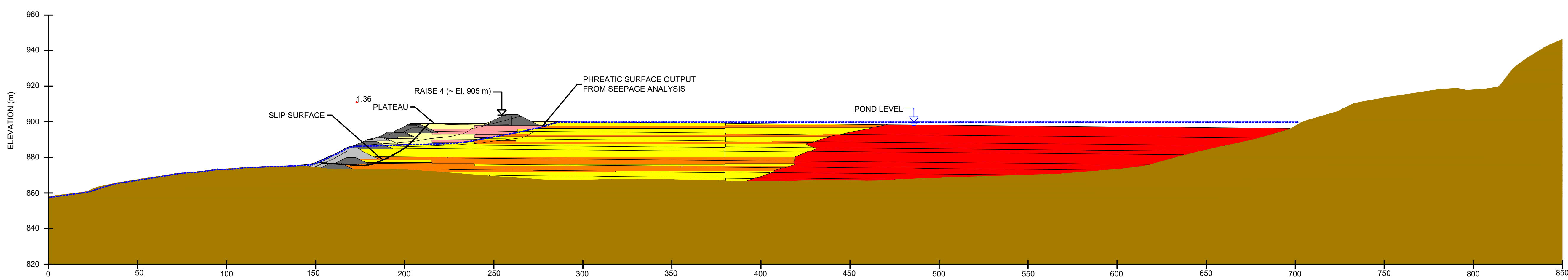

CASE 1-07C - PLATEAU TO TOE

1:2,500 0 25 50 m BASED ON A 11"X 17" DRAWING SIZE

NOTES:

1. ALL DIMENSIONS AND ELEVATIONS ARE IN METERS UNLESS STATED OTHERWISE.
2. MATERIAL PARAMETERS ARE OUTLINED IN APPENDIX E.
3. ONLY SLIP SURFACES CONSIDERED MOST CRITICAL ARE PRESENTED.

LEGEND:

- COARSE TAILINGS
- FINE TAILINGS
- COMPACTED BERM FILL (TAILINGS)
- COMPACTED BERM FILL (RESIDUAL SOIL)
- FOUNDATION SOIL
- SLIMES
- COARSE TAILINGS (DRAINED)
- FINE TAILINGS (DRAINED)
- PHREATIC SURFACE
- POND LEVEL

CLIENT

PROJECT
REPORT OF THE EXPERT PANEL ON THE TECHNICAL CAUSES OF THE FAILURE OF FEIJÃO DAM 1

TITLE
STABILITY ANALYSIS RESULTS
SECTION 1-1' - EL. 905 m
PEAK STRENGTH

SCALE	PROJECT No.	FIG. No.
1:2,500	A03355A01	8

KCB-FIG-B-L

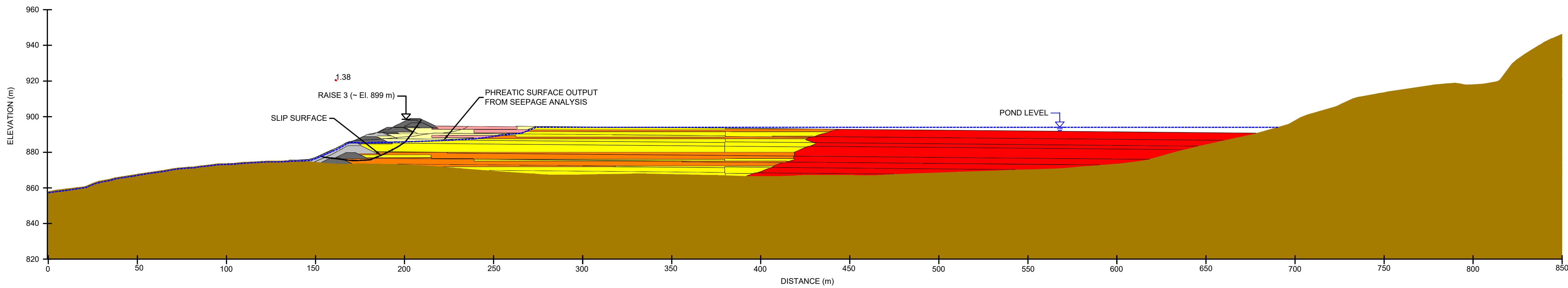

CASE 1-08A - CREST TO TOE

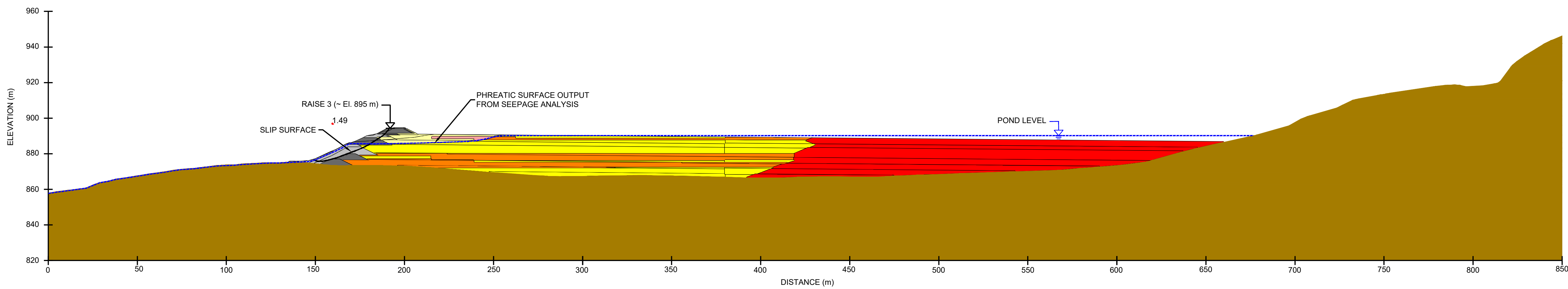

CASE 1-09A - CREST TO TOE

1:2,500 0 25 50 m BASED ON A 11"X 17" DRAWING SIZE

NOTES:

1. ALL DIMENSIONS AND ELEVATIONS ARE IN METERS UNLESS STATED OTHERWISE.
2. MATERIAL PARAMETERS ARE OUTLINED IN APPENDIX E.
3. ONLY SLIP SURFACES CONSIDERED MOST CRITICAL ARE PRESENTED.

LEGEND:

- COARSE TAILINGS
- FINE TAILINGS
- COMPACTED BERM FILL (TAILINGS)
- COMPACTED BERM FILL (RESIDUAL SOIL)
- FOUNDATION SOIL
- SLIMES
- COARSE TAILINGS (DRAINED)
- FINE TAILINGS (DRAINED)
- PHREATIC SURFACE
- POND LEVEL

CLIENT

PROJECT
REPORT OF THE EXPERT PANEL ON THE TECHNICAL CAUSES OF THE FAILURE OF FEIJÃO DAM 1

TITLE
STABILITY ANALYSIS RESULTS
SECTION 1-1' - EL. 899 m AND 895 m
PEAK STRENGTH

SCALE	PROJECT No.	FIG. No.
1:2,500	A03355A01	9

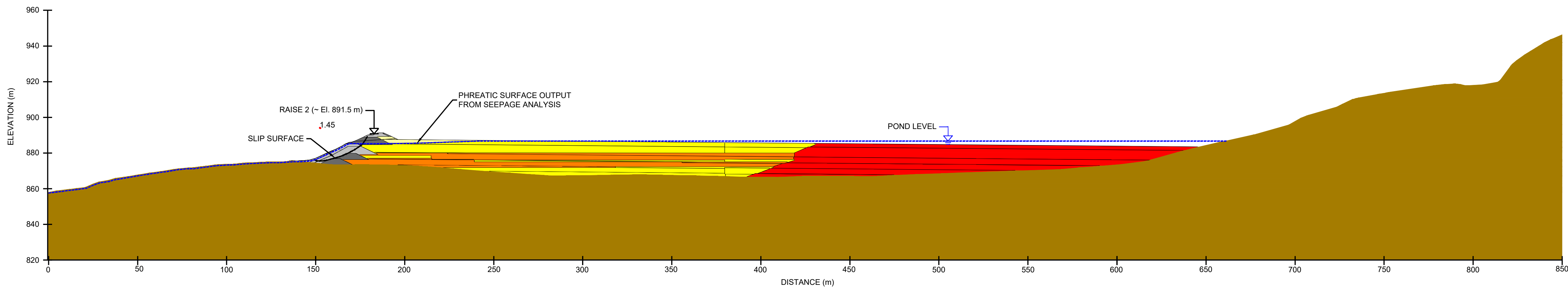

CASE 1-10A - CREST TO TOE

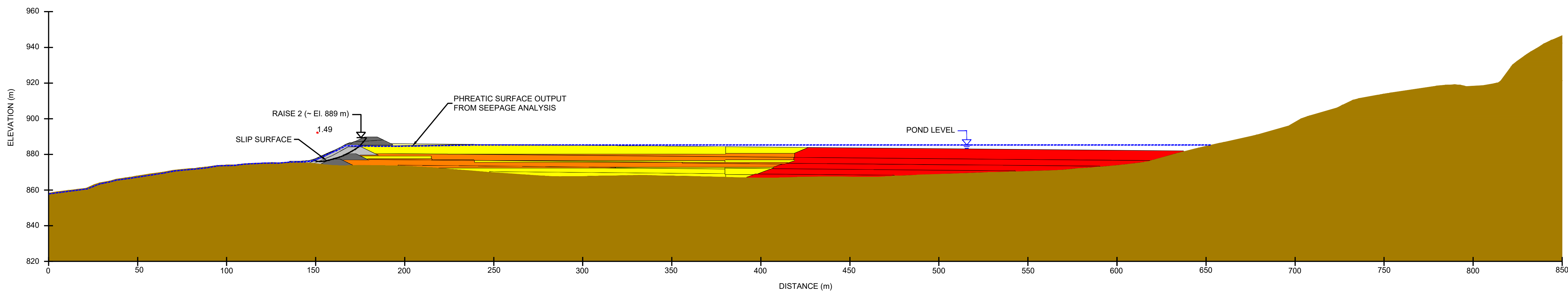

CASE 1-11A - CREST TO TOE

1:2,500 0 25 50 m BASED ON A 11"X 17" DRAWING SIZE

NOTES:

1. ALL DIMENSIONS AND ELEVATIONS ARE IN METERS UNLESS STATED OTHERWISE.
2. MATERIAL PARAMETERS ARE OUTLINED IN APPENDIX E.
3. ONLY SLIP SURFACES CONSIDERED MOST CRITICAL ARE PRESENTED.

LEGEND:

- COARSE TAILINGS
- FINE TAILINGS
- COMPACTED BERM FILL (TAILINGS)
- COMPACTED BERM FILL (RESIDUAL SOIL)
- FOUNDATION SOIL
- SLIMES
- COARSE TAILINGS (DRAINED)
- FINE TAILINGS (DRAINED)
- PHREATIC SURFACE
- POND LEVEL

CLIENT

PROJECT
REPORT OF THE EXPERT PANEL ON THE TECHNICAL CAUSES OF THE FAILURE OF FEIJÃO DAM 1

TITLE
STABILITY ANALYSIS RESULTS
SECTION 1-1' - EL. 891.5 m AND 889 m
PEAK STRENGTH

SCALE	PROJECT No.	FIG. No.
1:2,500	A03355A01	10

KCB-FIG-B-L

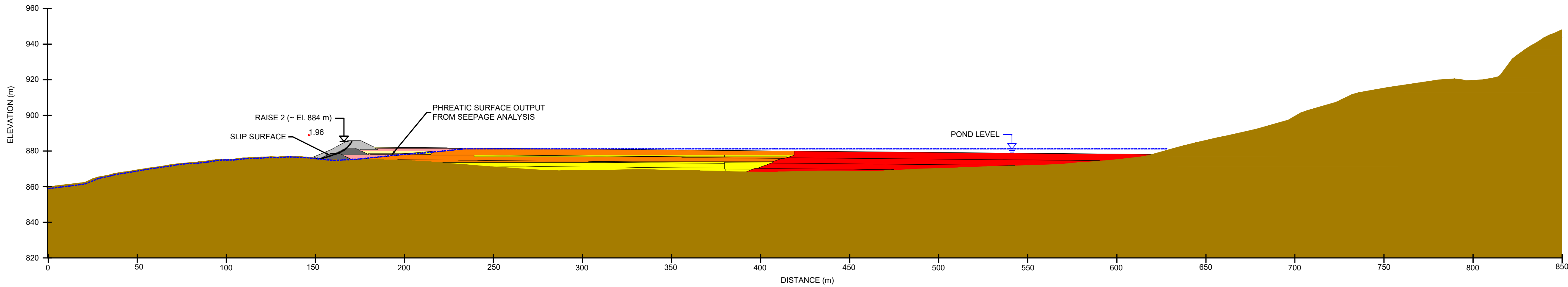

CASE 1-12A - CREST TO TOE

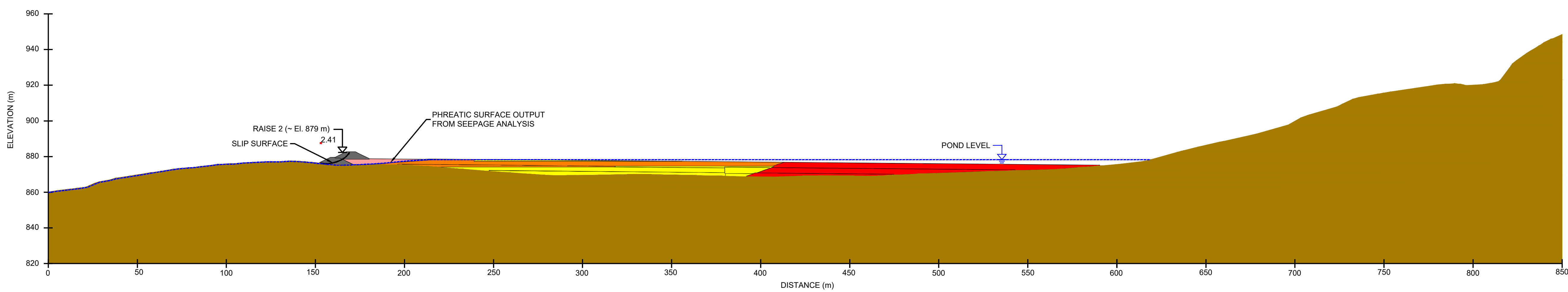

CASE 1-13A - CREST TO TOE

1:2,500 0 25 50 m BASED ON A 11"X 17" DRAWING SIZE

NOTES:

1. ALL DIMENSIONS AND ELEVATIONS ARE IN METERS UNLESS STATED OTHERWISE.
2. MATERIAL PARAMETERS ARE OUTLINED IN APPENDIX E.
3. ONLY SLIP SURFACES CONSIDERED MOST CRITICAL ARE PRESENTED.

LEGEND:

- COARSE TAILINGS
- FINE TAILINGS
- COMPACTED BERM FILL (TAILINGS)
- COMPACTED BERM FILL (RESIDUAL SOIL)
- FOUNDATION SOIL
- SLIMES
- COARSE TAILINGS (DRAINED)
- FINE TAILINGS (DRAINED)
- PHREATIC SURFACE
- POND LEVEL

CLIENT

PROJECT
REPORT OF THE EXPERT PANEL ON THE TECHNICAL CAUSES OF THE FAILURE OF FEIJÃO DAM 1

TITLE
STABILITY ANALYSIS RESULTS
SECTION 1-1' - EL. 884 m AND 879 m
PEAK STRENGTH

SCALE	PROJECT No.	FIG. No.
1:2,500	A03355A01	11

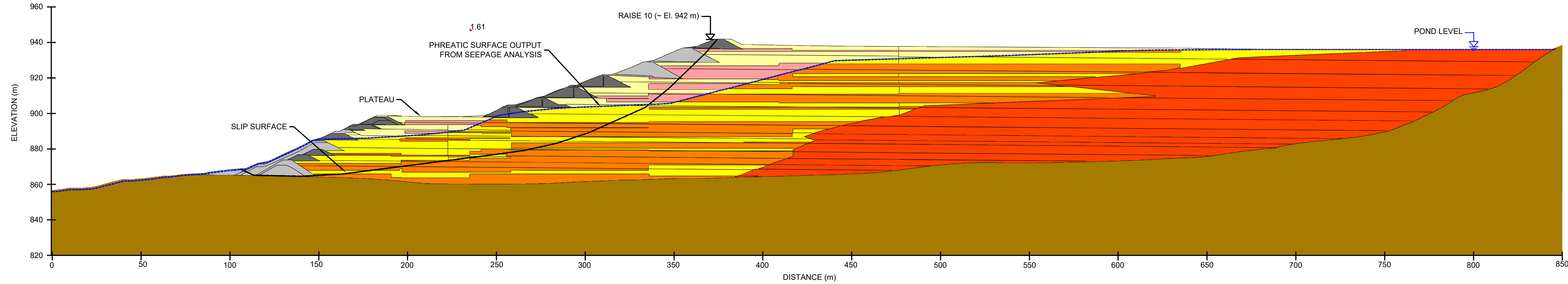

CASE 2-01A - CREST TO TOE

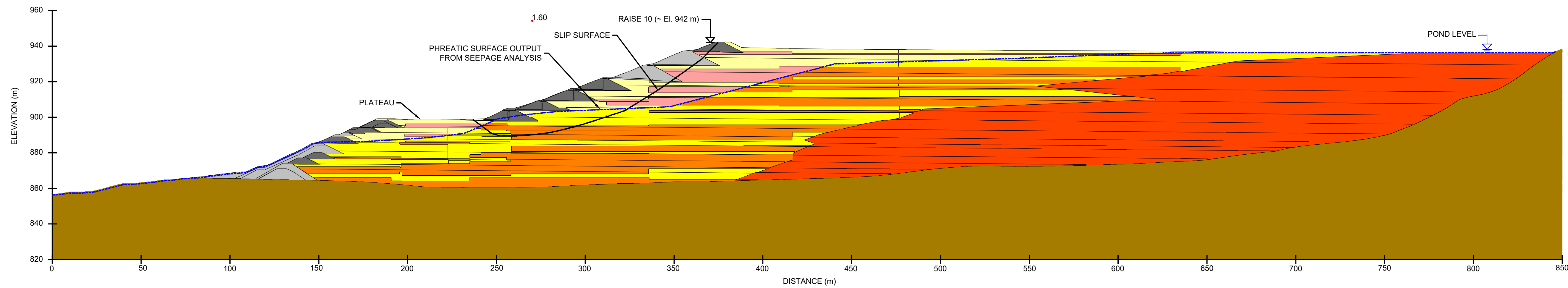

CASE 2-01B - CREST TO PLATEAU

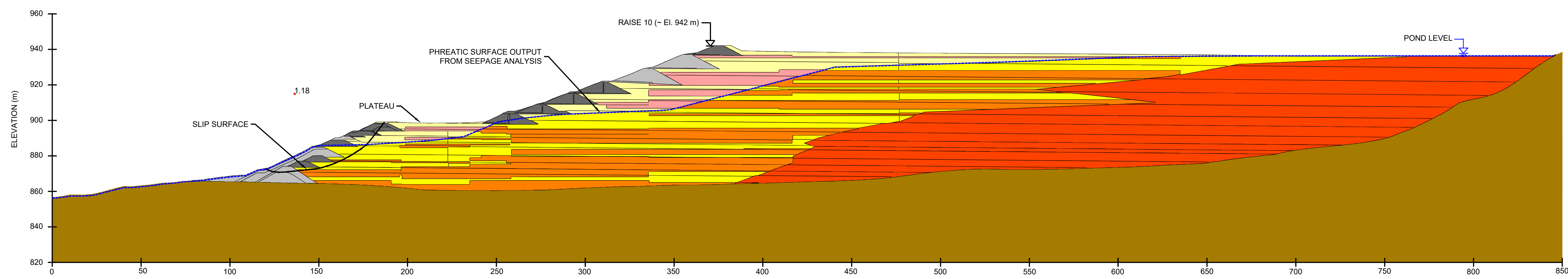

CASE 2-01C - PLATEAU TO TOE

1:2,500 0 25 50 m BASED ON A 11"X 17" DRAWING SIZE

NOTES:

1. ALL DIMENSIONS AND ELEVATIONS ARE IN METERS UNLESS STATED OTHERWISE.
2. MATERIAL PARAMETERS ARE OUTLINED IN APPENDIX E.
3. ONLY SLIP SURFACES CONSIDERED MOST CRITICAL ARE PRESENTED.

LEGEND:

- COARSE TAILINGS
- FINE TAILINGS
- COMPACTED BERM FILL (TAILINGS)
- COMPACTED BERM FILL (RESIDUAL SOIL)
- FOUNDATION SOIL
- SLIMES
- COARSE TAILINGS (DRAINED)
- FINE TAILINGS (DRAINED)
- PHREATIC SURFACE
- POND LEVEL

CLIENT

PROJECT
REPORT OF THE EXPERT PANEL ON THE TECHNICAL CAUSES OF THE FAILURE OF FEIJÃO DAM 1

TITLE
STABILITY ANALYSIS RESULTS
SECTION 2-2' - EL. 942 m
PEAK STRENGTH

SCALE	PROJECT No.	FIG. No.
1:2,500	A03355A01	12

KCB-FIG-B-L

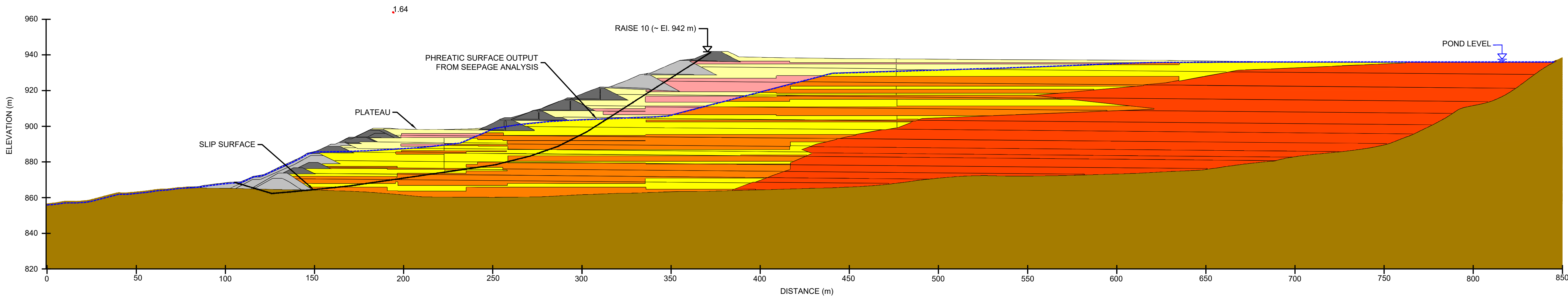

CASE 2-01D - CREST TO TOE

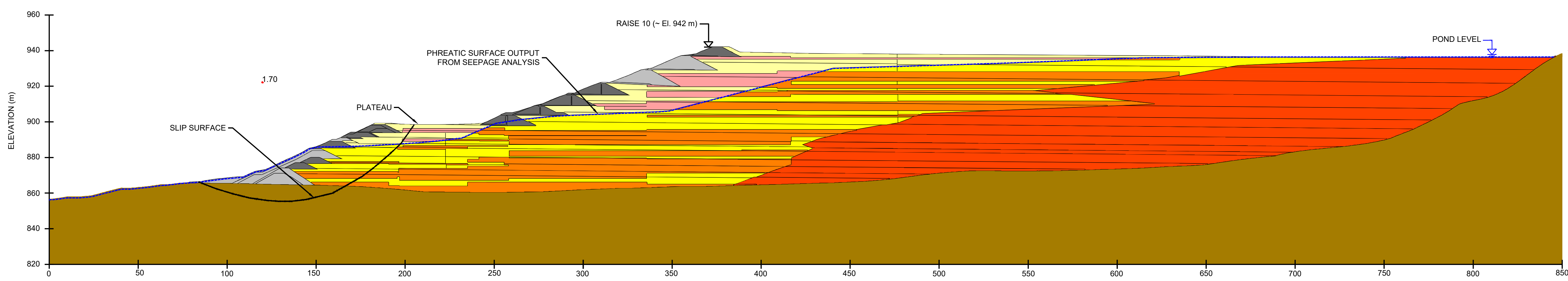

CASE 2-01E - PLATEAU TO TOE

1:2,500 0 25 50 m BASED ON A 11"X 17" DRAWING SIZE

NOTES:

1. ALL DIMENSIONS AND ELEVATIONS ARE IN METERS UNLESS STATED OTHERWISE.
2. MATERIAL PARAMETERS ARE OUTLINED IN APPENDIX E.
3. ONLY SLIP SURFACES CONSIDERED MOST CRITICAL ARE PRESENTED.

LEGEND:

- COARSE TAILINGS
- FINE TAILINGS
- COMPACTED BERM FILL (TAILINGS)
- COMPACTED BERM FILL (RESIDUAL SOIL)
- FOUNDATION SOIL
- SLIMES
- COARSE TAILINGS (DRAINED)
- FINE TAILINGS (DRAINED)
- PHREATIC SURFACE
- POND LEVEL

CLIENT

PROJECT
REPORT OF THE EXPERT PANEL ON THE TECHNICAL CAUSES OF THE FAILURE OF FEIJÃO DAM 1

TITLE
STABILITY ANALYSIS RESULTS
SECTION 2-2' - EL. 942 m
PEAK STRENGTH

SCALE	PROJECT No.	FIG. No.
1:2,500	A03355A01	13

KCB-FIG-B-L

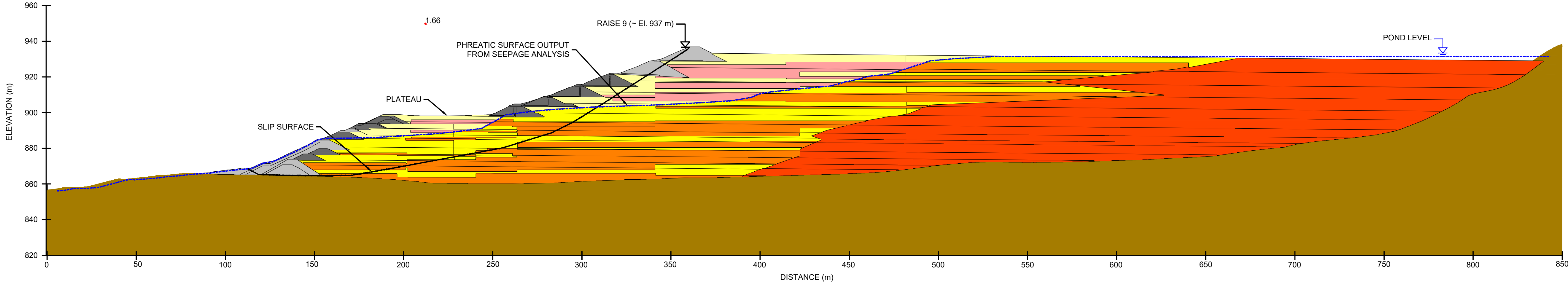

CASE 2-02A - CREST TO TOE

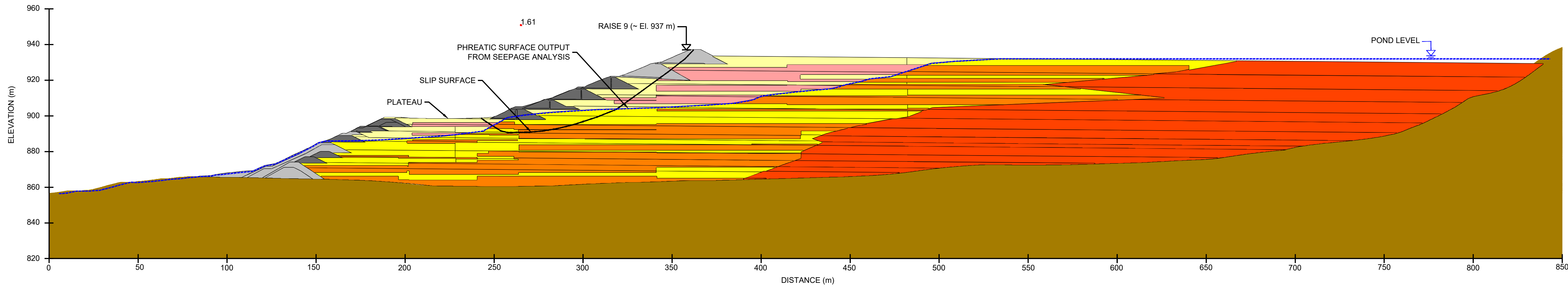

CASE 2-02B - CREST TO PLATEAU

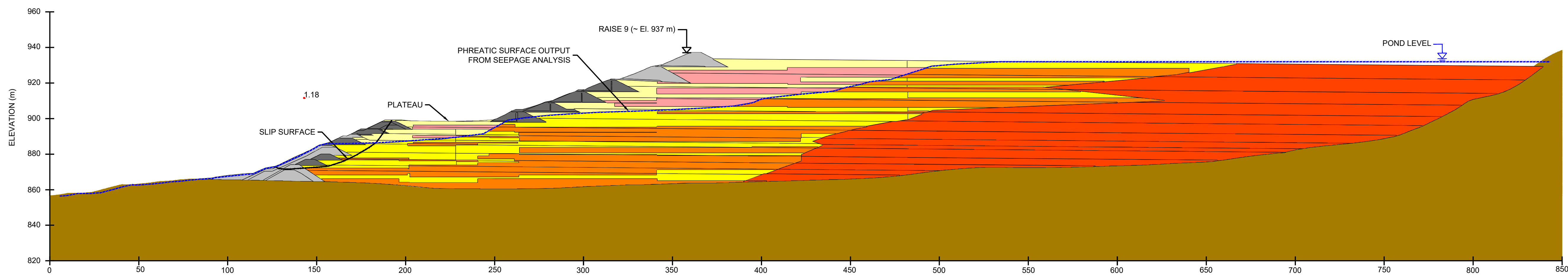

CASE 2-02C - PLATEAU TO TOE

1:2,500 0 25 50 m BASED ON A 11"X 17" DRAWING SIZE

NOTES:

1. ALL DIMENSIONS AND ELEVATIONS ARE IN METERS UNLESS STATED OTHERWISE.
2. MATERIAL PARAMETERS ARE OUTLINED IN APPENDIX E.
3. ONLY SLIP SURFACES CONSIDERED MOST CRITICAL ARE PRESENTED.

LEGEND:

- COARSE TAILINGS
- FINE TAILINGS
- COMPACTED BERM FILL (TAILINGS)
- COMPACTED BERM FILL (RESIDUAL SOIL)
- FOUNDATION SOIL
- SLIMES
- COARSE TAILINGS (DRAINED)
- FINE TAILINGS (DRAINED)
- PHREATIC SURFACE
- POND LEVEL

CLIENT

PROJECT
REPORT OF THE EXPERT PANEL ON THE TECHNICAL CAUSES OF THE FAILURE OF FEIJÃO DAM 1

TITLE
STABILITY ANALYSIS RESULTS
SECTION 2-2' - EL. 937 m
PEAK STRENGTH

SCALE	PROJECT No.	FIG. No.
1:2,500	A03355A01	14

KCB-FIG-B-L

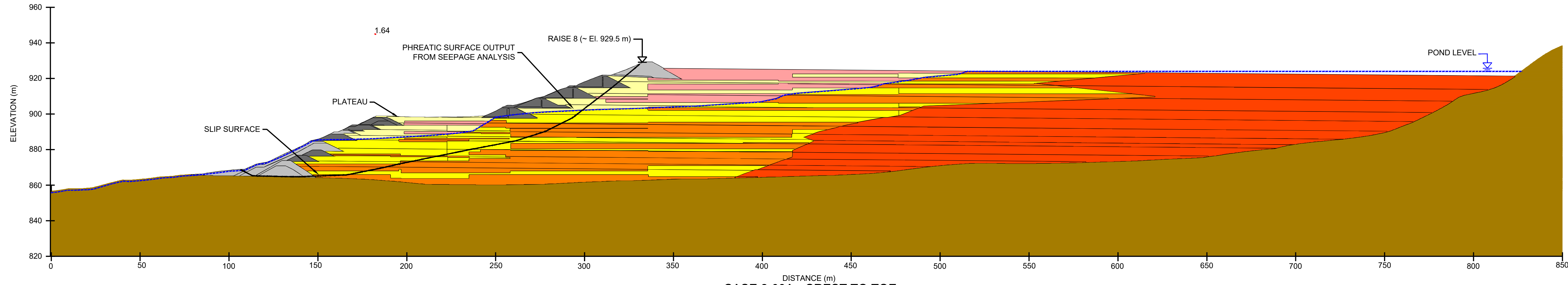

CASE 2-03A - CREST TO TOE

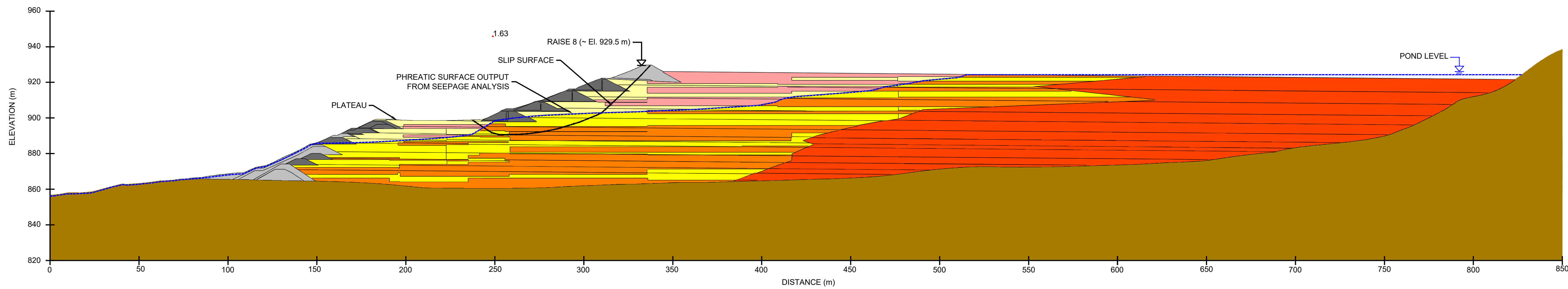

CASE 2-03B - CREST TO PLATEAU

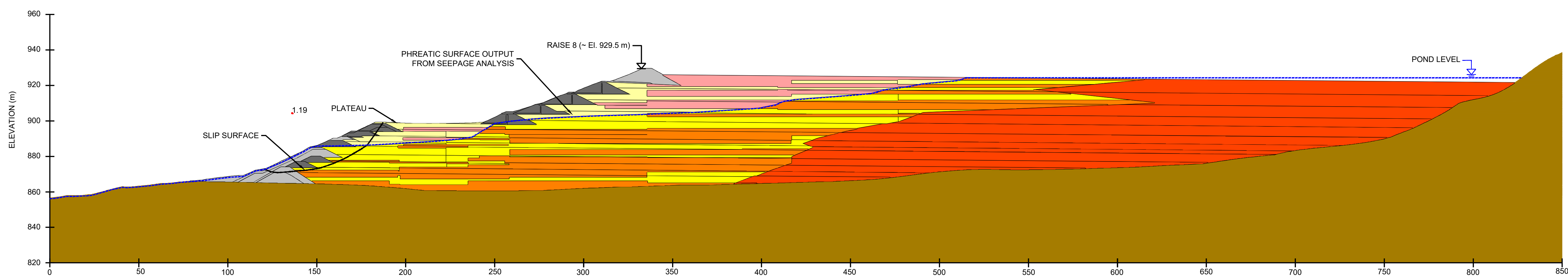

CASE 2-03C - PLATEAU TO TOE

1:2,500 0 25 50 m BASED ON A 11"X 17" DRAWING SIZE

NOTES:

1. ALL DIMENSIONS AND ELEVATIONS ARE IN METERS UNLESS STATED OTHERWISE.
2. MATERIAL PARAMETERS ARE OUTLINED IN APPENDIX E.
3. ONLY SLIP SURFACES CONSIDERED MOST CRITICAL ARE PRESENTED.

LEGEND:

- COARSE TAILINGS
- FINE TAILINGS
- COMPACTED BERM FILL (TAILINGS)
- COMPACTED BERM FILL (RESIDUAL SOIL)
- FOUNDATION SOIL
- SLIMES
- COARSE TAILINGS (DRAINED)
- FINE TAILINGS (DRAINED)
- PHREATIC SURFACE
- POND LEVEL

CLIENT

PROJECT
REPORT OF THE EXPERT PANEL ON THE TECHNICAL CAUSES OF THE FAILURE OF FEIJÃO DAM 1

TITLE
STABILITY ANALYSIS RESULTS
SECTION 2-2' - EL. 929.5 m
PEAK STRENGTH

SCALE	PROJECT No.	FIG. No.
1:2,500	A03355A01	15

KCB-FIG-B-L

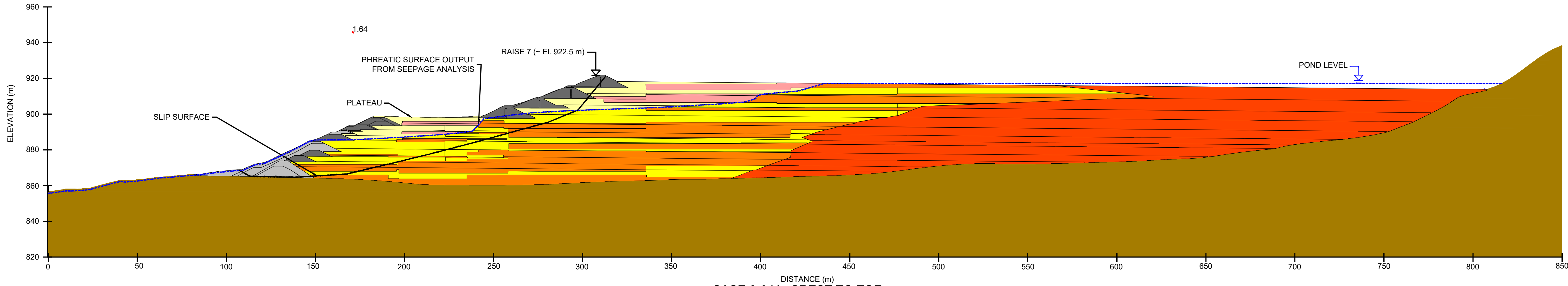

CASE 2-04A- CREST TO TOE

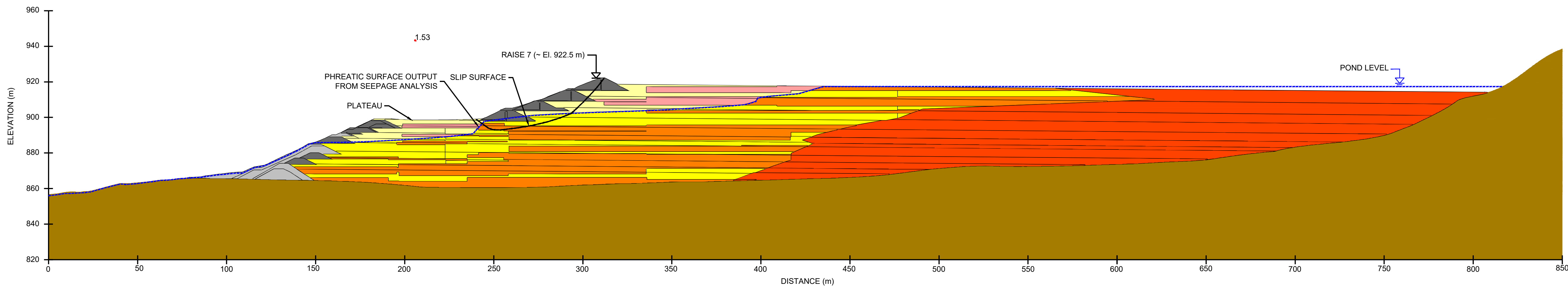

CASE 2-04B - CREST TO PLATEAU

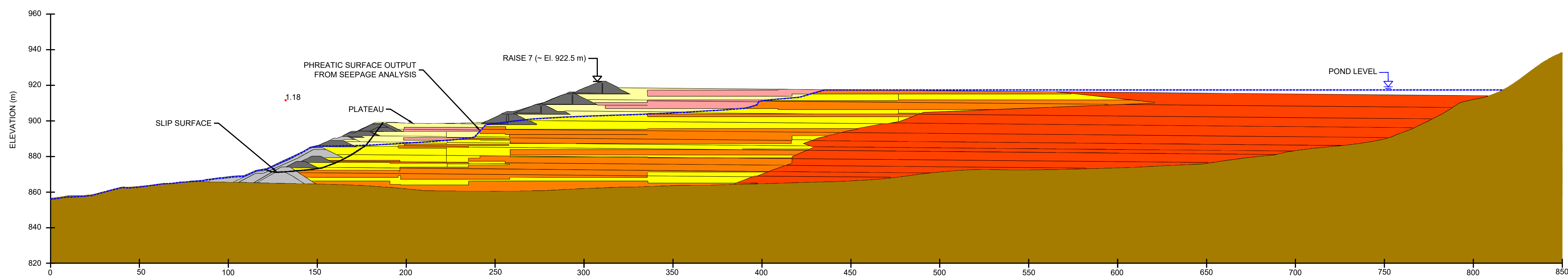

CASE 2-04C - PLATEAU TO TOE

1:2,500 0 25 50 m BASED ON A 11"X 17" DRAWING SIZE

NOTES:

1. ALL DIMENSIONS AND ELEVATIONS ARE IN METERS UNLESS STATED OTHERWISE.
2. MATERIAL PARAMETERS ARE OUTLINED IN APPENDIX E.
3. ONLY SLIP SURFACES CONSIDERED MOST CRITICAL ARE PRESENTED.

LEGEND:

- COARSE TAILINGS
- FINE TAILINGS
- COMPACTED BERM FILL (TAILINGS)
- COMPACTED BERM FILL (RESIDUAL SOIL)
- FOUNDATION SOIL
- SLIMES
- COARSE TAILINGS (DRAINED)
- FINE TAILINGS (DRAINED)
- PHREATIC SURFACE
- POND LEVEL

CLIENT

PROJECT
REPORT OF THE EXPERT PANEL ON THE TECHNICAL CAUSES OF THE FAILURE OF FEIJÃO DAM 1

TITLE
STABILITY ANALYSIS RESULTS
SECTION 2-2' - EL. 922.5 m
PEAK STRENGTH

SCALE	PROJECT No.	FIG. No.
1:2,500	A03355A01	16

KCB-FIG-B-L

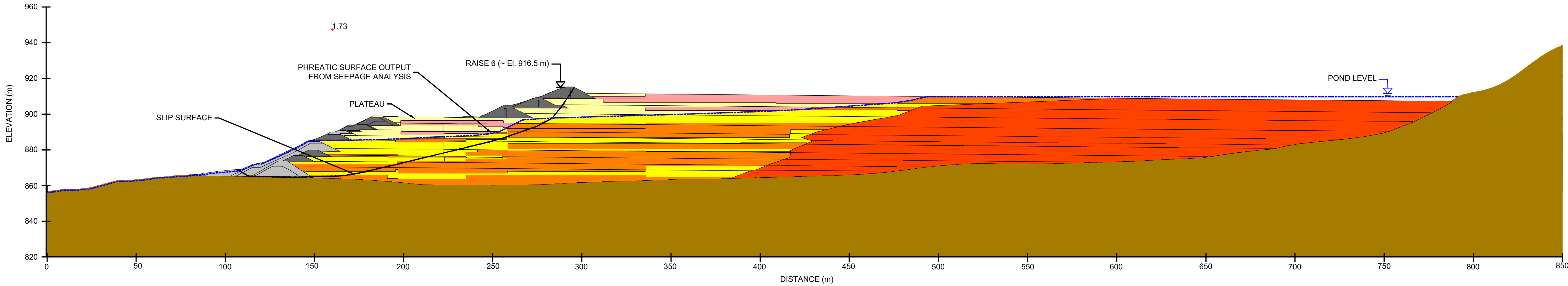

CASE 2-05A - CREST TO TOE

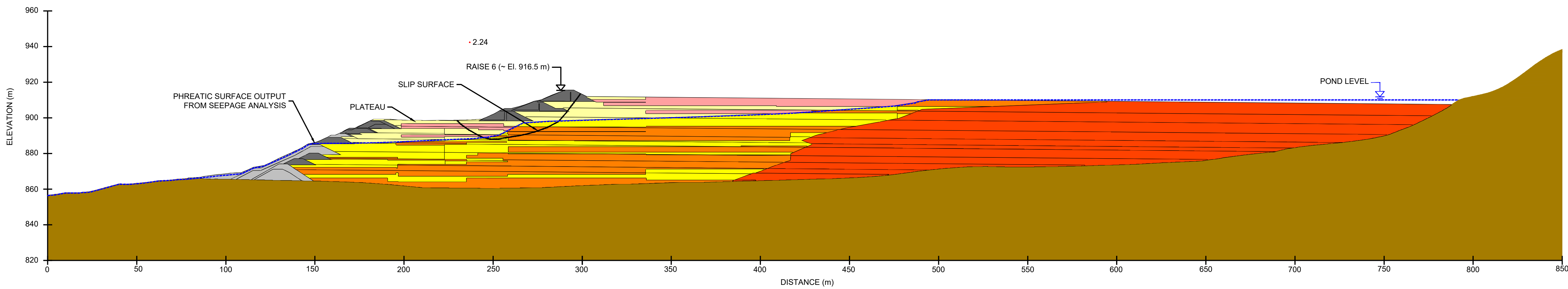

CASE 2-05B - CREST TO PLATEAU

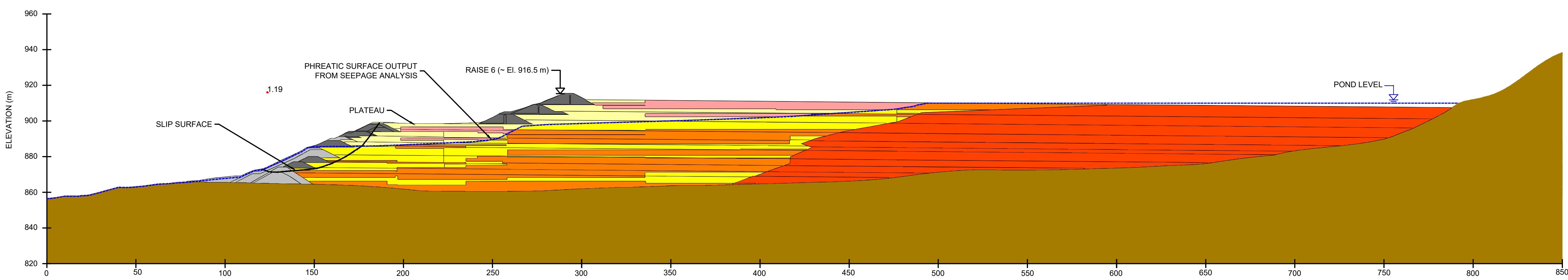

CASE 2-05C - PLATEAU TO TOE

1:2,500 0 25 50 m BASED ON A 11"X 17" DRAWING SIZE

NOTES:

1. ALL DIMENSIONS AND ELEVATIONS ARE IN METERS UNLESS STATED OTHERWISE.
2. MATERIAL PARAMETERS ARE OUTLINED IN APPENDIX E.
3. ONLY SLIP SURFACES CONSIDERED MOST CRITICAL ARE PRESENTED.

LEGEND:

- COARSE TAILINGS
- FINE TAILINGS
- COMPACTED BERM FILL (TAILINGS)
- COMPACTED BERM FILL (RESIDUAL SOIL)
- FOUNDATION SOIL
- SLIMES
- COARSE TAILINGS (DRAINED)
- FINE TAILINGS (DRAINED)
- PHREATIC SURFACE
- POND LEVEL

CLIENT

PROJECT
REPORT OF THE EXPERT PANEL ON THE TECHNICAL CAUSES OF THE FAILURE OF FEIJÃO DAM 1

TITLE
STABILITY ANALYSIS RESULTS
SECTION 2-2' - EL. 916.5 m
PEAK STRENGTH

SCALE	PROJECT No.	FIG. No.
1:2,500	A03355A01	17

KCB-FIG-B-L

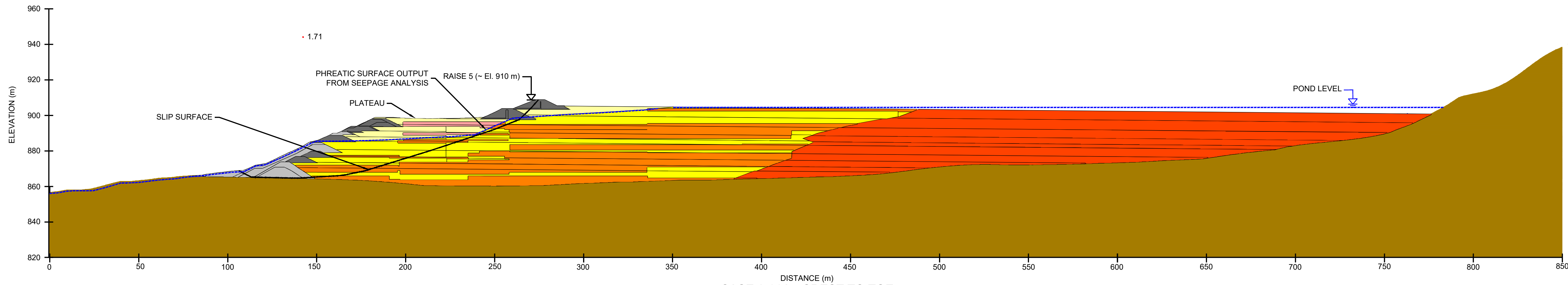

CASE 2-06A - CREST TO TOE

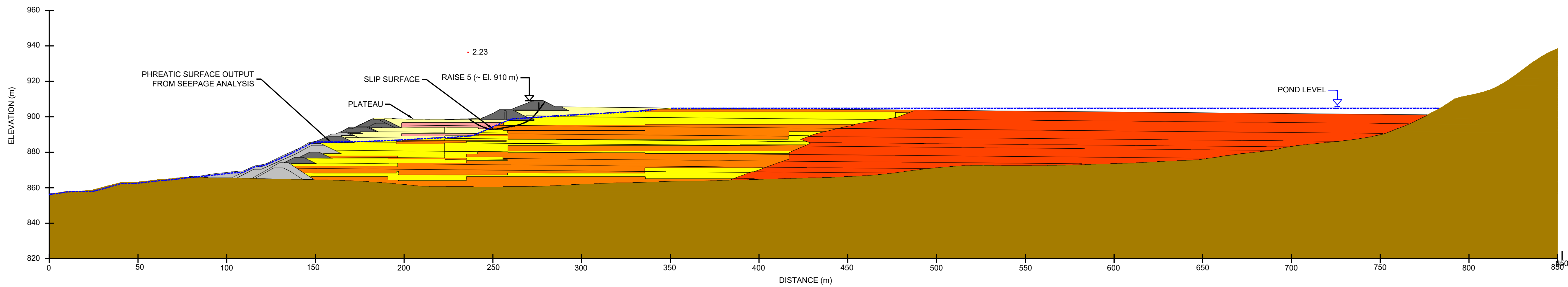

CASE 2-06B - CREST TO PLATEAU

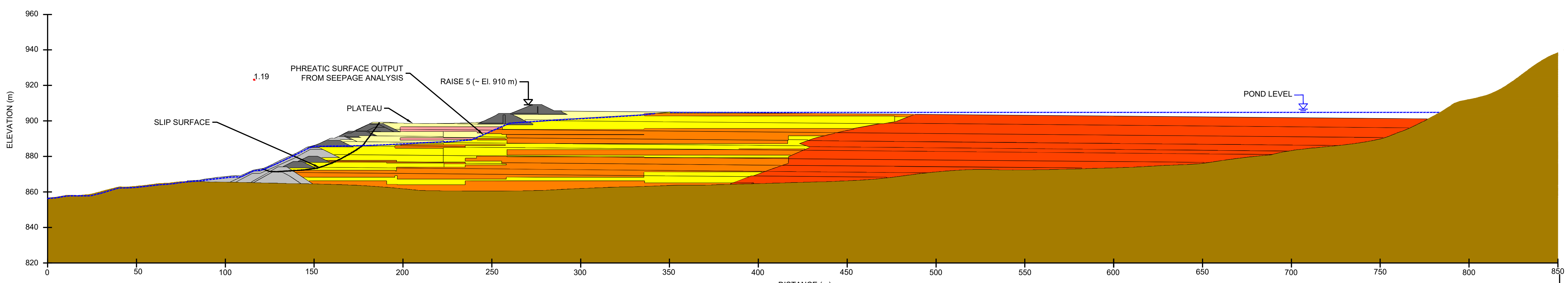

CASE 2-06C - PLATEAU TO TOE

1:2,500 0 25 50 m BASED ON A 11"X 17" DRAWING SIZE

NOTES:

1. ALL DIMENSIONS AND ELEVATIONS ARE IN METERS UNLESS STATED OTHERWISE.
2. MATERIAL PARAMETERS ARE OUTLINED IN APPENDIX E.
3. ONLY SLIP SURFACES CONSIDERED MOST CRITICAL ARE PRESENTED.

LEGEND:

- COARSE TAILINGS
- FINE TAILINGS
- COMPACTED BERM FILL (TAILINGS)
- COMPACTED BERM FILL (RESIDUAL SOIL)
- FOUNDATION SOIL
- SLIMES
- COARSE TAILINGS (DRAINED)
- FINE TAILINGS (DRAINED)
- PHREATIC SURFACE
- POND LEVEL

CLIENT

PROJECT
REPORT OF THE EXPERT PANEL ON THE TECHNICAL CAUSES OF THE FAILURE OF FEIJÃO DAM 1

TITLE
STABILITY ANALYSIS RESULTS
SECTION 2-2' - EL. 910 m
PEAK STRENGTH

SCALE	PROJECT No.	FIG. No.
1:2,500	A03355A01	18

KCB-FIG-B-L

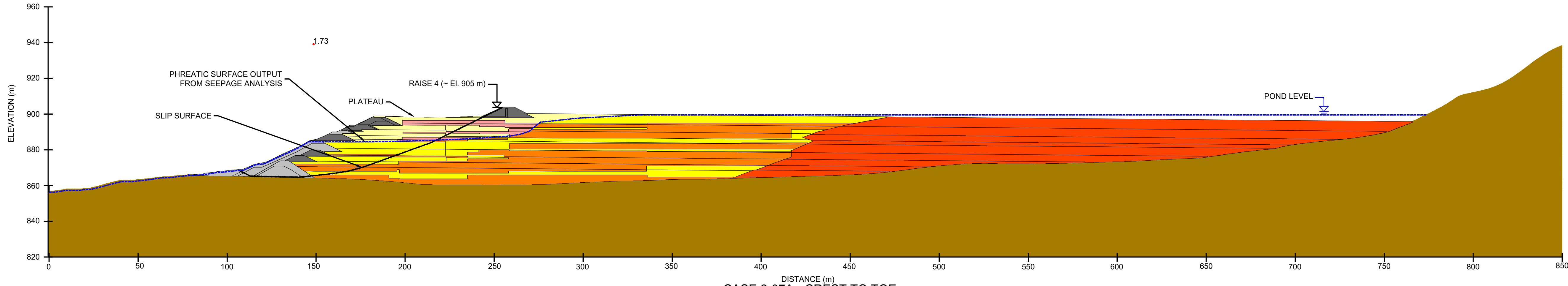

CASE 2-07A - CREST TO TOE

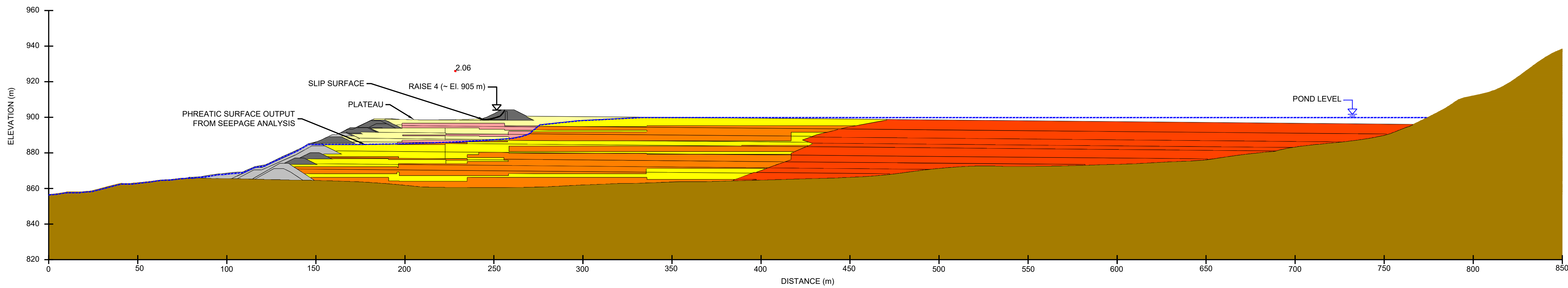

CASE 2-07B - CREST TO PLATEAU

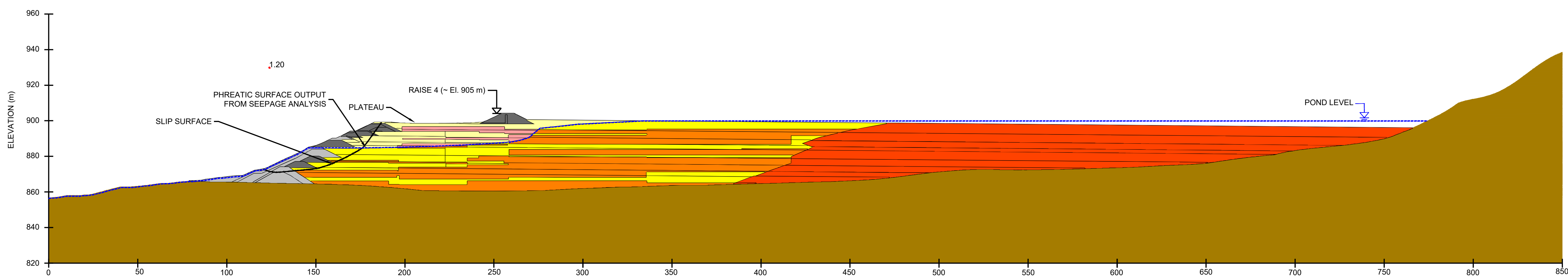

CASE 2-07C - PLATEAU TO TOE

1:2,500 0 25 50 m BASED ON A 11"X 17" DRAWING SIZE

NOTES:

1. ALL DIMENSIONS AND ELEVATIONS ARE IN METERS UNLESS STATED OTHERWISE.
2. MATERIAL PARAMETERS ARE OUTLINED IN APPENDIX E.
3. ONLY SLIP SURFACES CONSIDERED MOST CRITICAL ARE PRESENTED.

LEGEND:

- COARSE TAILINGS
- FINE TAILINGS
- COMPACTED BERM FILL (TAILINGS)
- COMPACTED BERM FILL (RESIDUAL SOIL)
- FOUNDATION SOIL
- SLIMES
- COARSE TAILINGS (DRAINED)
- FINE TAILINGS (DRAINED)
- PHREATIC SURFACE
- POND LEVEL

CLIENT

PROJECT
REPORT OF THE EXPERT PANEL ON THE TECHNICAL CAUSES OF THE FAILURE OF FEIJÃO DAM 1

TITLE
STABILITY ANALYSIS RESULTS
SECTION 2-2' - EL. 905 m
PEAK STRENGTH

SCALE	PROJECT No.	FIG. No.
1:2,500	A03355A01	19

KCB-FIG-B-L

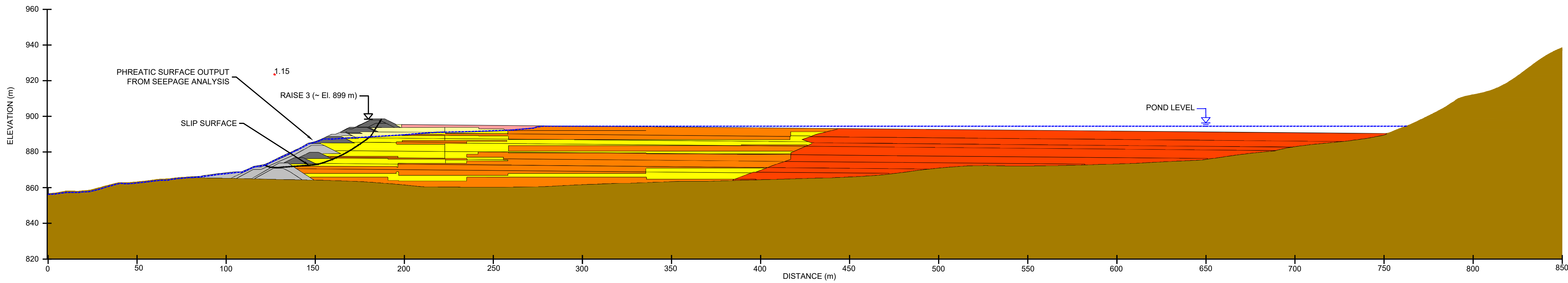

CASE 2-08A - CREST TO TOE

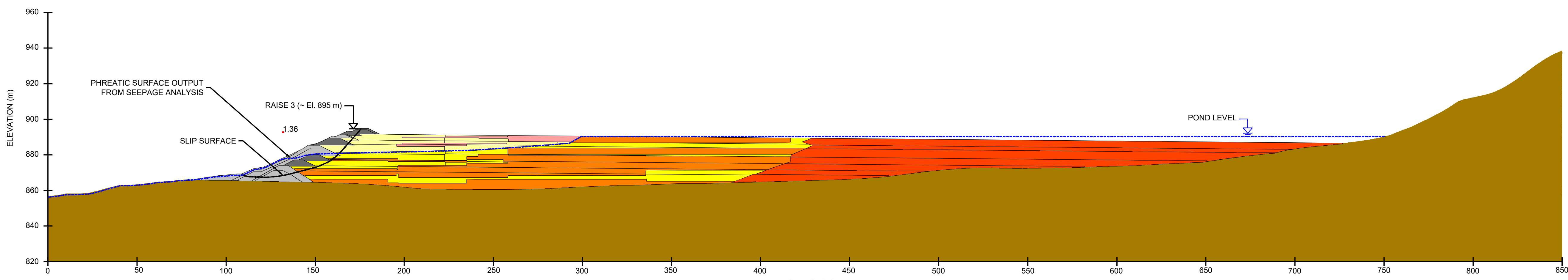

CASE 2-09A - CREST TO TOE

1:2,500 0 25 50 m BASED ON A 11"X 17" DRAWING SIZE

NOTES:

1. ALL DIMENSIONS AND ELEVATIONS ARE IN METERS UNLESS STATED OTHERWISE.
2. MATERIAL PARAMETERS ARE OUTLINED IN APPENDIX E.
3. ONLY SLIP SURFACES CONSIDERED MOST CRITICAL ARE PRESENTED.

LEGEND:

- COARSE TAILINGS
- FINE TAILINGS
- COMPACTED BERM FILL (TAILINGS)
- COMPACTED BERM FILL (RESIDUAL SOIL)
- FOUNDATION SOIL
- SLIMES
- COARSE TAILINGS (DRAINED)
- FINE TAILINGS (DRAINED)
- PHREATIC SURFACE
- POND LEVEL

CLIENT

PROJECT
REPORT OF THE EXPERT PANEL ON THE TECHNICAL CAUSES OF THE FAILURE OF FEIJÃO DAM 1

TITLE
STABILITY ANALYSIS RESULTS
SECTION 2-2' - EL. 899 m AND 895 m
PEAK STRENGTH

SCALE	PROJECT No.	FIG. No.
1:2,500	A03355A01	20

KCB-FIG-B-L

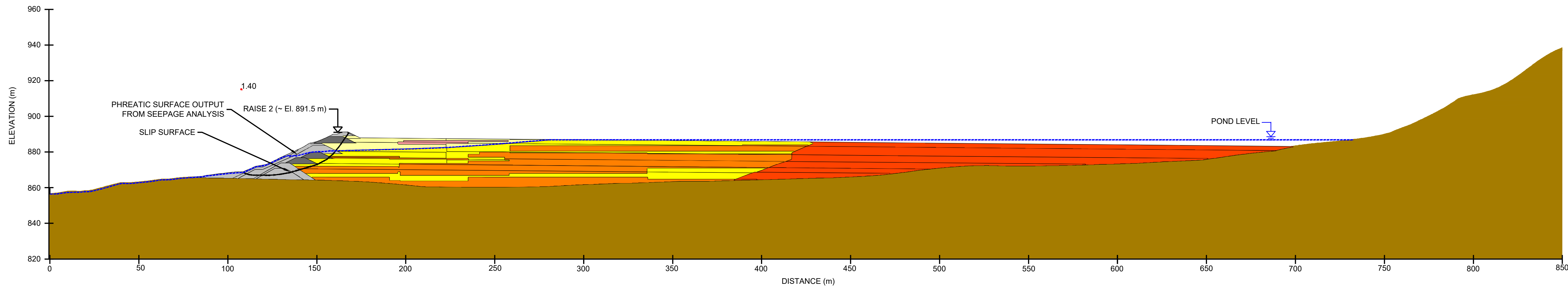

CASE 2-10A - CREST TO TOE

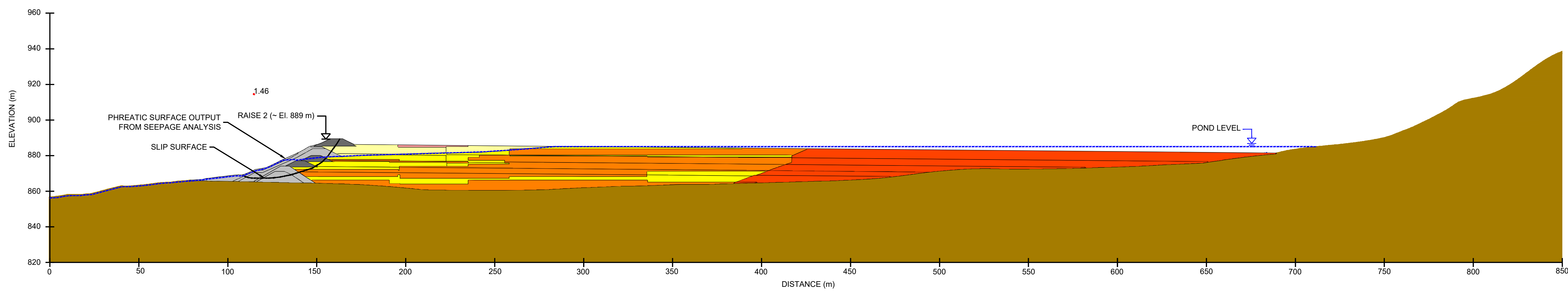

CASE 2-11A - CREST TO TOE

1:2,500 0 25 50 m BASED ON A 11"X 17" DRAWING SIZE

NOTES:

1. ALL DIMENSIONS AND ELEVATIONS ARE IN METERS UNLESS STATED OTHERWISE.
2. MATERIAL PARAMETERS ARE OUTLINED IN APPENDIX E.
3. ONLY SLIP SURFACES CONSIDERED MOST CRITICAL ARE PRESENTED.

LEGEND:

- COARSE TAILINGS
- FINE TAILINGS
- COMPACTED BERM FILL (TAILINGS)
- COMPACTED BERM FILL (RESIDUAL SOIL)
- FOUNDATION SOIL
- SLIMES
- COARSE TAILINGS (DRAINED)
- FINE TAILINGS (DRAINED)
- PHREATIC SURFACE
- POND LEVEL

CLIENT

PROJECT
REPORT OF THE EXPERT PANEL ON THE TECHNICAL CAUSES OF THE FAILURE OF FEIJÃO DAM 1

TITLE
STABILITY ANALYSIS RESULTS
SECTION 2-2' - EL. 891.5 m AND 889 m
PEAK STRENGTH

SCALE	PROJECT No.	FIG. No.
1:2,500	A03355A01	21

KCB-FIG-B-L

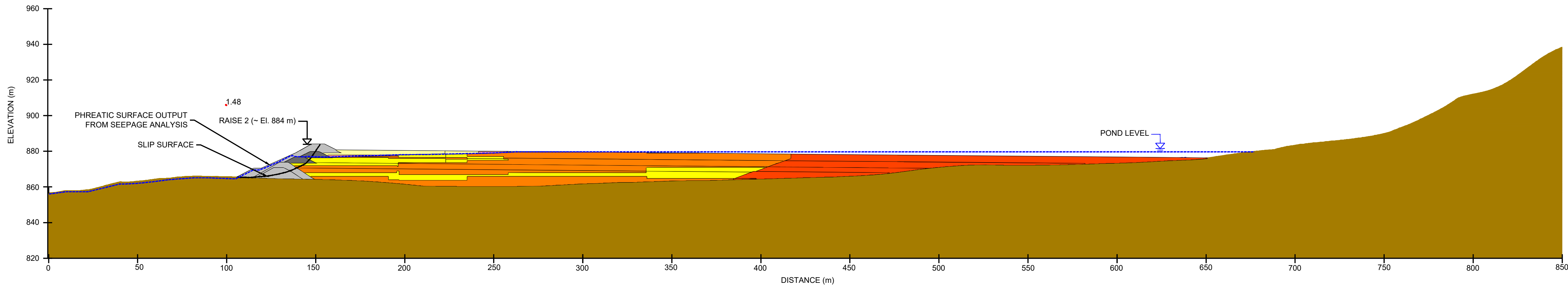

CASE 2-12A - CREST TO TOE

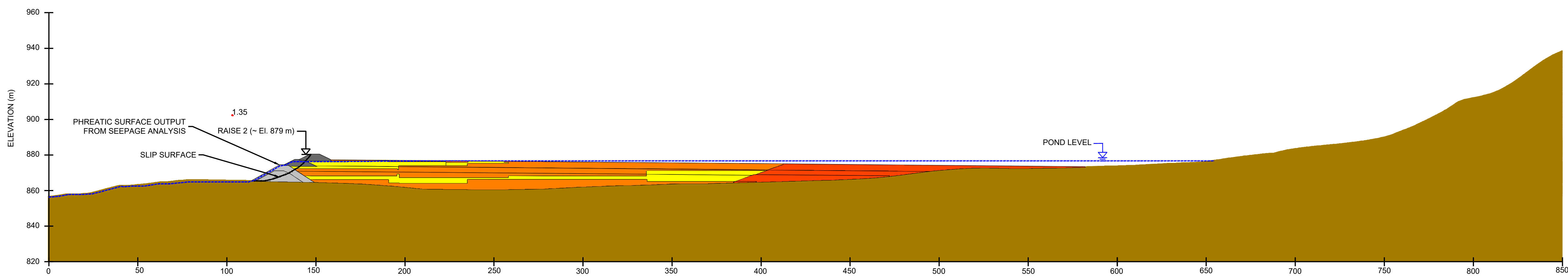

CASE 2-13A - CREST TO TOE

1:2,500 0 25 50 m BASED ON A 11"X 17" DRAWING SIZE

NOTES:

1. ALL DIMENSIONS AND ELEVATIONS ARE IN METERS UNLESS STATED OTHERWISE.
2. MATERIAL PARAMETERS ARE OUTLINED IN APPENDIX E.
3. ONLY SLIP SURFACES CONSIDERED MOST CRITICAL ARE PRESENTED.

LEGEND:

- COARSE TAILINGS
- FINE TAILINGS
- COMPACTED BERM FILL (TAILINGS)
- COMPACTED BERM FILL (RESIDUAL SOIL)
- FOUNDATION SOIL
- SLIMES
- COARSE TAILINGS (DRAINED)
- FINE TAILINGS (DRAINED)
- PHREATIC SURFACE
- POND LEVEL

CLIENT

PROJECT
REPORT OF THE EXPERT PANEL ON THE TECHNICAL CAUSES OF THE FAILURE OF FEIJÃO DAM 1

TITLE
STABILITY ANALYSIS RESULTS
SECTION 2-2' - EL. 884 m AND 879 m
PEAK STRENGTH

SCALE	PROJECT No.	FIG. No.
1:2,500	A03355A01	22

KCB-FIG-B-L

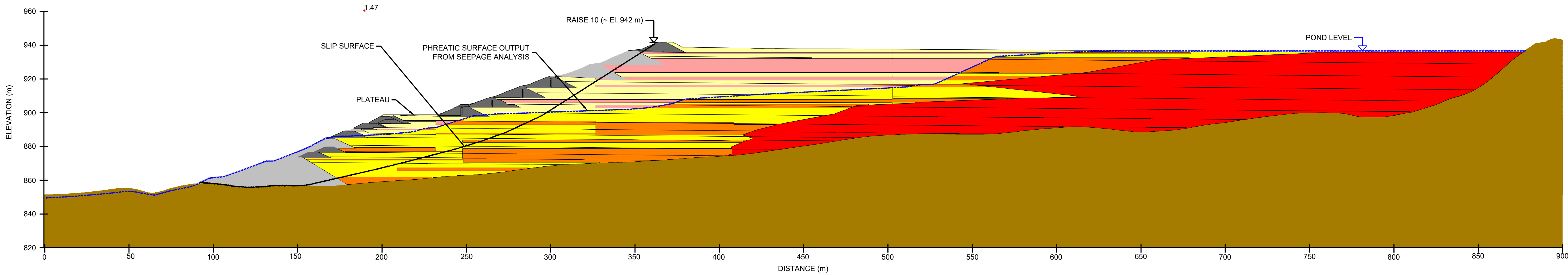

CASE 3-01A - CREST TO TOE

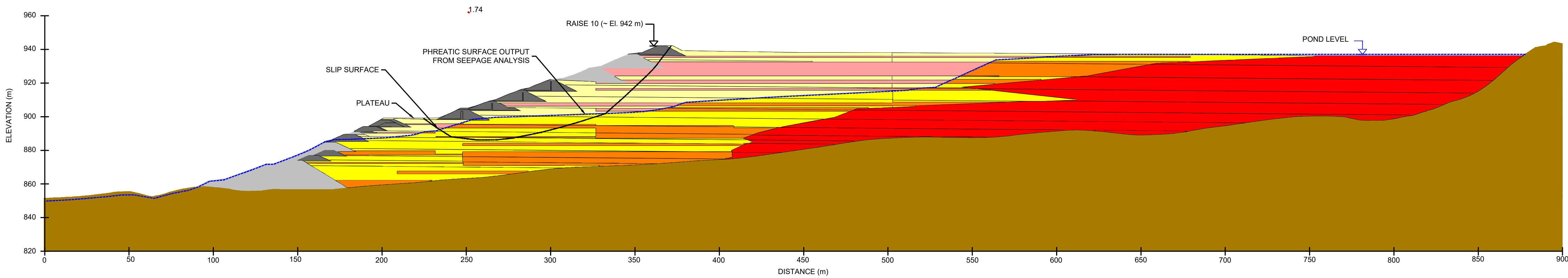

CASE 3-01B - CREST TO PLATEAU

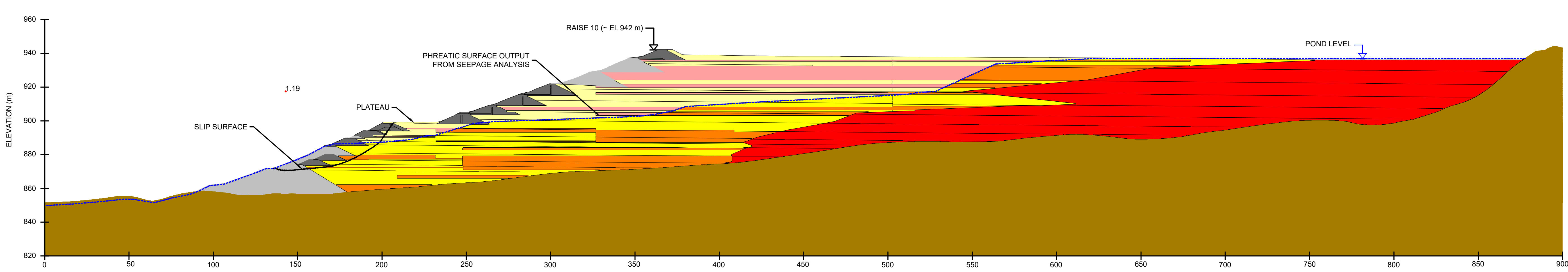

CASE 3-01C - PLATEAU TO TOE

1:2,500 0 25 50 m BASED ON A 11"X 17" DRAWING SIZE

NOTES:

1. ALL DIMENSIONS AND ELEVATIONS ARE IN METERS UNLESS STATED OTHERWISE.
2. MATERIAL PARAMETERS ARE OUTLINED IN APPENDIX E.
3. ONLY SLIP SURFACES CONSIDERED MOST CRITICAL ARE PRESENTED.

LEGEND:

- COARSE TAILINGS
- FINE TAILINGS
- COMPACTED BERM FILL (TAILINGS)
- COMPACTED BERM FILL (RESIDUAL SOIL)
- FOUNDATION SOIL
- SLIMES
- COARSE TAILINGS (DRAINED)
- FINE TAILINGS (DRAINED)
- PHREATIC SURFACE
- POND LEVEL

CLIENT

PROJECT
REPORT OF THE EXPERT PANEL ON THE TECHNICAL CAUSES OF THE FAILURE OF FEIJÃO DAM 1

TITLE
STABILITY ANALYSIS RESULTS
SECTION 3-3' - EL. 942 m
PEAK STRENGTH

SCALE	PROJECT No.	FIG. No.
1:2,500	A03355A01	23

KCB-FIG-B-L

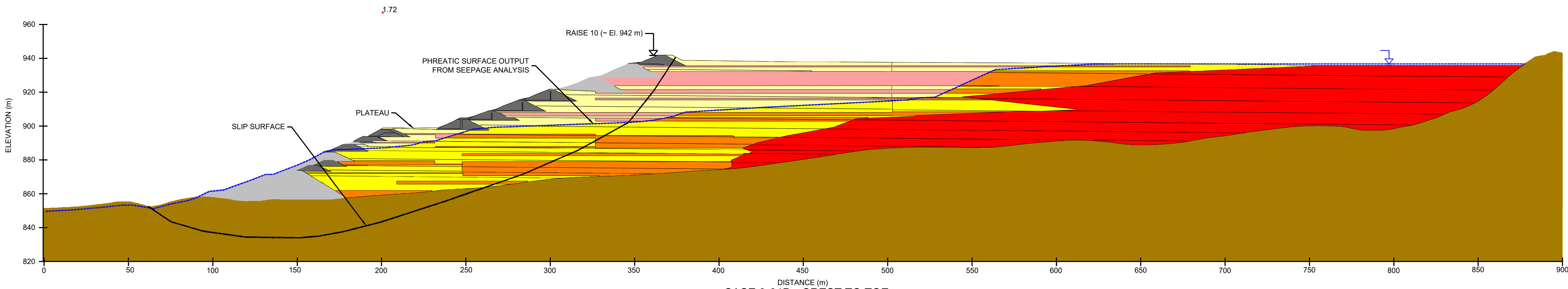

CASE 3-01D - CREST TO TOE

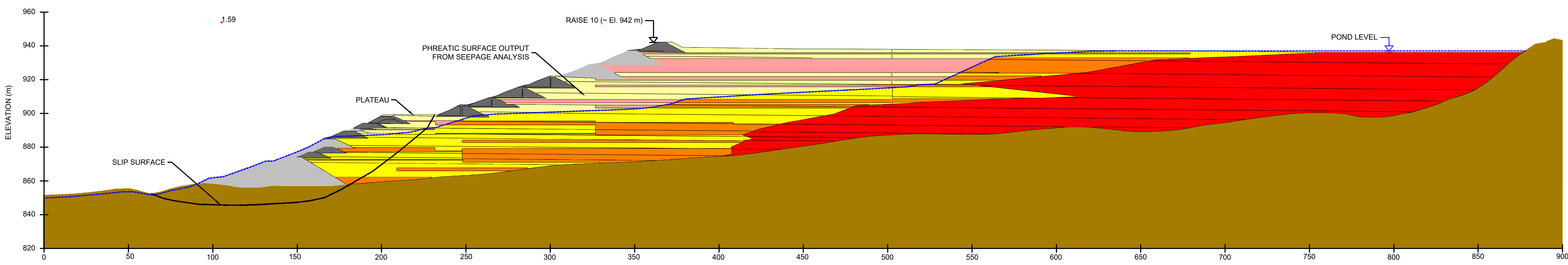

CASE 3-01E - PLATEAU TO TOE

1:2,500 0 25 50 m BASED ON A 11"X 17" DRAWING SIZE

NOTES:

1. ALL DIMENSIONS AND ELEVATIONS ARE IN METERS UNLESS STATED OTHERWISE.
2. MATERIAL PARAMETERS ARE OUTLINED IN APPENDIX E.
3. ONLY SLIP SURFACES CONSIDERED MOST CRITICAL ARE PRESENTED.

LEGEND:

- COARSE TAILINGS
- FINE TAILINGS
- COMPACTED BERM FILL (TAILINGS)
- COMPACTED BERM FILL (RESIDUAL SOIL)
- FOUNDATION SOIL
- SLIMES
- COARSE TAILINGS (DRAINED)
- FINE TAILINGS (DRAINED)
- PHREATIC SURFACE
- POND LEVEL

CLIENT

PROJECT
REPORT OF THE EXPERT PANEL ON THE TECHNICAL CAUSES OF THE FAILURE OF FEIJÃO DAM 1

TITLE
STABILITY ANALYSIS RESULTS
SECTION 3-3' - EL. 942 m
PEAK STRENGTH

SCALE	PROJECT No.	FIG. No.
1:2,500	A03355A01	24

KCB-FIG-B-L

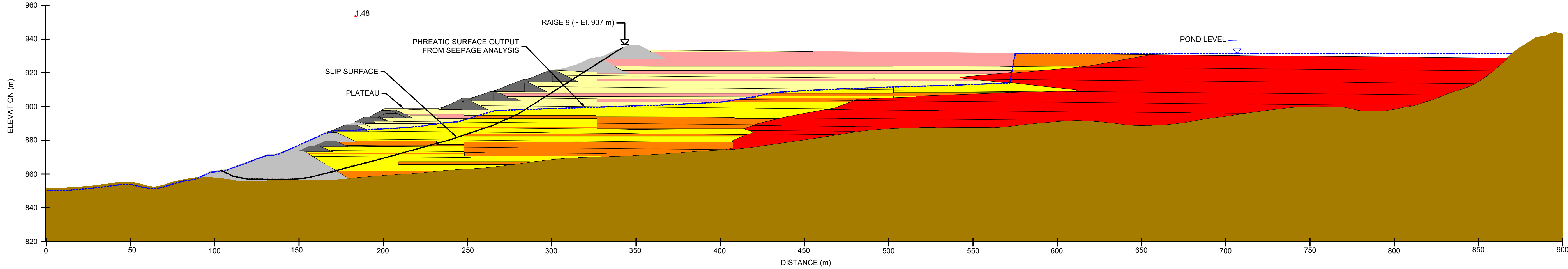

CASE 3-02A - CREST TO TOE

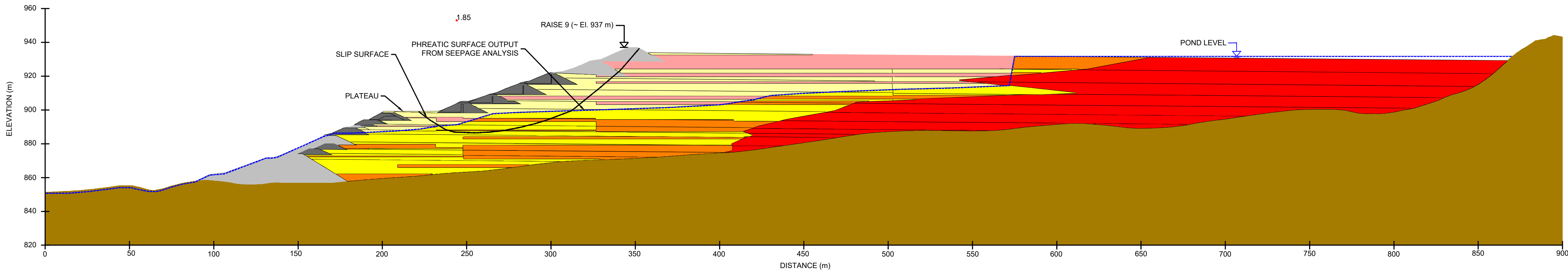

CASE 3-02B - CREST TO PLATEAU

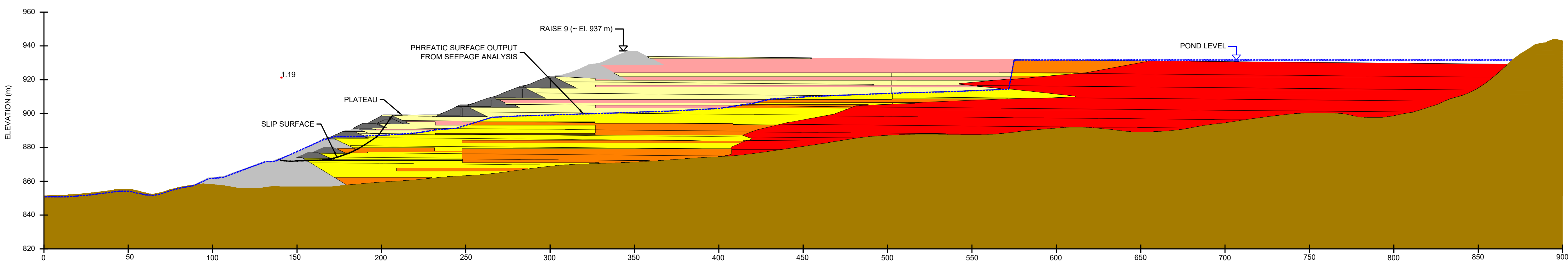

CASE 3-02C - PLATEAU TO TOE

1:2,500 0 25 50 m BASED ON A 11"X 17" DRAWING SIZE

NOTES:

1. ALL DIMENSIONS AND ELEVATIONS ARE IN METERS UNLESS STATED OTHERWISE.
2. MATERIAL PARAMETERS ARE OUTLINED IN APPENDIX E.
3. ONLY SLIP SURFACES CONSIDERED MOST CRITICAL ARE PRESENTED.

LEGEND:

- COARSE TAILINGS
- FINE TAILINGS
- COMPACTED BERM FILL (TAILINGS)
- COMPACTED BERM FILL (RESIDUAL SOIL)
- FOUNDATION SOIL
- SLIMES
- COARSE TAILINGS (DRAINED)
- FINE TAILINGS (DRAINED)
- PHREATIC SURFACE
- POND LEVEL

CLIENT

PROJECT
REPORT OF THE EXPERT PANEL ON THE TECHNICAL CAUSES OF THE FAILURE OF FEIJÃO DAM 1

TITLE
STABILITY ANALYSIS RESULTS
SECTION 3-3' - EL. 937 m
PEAK STRENGTH

SCALE	PROJECT No.	FIG. No.
1:2,500	A03355A01	25

KCB-FIG-B-L

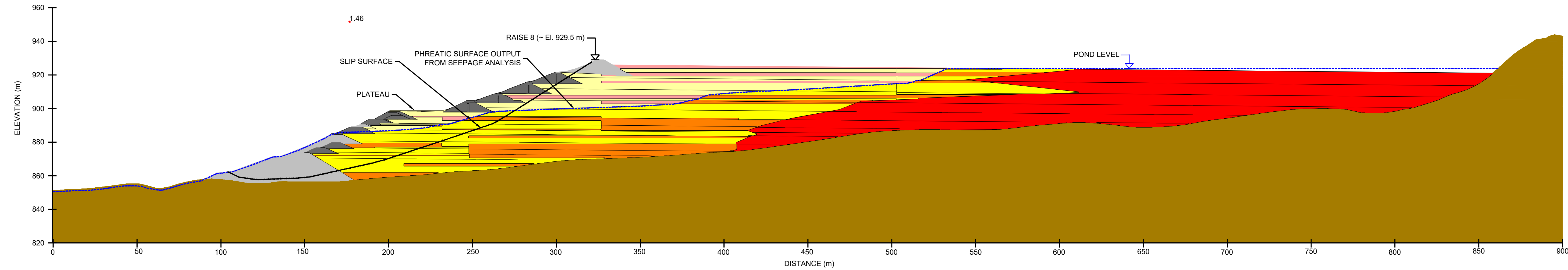

CASE 3-03A - CREST TO TOE

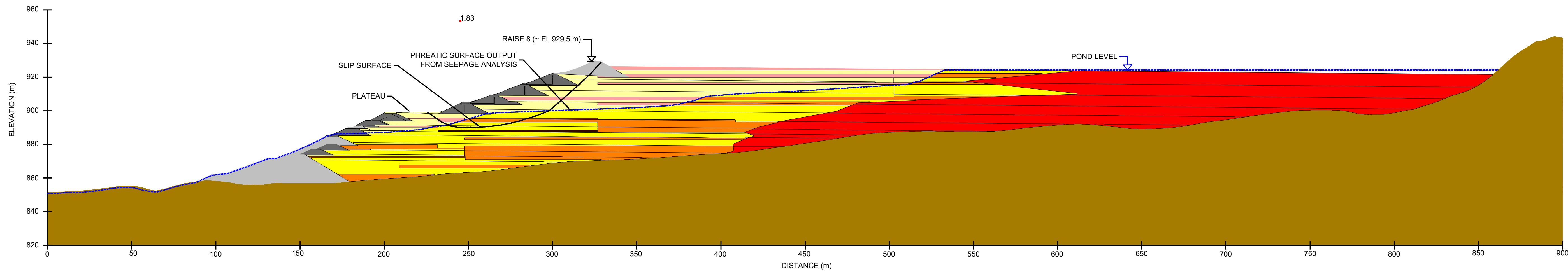

CASE 3-03B - CREST TO PLATEAU

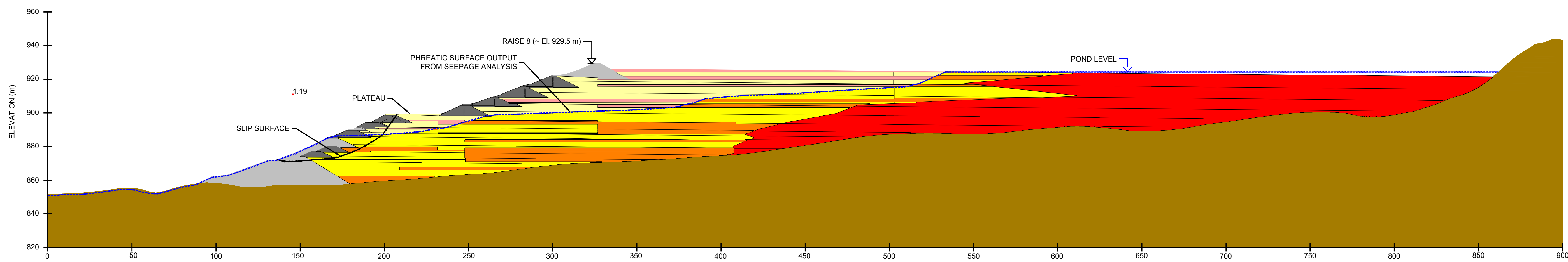

CASE 3-03C - PLATEAU TO TOE

1:2,500 0 25 50 m BASED ON A 11"X 17" DRAWING SIZE

NOTES:

1. ALL DIMENSIONS AND ELEVATIONS ARE IN METERS UNLESS STATED OTHERWISE.
2. MATERIAL PARAMETERS ARE OUTLINED IN APPENDIX E.
3. ONLY SLIP SURFACES CONSIDERED MOST CRITICAL ARE PRESENTED.

LEGEND:

- COARSE TAILINGS
- FINE TAILINGS
- COMPACTED BERM FILL (TAILINGS)
- COMPACTED BERM FILL (RESIDUAL SOIL)
- FOUNDATION SOIL
- SLIMES
- COARSE TAILINGS (DRAINED)
- FINE TAILINGS (DRAINED)
- PHREATIC SURFACE
- POND LEVEL

CLIENT

PROJECT
REPORT OF THE EXPERT PANEL ON THE TECHNICAL CAUSES OF THE FAILURE OF FEIJÃO DAM 1

TITLE
STABILITY ANALYSIS RESULTS
SECTION 3-3' - EL. 929.5 m
PEAK STRENGTH

SCALE	PROJECT No.	FIG. No.
1:2,500	A03355A01	26

KCB-FIG-B-L

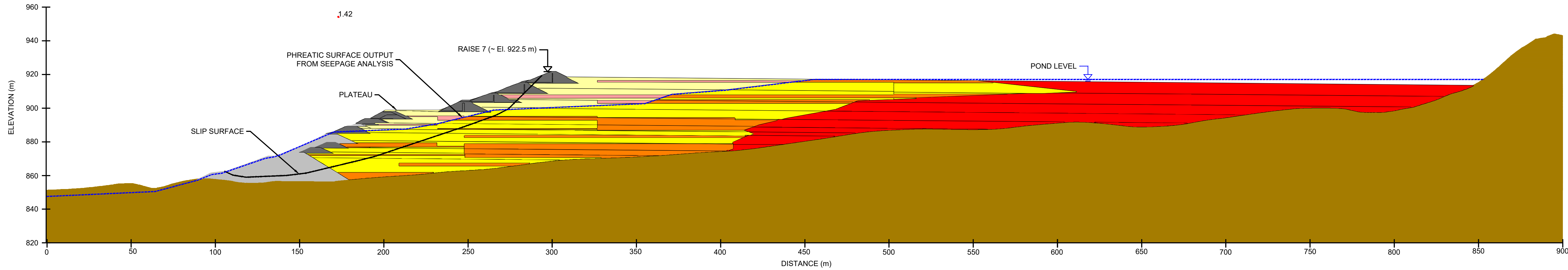

CASE 3-04A- CREST TO TOE

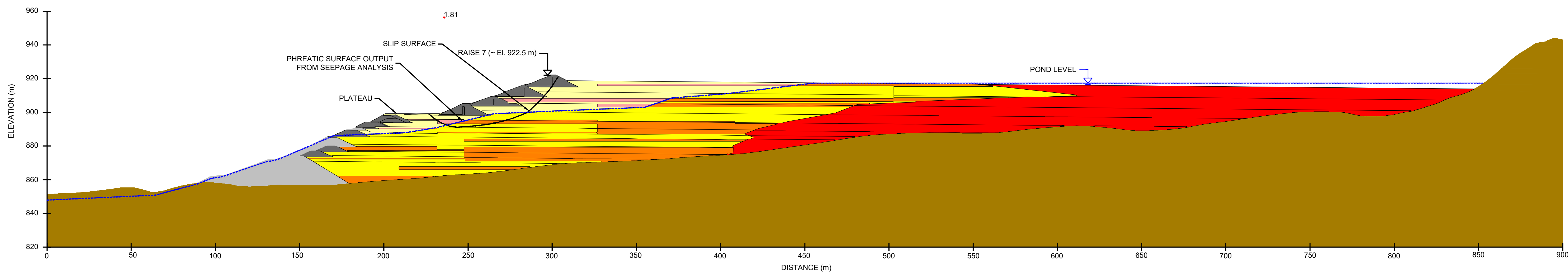

CASE 3-04B - CREST TO PLATEAU

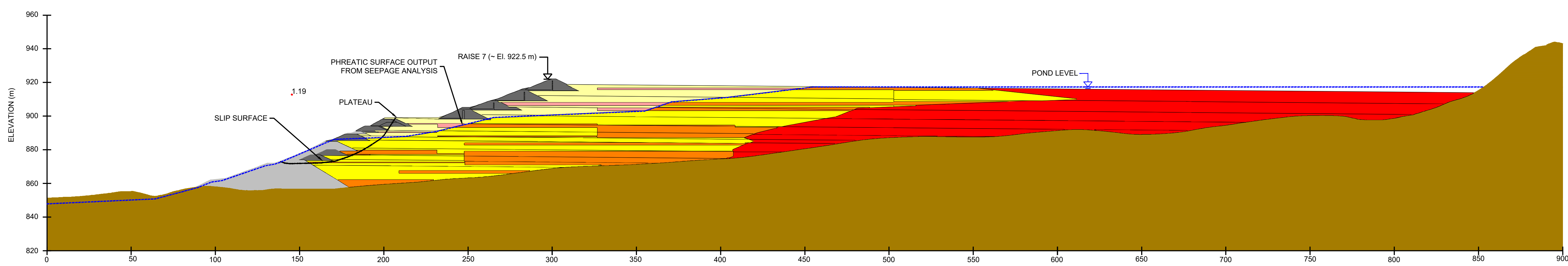

CASE 3-04C - PLATEAU TO TOE

1:2,500 0 25 50 m BASED ON A 11"X 17" DRAWING SIZE

NOTES:

1. ALL DIMENSIONS AND ELEVATIONS ARE IN METERS UNLESS STATED OTHERWISE.
2. MATERIAL PARAMETERS ARE OUTLINED IN APPENDIX E.
3. ONLY SLIP SURFACES CONSIDERED MOST CRITICAL ARE PRESENTED.

LEGEND:

- COARSE TAILINGS
- FINE TAILINGS
- COMPACTED BERM FILL (TAILINGS)
- COMPACTED BERM FILL (RESIDUAL SOIL)
- FOUNDATION SOIL
- SLIMES
- COARSE TAILINGS (DRAINED)
- FINE TAILINGS (DRAINED)
- PHREATIC SURFACE
- POND LEVEL

CLIENT

PROJECT
REPORT OF THE EXPERT PANEL ON THE TECHNICAL CAUSES OF THE FAILURE OF FEIJÃO DAM 1

TITLE
STABILITY ANALYSIS RESULTS
SECTION 3-3' - EL. 922.5 m
PEAK STRENGTH

SCALE	PROJECT No.	FIG. No.
1:2,500	A03355A01	27

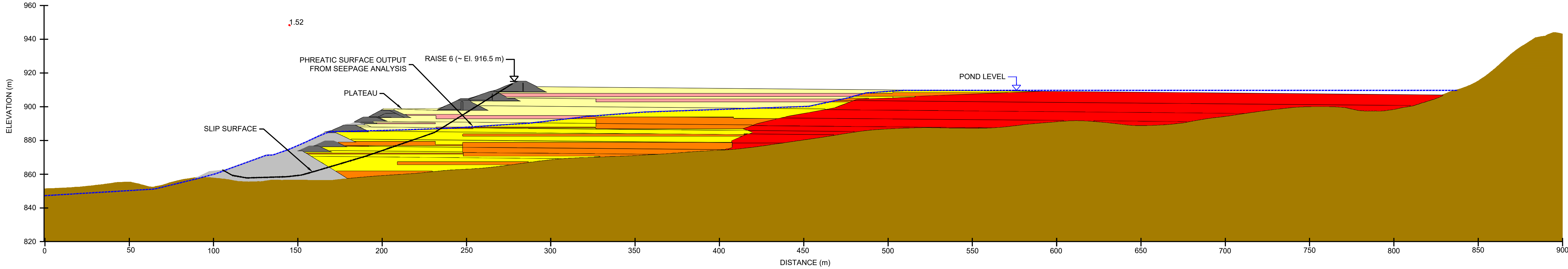

CASE 3-05A - CREST TO TOE

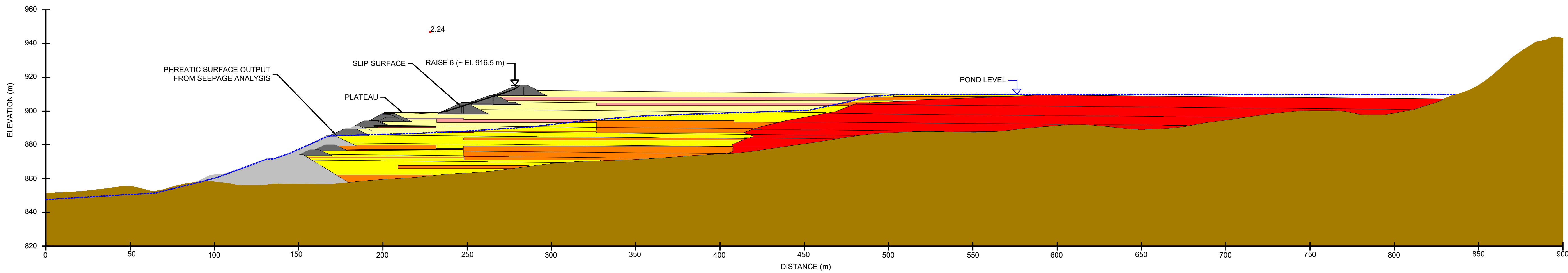

CASE 3-05B - CREST TO PLATEAU

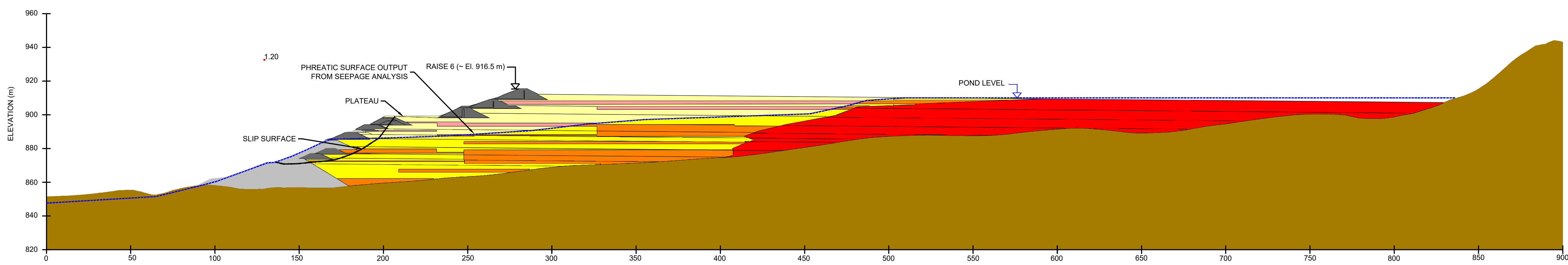

CASE 3-05C - PLATEAU TO TOE

1:2,500 0 25 50 m BASED ON A 11"X 17" DRAWING SIZE

NOTES:

1. ALL DIMENSIONS AND ELEVATIONS ARE IN METERS UNLESS STATED OTHERWISE.
2. MATERIAL PARAMETERS ARE OUTLINED IN APPENDIX E.
3. ONLY SLIP SURFACES CONSIDERED MOST CRITICAL ARE PRESENTED.

LEGEND:

- COARSE TAILINGS
- FINE TAILINGS
- COMPACTED BERM FILL (TAILINGS)
- COMPACTED BERM FILL (RESIDUAL SOIL)
- FOUNDATION SOIL
- SLIMES
- COARSE TAILINGS (DRAINED)
- FINE TAILINGS (DRAINED)
- PHREATIC SURFACE
- POND LEVEL

CLIENT

PROJECT
REPORT OF THE EXPERT PANEL ON THE TECHNICAL CAUSES OF THE FAILURE OF FEIJÃO DAM 1

TITLE
STABILITY ANALYSIS RESULTS
SECTION 3-3' - EL. 916.5 m
PEAK STRENGTH

SCALE	PROJECT No.	FIG. No.
1:2,500	A03355A01	28

KCB-FIG-B-L

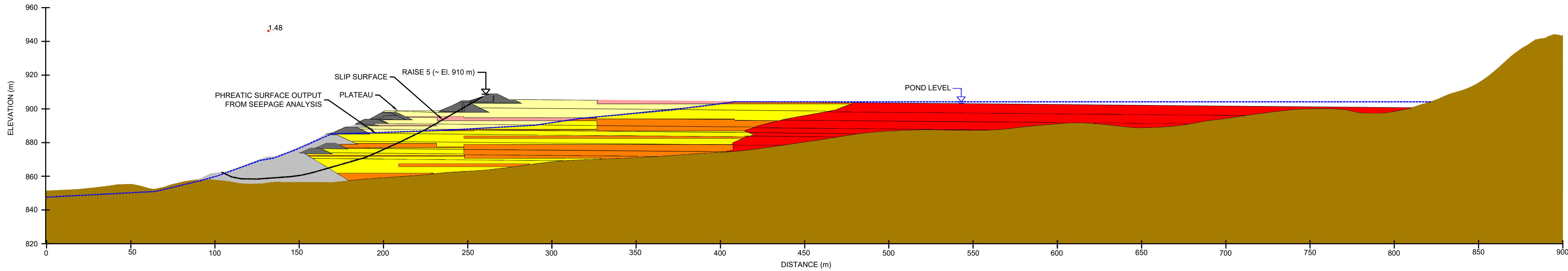

CASE 3-06A - CREST TO TOE

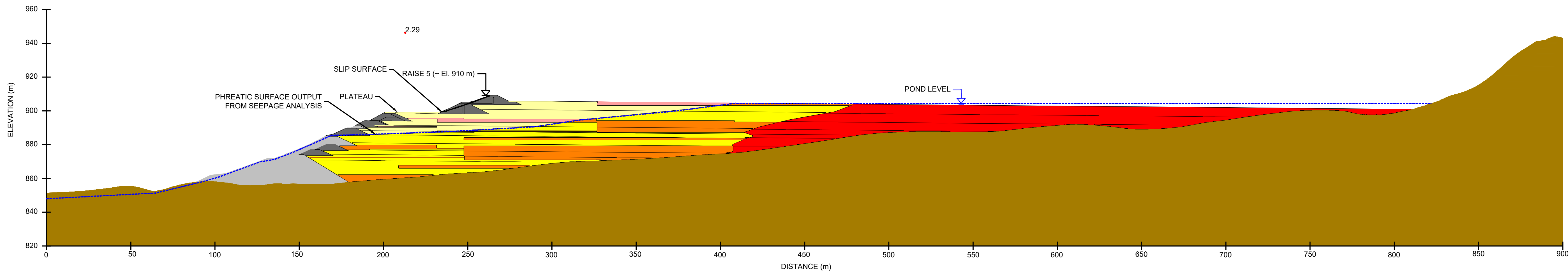

CASE 3-06B - CREST TO PLATEAU

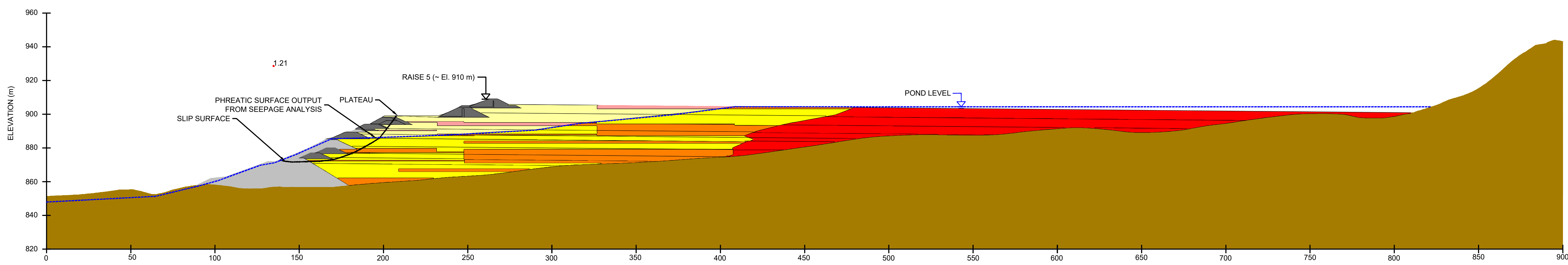

CASE 3-06C - PLATEAU TO TOE

1:2,500 0 25 50 m BASED ON A 11"X 17" DRAWING SIZE

NOTES:

1. ALL DIMENSIONS AND ELEVATIONS ARE IN METERS UNLESS STATED OTHERWISE.
2. MATERIAL PARAMETERS ARE OUTLINED IN APPENDIX E.
3. ONLY SLIP SURFACES CONSIDERED MOST CRITICAL ARE PRESENTED.

LEGEND:

- COARSE TAILINGS
- FINE TAILINGS
- COMPACTED BERM FILL (TAILINGS)
- COMPACTED BERM FILL (RESIDUAL SOIL)
- FOUNDATION SOIL
- SLIMES
- COARSE TAILINGS (DRAINED)
- FINE TAILINGS (DRAINED)
- PHREATIC SURFACE
- POND LEVEL

CLIENT

PROJECT
REPORT OF THE EXPERT PANEL ON THE TECHNICAL CAUSES OF THE FAILURE OF FEIJÃO DAM 1

TITLE
STABILITY ANALYSIS RESULTS
SECTION 3-3' - EL. 910 m
PEAK STRENGTH

SCALE	PROJECT No.	FIG. No.
1:2,500	A03355A01	29

KCB-FIG-B-L

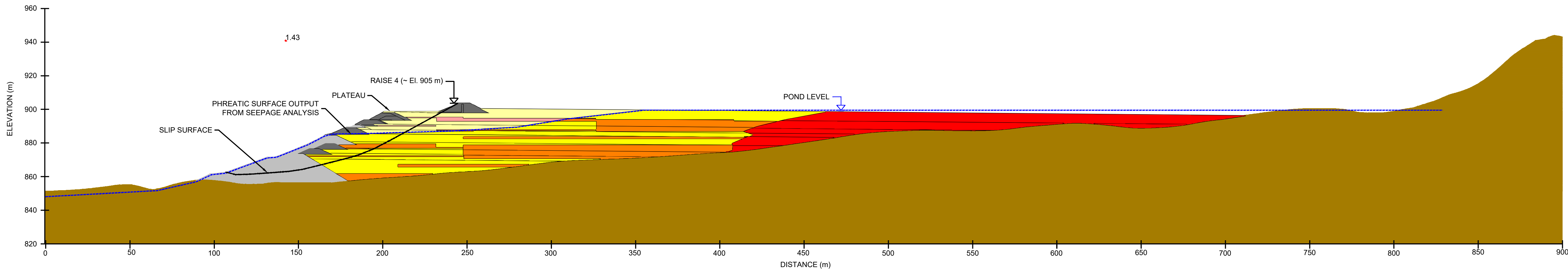

CASE 3-07A - CREST TO TOE

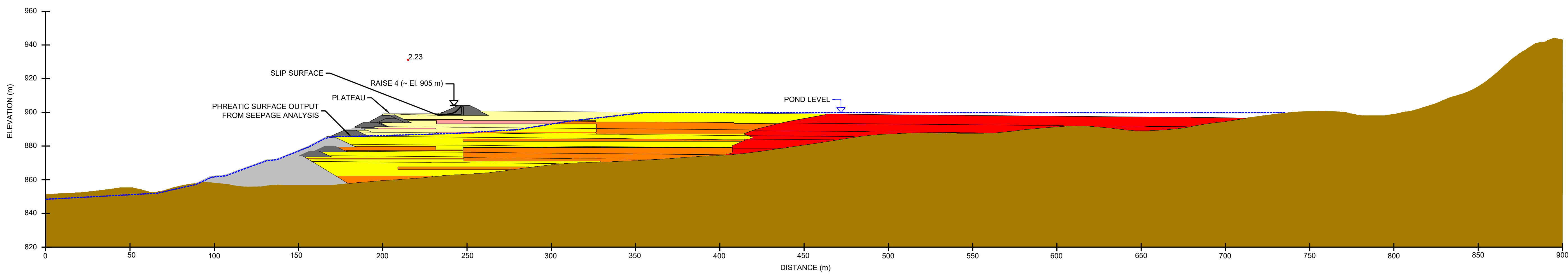

CASE 3-07B - CREST TO PLATEAU

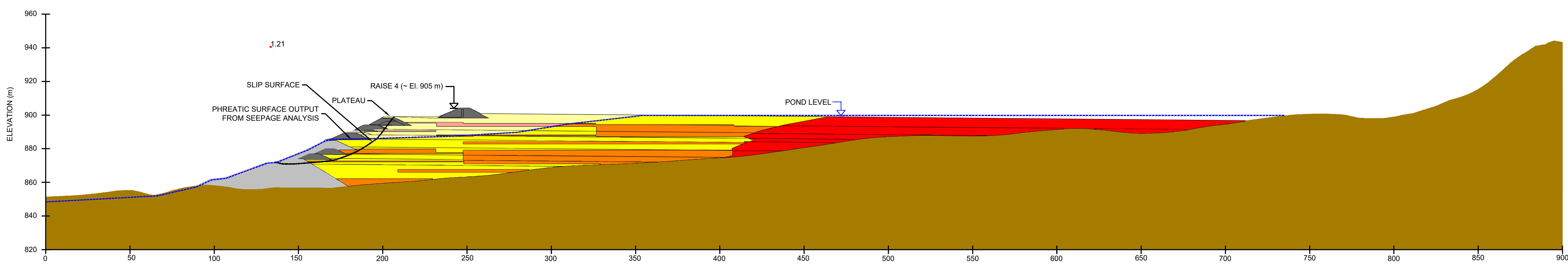

CASE 3-07C - PLATEAU TO TOE

1:2,500 0 25 50 m BASED ON A 11"X 17" DRAWING SIZE

NOTES:

1. ALL DIMENSIONS AND ELEVATIONS ARE IN METERS UNLESS STATED OTHERWISE.
2. MATERIAL PARAMETERS ARE OUTLINED IN APPENDIX E.
3. ONLY SLIP SURFACES CONSIDERED MOST CRITICAL ARE PRESENTED.

LEGEND:

- COARSE TAILINGS
- FINE TAILINGS
- COMPACTED BERM FILL (TAILINGS)
- COMPACTED BERM FILL (RESIDUAL SOIL)
- FOUNDATION SOIL
- SLIMES
- COARSE TAILINGS (DRAINED)
- FINE TAILINGS (DRAINED)
- PHREATIC SURFACE
- POND LEVEL

CLIENT

PROJECT
REPORT OF THE EXPERT PANEL ON THE TECHNICAL CAUSES OF THE FAILURE OF FEIJÃO DAM 1

TITLE
STABILITY ANALYSIS RESULTS
SECTION 3-3' - EL. 905 m
PEAK STRENGTH

SCALE	PROJECT No.	FIG. No.
1:2,500	A03355A01	30

KCB-FIG-B-L

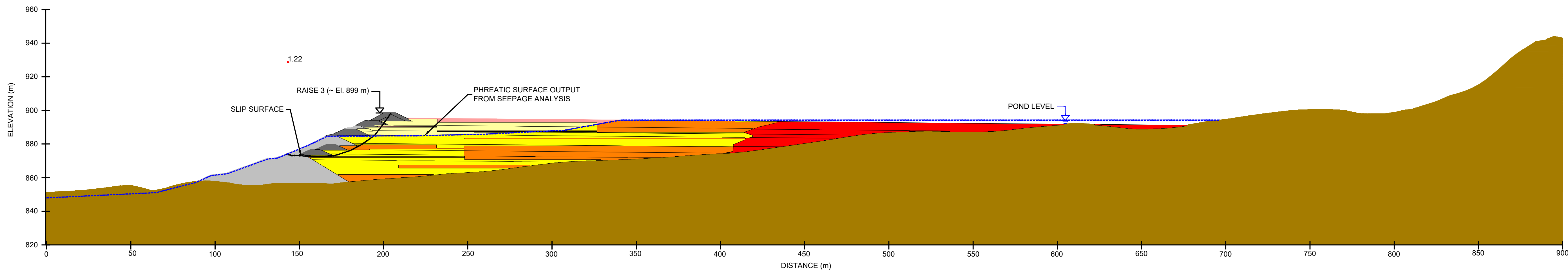

CASE 3-08A - CREST TO TOE

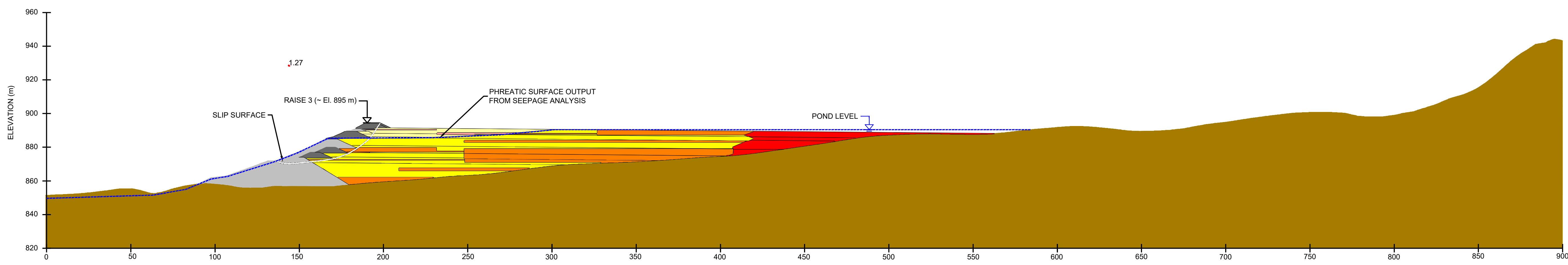

CASE 3-09A - CREST TO TOE

1:2,500 0 25 50 m BASED ON A 11"X 17" DRAWING SIZE

NOTES:

1. ALL DIMENSIONS AND ELEVATIONS ARE IN METERS UNLESS STATED OTHERWISE.
2. MATERIAL PARAMETERS ARE OUTLINED IN APPENDIX E.
3. ONLY SLIP SURFACES CONSIDERED MOST CRITICAL ARE PRESENTED.

LEGEND:

- COARSE TAILINGS
- FINE TAILINGS
- COMPACTED BERM FILL (TAILINGS)
- COMPACTED BERM FILL (RESIDUAL SOIL)
- FOUNDATION SOIL
- SLIMES
- COARSE TAILINGS (DRAINED)
- FINE TAILINGS (DRAINED)
- PHREATIC SURFACE
- POND LEVEL

CLIENT	
PROJECT	REPORT OF THE EXPERT PANEL ON THE TECHNICAL CAUSES OF THE FAILURE OF FEIJÃO DAM 1
TITLE	STABILITY ANALYSIS RESULTS SECTION 3-3' - EL. 899 m AND 895 m PEAK STRENGTH
SCALE	1:2,500
PROJECT No.	A03355A01
FIG. No.	31

KCB-FIG-B-L

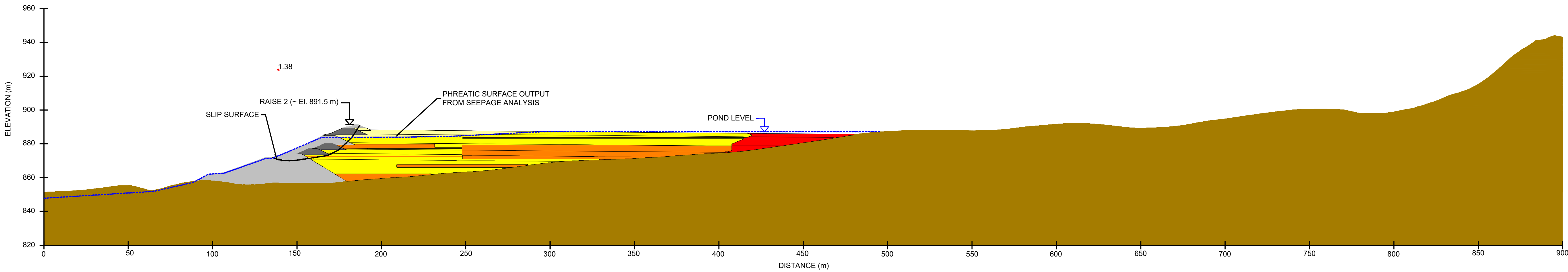

CASE 3-10A - CREST TO TOE

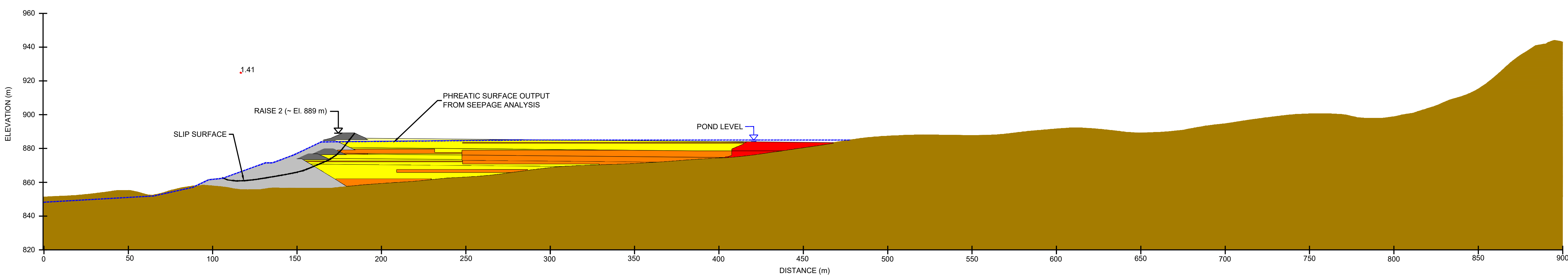

CASE 3-11A - CREST TO TOE

1:2,500 0 25 50 m BASED ON A 11"X 17" DRAWING SIZE

NOTES:

1. ALL DIMENSIONS AND ELEVATIONS ARE IN METERS UNLESS STATED OTHERWISE.
2. MATERIAL PARAMETERS ARE OUTLINED IN APPENDIX E.
3. ONLY SLIP SURFACES CONSIDERED MOST CRITICAL ARE PRESENTED.

LEGEND:

- COARSE TAILINGS
- FINE TAILINGS
- COMPACTED BERM FILL (TAILINGS)
- COMPACTED BERM FILL (RESIDUAL SOIL)
- FOUNDATION SOIL
- SLIMES
- COARSE TAILINGS (DRAINED)
- FINE TAILINGS (DRAINED)
- PHREATIC SURFACE
- POND LEVEL

CLIENT

PROJECT
REPORT OF THE EXPERT PANEL ON THE TECHNICAL CAUSES OF THE FAILURE OF FEIJÃO DAM 1

TITLE
STABILITY ANALYSIS RESULTS
SECTION 3-3' - EL. 891.5 m AND 889 m
PEAK STRENGTH

SCALE	PROJECT No.	FIG. No.
1:2,500	A03355A01	32

KCB-FIG-B-L

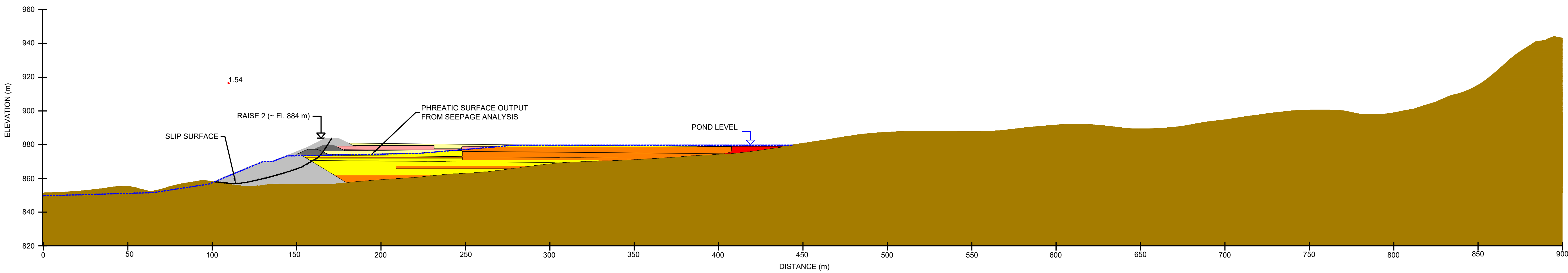

CASE 3-12A - CREST TO TOE

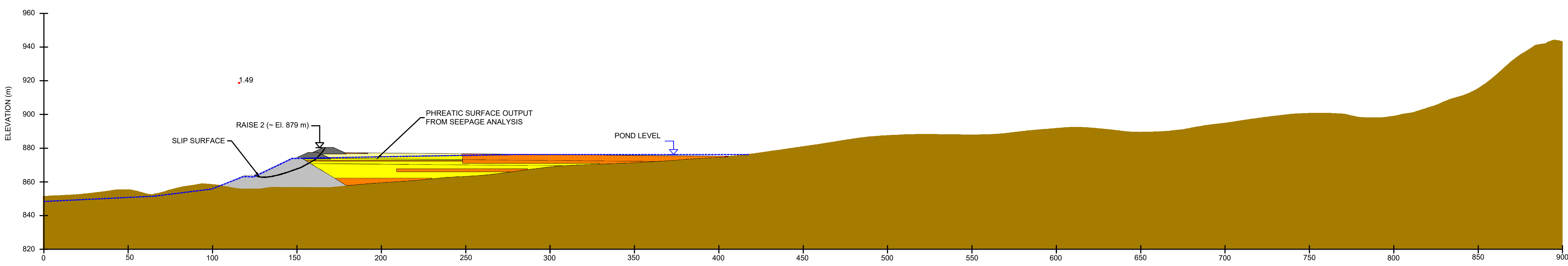

CASE 3-13A - CREST TO TOE

1:2,500 0 25 50 m BASED ON A 11"X 17" DRAWING SIZE

NOTES:

1. ALL DIMENSIONS AND ELEVATIONS ARE IN METERS UNLESS STATED OTHERWISE.
2. MATERIAL PARAMETERS ARE OUTLINED IN APPENDIX E.
3. ONLY SLIP SURFACES CONSIDERED MOST CRITICAL ARE PRESENTED.

LEGEND:

- COARSE TAILINGS
- FINE TAILINGS
- COMPACTED BERM FILL (TAILINGS)
- COMPACTED BERM FILL (RESIDUAL SOIL)
- FOUNDATION SOIL
- SLIMES
- COARSE TAILINGS (DRAINED)
- FINE TAILINGS (DRAINED)
- PHREATIC SURFACE
- POND LEVEL

CLIENT

PROJECT
REPORT OF THE EXPERT PANEL ON THE TECHNICAL CAUSES OF THE FAILURE OF FEIJÃO DAM 1

TITLE
STABILITY ANALYSIS RESULTS
SECTION 3-3' - EL. 884 m AND 879 m
PEAK STRENGTH

SCALE	PROJECT No.	FIG. No.
1:2,500	A03355A01	33

KCB-FIG-B-L

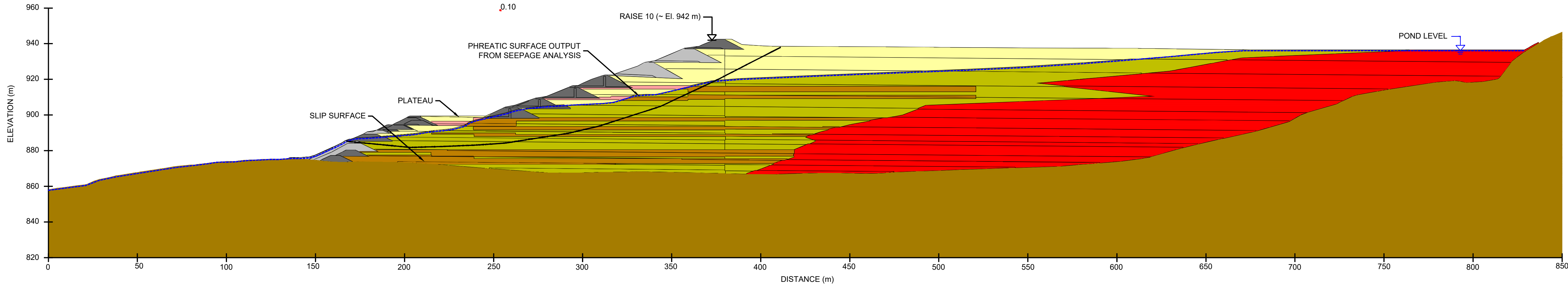

CASE 1-01F - CREST TO TOE

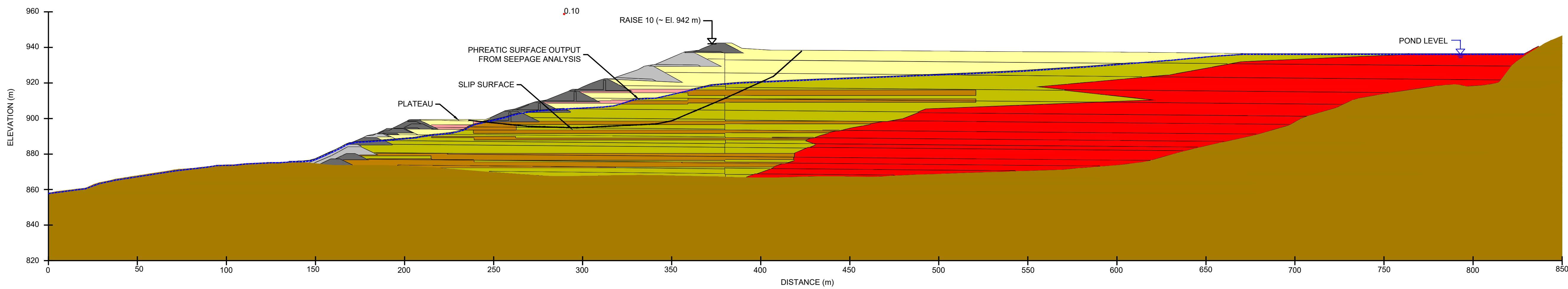

CASE 1-01G - CREST TO PLATEAU

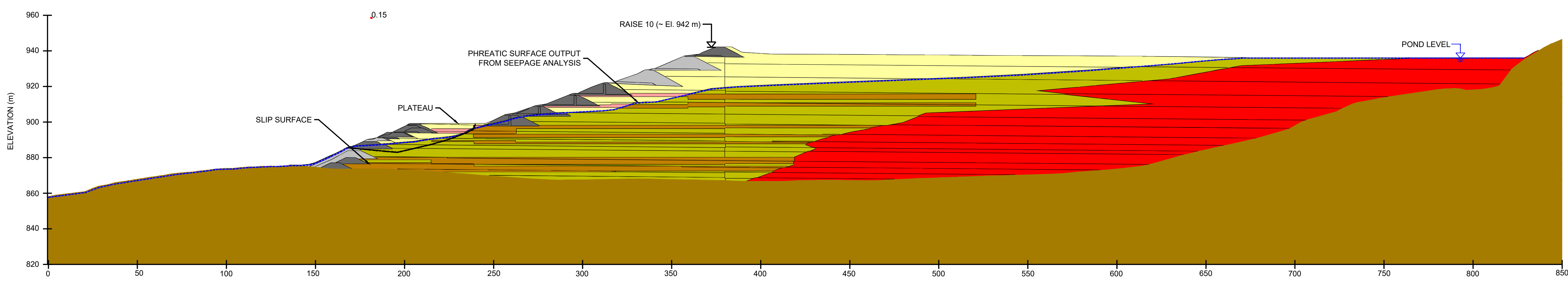

CASE 1-01H - PLATEAU TO TOE

1:2,500 0 25 50 m BASED ON A 11"X 17" DRAWING SIZE

NOTES:

1. ALL DIMENSIONS AND ELEVATIONS ARE IN METERS UNLESS STATED OTHERWISE.
2. MATERIAL PARAMETERS ARE OUTLINED IN APPENDIX E.
3. ONLY SLIP SURFACES CONSIDERED MOST CRITICAL ARE PRESENTED.

LEGEND:

- COARSE TAILINGS
- FINE TAILINGS
- COMPACTED BERM FILL (TAILINGS)
- COMPACTED BERM FILL (RESIDUAL SOIL)
- FOUNDATION SOIL
- SLIMES
- COARSE TAILINGS (DRAINED)
- FINE TAILINGS (DRAINED)
- PHREATIC SURFACE
- POND LEVEL

CLIENT

PROJECT
REPORT OF THE EXPERT PANEL ON THE TECHNICAL CAUSES OF THE FAILURE OF FEIJÃO DAM 1

TITLE
STABILITY ANALYSIS RESULTS
SECTION 1-1' - EL. 942 m
LIQUIFIED STRENGTH

SCALE	PROJECT No.	FIG. No.
1:2,500	A03355A01	34

KCB-FIG-B-L

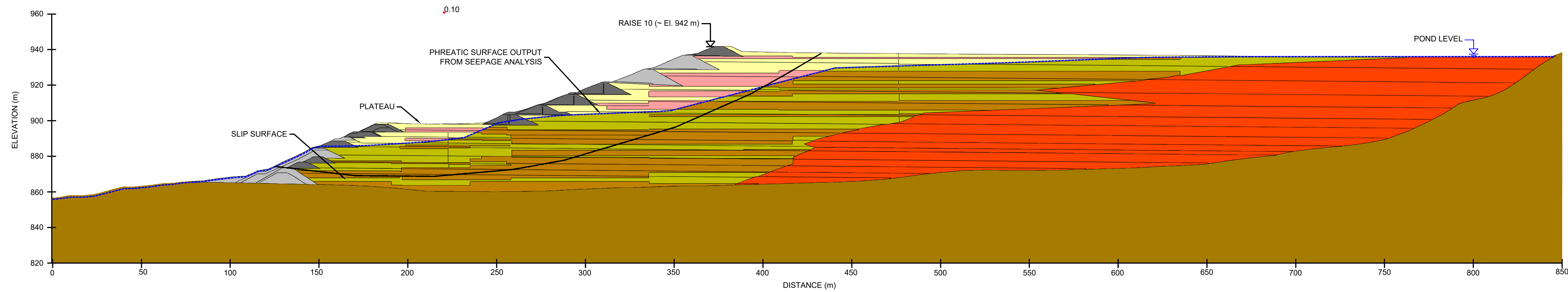

CASE 2-01F - CREST TO TOE

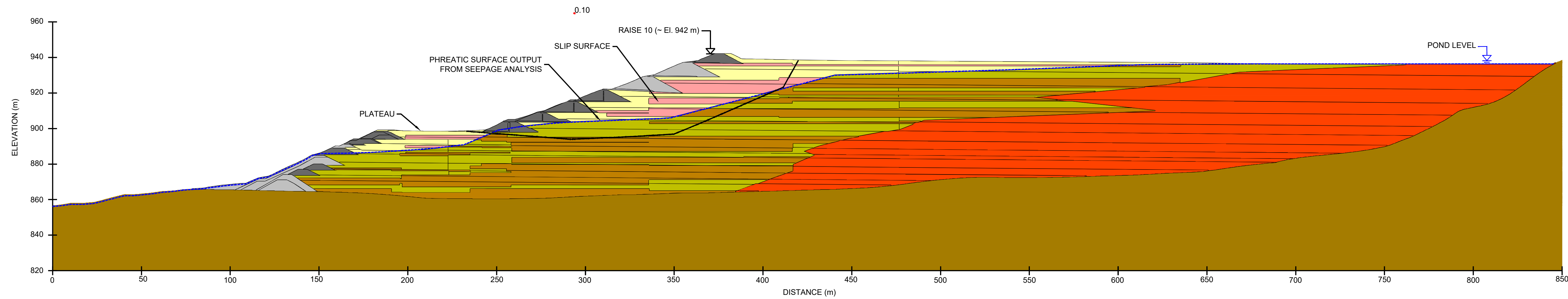

CASE 2-01G - CREST TO PLATEAU

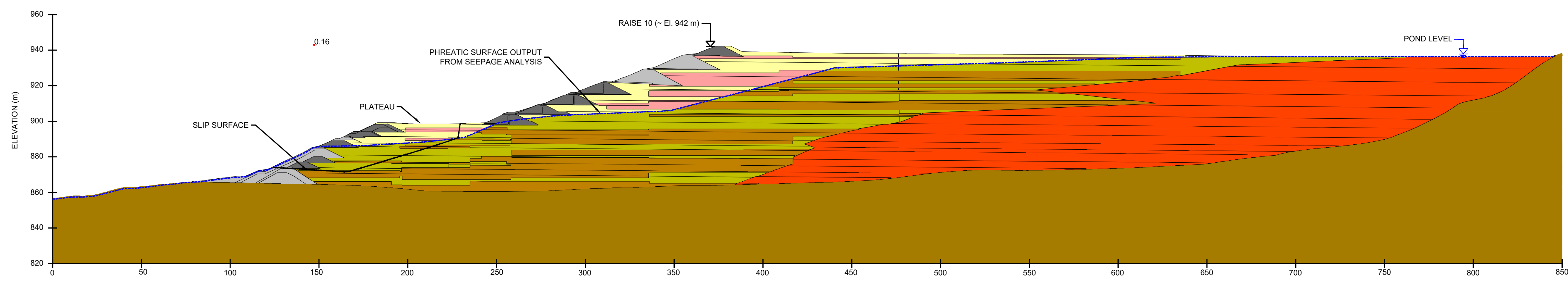

CASE 2-01H - PLATEAU TO TOE

1:2,500 0 25 50 m BASED ON A 11"X 17" DRAWING SIZE

NOTES:

1. ALL DIMENSIONS AND ELEVATIONS ARE IN METERS UNLESS STATED OTHERWISE.
2. MATERIAL PARAMETERS ARE OUTLINED IN APPENDIX E.
3. ONLY SLIP SURFACES CONSIDERED MOST CRITICAL ARE PRESENTED.

LEGEND:

- COARSE TAILINGS
- FINE TAILINGS
- COMPACTED BERM FILL (TAILINGS)
- COMPACTED BERM FILL (RESIDUAL SOIL)
- FOUNDATION SOIL
- SLIMES
- COARSE TAILINGS (DRAINED)
- FINE TAILINGS (DRAINED)
- PHREATIC SURFACE
- POND LEVEL

CLIENT

PROJECT
REPORT OF THE EXPERT PANEL ON THE TECHNICAL CAUSES OF THE FAILURE OF FEIJÃO DAM 1

TITLE
STABILITY ANALYSIS RESULTS
SECTION 2-2' - EL. 942 m
LIQUIFIED STRENGTH

SCALE	PROJECT No.	FIG. No.
1:2,500	A03355A01	35

KCB-FIG-B-L

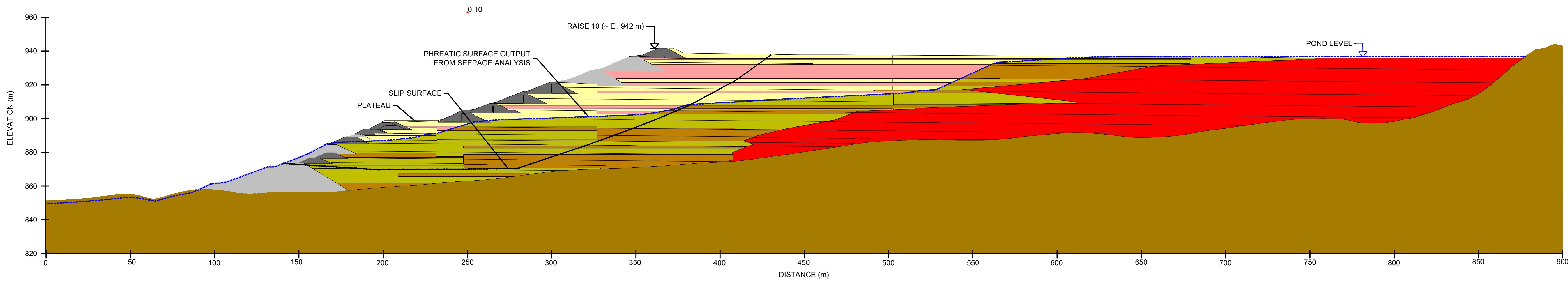

CASE 3-01F - CREST TO TOE

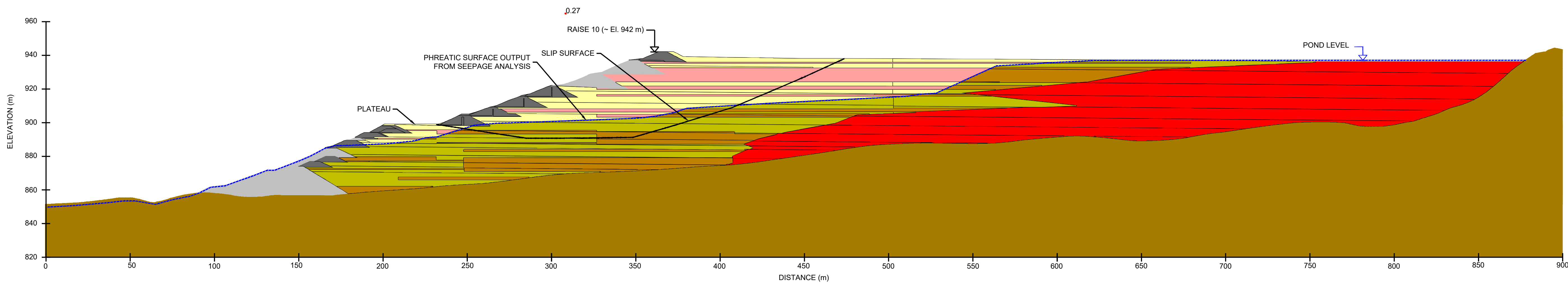

CASE 3-01G - CREST TO PLATEAU

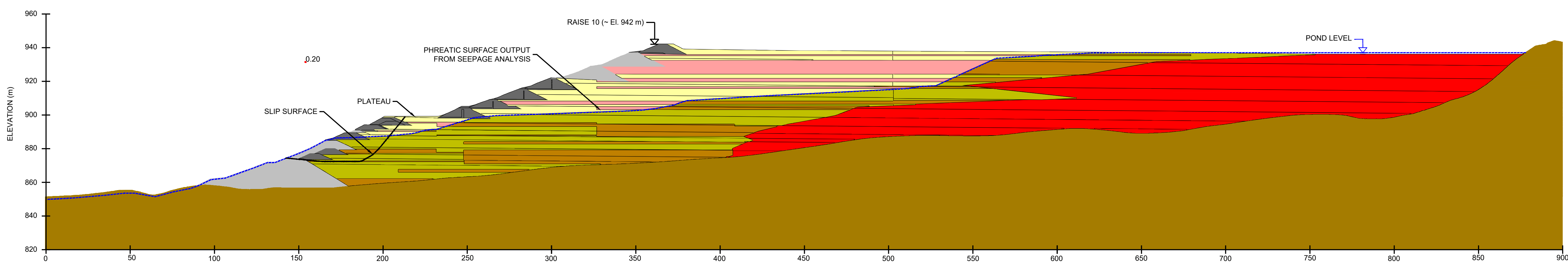

CASE 3-01H - PLATEAU TO TOE

1:2,500 0 25 50 m BASED ON A 11"X 17" DRAWING SIZE

NOTES:

1. ALL DIMENSIONS AND ELEVATIONS ARE IN METERS UNLESS STATED OTHERWISE.
2. MATERIAL PARAMETERS ARE OUTLINED IN APPENDIX E.
3. ONLY SLIP SURFACES CONSIDERED MOST CRITICAL ARE PRESENTED.

LEGEND:

- COARSE TAILINGS
- FINE TAILINGS
- COMPACTED BERM FILL (TAILINGS)
- COMPACTED BERM FILL (RESIDUAL SOIL)
- FOUNDATION SOIL
- SLIMES
- COARSE TAILINGS (DRAINED)
- FINE TAILINGS (DRAINED)
- PHREATIC SURFACE
- POND LEVEL

CLIENT

PROJECT
REPORT OF THE EXPERT PANEL ON THE TECHNICAL CAUSES OF THE FAILURE OF FEIJÃO DAM 1

TITLE
STABILITY ANALYSIS RESULTS
SECTION 3-3' - EL. 942 m
LIQUIFIED STRENGTH

SCALE	PROJECT No.	FIG. No.
1:2,500	A03355A01	36

KCB-FIG-B-L